STUDY OF CELLULAR AUTOMATA TECHNIQUES FOR URBAN GROWTH SIMULATION IN GIS DOMAIN

A THESIS

Submitted in partial fulfilment of the
requirements for the award of the degree
of
DOCTOR OF PHILOSOPHY
in
ARCHITECTURE AND PLANNING

by

SANDEEP MAITHANI

DEPARTMENT OF ARCHITECTURE AND PLANNING
INDIAN INSTITUTE OF TECHNOLOGY ROORKEE
ROORKEE - 247 667 (INDIA)

AUGUST, 2008

INDIAN INSTITUTE OF TECHNOLOGY ROORKEE
ROORKEE

CANDIDATE'S DECLARATION

I hereby certify that the work which is being presented in the thesis entitled **STUDY OF CELLULAR AUTOMATA TECHNIQUES FOR URBAN GROWTH SIMULATION IN GIS DOMAIN** in partial fulfilment of the requirements for the award of the Degree of Doctor of Philosophy and submitted in the Department of Architecture and Planning of the Indian Institute of Technology Roorkee, Roorkee is an authentic record of my own work carried out during a period from January 2004 to August 2008 under the supervision of Prof. R. K. Jain, Associate Professor, Department of Architecture and Planning, Indian Institute of Technology Roorkee, Roorkee and Prof. Manoj K. Arora, Professor, Department of Civil Engineering, Indian Institute of Technology Roorkee, Roorkee.

The matter presented in this thesis has not been submitted by me for the award of any other degree of this or any other Institute.

(SANDEEP MAITHANI)

This is to certify that the above statement made by the candidate is correct to the best of our knowledge.

(Manoj K. Arora)
Supervisor

(R.K. Jain)
Supervisor

Date:...29/8/08.......

The Ph.D. Viva-Voce Examination of **Mr. Sandeep Maithani,** Research Scholar, has been held on............................

Signature of Supervisors

Signature of External Examiner

Abstract

Land transformation is one of the foremost fields of human-induced environmental change with an extensive history dating back to antiquity. The process of land transformation has not abated, but rather accelerated and diversified with the onset of industrial revolution and the expansion of population and technological capacity. Settlement refers to the occupation of land for human living.

Monitoring and evaluating the growth of urban settlements is essential in order to avoid environmental problems such as, depletion of natural resources, increased pollution levels, loss of green cover etc., especially in developing countries where cities are experiencing a rapid growth. It is of vital importance for urban planners to not only understand the past and present urban growth patterns but also be able to predict the future growth patterns. This is where spatial models of urban growth become useful. These models not only provide an understanding of urban dynamics, but also provide realizations of the numerous potential scenarios that an urban system may take.

In recent years, Cellular Automata (CA) techniques have evolved as possible alternatives for urban growth simulation due to their potential for dynamic spatial simulation capability and affinity towards GIS and remote sensing. However, the CA based models highly depend on formation of transition rules, which is often subjective, as these are based on expert's opinions. Secondly in Indian context, very few attempts have been made to develop CA based models for assessing the urban growth.

The present research aims to apply CA based models to simulate urban growth in two typical Indian cities having markedly different growth patterns and to examine the efficacy of Artificial neural networks (ANN) in formation of transition rules for CA based modeling and its comparison *vis a vis* multi-criteria evaluation technique (MCE). Besides, the effect of

different neighbourhoods *viz* Von Neumann and Moore neighbourhood in CA modelling has also been investigated. The simulated urban growth has been evaluated, based on cell by cell match using Percent correct match (PCM) and spatially using Moran Index and Entropy. Finally using ANN, an urban growth zonation map depicting zones having different growth potential at an ordinal scale has also been generated and evaluated.

The proposed CA based models have been implemented in two Indian cities namely Dehradun with geographical extents 30°15' N to 30°25' N and 77°55' E to 78°10' E. The region is experiencing a fast urban growth, which is taking place in a dispersed manner mainly along the roads and Saharanpur with geographical extents 29°55' N to 30°0' N and 77°30' E to 77°35' E. The city is expanding onto the nearby fertile agricultural land in a compact manner, mainly along the roads. The following datasets have been used to generate various thematic data layers for the two study area:

a) Remote sensing data: IRS-1C LISS-III and IRS-P6 LISS IV multispectral, PAN, and aerial photographs
b) Survey of India toposheets at 1:50,000 scale (53J/3,53F/15 and 53G/9)
c) Guide map at 1:20,000 scale
d) Master plans at 1:20,000 scale

The ERDAS Imagine image processing software has been used for processing and analysis of remote sensing data. The GIS analysis has been carried out using ArcGIS software while ANN processing has been done in Neural Network Tool Box of MATLAB software.

The following GIS data layers have been generated from remote sensing data and other data sources,

i) Land cover maps showing built-up/non built-up areas for years 1997, 2001, 2005 from digital image classification of IRS LISS III images of Dehradun city. For Saharanpur city, built-up/non built-up areas maps for years 1993 and 2001 through visual interpretation of aerial photographs (1:10,000 scale) and IRS PAN image

ii) Road network maps from LISS III and PAN images, master plan and guide maps

iii) City core map after consultation with local planning authorities. In these GIS layers, the boundary of reserved forests, restricted areas and public lands have been masked out.

The proposed CA models take into consideration only the physical factors affecting urban growth. Social and economic factors have not been considered due to non availability of accurate data pertaining to these factors. The three physical factors considered are,

i) Distance to city core
ii) Accessibility to infrastructural facilities
iii) Distance to road network

Corresponding to these three factors, following four raster maps have been created in GIS,

i) Map showing Euclidian distance of each cell from the nearest road
ii) Map showing Euclidean distance of a cell from the nearest built-up
iii) Map showing Euclidian distance of each cell from the city core
iv) Map showing amount of built-up cells in neighbourhood

In the MCE based CA model (MCE-CA), the urban growth suitability is first generated using the MCE technique. The weights are assigned to the three factors using Analytical Hierarchical Process (AHP) technique. Taking the MCE generated suitability map as an input, the MCE-CA model is run iteratively for user-defined number of iterations and the amount of built-up in the neighourhood is estimated using Von Neumann and Moore neighbourhoods of sizes varying from 3x3 cells to 39x39 cells. Using different combinations of the neighborhood and model iterations, the MCE-CA model has been executed several times for each of the study areas, so as to determine the optimum values of the parameters. For the Dehradun city, the model has been calibrated for the period 1997-2001. Since for this city, the actual growth for the period 2001-2005 is available, the model is validated for year 2005. For Saharanpur city, the model has been calibrated for the period 1993-2001. Using the calibrated model, future urban growth simulation for year 2011 has been carried out for both the study areas.

In the ANN based CA model (ANN-CA), a multilayered feed forward ANN with one input layer, one or two hidden layers and one output layer has been designed and trained using backpropagation algorithm. The input layer consists of 4 neurons corresponding to the four variables. The output layer consists of 1 neuron corresponding to whether a cell location changed from non-built-up to built-up (1=change, 0=no change). The number of neurons in the hidden layer has been finalized in two ways: i) based on literature driven thumb rules and ii) by trial and error. The ANN, producing the highest accuracy has been selected for simulation. The output from ANN is a map showing the development potential of cells. All the cells have not transitioned immediately to built-up. Only the cells that have a development potential above a certain threshold are changed. The size of neighbourhoods has been fixed as 5x5 cells for Dehradun city and 13x13 cells for Saharanpur city, as identified from MCE-CA model.

The accuracy of the simulated urban growth has been determined using two measures:

i) Percent correct match (PCM) for cell by cell assessment and ii) Moran Index (I), a spatial statistical indicator to assess the pattern of growth.

An urban growth zonation map has also been generated based on the ANN outputs. The ANN output shows the development potential of each cell, based on which the study area has been categorized into three zones (i.e. high, medium and low) showing the urban growth potential on an ordinal scale. Since the ANN outputs are not normally distributed, a logit transformation has been applied to make the data normally distributed. The transformed data has then been categorized into three classes as low potential zone < (μ-σ), (μ-σ) < medium potential zone < (u+ σ), (u+ σ) < high potential zone, where μ is mean and σ is the standard deviation. These urban growth zonation maps have been validated by overlaying them with the actual urban growth maps for the respective years, to find the spatial distribution of actual urban growth in each zone.

Further, the simulated growth patterns for both study areas have also been evaluated using relative entropy. It is a structural measurement index that assesses the goodness of fit according to the spatial domain of interest, which in this case is the distribution of urban growth with respect to distance from roads and distance from the city core.

The results show that for Dehradun city which has a dispersed growth pattern, Von Neumann neighbourhood of small size produces the highest accuracy, in terms of pattern and location of urban growth. While for Saharanpur city which has a compact growth pattern, large neighbourhoods, produces the most optimum results irrespective of the neighbourhood. It has also been observed that large number of model iterations does not increase the model accuracy, as they have resulted in an increasingly compact patterns as compared to the actual growth. This may be due to unplanned and stochastic behavior of urban growth process in Indian cities, which the CA models have not been able to simulate completely.

The ANN-CA model also produces comparable results as obtained from the MCE-CA model. This shows that the ANN are able to define the CA transition results directly from the database without human intervention, which proves the usefulness of ANN in urban growth simulation. In ANN-CA model, the ANN architecture based on literature driven thumb rules produces better or comparable results than those obtained from the optimal network from trail and error.

The urban growth zonation maps, obtained from ANN outputs show that most of the simulated growth has taken place in the high potential zone followed by the medium and low potential zone. Thus, the delineated urban growth zones matched with the actual growth pattern. These results demonstrate that ANN can be used effectively in reducing the subjectivity involved in the urban zonation process.

The simulation results have also been evaluated at a macro level using relative entropy. The evaluation of the simulation results using relative entropy, indicate that the model has been able to simulate the distribution of urban growth with respect to roads and city core accurately. The study also demonstrates the usefulness of PCM and Moran Index as simple indicators for evaluating the simulation results on a cell by cell basis and at spatial level respectively.

Thus, the proposed CA based models and the urban growth zonation approach developed in this research can be very fruitful for the urban planners in planning and regulating the future growth in Indian cities.

Acknowledgement

I would like to express my sincere gratitude to my supervisors **Prof. R. K. Jain** and **Prof. (Dr.) Manoj K. Arora**, for their support, enthusiastic guidance and advice. They were a constant source of inspiration for the completion of this research work.

Prof. R. K. Jain will forever remain my creditor for his caring attitude and emotional backing. The amount of freedom given by him to think and in coping up with problems that inevitably arose in the course of research deserves a special mention.

Prof. (Dr.) Manoj K. Arora on the other hand taught me the nuances and fruits produced by hard work. Whether he was in office, home or out of station, but he has always provided his guidance, expertise, moral support and encouragement through personal meetings in his office, telephone or Internet. He helped me to understand this research work through dividing all objectives into small parts and completing them step-by-step. Despite his busy schedule, he provided his precious time for long hours of discussion whenever required to understand this research work. This research would not have been possible without his active support.

I am thankful to the **Director, National Remote Sensing Agency, Hyderabad,** who permitted to join Indian Institute of Technology Roorkee for Ph.D. research work.

I express my deep sense of gratitude to **Dr. Vinay K. Dadhwal,** Dean, IIRS, Dehradun, for his guidance and academic support at Indian Institute of Remote Sensing, Dehradun. Whenever I met him, he always enquired about the status of my research work.

I am also highly indebted to **Prof. B. S. Sokhi**, my divisional Head at IIRS for all his help and guidance. Despite his busy schedule, he spared time for inspiring lengthy discussions on my research work and also spared me from some of the routine office jobs which allowed me to complete this research work in time.

I am also highly indebted to **Dr. A. P. Subudhi**, my senior colleague at IIRS, for teaching me the concepts of GIS and was always at hand for solving my problems especially related to GIS.

I acknowledge the support provided by **B. R. Nikam**, **Dr. K. P. Sharma, S. C. Dangwal, Dr. A. K. Mishra, B. D. Bharath, S. Jain, V. P. Sharma, A. K. Kamboj, R. N. Arun and Jeetendru,** who have contributed directly or indirectly in a significant way towards the completion of this thesis.

I am thankful to **T. S. Brar** and **P. Kumar** for all their help and hospitability during my stay at IIT Roorkee.

Finally, I owe a deep sense of gratitude to my **parents**, my wife **Archana** and son **Adithya**, who provided me the perseverance, inspiration and strength to carry on even when the going was tough. Without their support and contribution, I would have never seen this day.

Maithani

(Sandeep Maithani)

Contents

LIST OF FIGURES

Figure No.	Title	Page No.
Figure 4.3	Urban growth suitability map generated using MCE (study area II)	119
Figure 4.4	Flowchart of MCE based CA model	123
Figure 4.5	PCM as a function of different Von Neumann neighbourhood sizes (study area I)	133
Figure 4.6	PCM as a function of different Moore neighbourhood sizes (study area I)	135
Figure 4.7	Moran Index as a function of different Von Neumann neighbourhood sizes (study area I)	137
Figure 4.8	Moran Index as a function of different Von Neumann neighbourhood sizes (study area I)	139
Figure 4.9	PCM as a function of different Von Neumann neighbourhood sizes (study area II)	143
Figure 4.10	PCM as a function of different Moore neighbourhood sizes (study area II)	145
Figure 4.11	Moran Index as a function of different Von Neumann neighbourhood sizes (study area II)	147
Figure 4.12	Moran Index as a function of different Moore neighbourhood sizes (study area II)	149
Figure 4.13a	Simulated urban growth pattern for 1997-2001 (study area I)	155
Figure 4.13b	Actual urban growth pattern during 1997-2001 (study area I)	157
Figure 4.14a	Simulated urban growth pattern for 2001-2005 (study area I)	159
Figure 4.14b	Actual urban growth pattern during 2001-2005 (study area I)	161
Figure 4.15	Simulated urban growth pattern for 2001-2011 (study area I)	163
Figure 4.16a	Simulated urban growth pattern for 1993-2001 (study area II)	167
Figure 4.16b	Actual urban growth pattern during 1993-2001 (study area II)	169
Figure 4.17	Simulated urban growth pattern for 2001-2011 (study area II)	171
Figure 5.1	A MLP feedforward ANN architecture	175
Figure 5.2	Stopping criteria to prevent the over-training of ANN	181
Figure 5.3	A schematic diagram of the ANN-CA model	183
Figure 5.4a	Simulated urban growth pattern for 1997-2001 using ANN-CA model (study area I)	197
Figure 5.4b	Actual urban growth pattern during 1997-2001 (study area I)	199
Figure 5.5a	Simulated urban growth pattern for 2001-2005 using ANN-CA model (study area I)	203
Figure 5.5b	Actual urban growth pattern for 2001-2005 (study area I)	205

LIST OF TABLES

Chapter 1

Introduction

1.1 Motivation

India is undergoing a rapid pace of urbanization. The urban population of India increased from 217.6 million to 285 million in the last decade and presently constitutes 27.8% of the total population (Census of India, 2001), it is expected to increase to 40% of the total Indian population by the year 2021 (GGIM, 2005). In India, urban growth has two contradictory facets; on one hand, cities act as engines of economic growth and on the other, it is accompanied by environmental degradation, as the surrounding agricultural lands, forests, surface water bodies get converted to urban use and are irretrievably lost (Kulshrestha, 2004, 2007a, 2007b; Gowda and Sridhara, 2000; Tayal and Bharat, 1997). Faced with these severe negative impacts, there is an urgent need for urban planners to manage urban growth more scientifically in the near future (Jain, 2002, 2003; Routray, 1993, 2000). A number of studies and national projects have been conducted in India to monitor the urban growth using images acquired by a series of Indian Remote Sensing (IRS) satellites (e.g., Kumar *et al.*, 2007; Pathan *et al.*, 1989, 1991, 1993; Pathan, 2004, 2005, 2006; Sudhira *et al.*, 2003; Lata *et al.*, 2001; Fazal, 2000; Rashid *et al.*, 1993, 1999a, 1999b; Mahavir and Galema, 1991). However, these studies were limited to mapping and monitoring of urban growth and did not attempt to develop any predictive urban growth model. Hence, a follow up task may be to model the urban growth for the purpose of decision making in urban planning. This has been the major rational behind this study wherein simulation of spatial and temporal urban growth has been assessed through suitable models.

1.2 Issues in urban modelling

Urban modelling bloomed in the late 1950s and throughout the 1960s in both USA and Western European countries. Most of the models developed during this time conceived the city as being static, and attempted to simulate how land uses are located with respect to each other at a cross-section of time. Linear econometric models, in which spatial interaction was implicit, formed one class of models, in contrast to the non-linear models such as Lowry Pittsburgh model which attempted to model spatial interaction explicitly (Reif, 1973). All these spatial interaction models were static and operated at a fairly aggregate level, i.e., census tracts and traffic zones formed the level at which cities were represented. Forrester (1969) proposed a model of urban dynamics in 1969 where the life-cycle of an urban area was examined using stock and flows equations. The model was non spatial in nature and was run on an abstract city, hence the model parameters were defined intuitively. However, all these models were criticized by Lee (1973) for being hyper comprehensive, data hungry and complicated. Towards the mid 1980s, Cellular Automata (CA) based models were proposed as an alternative, due to the following reasons (Sullivan and Torrens, 2000a):

i) Simplicity

ii) Potential for dynamic spatial simulation

iii) Capability for high resolution modelling

iv) An innovative bottom up approach

v) Affinity to Geographic Information Systems (GIS) and remote sensing data

At the most rudimentary level, a CA is a lattice of regular cells. At any time (t), a particular cell is in one of a finite number of allowed states, and the state of the cell at time (t+1) will change according to a uniformly applied set of transition rules, which are based on the states of the neighbouring cells in the lattice. Cells alter their states iteratively and synchronously through the repeated application of these transition rules. A CA is thus composed of five principal elements (Torrens, 2000):

i) A lattice

ii) Cells

iii) A set of allowed states

iv) Neighborhoods

v) Transition rules.

The notion of neighbourhood and transition rules is central to the CA paradigm, but their definitions are strongly dependent on domain knowledge and individual preference of the model builder. Thus, a critical issue in CA based modelling is how to reduce the subjectivity in defining the transition rules and to fix the size and shape of neighbourhoods.

Further, most of the studies based on CA models evaluate the simulation results visually or at the most using overall classification accuracy only (Barredo *et al.*, 2003, 2004; Cabaral and Zamyatin, 2006; Li and Yeh, 2001, 2002). The use of other quantitative indices for comparing the simulated growth patterns with the actual ones has been lacking. Thus, there is a need for quantitative indices that can comparatively evaluate the pattern of the CA based simulations with actual growth patterns in an effective way.

1.3 Indian scenario

In the Indian context, very few attempts have been made to develop CA based models for urban growth simulation. Jacob *et al.* (2006) developed a CA model for simulating land use dynamics for degradation prone areas in the State of Andhra Pradesh. In the unpublished works of Singh (2003) and Sudhira (2004), a CA model for land cover simulation for Shimla District and Manglore city has been developed. These models evaluated the simulation results visually or using overall classification accuracy. The use of other quantitative indices such as Moran Index, Shannon entropy, fractal dimension and other shape indexes for quantitative and comparative analysis of simulated growth pattern with the actual one may be more informative. Thus, not much work has been reported on urban growth simulation using CA based models in India. Nevertheless, the CA based models can be quite useful in the Indian context, as the present day focus of the Indian Government is on infrastructure development in urban areas.

1.4 Role of GIS in CA based modelling

In order to be useful and realistic, urban models depend on 'real-world' data such existing urban land uses and growth patterns, existing road network, location of various facilities, availability of infrastructure facilities etc., that can be integrated and mapped in a modelling scenario. Geographic Information Systems (GIS) has emerged as a prime framework for the integration and management of a range of spatial real world data. However, to use GIS alone as modelling tool have been received with skepticism, as it has limited modelling functionalities and has constraints in handling temporal datasets. Nevertheless, GIS and CA in combination can be used as a strong couple to model the urban growth to take advantages of both the techniques. For example, although the capacity of CA to explore complex systems has been well established (Itami, 1994), its capacity to represent real patterns is yet to be proven. In case of GIS, its spatial data analysis capacities may be insufficient to handle complex urban dynamics. The integration of the dynamic strength of CA with the effective spatial representation found in GIS thus may be beneficial to achieve realistic representation of a phenomenon such as urban growth (Wolff and Wu, 2004).

Based on this premise, the present study has been aimed to simulate growth of Indian cities. An extensive literature review on the usage of CA based models for urban growth simulation has been presented in chapter 2. A number of CA based models have been developed by various authors, while models have been developed for abstract cities, some have also attempted to simulate the growth of real cities. It has been observed that the critical issue in CA based modelling is the definition of transition rules, which in most of the cases depends on the experience and expertise of the individual. Some authors have attempted to use Multi-Criteria Evaluation (MCE) and more objective methods like Artificial Neural Networks (ANN) to reduce the subjectivity in transition rule definition. Besides transition rule definition, the shape and size of neighbourhood, indices for evaluating the simulation results are also other important issues in CA modelling. From the review, in chapter 2, certain research gaps, as listed below have been identified, which form the basis of formulating the objectives of this research,

i) The applicability of CA based models to Indian cities having varied growth patterns, have been lacking.

ii) Focus has to be placed on development and use of techniques such as ANN to bring objectivity in the definition of transition rules for CA based models.

iii) Research needs to be conducted on optimization of parameters such as neighbourhood type and neighbourhood size for calibration of CA based models.

iv) There is limited amount of work on quantitative evaluation of model simulation results, as the assessment is mostly based on visual inspection.

v) As urban planners are often interested in targeting areas that have very high to high potential of urban growth, thus, availability of urban growth zonation maps may be useful, as these can form key inputs to various planning exercises. The research in this direction is lacking.

1.5 Research Objectives

The main aim of this research is to advance the work on CA based urban growth modelling. Based on the identified research gaps, the following objectives have been framed:

i) To implement the proposed CA based models to simulate urban growth in two typical Indian cities having markedly different growth patterns.

ii) To evaluate the efficacy of ANN in formation of transition rules for CA based modeling and its comparison with the traditional MCE based CA model.

iii) To investigate the effect of different neighbourhood sizes and neighbourhood types in calibration of CA based models.

iv) To evaluate the performance of CA based models using Moran, Percent correct match and Shannon's entropy.

v) To generate ANN based urban growth zonation maps depicting zones of urban growth potential at an ordinal scale.

1.6 Scope and Limitations

The scope of the study carried out in this thesis is limited to the following:

i) Urban growth has been defined in terms of increase in built-up area, as mapped from the remote sensing data. The classification system in the model is based on the dichotomy of built-up and non built-up areas only.

ii) The model takes into consideration only the physical factors affecting urban growth. Social and economic factors have not been considered due to non availability of accurate data pertaining to these factors.

iii) Certain areas that do not have any developmental potential have been treated as exclusionary zones and excluded from the model. These areas include strategic locations, reserved forests, water bodies, public grounds and gardens.

1.7 Organization of the thesis

The thesis has been divided into seven other chapters. All the illustrations and tables have been put along with text relevant to them, the references have been placed at the end of the thesis. In the present chapter, an overview of the problem and research objectives has been identified.

Chapter 2 undertakes a critical review of traditional urban models and identifies their shortcomings. The advantages of using CA models as compared to the traditional models have been highlighted. The concepts and issues in CA based urban growth modelling with an emphasis on combining CA models with GIS have also been discussed. This review forms the basis of understanding the existing work done in the area of CA based urban growth modelling.

In chapter 3, the characteristics and growth trend of the two Indian cities, on which the proposed CA models have been applied, are described. The factors driving the urban growth in the study area have been dealt in detail. The chapter concludes with a description of various aspects related to the database creation for the two Indian cities taken as the study areas here.

The concepts of the MCE based CA (MCE-CA) model have been explained in chapter 4. Various model parameters, viz., neighbourhood type and size, model iterations, stopping criteria and model calibration have been discussed in detail. The simulation results after implementation of proposed models have been illustrated using various indices namely Moran Index and Percentage correct match. Finally, simulation of future urban growth has been described for both the study areas.

Chapter 5 discusses the concepts of ANN based CA (ANN-CA) model. Various parameters in the ANN based CA model, viz., the network architecture, training and testing of network, have been explained in detail. The analysis of simulation result and its comparison with the MCE-CA model has been highlighted.

Chapter 6 discusses the technique and advantage of ANN based urban growth zonation, which is followed by an evaluation of the zoning results for the two study areas.

The analysis of simulated results using structural measures like Shannon entropy has been described in chapter 7. The Shannon entropy is calculated for simulated and actual growth and results have been evaluated.

In chapter 8, based on the results and their analysis of the proposed models, certain conclusions have been drawn from this study, recommendations and pointers to future works have been stated.

Chapter 2

Urban Growth Modelling and Cellular Automata

2.1 General

It is generally argued that although traditional urban modelling approaches of the 1960s were based on sound theories, they had significant weaknesses such as poor handling of space-time dynamics, coarse representation of data and top-down approach, which ultimately failed to reproduce realistic simulations of urban systems.

Urban modelling has gradually moved from these static approaches to other dynamic spatio-temporal based approaches such as Cellular Automata (CA), which were developed in the 1940s to explore complex phenomena like urban growth. These are now progressively being adopted and adjusted to address the criticism raised by traditional models.

CA based approach has also found place in urban modelling due to its affinity towards GIS (Torrens, 2000, 2001). GIS has emerged as a prime framework for the management of a range of spatial data (Routray, 1990). Thus, the integration of CA with GIS opens up new vistas to improve urban modelling. The aim of this chapter is to present the state of knowledge on urban modelling, specifically in relation to GIS based urban CA modelling.

2.2 Spatial models in urban simulation

Any data that shows location of features in space with respect to a reference system is known as spatial data. Geospatial data implies a subset of spatial data applied specifically to the earth surface or data showing the location of features on the earth surface (Laurini and Thompson, 1996; Burrough and McDonnell, 1998). However, in this thesis, the terms geospatial data and spatial data have been used interchangeably.

Spatial data can be represented by a physical or abstract model. Physical models are scaled down replicas of the real world, whereas in an abstract model, the real world is represented by symbols (i.e., line, points, polygons or cells). The conventional maps and spatial databases created in a GIS may be regarded as the abstract spatial data models (Batty, 2001; Wegener, 2000). The spatial models can also be categorized as static or dynamic models (Reif, 1973).

Static models simulate the spatial distribution of various activities in an urban area, at one point of time. These represent a cross section of the urban system at some time or date. Dynamic models focus on the process of change rather than the final state of the urban system. A static model considers the system as in equilibrium, whereas a dynamic model develops multiple discrete or continuous timeframes within the system under investigation.

The urban growth is expressed in terms of spatial factors, which vary from one study or the other. These factors are interrelated by mathematical functions that represent the dynamism of the urban system. Thus, for the study of spatial temporal processes such as urban growth, there is a need to develop abstract spatial dynamic models. The dynamic spatial models can be solved using two methods:

i) Analytical method

ii) Simulation method

Analytical method refers to the use of deductive reasoning of mathematical theory to provide a model solution. In analytical methods, the model is expressed in some particular format (e.g., linear algebraic equations or continuous linear differential equations). The system must be approximated or abstracted in order to derive a model that fits a mathematical equation.

Simulation methods involve application of numerical or computational procedures for solving the model. It is a step-by-step process of solving the dynamic model numerically in time domain. As a result, the current values at any step of the computation represent the state of the system being modeled at that point of time. Compared to the analytical method, simulation methods are computationally intensive and produce general solutions rather than specific solutions. Further, simulation method is useful when the model contains non linear stochastic expressions that are difficult to evaluate analytically.

Moreover, urban growth is a spatio-temporal process which is complicated and ill defined. Thus, it may not be possible to propose a universal solution that may explain the growth in different cities. Hence, simulation method appears effective in understanding the urban growth and its prediction.

2.3 Traditional models of urban growth

Since the beginning of 19th century, various models and theories have been proposed to explain urban growth. Burgess concentric zone theory in 1925, was based on the idea that the growth of a city took place outwards from its central area to form a series of concentric zones of various land uses. However, discrepancies between the concentric model and the actual distribution of urban land use patterns encouraged the formulation of various theories, notably among these was the sector theory proposed by Hoyt and Davie in 1939. According to this theory, patterns of urban land use were influenced by the road network radiating outwards from the city centre. The accessibility to roads created a sectoral pattern of land values, which in turn influenced the urban land use pattern. However, both the concentric zone and sector theories assumed that the city grew around single nucleus, but actual pattern of urban growth is generally far more complex and varied than any of the models suggested. Consequently, Harris and Ullman in 1945 proposed the multiple-nuclei theory, and suggested that urban growth in large cities took place around a number of nuclei rather than a single nucleus (Knowles and Wareing, 1976).

Thus, with the help of these theories, attempts were made to formulate comprehensive models of urban growth. However, none was entirely satisfactory, as these theories were rigid and static in nature and sought only to represent visually the spatial arrangement of hypothetical urban socio- economic systems (Ramachandran, 1991).

Urban growth modelling bloomed in the 1950s and 1960s. Most of these models developed were spatial interaction models. Spatial interaction models drew from the original efforts of Reilly in 1931 and Zipf in 1946 to model human activities. The model formula, in its most basic form, was based on Newton's Law of Gravitation. Models included in this group were the well known gravity type models and their reincarnated formulations such as Lowry and Grain-Lowry model. The spatial interaction models were used to study a variety of intersections arising out of human activities within the urban system, such as journey to work, land use transport interactions and urban growth in general. However, these models had significant limitations; they were very complicated, required lot of data, their resolution was coarse and they were static in nature.

Forrester (1969) introduced the concept of industrial dynamics, for simulating industrial processes in firms and attempted to apply this idea to model the growth dynamics of an abstract city using differential equations (referred as stock and flow equations). Since the model was developed for an abstract city, it was not calibrated for real world. Besides, the model also ignored the spatial dimension of urban growth. According to Batty and Torrens (2001), it was not appropriate to treat this model as a generalized model of a city. Although, Forrester model played an important role in introducing the dynamic view of the urban systems, but it was Lowry model, with extensions and modifications that found widespread use.

2.4 Cellular Automata for urban growth modelling

CA offers a range of advantages for urban modelling and in several ways it gets over the deficiencies of the traditional models. CA based models are inherently spatial, dynamic and have a natural affinity towards GIS (Couclelis, 1997; Torrens, 2000, 2001).

2.4.1 Concept of Cellular Automata

Cellular automata (CA) were originally conceived by Ulam and Von Neumann in the 1940s to provide a framework for investigating the behavior of complex systems (Torrens, 2000). The concept of self-organization, which is one of the main characteristics of complex systems, is central to CA based modelling. Self-organization refers to the tendency of system to spontaneously develop ordered patterns, often on a large scale from local decision making processes (Torrens and Sullivan, 2001). Thus, CA are able to simulate processes such as urban growth where global or centralized order emerges as a consequence of local or decentralized rules.

At the most rudimentary level, a CA is an array (or lattice) of regular cells. At any given time, a cell is in one of the finite number of allowed states. The cell changes its state based on the state of its neighbouring cells in the lattice, as per uniformly applied set of transition rules. Cells change their states iteratively and synchronously through repeated application of these transition rules. CA is thus composed of five principal elements (Torrens, 2000, 2001),

i) Lattice: A regular uniform and infinite 'lattice' or 'array' with discrete variables at each cell. Lattice space can have *n* dimensions, but two-dimensional CA is the most common in urban simulation.

ii) State: A state is a variable, which takes different values at each cell. It can be a property, a number or word (0 or 1, urban or non-urban).

iii) Cell: A cell is the sub-unit of the lattice or the regular geometrical grid. A cell at any instant of time can be in only one state out of a given number of states. The states of all cells in a grid are updated during CA iterations.

iv) Neighbourhood: In a lattice, there are normally the cells that are physically closest to the central cells, which influence the state of the central cell in the next step. The neighbourhood cells act as immediate areas of interest for the central cell, as the transition rules which decide the state of the central cell in next step are based on the neighbourhood values. The neighbourhood also includes the central cell itself. The two commonly used neighburhoods are the Von Neumann and Moore neighbourhoods. A 3x3 cell Von Neumann and Moore neighborhoods are shown in Figure 2.2. The black cell (which represents the cell under consideration) and the surrounding grey cells (4 in case of Von Neumann and 8 in case of Moore neighbourhood) together constitute the neighbourhood. The neighbourhoods can also be extended from their 3x3 cells size to other larger odd numbered sizes (e.g. 5x5, 7x7, 9x9 and so on).

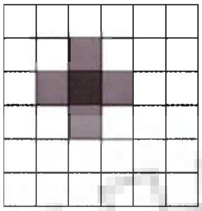

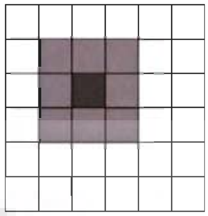

Fig 2.1: Von Neumann neighborhood Moore neighborhood

v) Transitional rules: These are a set of conditions or functions that define the state of change in each cell in response to its current state and that of its neighbors. The future state of cells is determined by the transitional rules in a discrete time frame.

Mathematically, CA can be defined as:

$$\{S_{t+1}\} = f(\{S_t\}\{I^h_t\})$$

where, $\{ S_{t+1} \}$ is the state of the cell at time (t+1), $\{ S_t \}$ is the state of the cell at time (t) and $\{ I_t^h \}$ refers to the neighbourhood, function f refers to the transition rules, t is the time steps in temporal space, h is the neighbourhood size.

Hence, it is the capacity to integrate spatial and temporal dimensions that makes CA appealing for the development of robust and reliable urban dynamics models.

2.4.2 Limits and strengths of cellular automata

Conceptually and theoretically, CA for urban studies has some limitations and strengths with regard to the development of an urban dynamics framework. This section first discusses some of the limitations of CA and then expands on its strengths to model complex phenomena like urban growth.

The original framework of CA is not appropriate to support realistic urban dynamics (Wolfram, 1986). For instance, the overall original structure of CA is too simplistic and constrained to apply in real urban applications (Sipper, 1997). Similarly, it is not reasonable to apply the concept of an infinite space plane (two-dimensional) and uniform regular space to the city because cities are not infinite, regular, or uniform. Moreover, the notion of neighbourhood is too coarse and does not take external factors and distance-decay actions into consideration.

Another criticism is that cellular automata only assumes a bottom-up approach, and accounts for local specificities that ultimately define the overall representation of the space generally. All constituents of urban systems, however, do not exhibit bottom-up behaviour like, urban planning decisions, national policies, macro-economy, and so on. These factors operate from top to bottom and serve to constrain the urban growth.

In the original CA, transition rules were universal and applied synchronically to all cells. In real urban growth processes, however, no single rule governs the behaviour of the entire system. To solve the rigid transitional rules, urban dynamics CA transition rules are formulated using Boolean statements, and probabilistic expressions such as {< IF >, < THEN >, < ELSE >}. The flexibility thus gained in these expressions, simplifies the representation of more complex systems (Batty, 2000).

The simulation of urban dynamics is an area of research where CA has been recently implemented. Here, CA represents a useful tool for understanding urban dynamics, improving theory, achieving realistic and operational urban models (White, 1998). White and Engelen (1993) have demonstrated that a cellular automata approach can lead to a better understanding of spatial patterns as well as representing realistic patterns. In the spatial modelling perspective, the strengths of CA lie in their capacity to perform dynamic spatial modelling over a discrete and continuous Euclidean space. Similarly, CA has the ability to exhibit explicit spatio-temporal dynamics. Several studies (e.g., Bivand and Lucas, 2000; Openshaw and Abrahart, 2000) have shown how CA models can be integrated with other spatio-temporal models, to improve the representation of urban features. Finally, the flexibility of transitional rules embedded into CA architecture favours an effective control over the dynamic patterns that are generated.

The role of CA is to discover, understand and explain how cities emerge and change (Couclelis, 1985; White and Engelen, 1994; Portugali, 2000; Ward *et al.*, 2000). The introduction of CA approaches in geography may be traced back to the work of Hägerstrand (1968), who highlighted the major components of current CA architectures as, discrete time and state, cell, neighbourhood, uniform transitional rules and lattice. The investigation of Hägerstrand was limited by the capacity of the simulation (e.g., less than 200 cells), yet it was theoretically and conceptually well formulated. Tobler (1970) further developed a forecasting model based on urban growth. In fact, Tobler's study laid the theoretical and conceptual foundation of CA for future applications in geography. In 1979, he published a paper formalizing the concept of CA (Tobler, 1979), which opened the gates for geographers to use CA for urban planning applications, spatial modelling and simulation. However, the temporal dimension of Tobler's CA was considered weak because the simulated maps developed for each year were very different from the actual growth simulation (Wegener, 2000).

Tobler's work was improved by Couclelis (1985, 1989, 1997), Batty and Longley (1986, 1994) and Batty and Xie (1994c, 1997), who enhanced the theoretical and methodological aspects of CA for analysing and modelling complex urban dynamics. In the same spirit, Couclelis (1989) demonstrated the use of CA as a metaphor to study different varieties of urban dynamics. Couclelis claimed that although CA was not originally intended to produce realistic representations of urban dynamics, it could be reformulated and integrated with some spatial models to form better predictive models. White and Engelen (1993, 1994) went further to advocate that CA was capable of generating real patterns of urban land-use change. Thus, it is during the last two decades or so, impetus on the use of CA models for urban growth simulation can be seen. The following sections demonstrates the uses of CA; first as a hypothesis to explore the urban growth dynamics of fictitious cities, and then in the simulation of real urban growth.

2.4.3 Hypothetical urban simulation with cellular automata

A number of researchers have shown the use of CA to explore urban theories and growth patterns (Batty and Longley, 1986; Batty and Xie, 1994; Sullivan and Torrens, 2000b). Earlier CA models such as Tobler's (1970) model of Detroit, and Coucleli's (1985) model of the Los Angeles, were used to demonstrate how global patterns emerge from local transitional rules. Cecchini (1996), for instance, demonstrated that CA could provide a comprehensive understanding of land use change in fictitious cities. In other examples, Batty (1994) applied CA to verify urban dynamics theories and to test some hypotheses of urban changes. Similarly, Semboloni (1997) assessed the aspects of economic theory by applying CA for the simulation of urban growth in a hypothetical city. Benati (1997) also used CA to simulate the location of competitors on a discrete and bi-dimensional market place using equilibrium theory. Phipps and Langlois (1997) applied CA to test the Von Thünen model in order to establish CA suitability for the interpretation of real patterns. This work was interesting in the sense that it showed another way of understanding a well-established geographical model. In another example, Wu (1998a) and Batty (1998) demonstrated the use of CA to explore the development of polymorphous-polycentric cities. CA was also used to investigate intra-urban land use transformations (White and Engelen, 1994) and long-term spatial urban sprawl (Batty, 1996). Portugali *et al.* (1994) demonstrated the use of CA to simulate spatial segregation between different social groups.

One of the most significant improvements to CA models came from Wu (1998b) work, who applied CA in a generic city to highlight the fact that CA could significantly improve the understanding of growth patterns of polycentric urban forms. Wu and Webster (1998, 2000) also applied CA to explore the sustainability of urban forms. Two main difficulties, however, limited the applicability of these experiments into actual urban areas. First, the limited size of the space considered reduced the potentiality of these applications in real world situations (Batty, 2000). Second, was the difficulty experienced in spatially reflecting some fundamental formulations of CA. For example, the model did not address the concept of CA's explicit representation of change of state based on general rules and attributes of the neighbouring elements. In light of these key questions, researchers had to readjust the structure of CA or seek alternative integration with other spatial models that can better handle real world data in a simple manner.

2.4.4 Modelling real cities with CA

Since the 1970s, CA has been regarded as a useful tool to simulate and model various urban systems. Although, initial CA applications were limited to test hypothesis, theories and generating fictitious cities, real applications have been rare. This may be partially due to the rigid conceptual framework of the original CA. In the 1990s, however, operational urban CA models started to emerge owing to the progress in conceptual urban CA, the development in the rapport between CA and real data interfaces and computing power. In these models (Meaille and Wald, 1990; Clarke *et al.*, 1997, 1998; Almeida *et al.*, 2003), some CA principles have been relaxed as a means of achieving more realistic simulations. This section reviews some examples of CA urban modelling applied to real cities highlighting the achievements made, and also points out some of the limitations of CA models.

White and Engelen (1993) used CA to explore the spatial structure and temporal dimension of urban land use and to test general theories of structural evolution. The cellular model generated patterns for each land use type, which were then, compared with data from a set of US cities using fractal dimension. The results showed realistic representations of actual urban form. In another example, White and Engelen (1997) and White *et al.* (1997), implemented CA, to model and predict the land use of the Carribean island of St. Lucia and in USA. In both studies, the transition rules were based on the suitability value of a cell for different land uses and neighbourhood information. The model for Cincinnati was calibrated by trial and error process, whereas in case of St. Lucia, the final calibration was not done and one scenario was described, in order to illustrate the behavior of the model. The simulation results for Cincinnati were evaluated using two measures:

i) Visual comparison of simulated land use with the actual land use.

ii) Comparison of the fractal dimension of the simulated and actual land uses.

From visual comparison, it was found that the simulation result appeared to be the actual growth. As a more precise measure of the urban form, the fractal dimension associated with the area-radius plot of various land uses was used. Plots of area occupied by a particular land use against the radial distance from the city centre were prepared for both the simulated and actual city of Cincinnati. Results showed that plots for actual and simulated land uses did not match exactly, but the patterns were similar. Thus, the model results were realistic and the model was able to simulate the land use pattern of Cincinnati. In all the three models thus far discussed, the neighbourhood used was of circular shape and included the cell itself and the cells lying within a radius of six cells.

Barredo *et al.* (2003, 2004) also developed a CA model for predicting the land use of Dublin and Lagos, Nigeria respectively. The model was based on 22 states, which were classified as fixed classes (water bodies, airport, rail and road network etc.), passive states (arable land, forests, shrub, sparsely vegetated and wetlands) and active states (different categories of residential areas, industrial, commercial, public services, port areas and abandoned lands). The transition rules were based on accessibility, neighbourhood, suitability of a cell and zoning status. The neighbourhood used was of circular shape and included the cell itself and the cells lying within a radius of eight cells. The model parameters were determined heuristically. For Dublin, the simulation results were evaluated using three indices:

i) Visual comparison with actual land use,

ii) Comparison matrix which evaluated the simulation results with the actual land use on a cell by cell basis,

iii) The distribution of land use pattern through relatively abstract measures such as fractal dimension.

The visual comparison of the simulated and actual land use map showed similarity between the two maps. However, the simulated land use was less fragmented than the actual land use. The fractal dimension was calculated by calculating the total area occupied by individual land uses with a given radius from the city using a set of increasing radii. Despite marginal difference in the area-radius plot, the general agreement of the plots for simulated and actual land use indicates the similarity of the pattern distribution in both maps. Each land use was compared on cell by cell basis using comparison matrix. A maximum accuracy of 92% was reported for residential uses and the minimum accuracy of 64% was reported for industrial uses. For Lagos, the results were evaluated based on :

i) Comparison matrix

ii) Spatial metrics such as mean patch area, total edge, shape index proximity index splitting index and Simpson diversity index.

The statistics obtained from the comparison matrix showed an acceptable fit between the simulated and actual land use maps. The maximum accuracy of 85% was obtained for residential uses and a minimum accuracy of 63% for informal settlements. To compare the pattern similarity between the actual and simulated land uses, various spatial metrics were computed for actual and simulated land use and compared using regression analyses. The correlation coefficient varied from 0.84 to 0.98. The spatial metrices showed a high degree of similarity between the actual and simulated maps in terms of pattern.

Clarke *et al.* (1997) developed the Urban Growth model (UGM) based on integration of GIS and cellular automata approaches. The UGM simulates the urban growth transition from non-urban to urban land. In UGM, the input factors were the local (roads, existing urban areas and slope), and temporal (historical patterns of growth). The simulation was controlled by five parameters, which carry respective weights or coefficients: slope resistance, road gravity, breed, dispersion and spread. The coefficient of each parameter was determined by running four rigorous calibration phases: coarse, fine, final and averaging best results. The weighted probabilities of each parameter were then used as input into the growth prediction. Clarke and Gaydos (1998) gave the SLEUTH model, which is a CA-based urban growth model(UGM) coupled with a land cover change model (US Geological Survey 2003).The

SLEUTH, stands for slope, land cover, exclusion area, urban extent, transportation network and hillshade. These characters constitute the five main categories of data input. Whereas UGM was designed for local application, SLEUTH was more ambitious and claimed to be used for forecasting urban growth at a regional and continental scale. The results from the model were evaluated on the basis of a single composite measure, which was generated on the basis of the following factors:

i) R^2 fit between the actual and predicted number of urban pixels

ii) R^2 fit between the actual and predicted number of edges in the image

iii) R^2 fit between the actual and the predicted number of separate clusters in the urban distribution

iv) Modified Lee-Sallee shape index.

UGM and SLEUTH models have been applied in the study of many planned cities in North America such as San Francisco (Clarke *et al.*, 1997), Chicago, Washington-Baltimore area (Clarke and Gaydos, 1998), Sioux Falls, California, and Philadelphia (Varanka, 2001); Lisbon and Porto (Silva and Clarke, 2002) in Portugal (Europe); and Porto Alegre (Leao, 2002) in Brazil South America.

In order to derive behavior oriented transition rules in CA, the Analytical Hierarchical Process (AHP) of MCE was also used by various authors. Jacob *et al.* (2006) implemented a MCE based CA model for simulating the land degradation process in degradation prone districts of Andhara Pradesh, India. The land use classes were grouped into three classes: degraded land, non degraded land and land prone to degradation. The suitability of each cell for various classes was determined using the AHP method. The transition rules were based on the suitability value of each cell. A 3x3 cells Von Neumann neighbourhood was used in the model. The model was calibrated heuristically and the simulated results were evaluated using a comparison matrix. An overall accuracy of 78% was achieved during the validation. Cabral and Zamyatin (2006), also used a MCE based CA model for simulating the urban growth in Sintra-Cascais municipality, Portugal. The suitability of each cell for built-up was determined using the AHP method. The transition rules were based on these suitability values. Various neighbourhoods size were attempted. The results were evaluated using five indices: percent correct, $K_{standard}$, K_{no}, $K_{location}$ and $K_{quantity}$. $K_{standard}$ is the standard Kappa index of agreement and compares the observed proportion correct to the proportion correct due to chance. K_{no} denotes kappa for no information and indicates the proportion classified correctly relative to the expected proportion classified correctly by a simulation with no ability to specify accurately quantity or location. $K_{location}$ denotes kappa for location and indicates the extent to which the simulated and actual maps agree in terms of location of each category, given the specified quantities. $K_{quantity}$ denotes kappa for quantity and indicates the extent to which the two maps agree in terms of quantity of each category, given the specified locations. The values obtained for these indices during model validation were: 83.95%, 66.28%, 67.9%, 68.57% and 96.66% respectively.

Li and Yeh (2001, 2002) developed CA based urban growth models for Dongguan city of China. The ANN derived weights acted as the transition rules derived directly from the database, instead of the user defining them as in case of MCE based CA models. Li and Yeh (2001), applied the ANN based CA model to predict the urban growth in Dongguan city. The model was based on the dichotomy of built-up and non built-up areas. A 7x7 cells Von Neumann neighbourhood was used in the model. The ANN was first trained and then using this trained network, the urban growth was simulated. The simulated result was evaluated using comparison matrix and an overall accuracy of 79% was reported. Li and Yeh (2002) used the same model to simulate land cover classes, like cropland, construction sites orchard built-up areas, forest and water in Dongguan city. The results were again evaluated using comparison matrix and the overall accuracy of 83% was reported. Thus, the ANN was able to extract the transition rules from the database without much human intervention.

These studies suggest that even in cases where CA has been extensively used as an urban simulator, its implementation on real world data sets has to go a long way.

2.5 Integrating GIS and CA for urban dynamics modelling

Yeh and Li (2001b, 2002, 2003) and Batty (2001) have shown that GIS can act as a key tool to make effective use of urban dynamics models such as those based on CA. The concept of integrating GIS and CA tools is based upon their resemblance to each other. For instance, a raster GIS structure can be represented in a CA environment by the cells and lattice. This section extends the discussion on the similarities between CA and GIS and then explores the potentialities for a workable integration. After expressing the theoretical framework of an integrated GIS based CA model, some examples have been presented to illustrate existing approaches that claim to achieve successful and accurate modelling of urban dynamics.

2.5.1 Reasons for linking GIS and CA for urban dynamics modelling

A number of important points have been raised in the literature about the benefits of linking GIS and CA to improve urban dynamics modelling. GIS and CA have been argued to have significant common features and complementary functionalities, and can therefore supplement and complement each other (Wagner, 1997; White, 1998). Couclelis (1985, 1989) discussed the theoretical considerations for the integration of GIS and CA as well as their potentialities in improving the quality of spatial urban dynamics models. Couclelis also (1997) pointed out the natural affinity between CA and GIS and advocated a more interactive and visual integration of GIS and CA to improve the patterns of realism in urban modelling and simulation.

Sui and Zeng (2001) recognized the advantage of GIS based CA urban modelling and simulation. One of the advantages cited is the bottom-up approach of CA, which enables the incorporation of various local factors into the modelling process in order to better represent their evolution. In doing so, the model can generate realistic urban dynamics thereby correcting the static representation of GIS.

In many ways, the deficiencies of GIS and CA can be compensated by each other. For example, although the capacity of CA to explore complex systems is well established (Wolfram, 1984; Itami, 1994), its capacity to represent real patterns has still to be proven. In case of GIS, its predictive and analytical capacities are insufficient to handle complex urban dynamics. The integration of the dynamic strength of CA with the realistic temporal and spatial representation found in GIS and remote sensing is, therefore, appealing as a practical means to achieve realistic representation. On one hand, GIS has much to offer in this integration as it can do data pre-processing, sorting, storage and retrieval of data, database querying, graphical display, input and output editing. On the other hand, CA may provide the power for database analysis, temporal dimensionality (for instance by handling multiple iterations), the flexibility to assign transitional rules and definition of the spatio-temporal neighbourhoods.

2.5.2 GIS and CA integration: a review of some studies

Urban researchers in principle have agreement on, the usefulness and necessity to link CA with GIS to achieve more realistic and informed urban dynamics models. However, implementation strategies are divergent in identifying the appropriate way to achieve optimum results.

One approach consists of building a CA modelling application using the programming language within a GIS language protocol (Batty and Xie, 1994a; 1994b; Yeh and Li, 2001b). This requires a certain level of familiarity with the programming language embedded in the GIS package in use. The flexibility of the language, however, is not always guaranteed and the scope for application of the skills learnt in the process is limited.

Another approach to integrate CA and GIS is to develop a stand-alone CA program that can use data from GIS. Data interchange and compatibility can be achieved through file conversion protocols (Yates and Bishop, 1998; Yeh and Li, 2002, 2003). However, if the program can not access and modify the data to and from the GIS environment, then the process of reformatting the input and output is not only more likely to mislead the representation, it may also be time consuming and error prone. For these reasons, 'loose' or 'tight' coupling are more likely to produce better integration models (Bivand and Lucas, 2000; Almeida *et al.*, 2003; Couclelis, 2002).

There are two dominant views that sustain the way in which realistic dynamics modelling may be achieved, if GIS and CA are to be used simultaneously. The difference lies in the extent to which the integration is achieved. Coupling is attractive because of the continuous expansion of GIS technology and its interchangeability with other spatial platforms and technologies (Waters, 2002). Another advantage of coupling is the possibility it creates to use different tools (e.g., statistics, image processing, stand-alone programs, GIS platform, etc.) to process all the information (Almeida *et al.*, 2003).

The first view is constructed around the argument that GIS functionalities and capabilities should be extended to respond to specific needs. Therefore, the integration of GIS and CA approaches may be successfully achieved through tight coupling. That is, new extensions, functionalities or dynamic tools are encoded into the GIS environment to expand its capabilities to perform tasks for which it has not been originally designed. In the perspective of urban spatial modelling by means of GIS, the tight coupling group supports the view that future GIS should be equipped with spatial dynamics modelling. This can, however, be achieved by incorporating GIS functionalities into a type of analytical engine of cellular automata; The CAM modelling machine developed by Toffoli and Margolus (1987) is one such example. Although, models generated through tight coupling are often suitable for a specific application, these are poorly replicable in a different context. Moreover, spatial models developed within GIS remain less flexible and the capabilities of handling other modelling functionalities are also weak. Thus, there are thresholds for the extension of CA or GIS functionalities and capacities. At least in the case of GIS, it is clear that the technology has not yet been designed to perform complex modelling operations (Longley and Batty, 1996; Alberti, 1999; Waddell, 2002).

An alternative view on the integration of GIS and spatial modelling approaches is that, it should be envisaged in respect of the sole strength and contribution of each set of tools. This technique is known as loose coupling. In loose coupling, both GIS and CA maintains their fundamental structure and functionalities, and only execute the operations, where they perform the best. In case of CA and GIS, for instance, a loose coupling approach is the first pragmatic choice when it comes to dynamics modelling and simulation of real data (Clarke and Gaydos, 1998). In case of loose coupling, there are many variants; from using GIS purely as the display environment to a more expanded coupling where the contribution of GIS is much wider (Batty *et al.*, 1999). In a sharing task, GIS may act as a data management, storage, retrieval and static visualization interface, whereas CA may perform other functions that cannot or are less effectively handled by GIS, such as dynamic exploration and data analysis, interaction with commands and functions, insertion of weighting parameters, iterations, calibration, modelling, dynamic visualization and simulation. If the synergy task is not carefully defined, however, there is a potential risk of role conflict, and also a possibility that the user may not have full control over the system and the data. When this difficulty can be avoided, loose coupling can be considered as a flexible and adjustable integration strategy that usually leads to more realistic simulations.

The loose coupling can also be achieved through the development of a macro language. Conceiving and building scripts using macro languages may achieve optimum and flexible integration of CA and GIS. This supplementary programming task, which takes place outside the GIS and CA environment has advantages since programming languages can be used and the knowledge gained may be re-used or expanded for other applications. Moreover, the scenario can be easily updated or adjusted. Also, many of these programs support conditional statements such as Boolean logic based ('if...then') iterations, calibration possibilities, and many other functions which help in modelling. In that respect, properties of Object-Oriented Programming (OOP) have been reported as appropriate for realistic urban modelling and simulation (Benenson and Torrens, 2004). For instance, the SWARM software tool uses OOP to simulate landscape behaviour based on the integration of GIS and CA (Wu, 1999). The integration can also be realized by creating a graphic user interface (GUI) that gets its input from a GIS to subsequently run a simulation based on a CA protocol (Wu, 1998b; Wu and Webester, 1998). Thus, it appears that the linkage between spatial models and modelling and simulation techniques can be effectively achieved through the loose coupling approach.

2.6 Summary

The review presented in this chapter has clearly indicated that the current research based on CA, GIS and their integration. Chronologically, the work can be divided into two periods, the first period (from 1940s to 1990s) was the development of the conceptual and theoretical frameworks. The second period (i.e., beyond 1990s) has been marked by the increasing interests in the applications of these dynamic approaches; first in fictitious cities, and then in real contexts.

In particular, the review demonstrates that in the area of urban modelling, there is evidence of growing awareness that the concept of equilibrium is no longer sustainable, and the theory of complex systems (i.e. dynamics) is prevailing. The realistic urban dynamics models should consider the equal representation of space, time and other key attributes, which can only be successfully conducted by the integration of many spatial tools. However, the process of coupling of technologies for realistic representation remains wide open for debate.

The second part of the review illustrates how the improvements in computing and GIS technologies have helped the developments in the area of urban dynamics modelling and simulation. In particular, the literature reflects that GIS may be appropriate for urban modelling and simulation as compared to CA, which although well suited, needs real-world data to generate informed and useful simulations. It is also apparent from the review that the integration of GIS and CA is the way forward to gain better insight into the process and form of urban dynamics simulation and modelling.

Nevertheless, some research gaps as follows, have been identified from this review, which need attention,

i) In most of the studies, the use of only one neighbourhood has been reported. The effect of using neighbourhood of different shapes and sizes on the simulation result has not been studied exhausitively.

ii) A comparative evaluation study of more objective approaches such as ANN for definition of transition rules in comparison to the subjective definition via MCE and other behavior oriented methods to examine their efficiency is required.

iii) There is a need for indices that can evaluate the growth pattern, with respect to various urban elements that influence urban growth (e.g., road network, distance to various facilities etc.).

iv) For evaluating the simulated growth pattern, different indices have been used in various studies. There is a need to devise simple indicators to ensure a straight forward comparison between various models.

v) The research is also lacking in development of urban growth zonation maps. These maps may depict zones having different growth potential and can serve as a important input in the planning process.

vi) Very few CA models have been implemented in Indian cities.

These research gaps have led to the formulation of research objectives of this thesis. To accomplish these objectives, some CA based models have been proposed and implemented on two markedly different urban cities in India, as discussed in the subsequent chapter.

Chapter 3

Study Area and Data Layer Generation

3.1 General

For carrying out the simulation studies, two Indian cities namely, Dehradun and Saharanpur having different growth patterns have been selected. Figure 3.1 shows the location of these two cities on the map of India. In this chapter, description of spatial databases generated for these study areas has been provided. These databases form the basis for analysis of growth trend of these two cities. Based on the growth trend analysis, the factors influencing urban growth have been identified. These factors become the indicators for various simulation studies as described in subsequent chapter.

3.2 Study area I: Dehradun city

3.2.1 Physical setting

Dehradun city, the capital of Uttarakhand Sate (India), is located in the picturesque Doon valley. The lower Himalayas are located in the north, Siwalik mountain range in the south, river Song in the east and river Tons in the west of the city. The hills which form the north and south boundaries of the study area are covered with dense patches of reserved forest (Figure 3.2). A number of civil and defense institutions of national level are located in the city. The city has also emerged as a vital service centre within the region, since the trade and commerce requirements of the region, higher order facilities of health, education, recreation and transportation are met by the city. The city and its adjoining areas are exuberant in fruit and agricultural products. During the last decades, the city has registered an unprecedented growth in its area and population.

In order to regulate the development of the city, the Town and Country Planning department has demarcated the Dehradun planning area, which consists of Dehradun city and the surrounding areas. The planning area is selected on the basis of the influence of the city on its surrounding areas. The geographical extents of the Dehradun planning area are 30°15' N to 30°25' N latitude and 77°55' E to 78°10' E longitude, and covers a total area of 360 km^2.

3.2.2 Demography

An analysis of the decadal population from 1971 to 2001 (Figure 3.3) reveals an increasing trend in population from 30.38% in 1971-1981 to 37.92 % in 1991-2001. The Town and Country Planning department has projected the future population on a decadal basis (Figure 3.3), and plans to develop the area with a gross density of 130 persons per hectare (Town and Country Planning Department, 2005).

As per 2001 census, 75% of the workforce is engaged in tertiary sector, 20% in secondary sector and 4% in primary sector. The employment of a large portion of the population in tertiary sector highlights the role of Dehradun as a major service and commercial centre in the region.

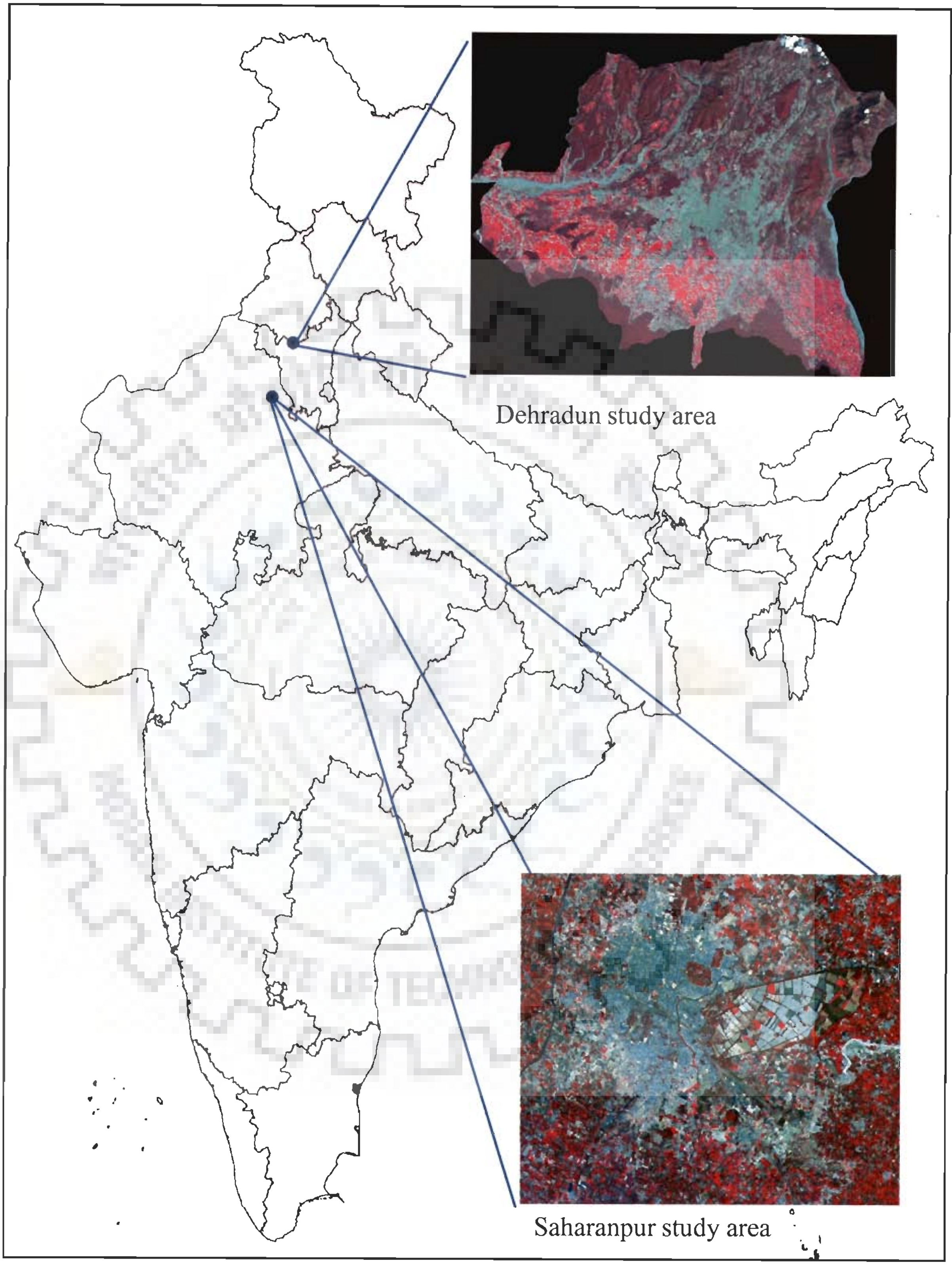

Figure 3.1: Location of study areas (Not to scale)

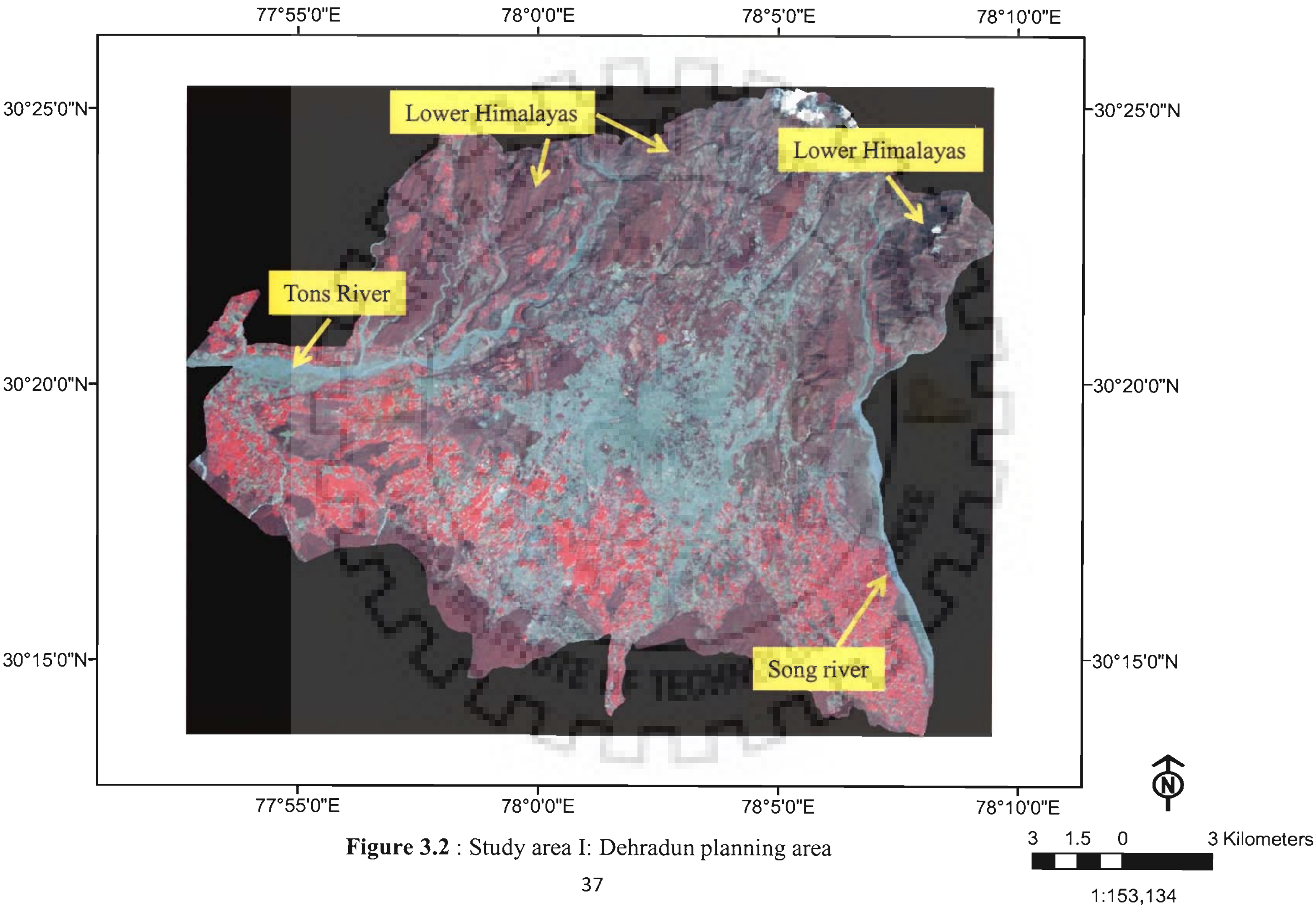

Figure 3.2 : Study area I: Dehradun planning area

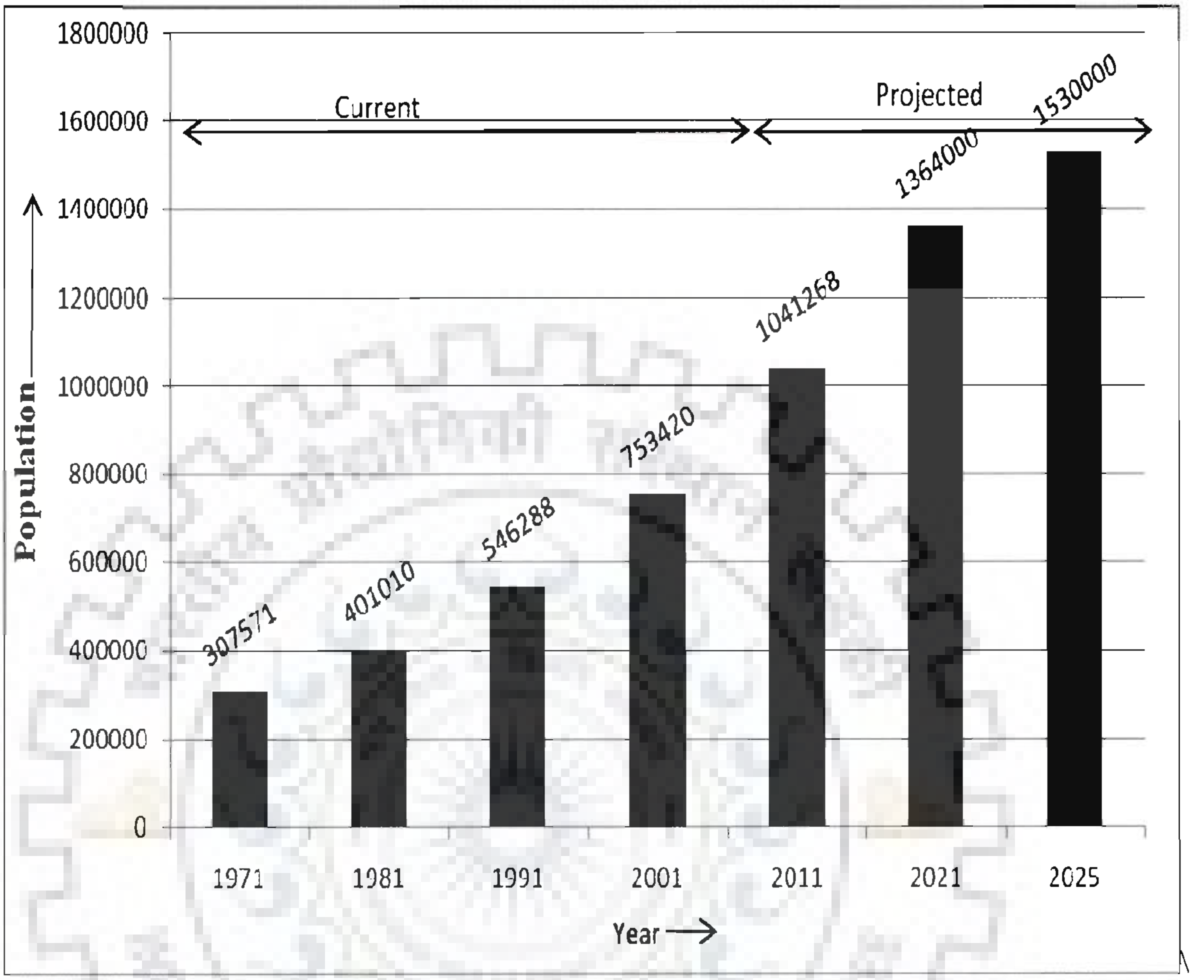

Figure 3.3: Demography of study area I

3.2.3 Major functions of the city

The major functions of Dehradun city are,

a) *Administrative*: Dehradun is the capital of Uttarakhand State, with the State Government functioning from here.

b) *Educational and Institutional:* Dehradun has several national level research institutes viz. Forest Research Institute, Indian Institute of Himalayan Geology, Wild Life Institute, Indian Institute of Remote Sensing and many others. A number of colleges and technical institutes are also located in the city.

c) *Commercial:* Dehradun is a clearing place for goods exported for the hill areas of the district and also for those imported from these areas. The trade of the city has followed two main channels: one between valley and plain and other between the valley and hills. After becoming capital of the State, the commercial activities have gained momentum. Dehradun is now considered as one of the largest service centre within the hilly region of Uttarakhand state.

d) *Industrial:* Dehradun has a number of industries that include information technology, biotechnology, agro based and food processing industry, floriculture and industry based on herbs and medicinal plants. In addition, tea and forest product industries also have potential of further evolution.

e) *Tourism:* As Dehradun is located in the picturesque Doon valley, it is endowed with immense importance as a place of tourist attraction. There are number of places and recreational spots within short distance from the city center. Dehradun is also a gateway to the hill stations located in the lower Himalayas.

f) *Defense:* Dehradun also occupies a strategic location in terms of military establishment of the country. A number of defense organisations viz. Indian Military Academy, Doon Cantonment, Clement town Cantonment, Ordinance Factory, Indo-Tibet border police, the President's body-guard offices etc., are located in the city.

3.3 Study area II: Saharanpur city

3.3.1 Physical setting

Saharanpur city is located in the fertile tract of Upper Ganga-Yamuna daob (tract of land between two confluent rivers) in the western part of Uttar Pradesh State (India). The city is a district headquarters and is well connected by several roads and railways transport to other important cities. Thus, the city in its regional setting also has a very significant place as a transport node. The city besides being a major market of food grains also acts as a service centre for the surrounding hinterland, as it provides education and medical facilities. The present city is bisected into two parts by a railway line. The old city area is located in the northern part, where most of the commercial facilities are located (Figure 3.4). Lately, due to the emergence of several industries (e.g., paper, strawboard, tobacco), the city has lost its agrarian fabric and, therefore, growing numbers of its labour force is presently employed in the secondary and tertiary sectors. The development of industry and services is attracting migrants not only from the city's hinterland but also from further away far areas. As a result, the city is expanding rapidly, onto the nearby surrounding fertile agricultural lands (Subudhi, 1998; Fazal, 2000). The study area II consists of Saharanpur city and its surroundings areas. The study area encompasses the geographical extents, 29°55' N to 30°0' N latitude and 77°30' E to 77°35' E longitude and covers a total area of about 80 km^2.

3.3.2 Demography

From the analysis of decadal population, it is evident that the city had a constant rate of population growth (Figure 3.5). The growth rate is 31.04% in 1971-81, 25.59% in 1981-1991 and 25.64% in 1991-2001 time periods. The Town and Country Planning department has projected the future population on a decadal basis (Figure 3.5) and plans to develop the area with a gross density of 140 persons per hectare (Town and Country Planning Department, 2001). According to 2001 census, 60% of the workforce is engaged in tertiary sector, 36% in secondary sector and 4% in primary sector, thus highlighting its role as a commercial and service centre in the region.

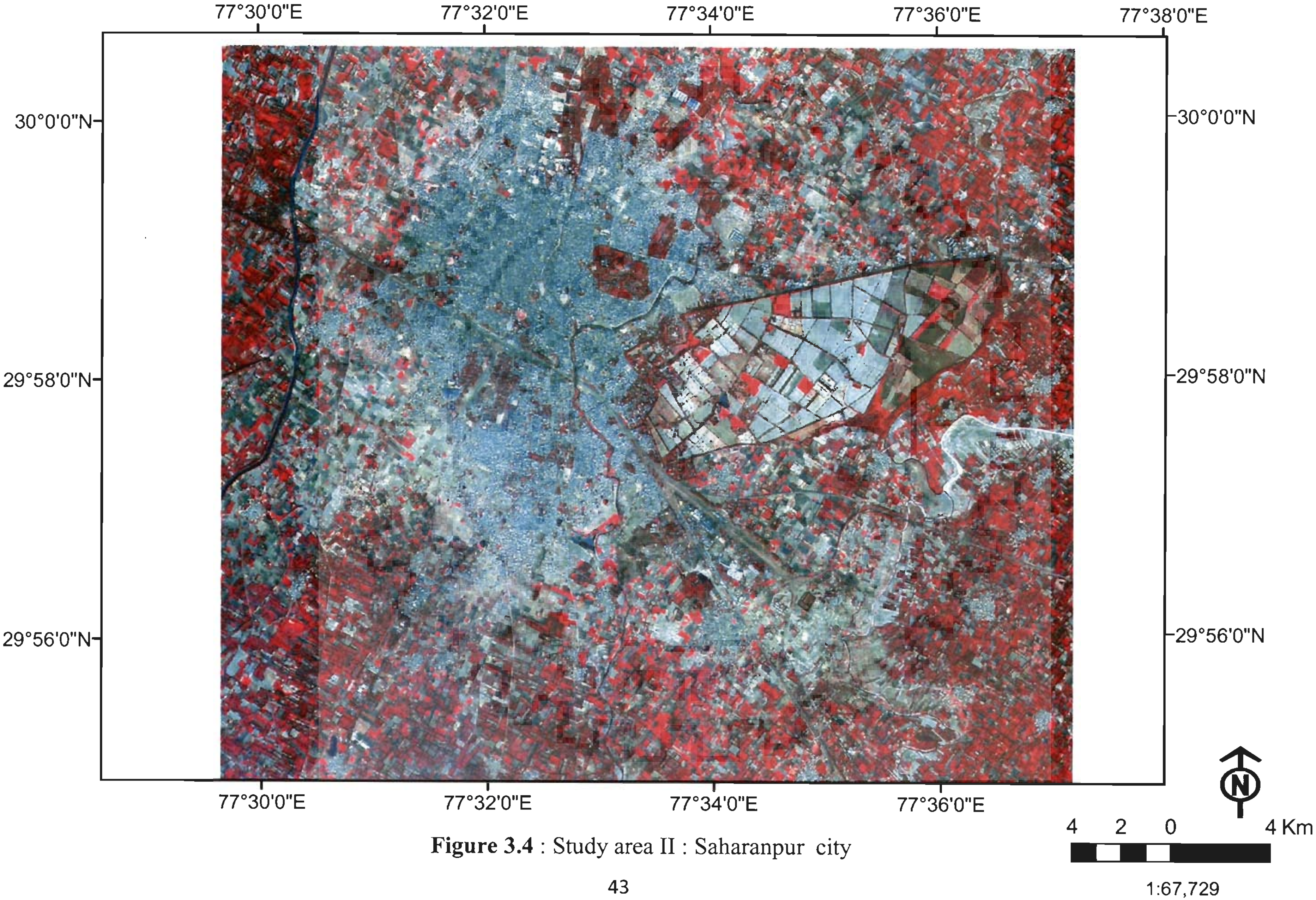

Figure 3.4 : Study area II : Saharanpur city

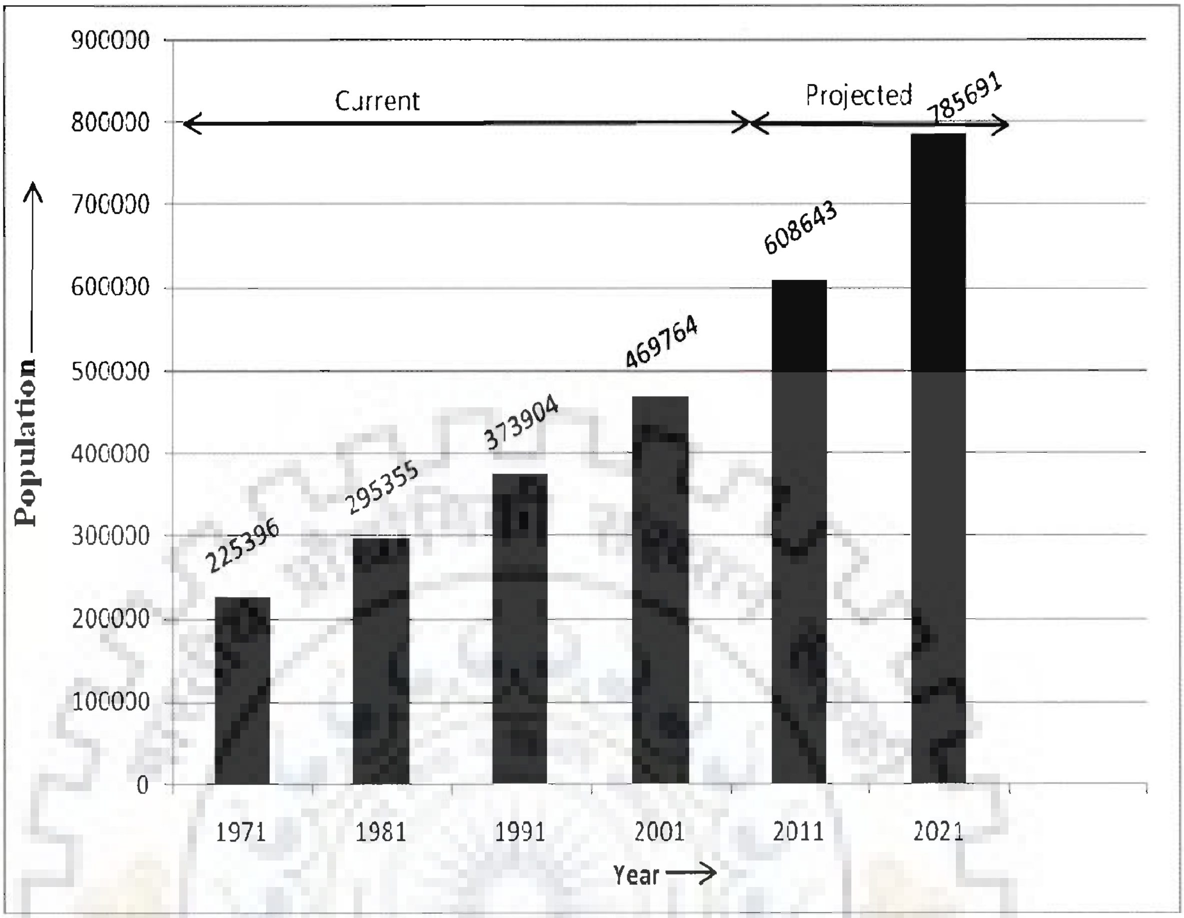

Figure 3.5: Demography of study area II

3.3.3 Major functions of the city

The major functions of the city are,

a) *Commercial:* Saharanpur is a leading commercial centre for its surrounding hinterland. It has a big wholesale market for various agro based products like rice, maize, groundnuts etc. It also provides other higher level economic and other services such as banking, agricultural equipments etc. to the surrounding areas.

b) *Industrial:* Saharanpur city is also important for its agro-based industries. The city has various small scale industries such wood carving, hosiery etc. These household industries also play an important role in defining the economic structure of the city.

c) *Transport:* The development of Saharanpur is highly attributed to its transport facilities. The city is also an important junction for traffic plying on various National and State highways, besides it is well connected by railways to the other parts of the country.

d) *Educational:* A number of colleges and technical institute's viz. horticulture research institute, pulp and paper technology department of IIT Roorkee are also located in the city.

3.4 Generation of spatial database

3.4.1 Software used

For the preparation of spatial databases, two key software namely ERDAS Imagine image processing software and ArcGIS software have been used. While ERDAS software has been mainly used for image geo-referencing, registration and classification operations, ArcGIS software is used for all GIS related operations.

3.4.2 Study Area I

3.4.2.1 Data sources used for creating spatial database

For analyzing the growth trend in study area I, maps depicting the built-up and non built-up area for years 1997, 2001 and 2005, have been produced from the remote sensing data acquired by sensors onboard Indian Remote Sensing (IRS) 1C/1D satellite. Table 3.1 lists the spatial and spectral resolutions and date of acquisition of the remote sensing data used. The topographical maps, as listed in the Table 3.1, have been used for image geo-referencing and as a reference data. Figure 3.6 shows the standard false colour composite (FCC) of the study area generated from green, red and near infrared bands of LISS-III sensor. The different tones of red color denote vegetation cover. Cyan colour with rough texture represents built-up area. The dry river beds have dark blue to cyan tone, and a smooth texture. The fallow land appears in greenish grey tone with smooth texture. The bare soil having no vegetation appears in bright white tone.

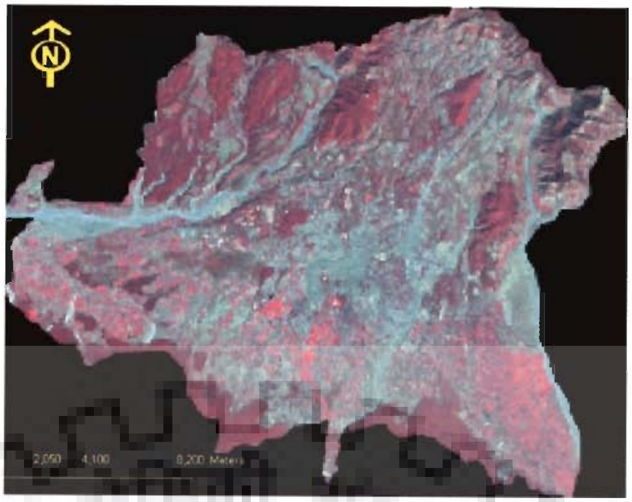

(a)

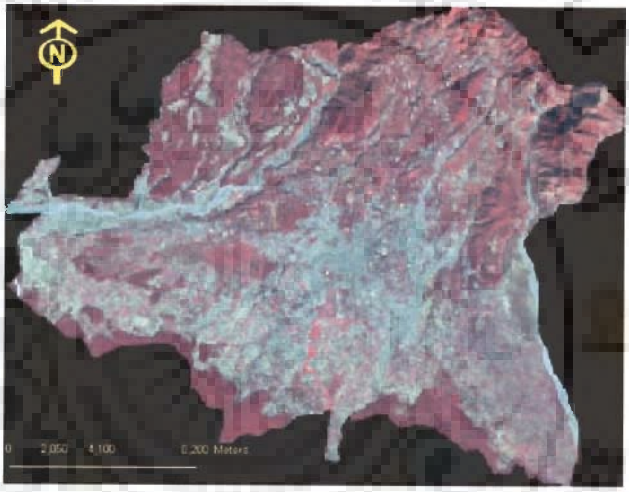

(b)

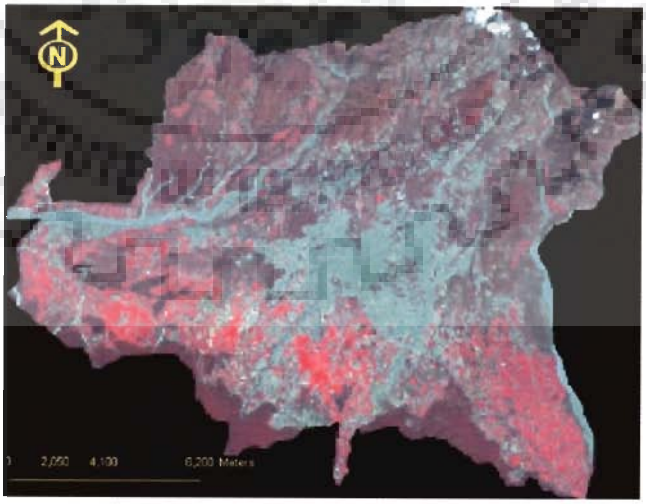

(c)

Figure 3.6: LISS III standard FCC of study area I :
(a) LISS III standard FCC of 11-2-1997
(b) LISS III standard FCC of 23-12-2001
(c) LISS III standard FCC of 13-3-2005

Table 3.1: Characteristics of remote sensing data and other data used for study area I

Satellite/Other data used	Sensor	Date of Acquisition
IRS -1C	LISS-III (Spatial resolution: 23.5 meters) operating in four bands(Green : 0.52-0.59μm, Red: 0.62-0.68μm, Near infra red: 0.77-0.86μm, Sort wave infra red: 1.55μm-1.77μm)	13-3-2005 23-12-2001 11-2-1997
IRS-1C	PAN (Spatial resolution: 5.8 meters), operating in single band 0.5-0.75 μm	14 -3- 1997 10 -10- 2001
IRS-P6	LISS-IV (Spatial resolution: 5.8 meters) operating in three bands(Green : 0.52-0.59μm, Red: 0.62-0.68μm, Near infra red: 0.77-0.86μm)	4-4-2005
Topographic maps	Sheet number: 53J/3and 53F/15 at 1:50,000 scale	1965-66
Guide map	1:20,000 scale	1968
Master plan of Dehradun for year 2025	1:20,000 scale	2005

3.4.2.2 Pre-processing of remote sensing data

For analyzing urban growth, the maps depicting the built-up/non built-up areas for years 1997, 2001 and 2005, must be accurately registered with each other. This, image to image registration of images of these years is pre-requisite, since the built-up/non built-up areas maps are derived from these images only. The LISS-III image of year 2005 is first geo-referenced to a topographical map using 28 well distributed ground control points (GCP). The GCP consists of road intersections and other distinct well defined and prominent features which could be identified in both image and topographical sheet. The registration has been performed to a sub pixel accuracy using first order polynomial transformation and the image has been resampled using nearest neighbor technique. The images of years 1997 and 2001 have then been registered to the georeferenced LISS-III image of 2005, using 35 and 30 GCP respectively. The root mean square error (RMSE) obtained is 0.09 and 0.11 pixels for 1997 and 2001 respectively.

3.4.2.3 Generation of maps showing built-up / non built-up areas

The built-up/non built-up maps have been produced from classification of LISS-III images of year 1997, 2001 and 2005 using the maximum likelihood classifier (MLC). The MLC is a parametric supervised classification algorithm. The various steps involved in the classification process are,

i) Classification system

The present study is based on the dichotomy of built-up and non built-up classes. Built-up class has been defined as land covered by structures and other impervious material. The non built-up class consists of fallow land, scrubland, agricultural and bare soil classes (Anderson *et al.*, 1976; Gautam, 1976; Kasetkasem *et al.*, 2005; Mundia and Aniya, 2005). The description of these classes along with their characteristics on the LISS-III imageries is discussed in Table 3.2 (Lillesand and Kiefer, 2000). After the classification of images into these classes, the classes have been merged into one class, i.e., non built-up.

Table 3.2: Characteristics of various land cover classes

Class attributes	Class name	Definition	Characteristic on LISS III standard FCC
1	Built-up	Land covered by structures, having block like appearance.	Cyan, bright and dull
2	Non Built-up	Non Built-up class includes the following sub classes (i.e., subclasses with attributes 21,22,23 and 24)	
21	Fallow land	Agricultural land presently lying vacant	Greenish grey with smooth texture
22	Scrubland	Land having sparse vegetation	Dull red to pink
23	Agricultural	Land used primarily for production of food and fiber.	Dull red and smooth appearance
24	Bare-soil	Land having thin soil, sand or rocks. Vegetation if any is scrubby.	Bright whitish

ii) Formation of training datasets

The MLC algorithm uses the statistical parameters derived from the training data to classify the remote sensing image into various classes. Thus, in order to obtain higher classification accuracy, the training data should be representative of the respective classes and should be collected from relative homogenous areas.

The quality of a training dataset can be analyzed by its histogram plots. A unimodal histogram following a normal distribution is representative of pure training dataset, while multimodal histograms indicate the presence of two or more classes in the dataset (Arora, 2002). Since the generation of training data set is a tedious process, therefore its size should be kept small. However, it should be large enough for accurate determination of various statistical parameters that are required by the classification algorithm. As a rule of thumb, in a training dataset, the number of training samples for each class may be 30n (Mather, 1999) where n is the number of spectral bands of remote sensing image. In this study, LISS-III data having four bands is being used, thus the minimum number of training samples in each class in the training dataset has been kept as 120 (Table 3.3). The histogram plots of the training dataset for each class, generated from 1997, 2001 and 2005 images have been found to be unimodal.

Table 3.3: Number of training pixels used in classification for each class

Remote sensing image → / Land cover classes ↓	1997 image	2001 image	2005 image
Built- up	160	184	156
Bare soil	130	162	157
Agricultural	174	195	152
Fallow land	157	152	142
Scrubland	157	141	178

iii) Separability analysis

Separability analysis is mostly performed on the training dataset in order to identify the combination of bands that is most effective in discriminating each class from all others. The aim is to remove the bands that provide redundant spectral information while retaining the maximum class separability, thereby reducing the dimensionality of dataset and processing time.

To find the band combination that gives maximum class separability. Transformed Divergence (TD), (Jensen, 1986) has been used in this study. The Transformed Divergence (TD) values range from 0-2000. A TD value of 2000 indicates excellent class separability, above 1900 provides good separability while values below 1700 are considered as poor. The band combinations which have yielded maximum TD values for the 1997, 2001 and 2005 images are shown in Table 3.4. These band combinations have then been used for classifying the LISS III images using MLC.

Table 3.4: Best band combinations and their average Transformed divergence (TD) values

Band 1 Green: 0.52-0.59μm; *Band 2* Red: 0.62-0.68μm
Band 3 NIR: 0.77-0.86μm; *Band 4* SWIR: 1.55μm-1.77μm

Year	Band combinations	Average TD
1997	1,3,4	2000
2001	1,3,4	1998
2005	2,3,4	2000

iv) Image classification

The best band combinations as of, the LISS III images of the three years have been classified using the maximum likelihood classification (MLC) algorithm. The MLC is based on the probability density function associated with a particular training data signature. Pixels are assigned to the most likely class based on a comparison of the posterior probability of each class. The image has thus been classified into one class of built-up and 4 classes of non built-up area. The later classes have then been merged into non built-up class. The maps thus produced show the built-up and non built-up class for years 1997, 2001 and 2005 and are shown in Figure 3.7, 3.8 and 3.9 respectively. These maps also show exclusionary areas which include restricted areas, reserved forests, water bodies, public grounds and gardens, these areas do not have any development potential. Mask corresponding to these areas have been generated using the survey of India topographical maps, guide map and Dehradun master plan (Figure 3.10) and these areas were masked before the classification.

v) Accuracy assessment

In order to determine the accuracy of classification, testing samples are collected from the classified image, which are compared with the corresponding samples on the ground or reference data. In this study the PAN and LISS-IV images providing data of higher spatial resolution than the LISS III image have been used as a reference data. The class attributes of testing data as observed on classified image and reference data are cross tabulated in the form of an error matrix. An error matrix is a square matrix of *n*x*n* dimensions, where *n* refers to the number of classes. The column represents the reference data, while the rows refer to the classified image. From this matrix, the overall accuracy is obtained, by dividing the number of correctly classified samples, along the diagonal by the total number of samples. The choice of a suitable sampling scheme and the determination of an appropriate sample size, plays an important role in determining the appropriate testing sample data (Arora and Agarwal, 2002). As a rule of thumb, the number of testing samples selected per class for accuracy assessment is 50, which can be increased to 75-100 when the study area is large or the numbers of classes are large (Congalton, 1991; Congalton and Green, 1999).

A stratified random sampling has been used here to select 100 testing pixels each from the built and non built-up classes. The overall accuracy for the three classified images of 1997, 2001 and 2005 have been found to be are 94%, 90.5% and 93% respectively, which are more than the minimum accuracy criteria of 85% overall accuracy as recommended by Anderson *et al.* (1976).

3.4.2.4 Generation of road network map

The road network has been derived from LISS III 1997 remote sensing data through visual image interpretation. The PAN data and the guide map of Dehradun have been used as data sources. The road network has not undergone any major modification during the period 1997-2005. Therefore the same road network has been used for 1997-2001 and 2001-2005 period. As can be seen from the map of road network (Figure 3.11), the road network is radial in nature, with the roads radiating outwards from the city core. These radiating roads are interconnected to each other by a network of roads.

3.4.2.5 Delineation of city core

The city core has been defined as that part of the city where most of the higher level facilities are located. In Dehradun study area, the city core has been identified after consultation with the local planning authorities (Figure 3.11). The city core consists mainly of the old portions of the city, which have formed the nucleus around which the city has grown. The master plan of 2005-2025 also proposes to further develop the economic activities in this city core area.

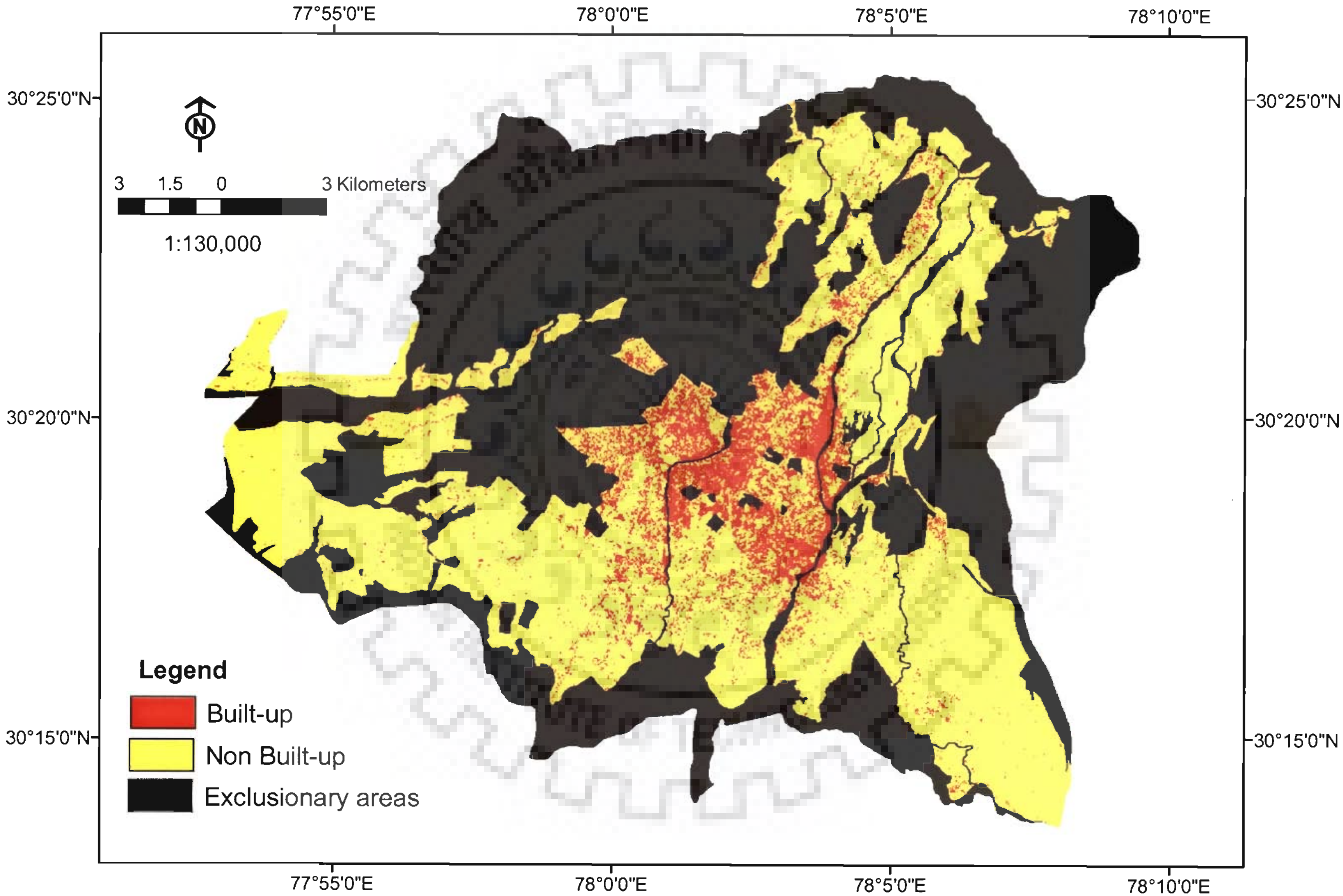

Figure 3.7: Built-up/ non built-up areas in year 1997 (study area I)

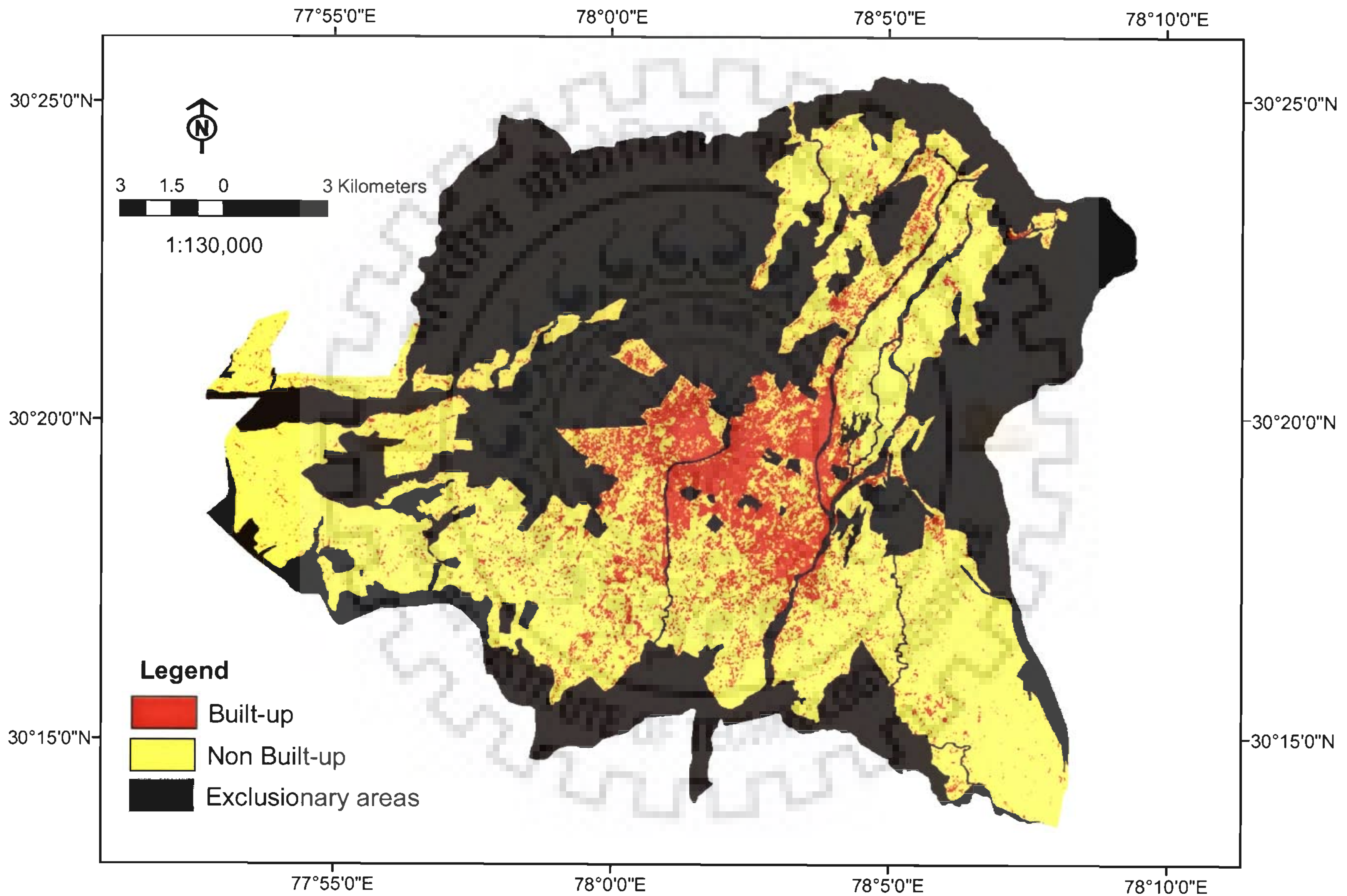

Figure 3.8: Built-up/ non built-up areas in year 2001 (study area I)

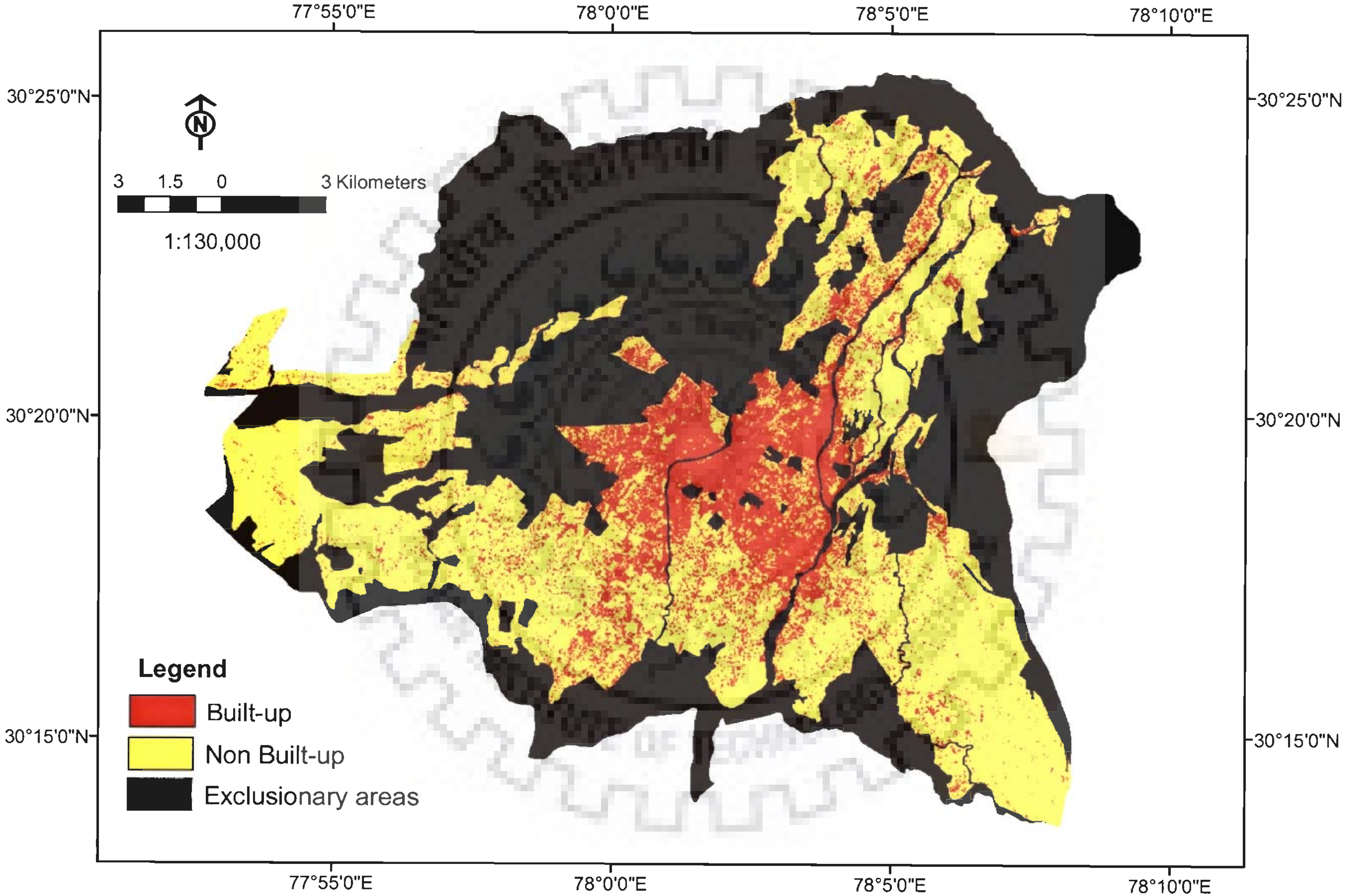

Figure 3.9: Built-up/ non built-up areas in year 2005 (study area I)

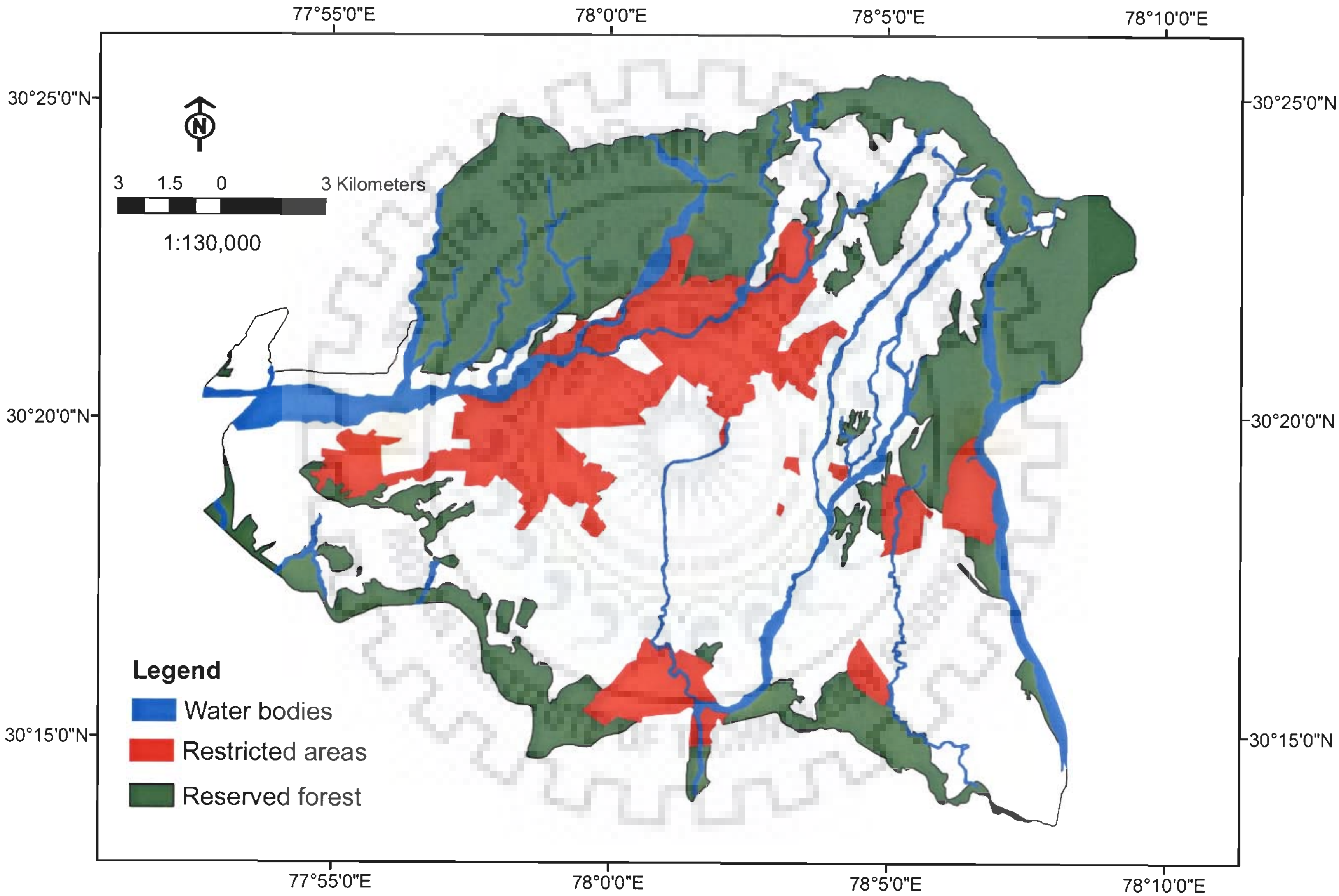

Figure 3.10: Exclusionary areas (study area I)

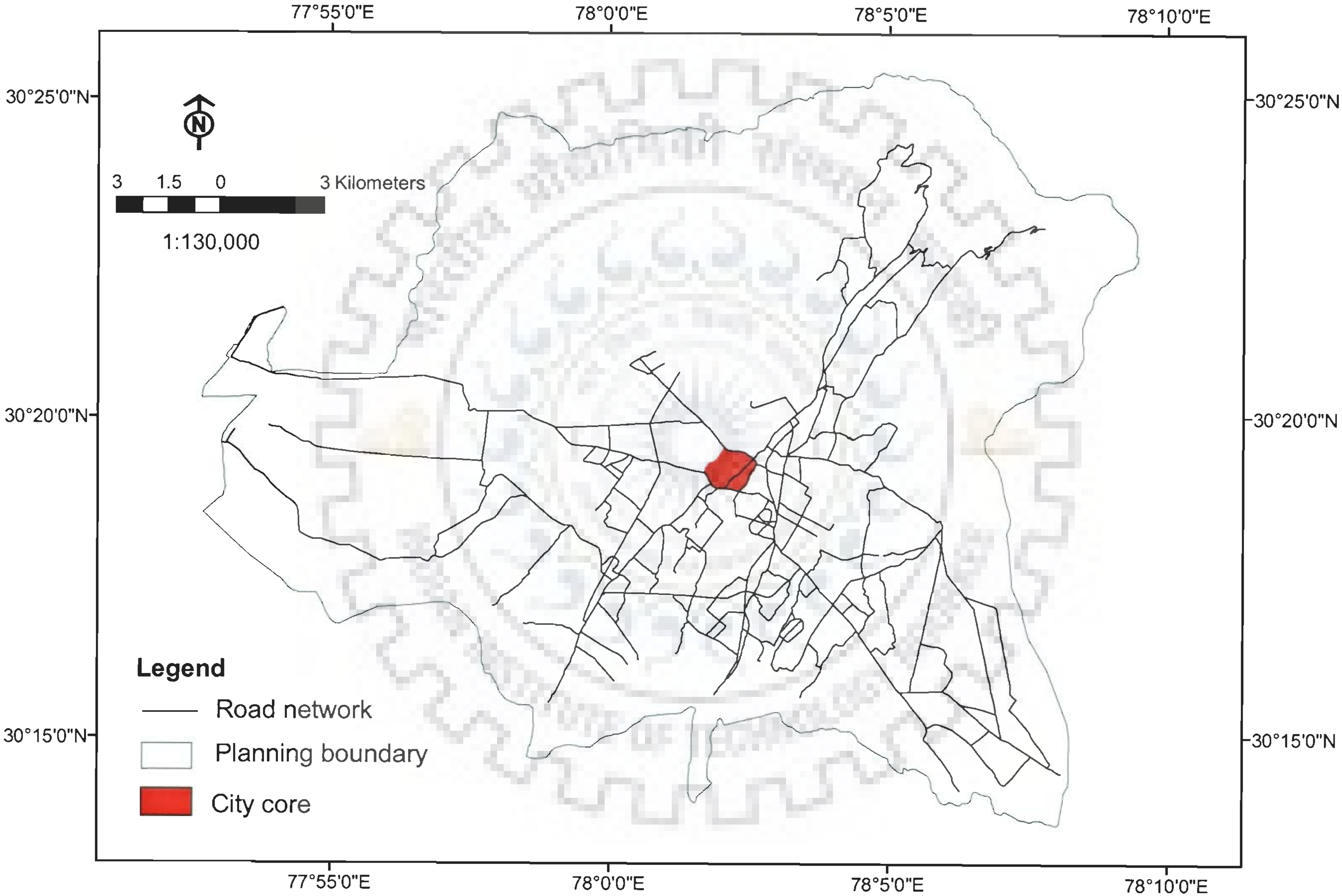

Figure 3.11: Road network and city core (study area I)

3.4.3 Study area II

3.4.3.1 Data Sources used for creating spatial database

Data used to produce the built-up/non built-up area maps of years 1993 and 2001 consisted of aerial photographs and remote sensing data acquired Indian Remote Sensing IRS 1C PAN sensor. Table 3.5 lists the scale and date of acquisition of the aerial photographs and the remote sensing data. Both the data products are panchromatic, so the built-up area has a blocky appearance with light tone. The vegetated areas have light to dark tone with rough texture. Bare soil has very light tone, while the water bodies have a dark tone.

The topographical map has been used for extraction of control points for geometric registration of the maps. The guide map and master plan have been used as a reference data, during the creation of different maps.

Table 3.5: Data products used for study area II

Data product	Scale	Date of Acquisition
Aerial Photograph in analogue form	1:10,000	1993
IRS-1C PAN data in analogue form (Spatial resolution: 5.8 meters, operating in single band 0.5-0.75 μm)	1:12,500	3-11-2001
Topographic maps	Sheet number 53G/9 at 1:50,000 scale	1965-66
Guide map of Saharanpur	1:20,000	1982
Master plan of Saharanpur for year 2021	1:20,000	2001

3.4.3.2 Generation of maps showing built-up / non built-up areas

Maps depicting the, built-up/non built-up for year 1993 and 2001 are prepared by visual image interpretation of the aerial photographs and IRS-1C PAN image (Figure 3.12 and 3.13 respectively). These maps are then scanned to convert them to digital format. In order to ensure a proper overlay between the two maps, the two maps are registered to each other. Firstly, 30 ground control points (GCP) well distributed across the 1993 map and also present in the topographical map are selected. Using these GCP, the 1993 map is georeferenced to the topographical map using first order polynomial transformation, resulting in a RMSE of less than half a pixel. The 2001 map is then registered to the geoferenced 1993 built-up/ non built-up areas map using 25 GCP and the RMSE obtained is 0.14 pixels.

The overall accuracy of these 1993 and 2001 year maps prepared by visual interpretation is 93% and 91% respectively. The restricted areas and water bodies have been treated as exclusionary zones. Mask corresponding to these areas have been generated based on Survey of India topographical map, guide map and Saharanpur master plan (Figure 3.14).

3.4.3.3 Generation of road network map

The road network map has been generated by visual image interpretation of 1993 aerial photographs (Figure 3.15). The guide map and master plan of Saharanpur city have also been used as data sources.

3.4.3.4 Delineation of city core

After consultation with the local planning authorities, the city core has been demarcated (Figure 3.15). Most of the commercial and institution facilities in Saharanpur city are located in the city core. This area constitutes the old part of the city and has a very high built-up area and population density. The city originates from here, and slowly spreads in the south and west directions.

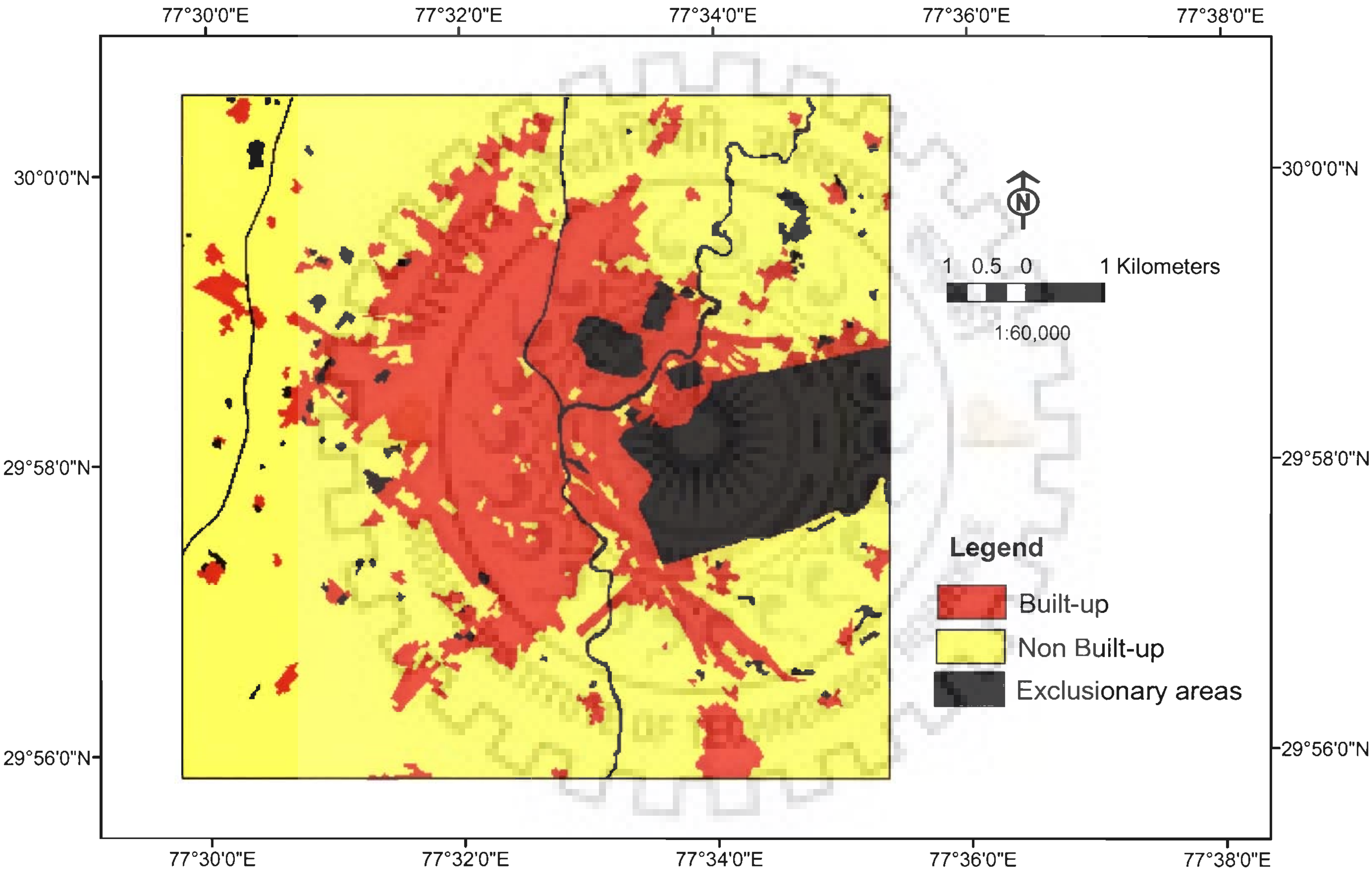

Figure 3.12: Built-up/ non built-up areas in year 1993 (study area II)

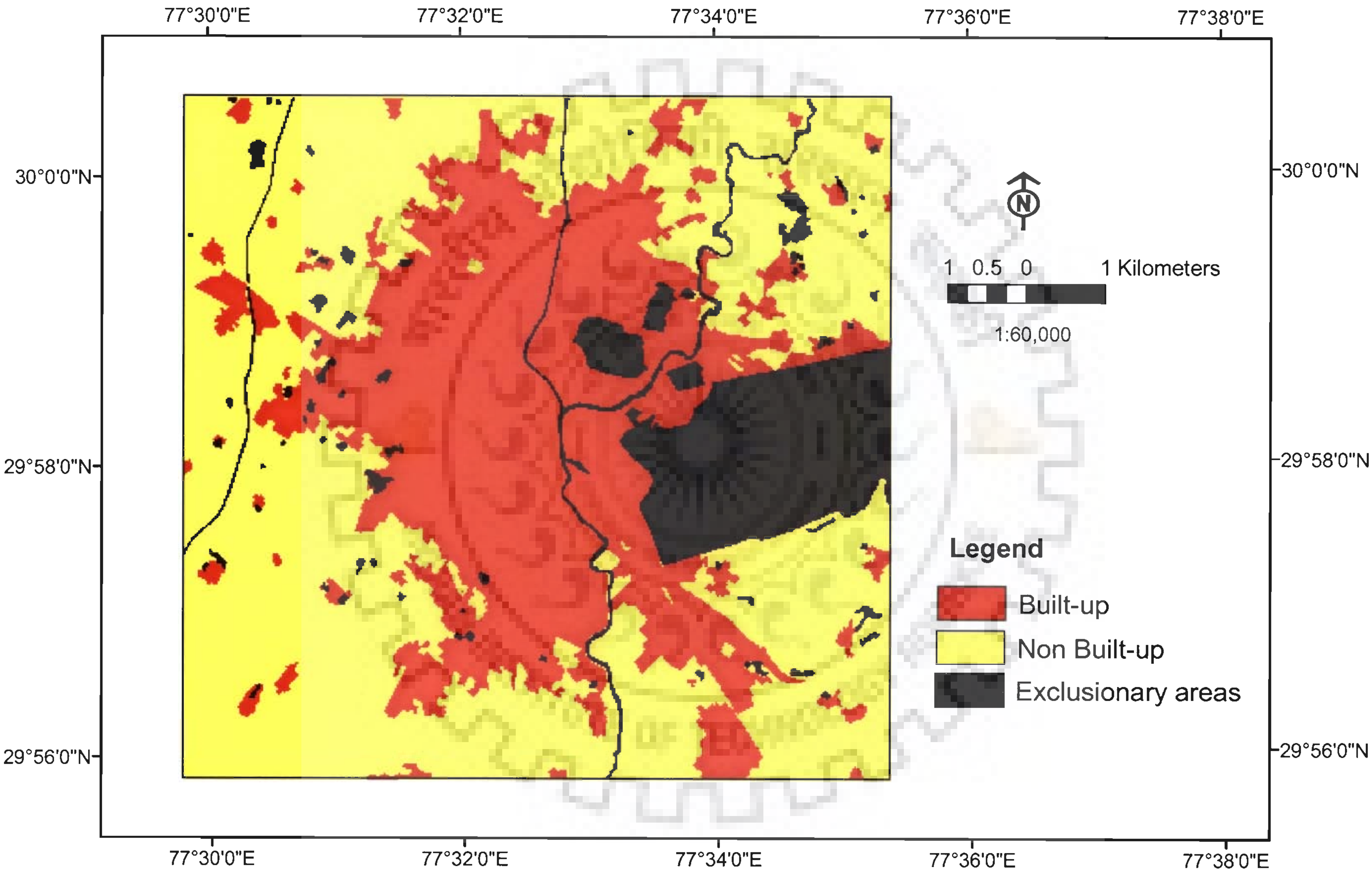

Figure 3.13: Built-up/ non built-up areas in year 2001(study area II)

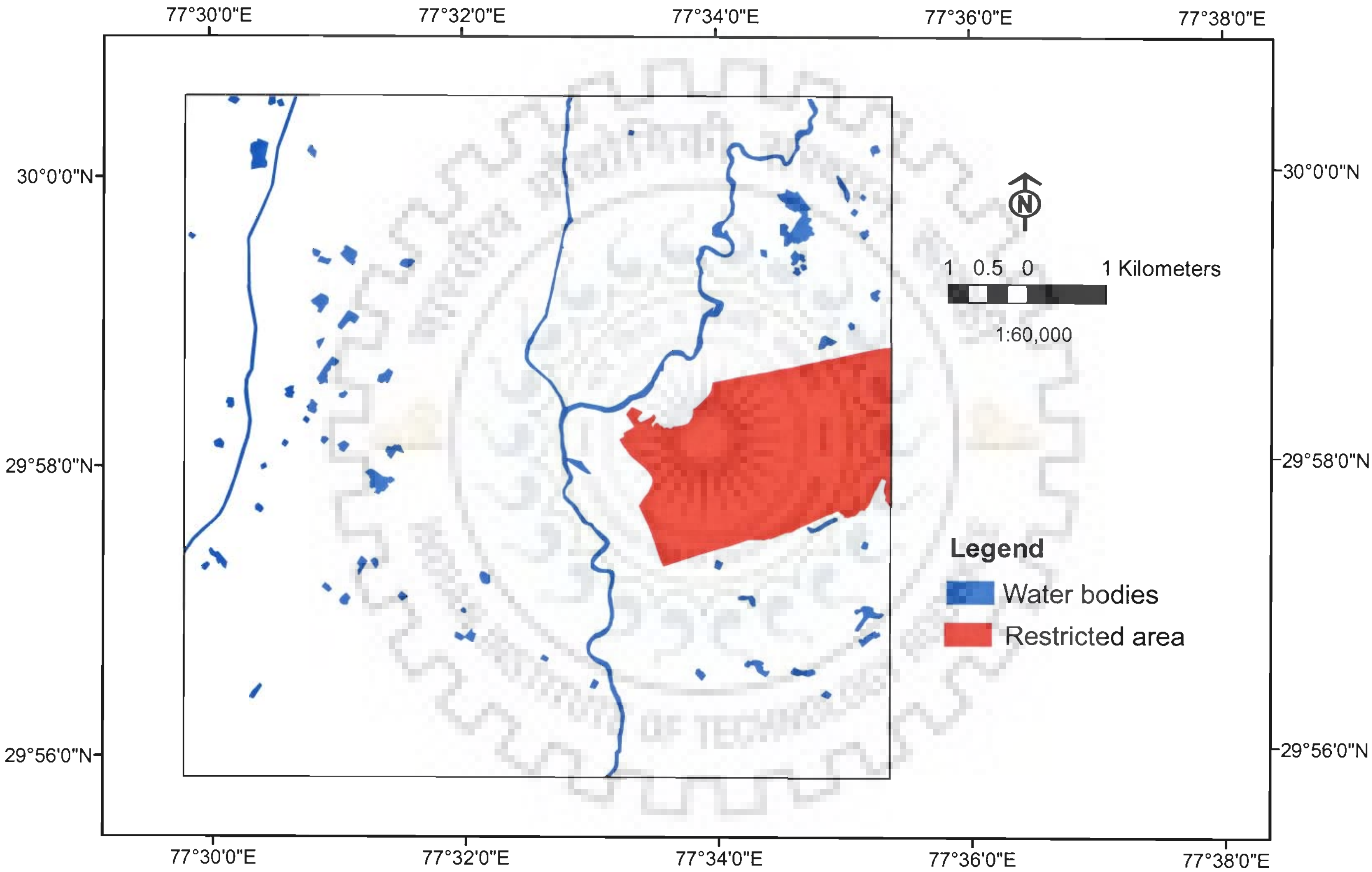

Figure 3.14: Exclusionary areas (study area II)

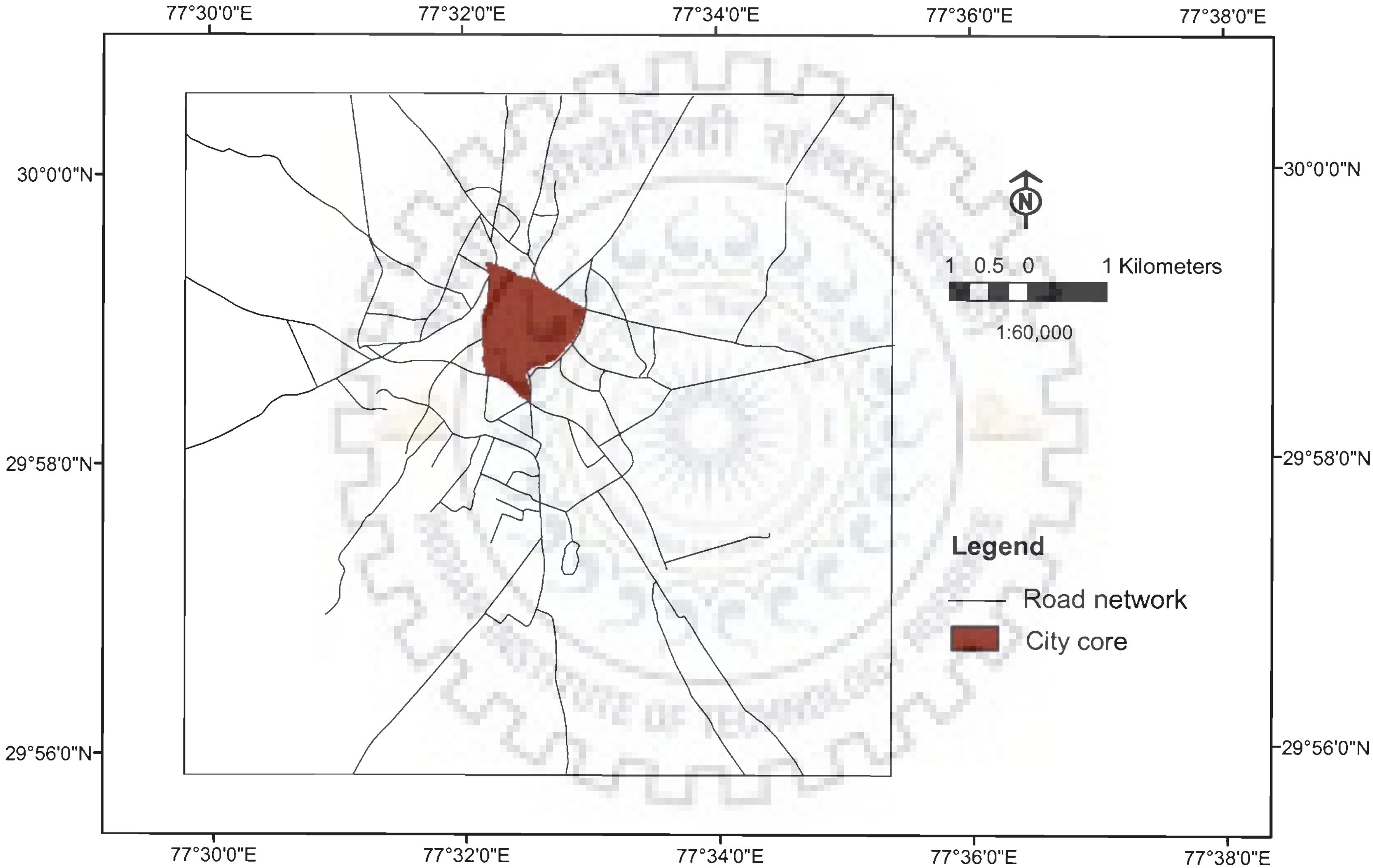

Figure 3.15: Road network and city core (study area II)

3.5 Analysis of urban growth trend

3.5.1 Study area I

As discussed in chapter one, urban growth has been quantified in terms of increase in the built-up area over a period of time .Thus, maps depicting built-up and non built-up area for years 1997, 2001 and 2005 have been prepared for monitoring the urban growth. The growth analysis for the two time periods 1997-2001 and 2001-2005 has been carried out in a GIS environment using overlay operation (Figures 3.16 and 3.17). The overlay analysis shows that during 1997-2001, the increase in built up area is 797 hectares and in 2001-2005 it is 1108 hectares respectively. The boundary of the planning area mainly in the north, east and south directions is hilly and covered with reserved forests, thereby restricting any growth. Large area of land is also occupied by defense establishments in the west, north-west, east and south directions. The tea plantation in the west also occupies a large tract of land. Due to these constraints, the city has not been able to grow in a compact and continuous manner, with growth taking place in a scattered manner mainly in pockets. The existing trend of physical development indicates that the city may expand in the south-east and south-west directions, where the terrain is flat, level of accessibility is good and not many constraints are there.

The growth pattern has also been analyzed in terms of distance from road network and city core. After consultation with the local planning authorities and based on field knowledge, different buffer zones have been created around the roads and city core (Tables 3.6 and 3.7), and have been overlaid with the growth maps of 1997-2001 and 2001-2005.

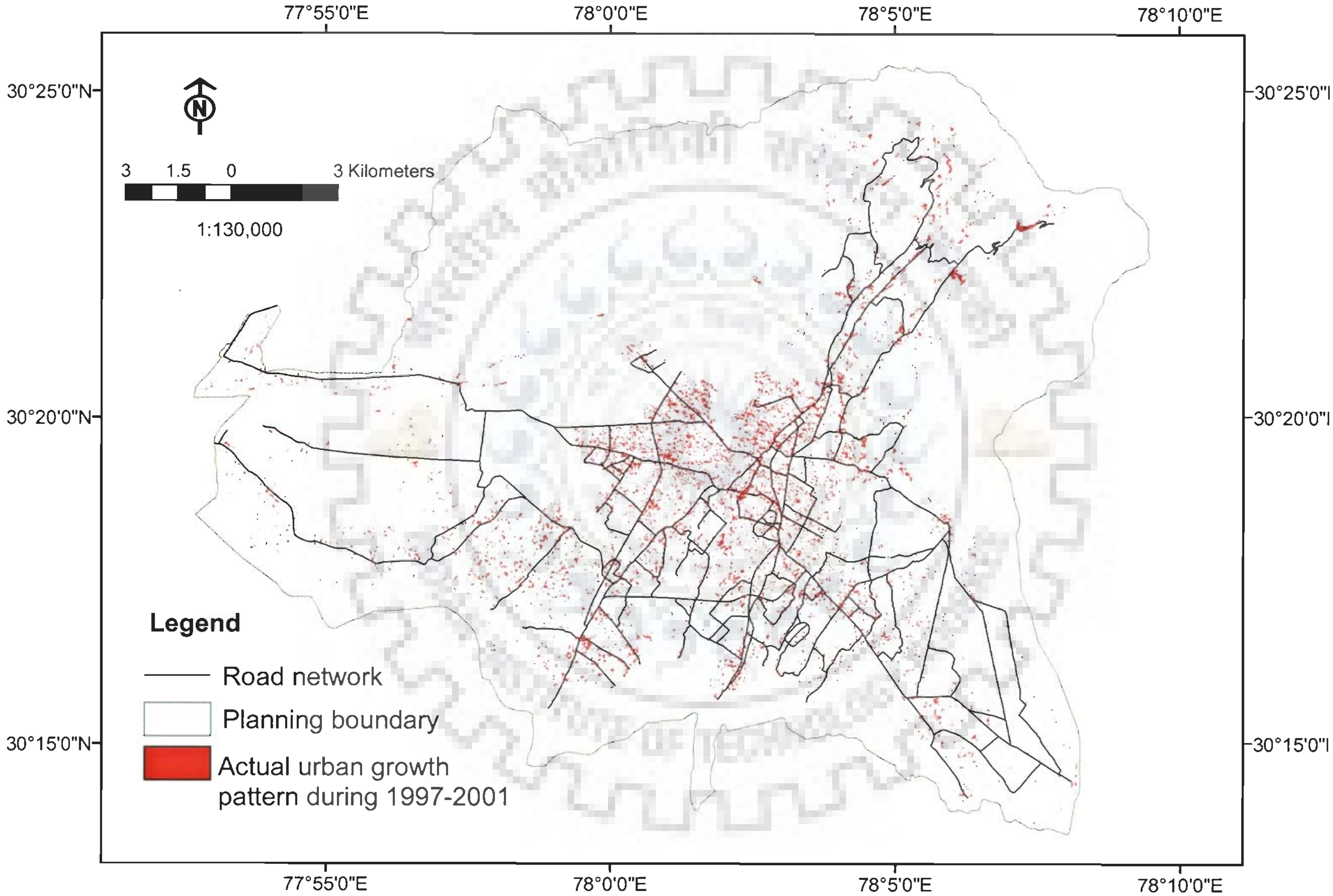

Figure 3.16: Urban growth pattern during 1997-2001 (study area I)

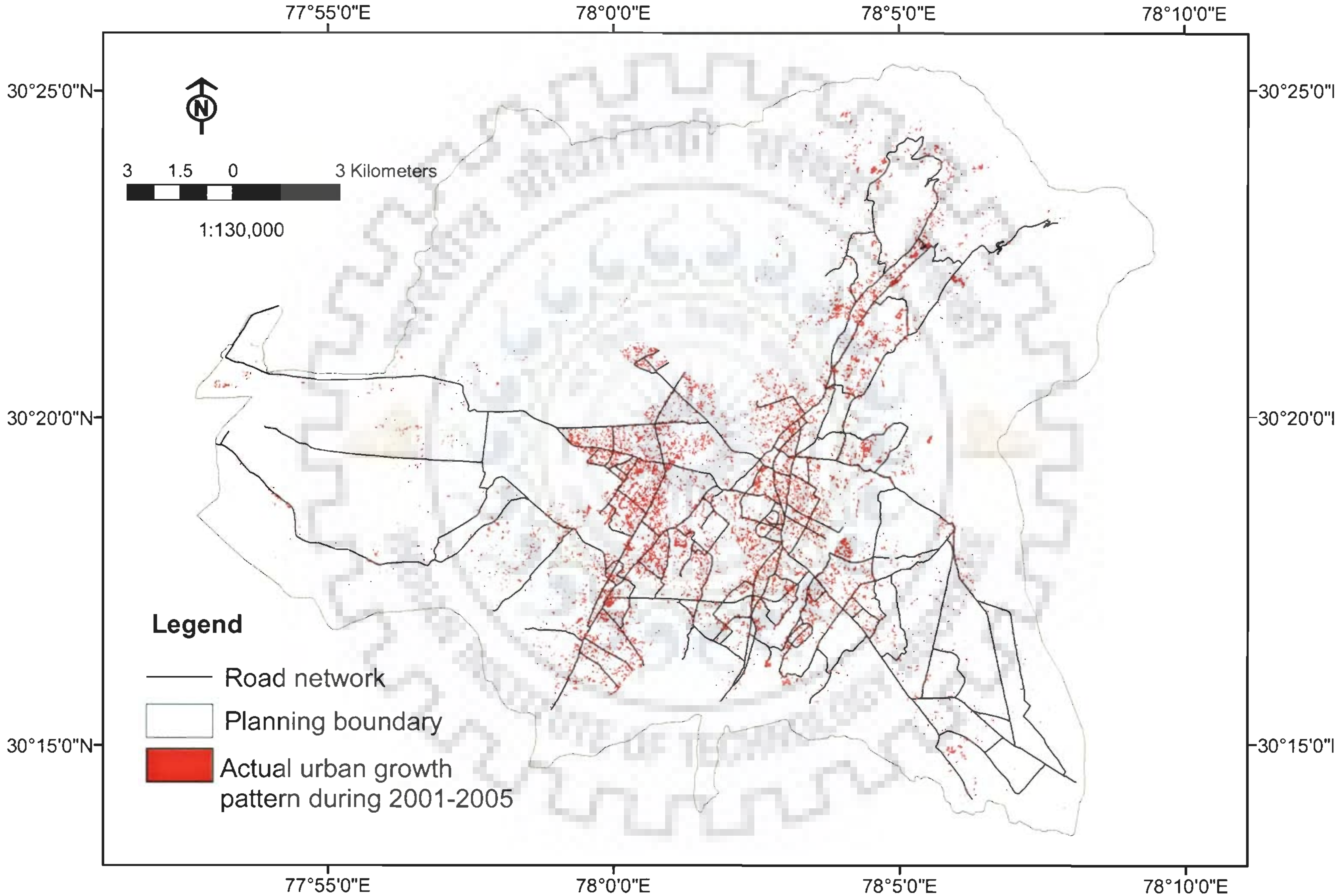

Figure 3.17: Urban growth pattern during 2001-2005 (study area I)

Table 3.6: Buffer zones with respect to roads

Zones	Distance from Roads (in meters)
I	0-200
II	200-400
III	400-800
IV	800-1600
V	>1600

Table 3.7: Buffer zones with respect to city core

Zones	Distance from city core (in meters)
I	0-1000
II	1000-2000
III	2000-3000
IV	3000-4000
V	>4000

a) Growth patterns with respect to roads

A study of Table 3.8 shows that in 1997-2001, 62.4%, of the total urban growth has taken place within zone I, which increased to 68.5% in 2001-2005. The growth in zone II remains the same, i.e., 21%. However, in zone III, the growth has decreased from 13% in 1997-2001 to 8.6% in 2001-2005. Thus, 83% of the total growth in 1997-2001 and 89% of the total growth in 2001-2005 has taken place within a distance of 400 meters from the roads. This highlights the importance of road accessibility in the growth process of the study area I.

Table 3.8: Percentage of growth in different distance zones from existing roads (study area I)

Zones	Distance from Roads (in meters)	% of Total Growth (1997 -2001)	% of Total Growth (2001-2005)
I	0-200	62.4	68.5
II	200-400	21.1	20.5
III	400-800	13.0	8.6
IV	800-1600	3.2	2.0
V	>1600	0.3	0.4

b) Growth with respect to city core

The urban growth during 2001-2005 in zone I is 8%, as compared to 13.4 % in 1997-2001 (Table 3.9). The total growth in Zone II, III and IV has increased to 54% in 2001-2005 from

43% in 1997-2001.Thus, distance from city core is also a important factor affecting the growth process in zone I.

Table 3.9: Percentage of growth in different distance zones from city core (study area I)

Zones	Distance from City Core (in meters)	% of Total Growth (1997 -2001)	% of Total Growth (2001-2005)
I	0-1000	13.4	8.0
II	1000-2000	16.6	18.0
III	2000-3000	16.2	19.7
IV	3000-4000	9.7	16.2
V	>4000	44.1	38.1

3.5.2 Study area II

The urban growth of Saharanpur has been analyzed for the period 1993 to 2001 (Figure 3.18), using maps depicting built-up/ non built-up areas for year 1993 and 2001. Results show that 630 hectares of land has changed from non built–up to built–up during the 1993-2001 period. This growth has taken place in the form of infilling of vacant areas and outgrowth from already built–up area in 1993. In the absence of any natural constraints, the city has grown in a concentric compact pattern, mainly along the roads and in contiguity of already built-up areas. Due to the presence of defense establishment, i.e., Remount Depot, in the east direction, the growth has been restricted in this direction. The growth pattern has also been analyzed with respect to distance from roads and distance from city core.

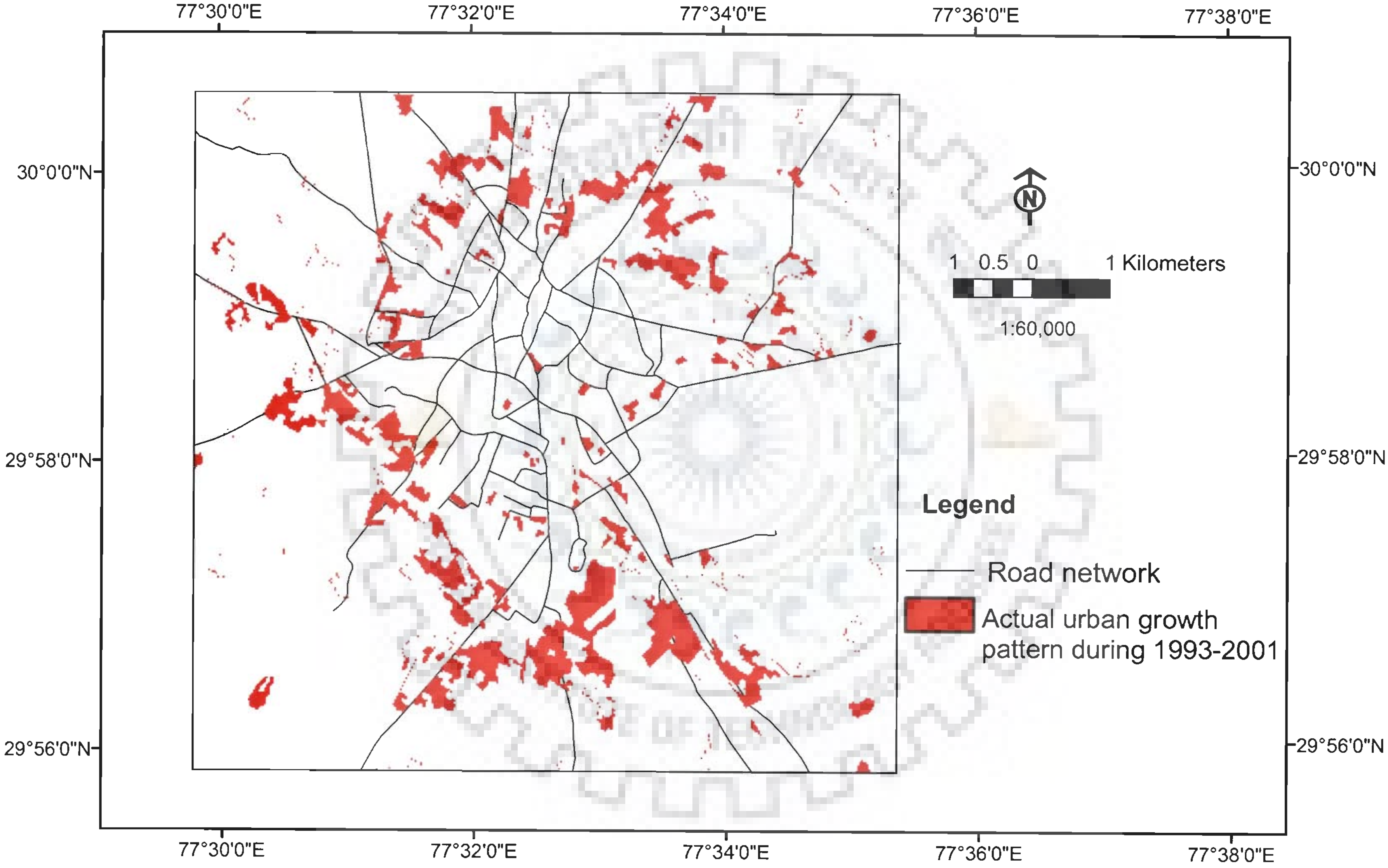

Figure 3.18: Urban growth during 1993-2001 (study area II)

a) Growth with respect to roads

From Table 3.10, it can be deduced that 79% of the total growth has taken place within zone I and II during 1993-2001. While 21.4 % of the total growth has taken place in zone III, IV and V respectively. This highlights the importance of road accessibility in the growth process of study area II.

Table 3.10: Percentage of growth in different distance zones from roads (study area II)

Zones	**Distance from Roads (in meters)**	**% of Total Growth (1993 -2001)**
I	0-200	51.6
II	200-400	27.0
III	400-800	18.3
IV	800-1600	2.9
V	>1600	0.2

b) Growth with respect to city core

In case of distance from city core (Table 3.11), it has been observed that 83% of the total growth has taken place in zone II, III and IV during 1993-2001. Thus, distance from city core is also an important factor affecting the growth process in study area II

Table 3.11: Percentage of growth in different distance zones from city core (study area II)

Zones	**Distance from City Core (in meters)**	**% of Total Growth (1997 -2001)**
1	0-1000	8.0
2	1000-2000	30.9
3	2000-3000	28.0
4	3000-4000	24.2
5	>4000	8.9

3.6 Factors driving the urban growth

As observed from growth trend in both the study areas, distance to roads and city core are two important factors that influence the growth process. However, besides these two factors, the accessibility to basic infrastructure facilities (i.e., water supply, sewerage, electricity, banks, shopping centre, medical centre etc.) also influences the urban growth process (Paul and Bharat, 1997; Gupta and Bawa, 2004; Gowda, 1998). Thus, urban growth in both study areas is defined as a function of the following three factors:

i) Distance to road network

ii) Accessibility to infrastructural facilities

iii) Distance to city core

The following raster maps corresponding to these three factors have been generated in GIS. The cell size of these raster maps has been kept as 23.5 meters, which corresponds to the spatial resolution of LISS III image used in this study,

i) Distance to road network

The distance to transport network has been measured in terms of Euclidian distance from the nearest road. Raster maps depicting the Euclidian distance of each cell from the nearest road have been generated in GIS for both the study area, as shown in Figure 3.19 and 3.20.

ii) Accessibility to infrastructural facilities

The accessibility to infrastructural facilities has been measured in terms of:

a) Distance from nearest built-up cells: The cost of connecting to urban services (e.g. water supply, sewerage, etc.) decreases with the distance from already built-up areas, as these facilities are already available in existing built-up areas. Raster maps showing the Euclidean distance of a cell from the nearest built-up cells have been generated and are shown in Figure 3.21 and 3.22

b) Amont of built–up cells in the neighbourhood: A larger proportion of built-up area in the neighbourhood implies availability of localized facilities, i.e., shopping centre, medical centre, banking, post office etc., necessary to support the population. Figure 3.23 and 3.24 show the amount of built-up cells in neighbourhood, calculated using a 5x5 cell Von Neumann neighbourhood.

iii) Distance to city core

The distance to city core has been measured in terms of Euclidean distance of each cell from the city core, where most of the higher level commercial facilities are located. Raster maps depicting the Euclidian distance of each cell from the city core have been generated and are shown in Figures 3.25 and 3.26

The database pertaining to factors driving the urban growth, as discussed in this chapter, forms the input to various CA based models implemented in this research.

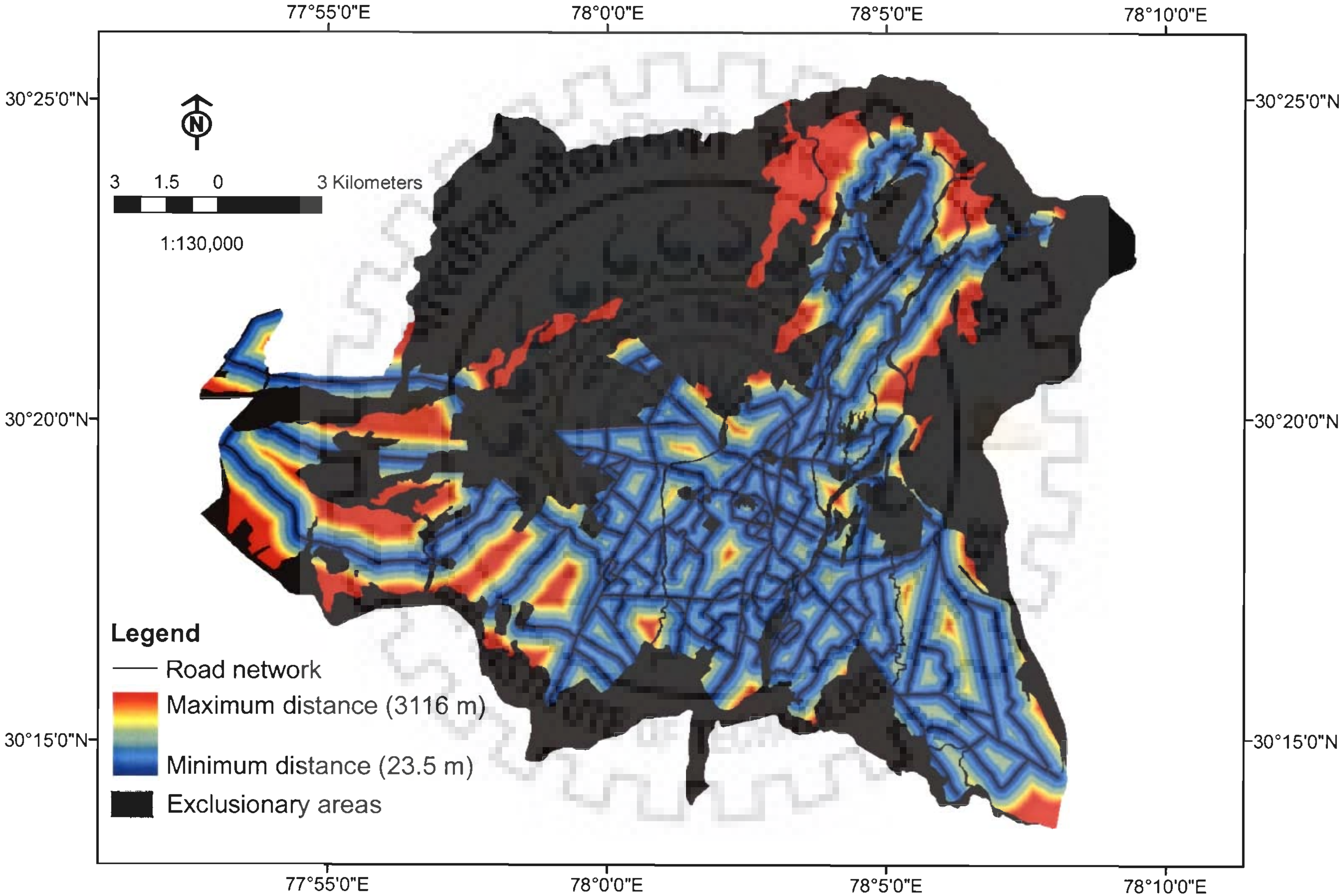

Figure 3.19: Distance from nearest road (study area I)

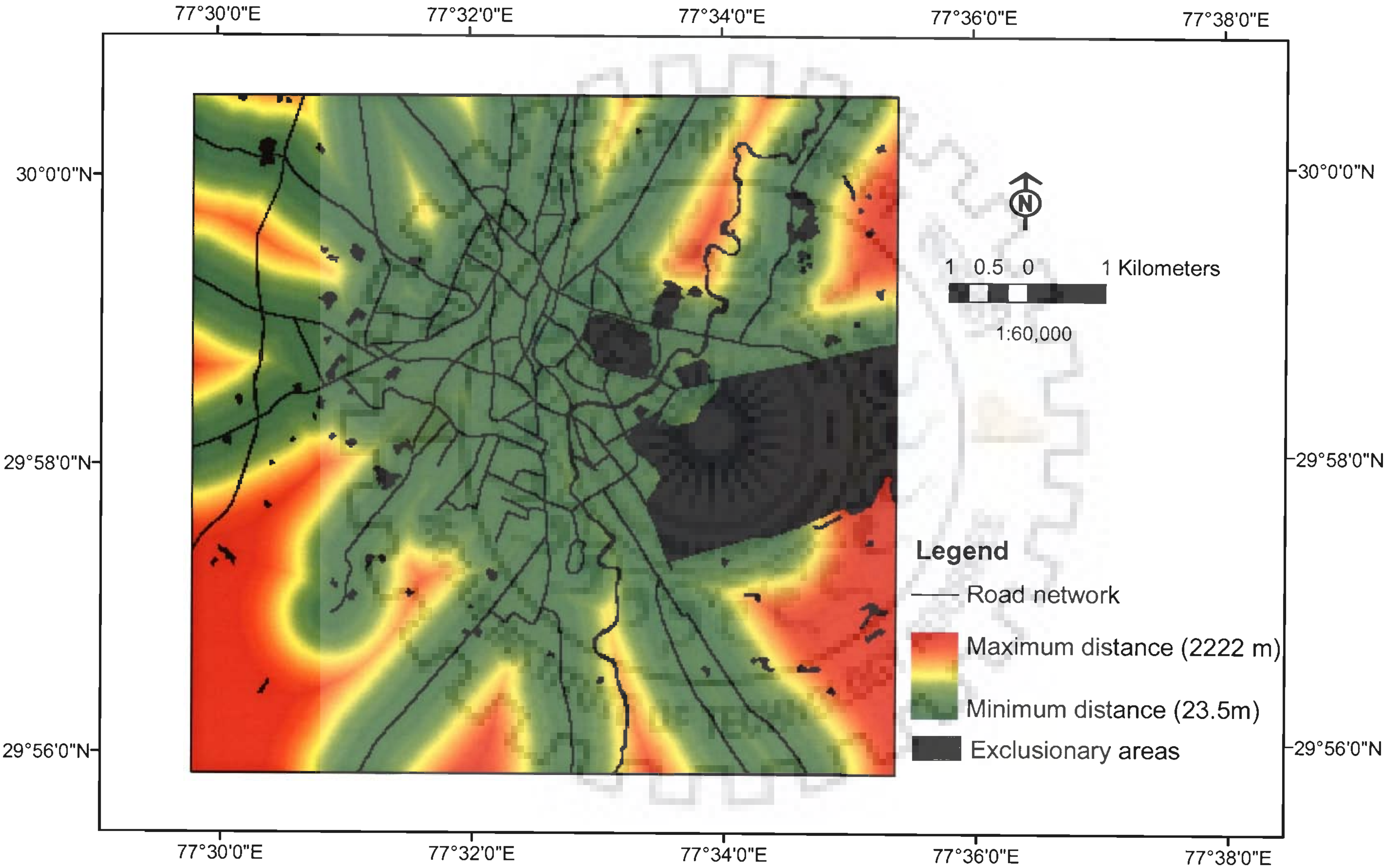

Figure 3.20 : Distance from nearest road (study area II)

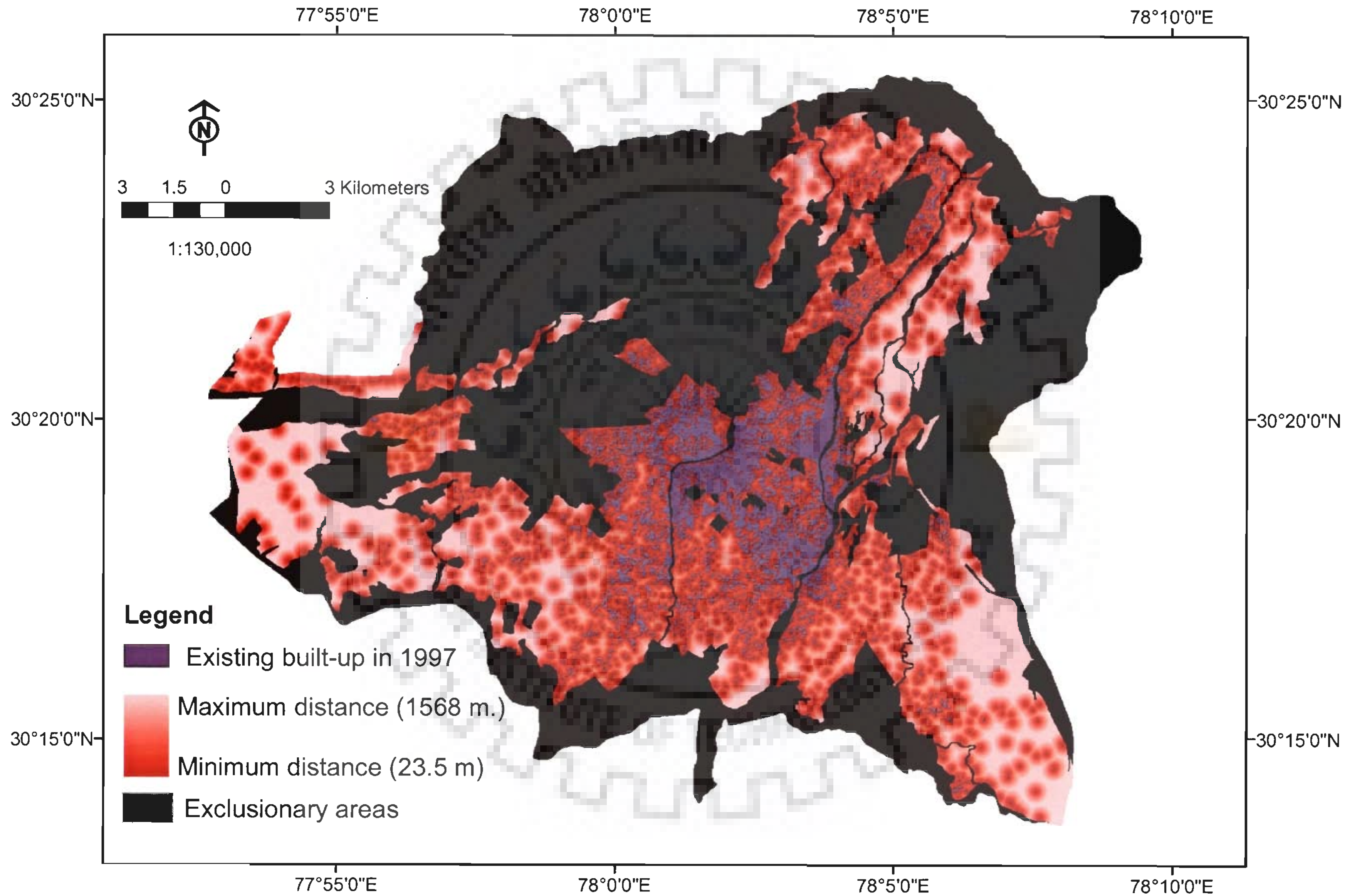

Figure 3.21: Distance from nearest built-up (study area I)

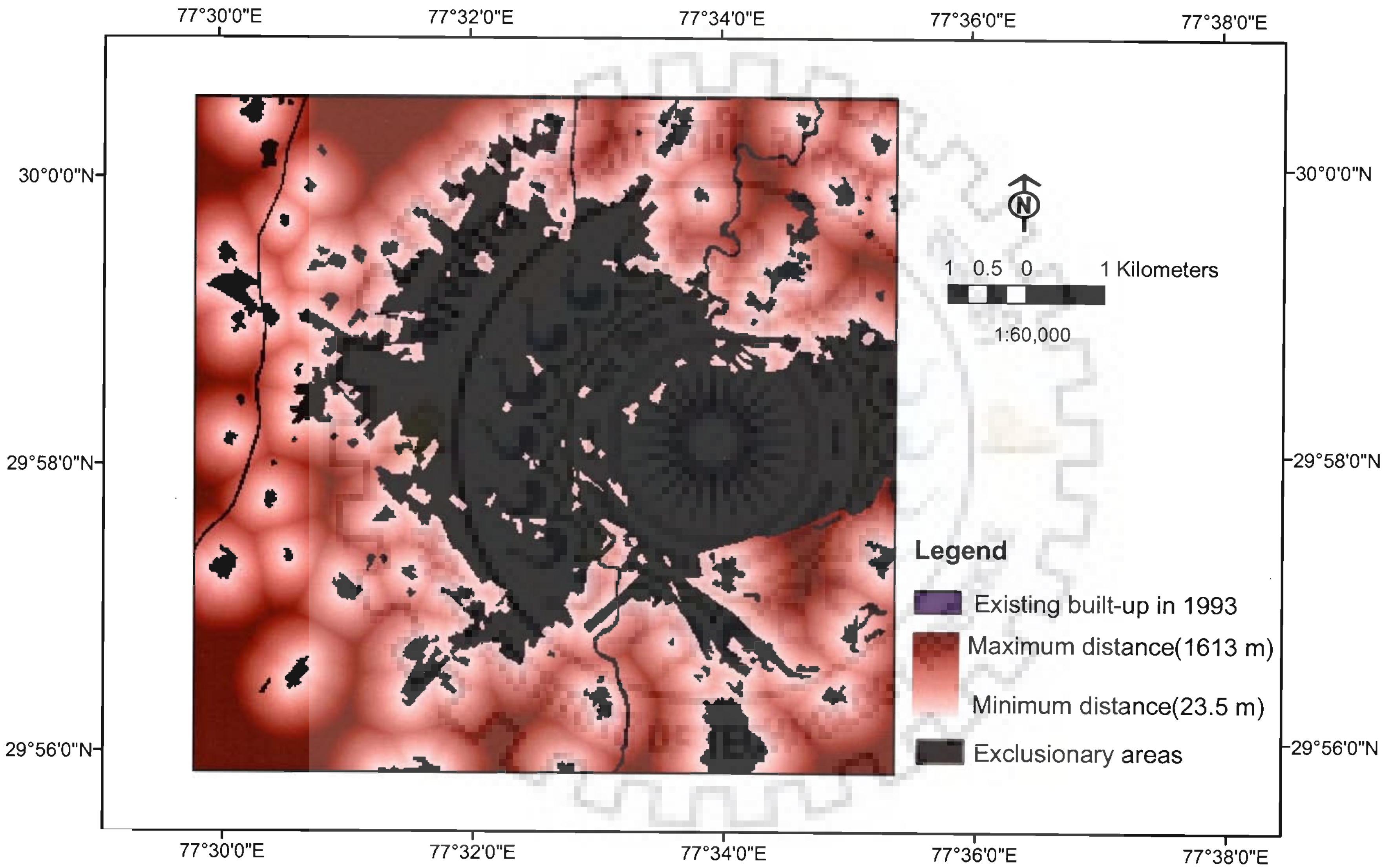

Figure 3.22: Distance from nearest built-up (study area II)

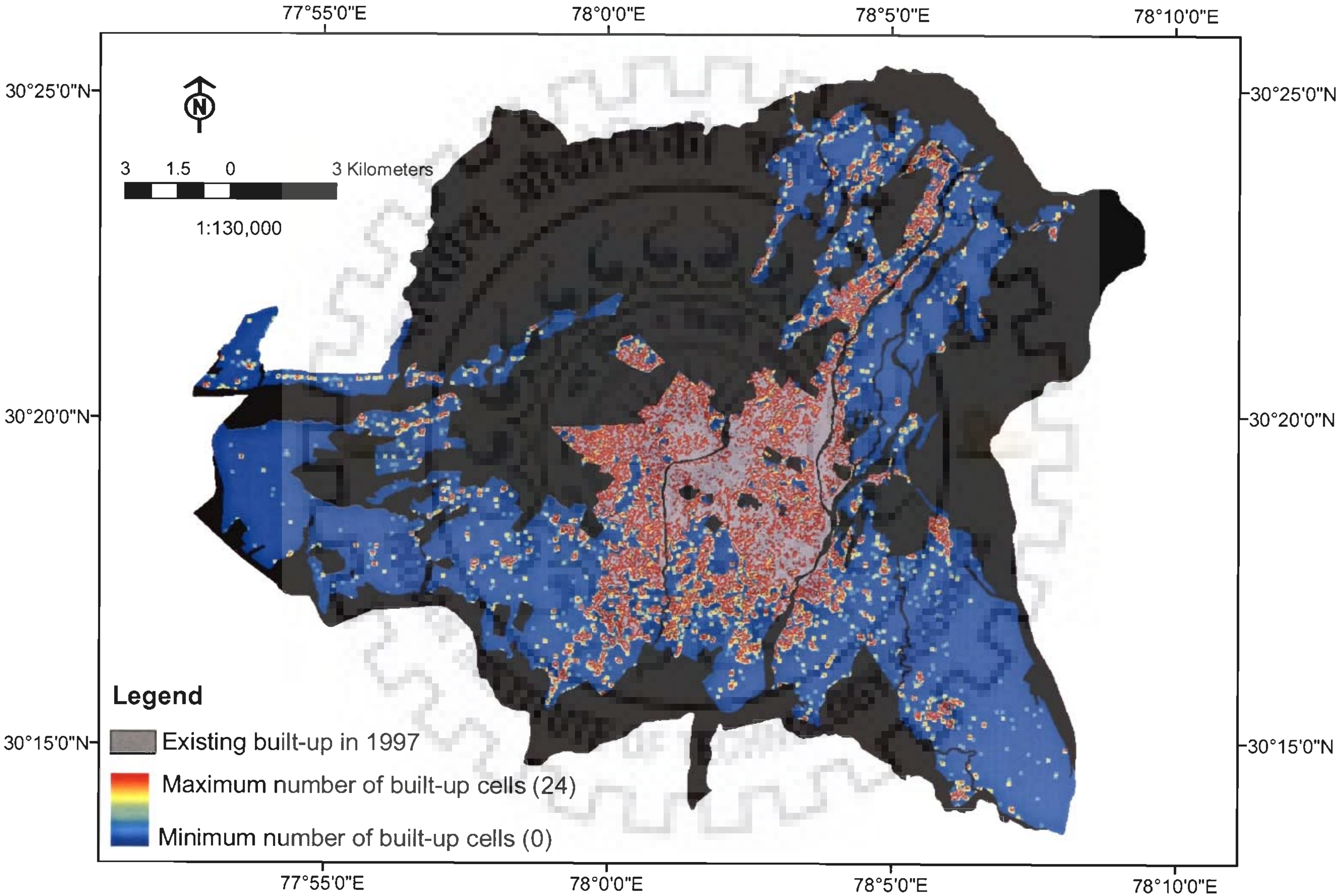

Figure 3.23: Number of built-up cells in neighbourhood (study area I) calculated using 5x5 cell Von Neumann neighbourhood

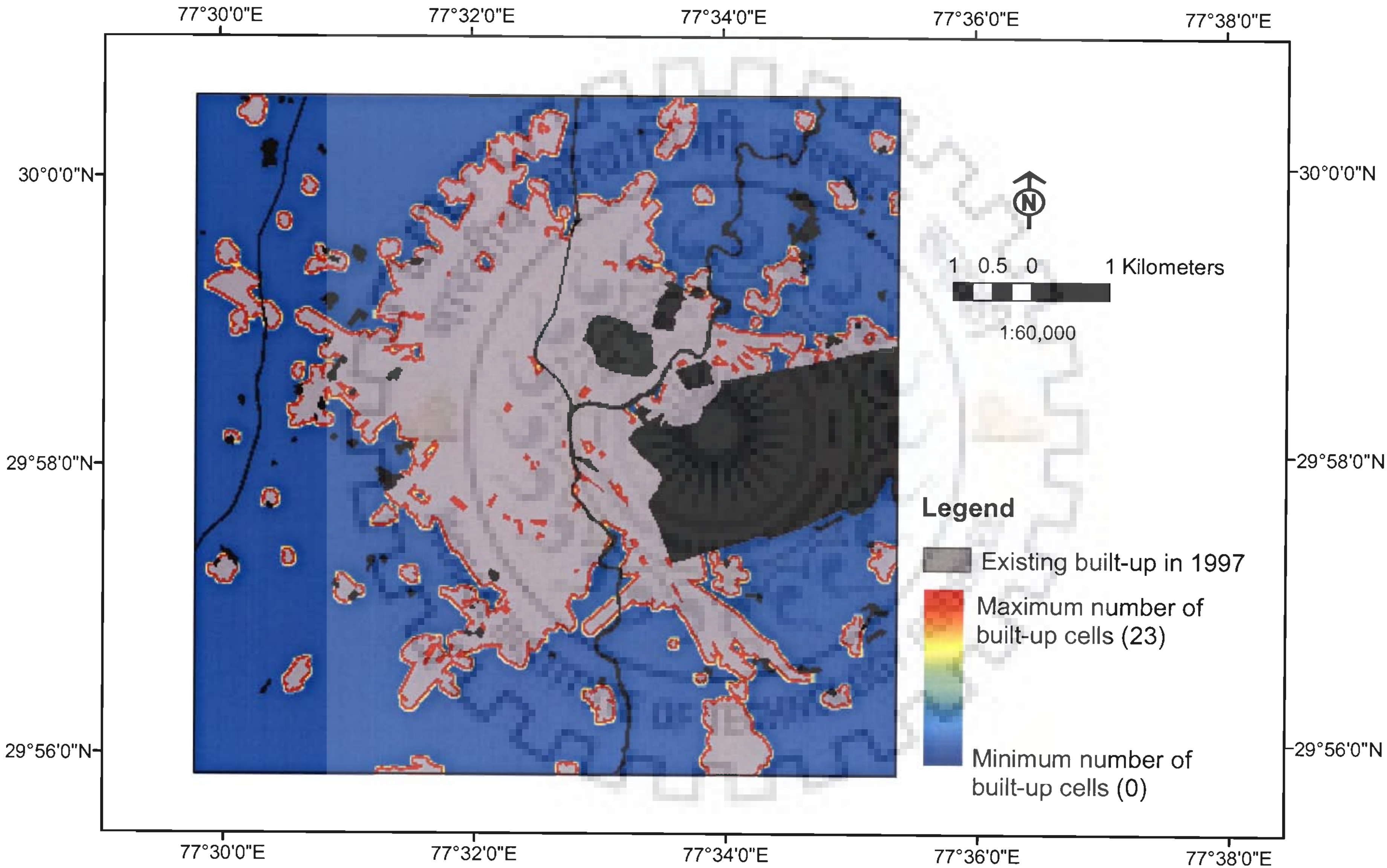

Figure 3.24: Number of built-up cells in neighbourhood (study area II) calculated using 5x5 cell Von Neumann neighbourhood

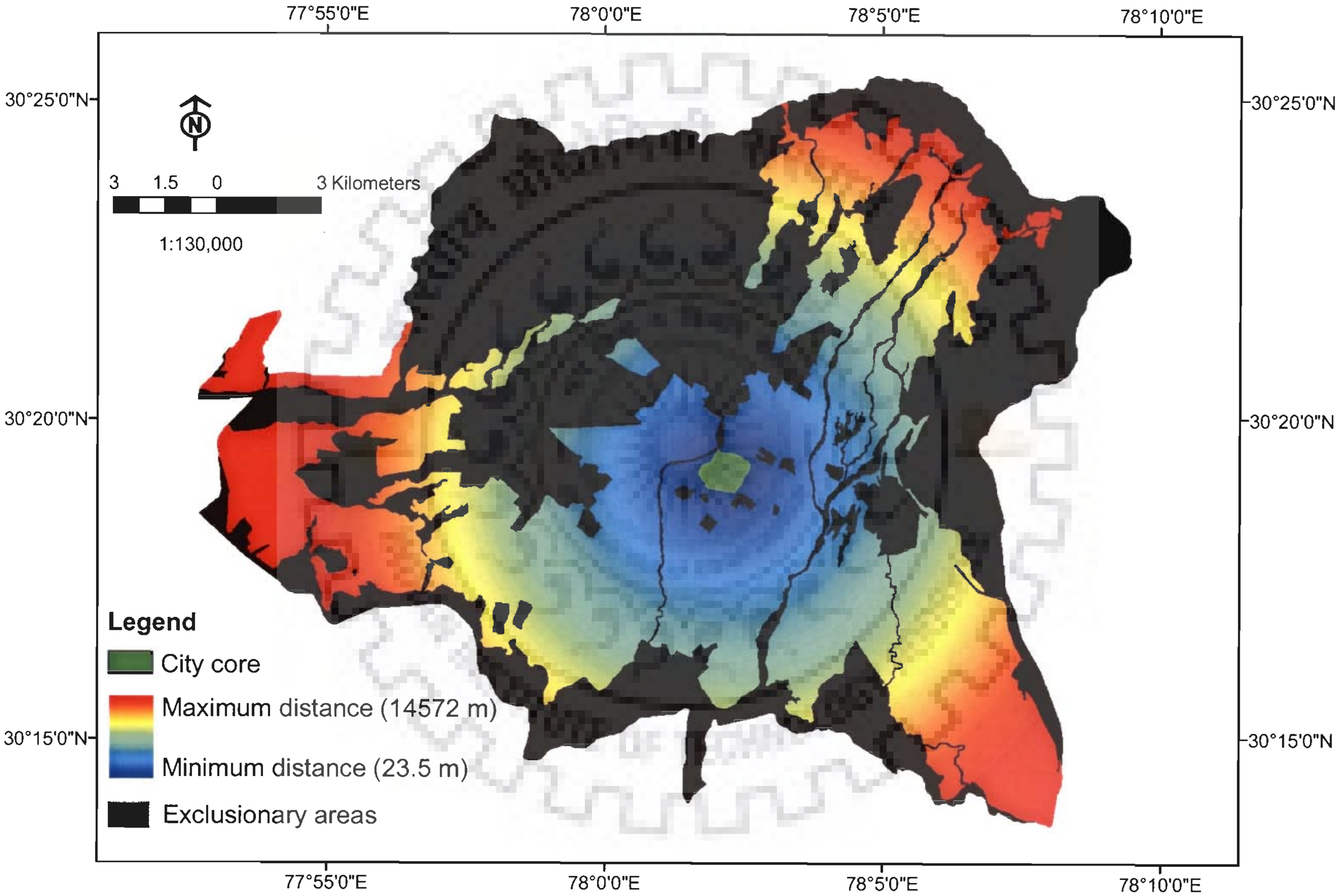

Figure 3.25: Distance from city core (study area I)

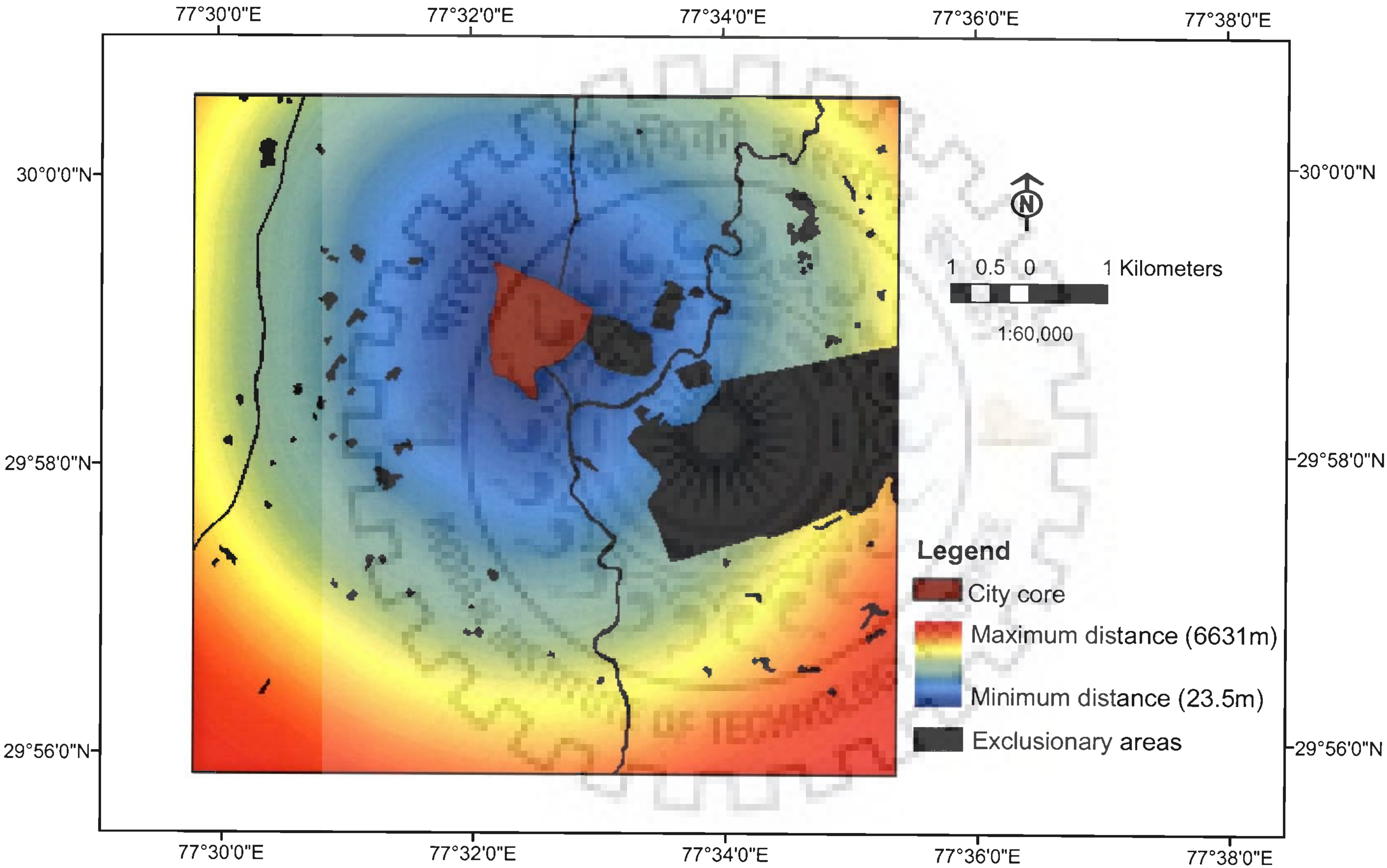

Figure 3.26: Distance from city core (study area II)

Chapter 4

Multi-Criteria Evaluation based CA model

4.1 Introduction

In this chapter, a Multi-Criteria Evaluation (MCE) based CA model to simulate urban growth, has been proposed. The model simulates urban growth as a function of the three factors, which were discussed in chapter 3. In the proposed model MCE is used to define the CA transition rules. The proposed MCE-CA model is calibrated for both the study areas and the calibrated results have been evaluated with respect to the actual growth on a cell by cell basis and spatial growth patterns. The calibration parameters, which produce the highest accuracy, have been used for future urban growth simulations in both the study areas.

4.2 Multi-criteria evaluation

The urban growth, in both the study areas, has been expressed as a function of following three factors,

i) Distance to city core

ii) Accessibility to infrastructural facilities

iii) Distance to road network

Corresponding to these three factors, the following raster maps have been created in GIS,

i) Euclidian distance of each cell from the city core

ii) Euclidean distance of a cell from the nearest built-up

iii) Euclidian distance of each cell from the nearest road

The Multi-Criteria Evaluation (MCE) technique has been used, in order to combine these three raster maps into a single raster map (suitability map), which depicts the potential or suitability of each cell for future urban growth. In implementing MCE, each factor has been assigned a weight, which indicates the relative importance of a factor with respect to other factors in determining the urban growth suitability of cells. In MCE, several weight assignment strategies, such as, ranking, rating, Analytical Hierarchical Process (AHP) and tradeoff methods are available. Amongst these, AHP method, given by Satty in 1980, is the most popular one (Malczewski, 1999, 2006) and has been used in the present study for deriving the weights of factors. These weights are then used for generating the urban growth suitability map. The AHP process consists of following three steps,

i) Generation of pair wise comparison matrix.

ii) Computation of factor weights.

iii) Estimation of consistency ratio.

4.2.1 Generation of pair wise comparison matrix

The three factors are compared pair wise and scores are assigned to the factors on a numerical scale ranging from 1 to 9 (Table 4.1) based on their relative importance with respect to each other in the urban growth process. The results of this comparison are displayed in the form of a pair wise comparison matrix. In the present study, the comparison matrix has been created based on the expert opinions from local planning authorities (Table 4.2). This matrix is reciprocal in nature and shows the pair wise score between all factors. For example, the factor distance to road network has strong importance as compared to the factor, distance to city core. Hence, distance to road network has been assigned a score of 5 and the factor, distance to city core, receives a score of 1/5 (Table 4.1).

Table 4.1: Definition of numerical scales for pair wise comparison

Numerical scale	Relative importance
1	Equal importance
2	Equal to moderate importance
3	Moderate importance
4	Moderate to strong importance
5	Strong importance
6	Strong to very strong importance
7	Very strong importance
8	Very to extremely strong importance
9	Extreme importance

Table 4.2: Pair wise comparison matrix

Factor	Distance to city core	Accessibility to infrastructural facilities	Distance to road network
Distance to city core	1	1/3	1/5
Accessibility to infrastructural facilities	3	1	1/3
Distance to road network	5	3	1

4.2.2 Computation of factor weights

The pair wise comparison matrix has been used for calculation of factor weights. The steps in weight calculation are:

i) The values in each column of the pair wise comparison matrix are summed

ii) Each element in the matrix is divided by its column total

iii) The average of the elements in each row is computed, i.e., the sum of each row is divided by the number of factors, which in the present case is 3

Thus, the computed factor weights are, distance to city core = 0.10, accessibility to infrastructural facilities = 0.26 and distance to road network = 0.64

4.2.3 Estimation of consistency ratio

Depending on the expert opinions, the factors can be assigned different scores and the corresponding factors weights calculated which at times can be subjective. Therefore, in order to determine the consistency of comparisons between the factors and computed weights, a measure namely, consistency ratio (CR) has been used. The CR is defined as the ratio between consistency index (CI) and random index (RI), as explained in Equation 4.1,

$$CR = \frac{CI}{RI} \qquad \ldots 4.1$$

Random index (RI) is the consistency index of a randomly generated pair wise comparison matrix. The value of RI used is 0.58, as found out from the Random Inconsistency indices table given by Satty (Malczewski, 1999).

Consistency index (CI) is defined as follows,

$$CI = \frac{\lambda - n}{n - 1} \qquad \ldots 4.2$$

Where,

λ = average value of the consistency vector

n = number of factors (n = 3 in present case, since three factors are considered)

The value of λ is calculated as (refer Table 4.3),

i) The weight of the factor, distance to city core (i.e., 0.12) , is multiplied by the first column of pair wise comparison matrix (refer Table 4.2), as shown in step I of Table 4.3

ii) The weight of the factor, distance to infrastructural facilities (i.e., 0.23), is multiplied by the second column of pair wise comparison matrix (refer Table 4.2), as shown in step I of Table 4.3

iii) The weight of the factor distance to road network (i.e., 0.65), is multiplied by the third column of pair wise comparison matrix (refer Table 4.2), as shown in step I of Table 4.3

iv) These values are summed over the rows as shown in step I of Table 4.3

v) The consistency vector is determined by dividing the weighted sum vector by the criterion weights as shown in section II of Table 4.3.

Table 4.3: Determination of consistency vector (Note: the values in brackets indicate the factor scores assigned in Table 4.2)

Factor	**Step I**	**Step II**
Distance to city core	(1)x0.10+ (1/3)x0.26+ (1/5)x0.64= 0.32	0.32 / 0.10 =3.2
Accessibility to infrastructural facilities	(3)x0.10+(1)x0.26+ (1/3)x0.64= 0.78	0.78 / 0.26 =3.0
Distance to road network	(5)x0.10+ (3)x0.26+ (1)x0.64 = 1.93	1.93/0.64 = 3.01

The value of λ is found out by averaging the value of the consistency vector obtained in Table 4.3 as,

$$\lambda = \frac{3.2+3.0+3.01}{3} = 3.07$$

The value of CI is then calculated using Equation 4.2 as,

$$CI= \frac{3.07 - 3}{3-1} = 0.04$$

Thus, CI=0.04 and RI=0.58, using Equation 4.1, the value of CR is calculated as,

$$CR = \frac{0.04}{0.58} = 0.07$$

If CR < 0.1, it indicates a reasonable level of consistency in pair wise comparison and the weights are accepted. On the other hand, if CR ≥ 0.1, it indicates inconsistent judgment and the scores in the comparison matrix need to be assigned again and the weights determined again. Since, the computed value of CR is 0.07 and less than 0.1, therefore the computed weights are accepted.

4.2.4 Generation of urban growth suitability map

The AHP derived factor weights have then been used for creating the urban growth suitability map. The raster maps corresponding to the three factors driving urban growth (discussed in section 4.2), are reclassified on a 0-1 linear scale. In these maps, the cells near to built-up area, road and city core receive a value of 1 and cells farther away receive lesser values. These three raster maps have been multiplied with their respective factor weights, and the products added together (Equation 4.3) as,

$$S = (D_{cc} * 0.10 + D_{nb} * 0.26 + D_{nr} * 0.64) \quad \text{.... 4.3}$$

Where,

S is the suitability map which shows the potential of each cell for urban growth

D_{nb} denotes the raster map distance to nearest built-up

D_{cc} denotes the raster map distance to city core

D_{nr} denotes the raster map distance to nearest road

The suitability map thus produced, shows the suitability of each cell for urban growth. Figure 4.1, depicts the process of suitability map creation. The suitability map produced for study areas I and II using the MCE technique are shown in Figure 4.2 and Figure 4.3 respectively. The areas with black colour represents cells that are already built-up and fall in exclusionary zones (discussed in chapter 3) and have thus been excluded from analysis. The cells with value 1 are the most suitable for future urban growth, while cells with lower values are less suitable for urban growth.

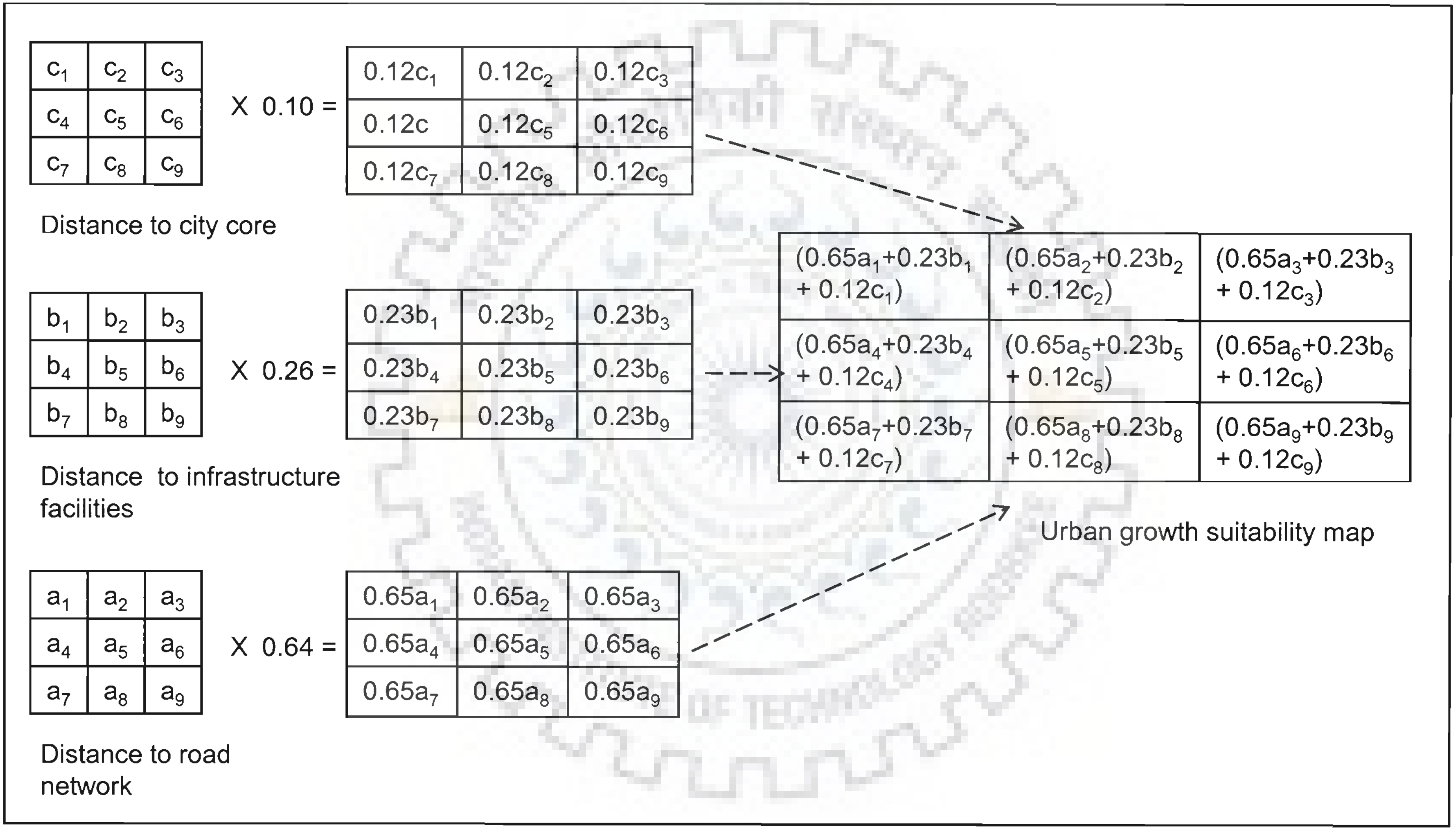

Figure 4.1: Process of generation of urban growth suitability map

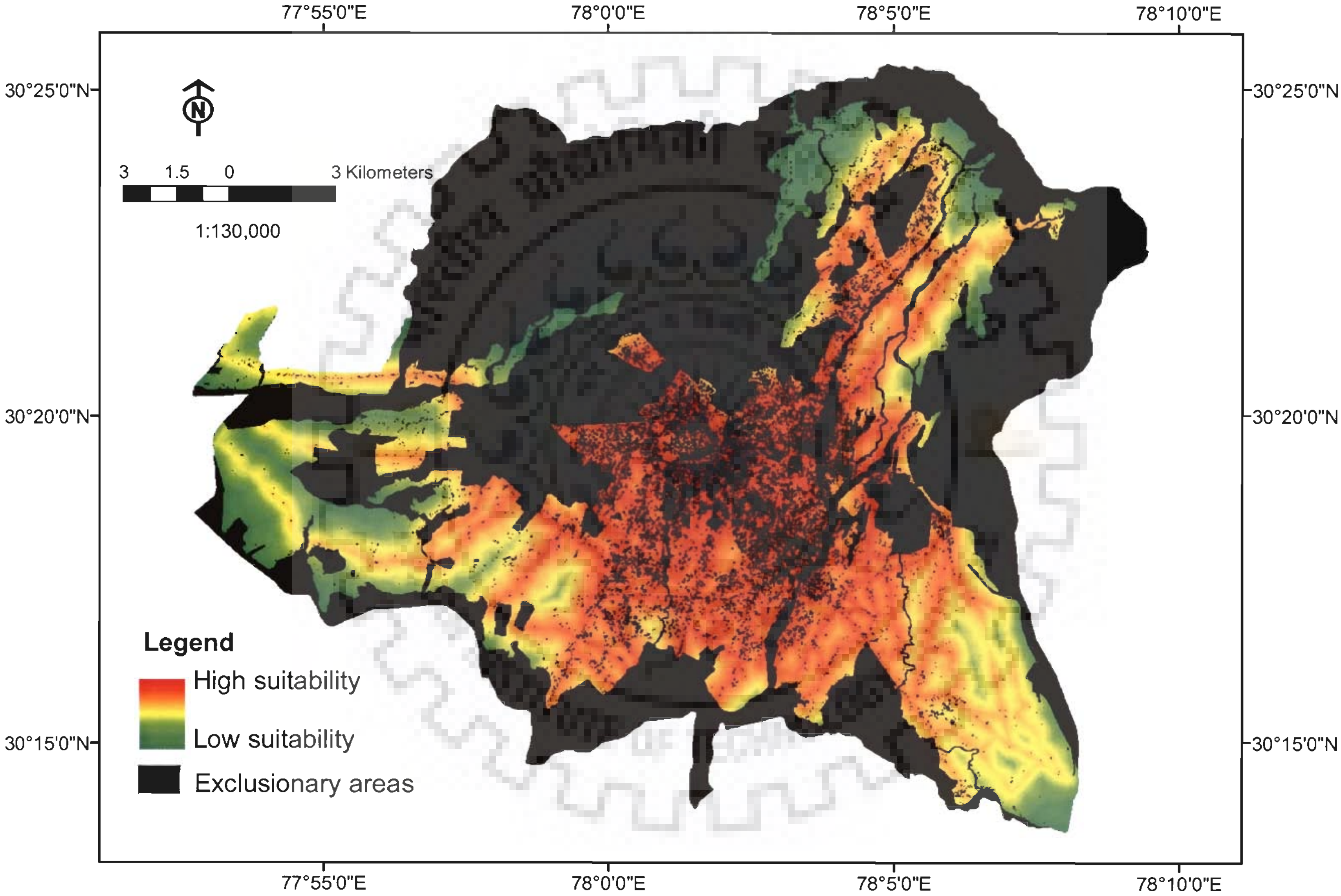

Figure 4.2: Urban growth suitability map generated using MCE (study area I)

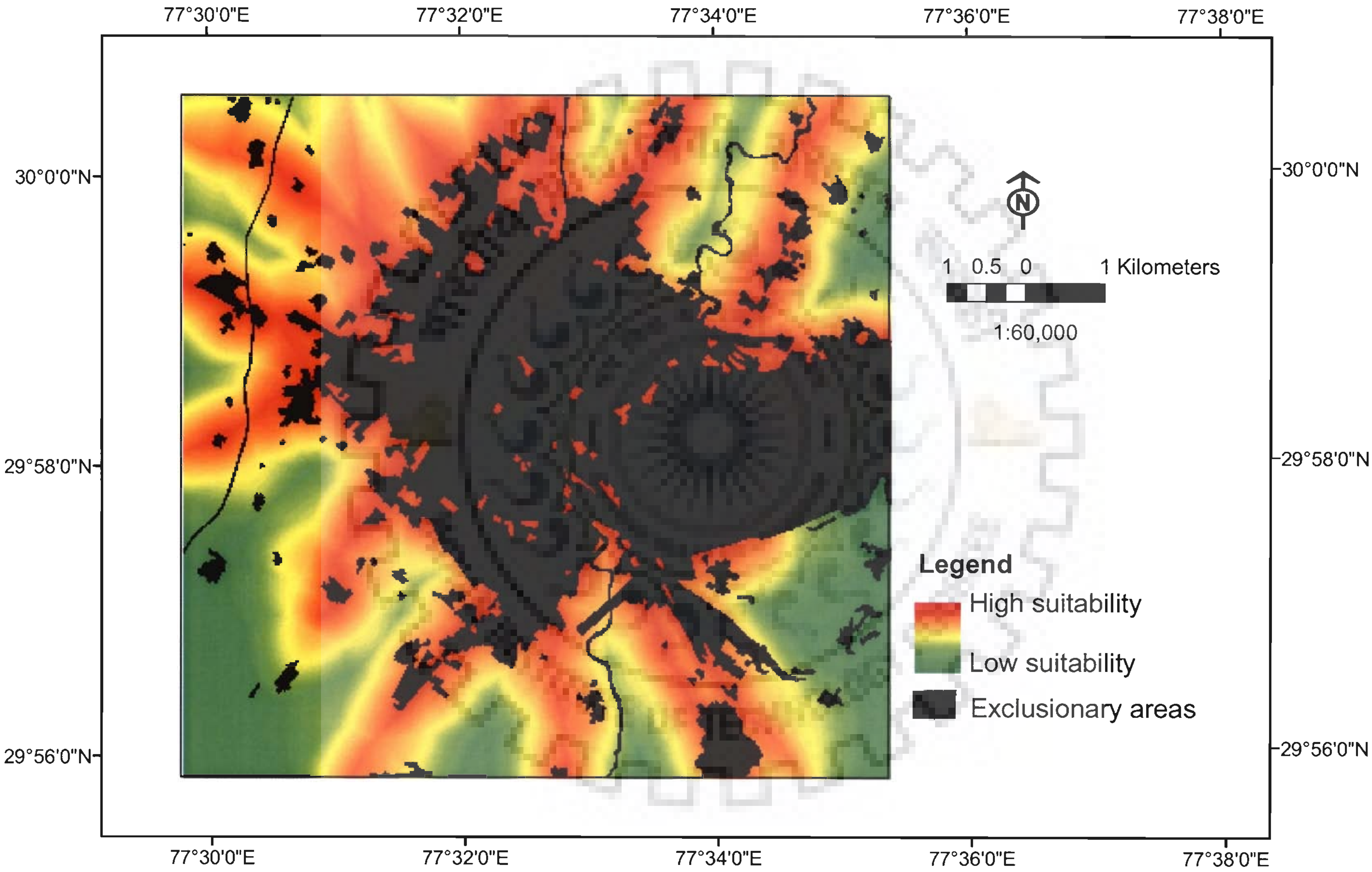

Figure 4.3: Urban growth suitability map generated using MCE (study area II)

4.3 MCE based CA model (MCE-CA)

The urban growth suitability maps are static in nature, since these are created by linear summation of factors which are also static in nature. For example, the values in the factor map, distance from roads, will only change when a new road is built. Similarly, the factors distance to city core and existing built up area are also static and will change only when some external forces act on them. However, urban growth is a dynamic process in space and time and can not be modelled using the static approach. Therefore, a MCE based CA (MCE-CA) model is proposed to capture the dynamic process of urban growth.

The proposed model uses the MCE derived suitability map as input. The potential of cell for future urban growth has been expressed as a function of the suitability of the cell and local level factors (i.e., amount of built-up in the neighbourhood). These factors interact at the local level in a recursive manner, initiate a non-linear dynamic process, which is able to capture the dynamics of urban growth.

The proposed model is based on the dichotomy of built-up and non built-up areas and simulates transition from non built-up to built-up areas with no reverse process. Therefore, the existing built–up areas and areas that do not have any development potential, e.g., restricted areas, reserved forests, water bodies, public grounds (discussed in chapter 2) have been treated as exclusionary areas. The proposed model makes no prediction of urban growth in these exclusionary areas. A schematic diagram of the model is shown in Figure 4.4.

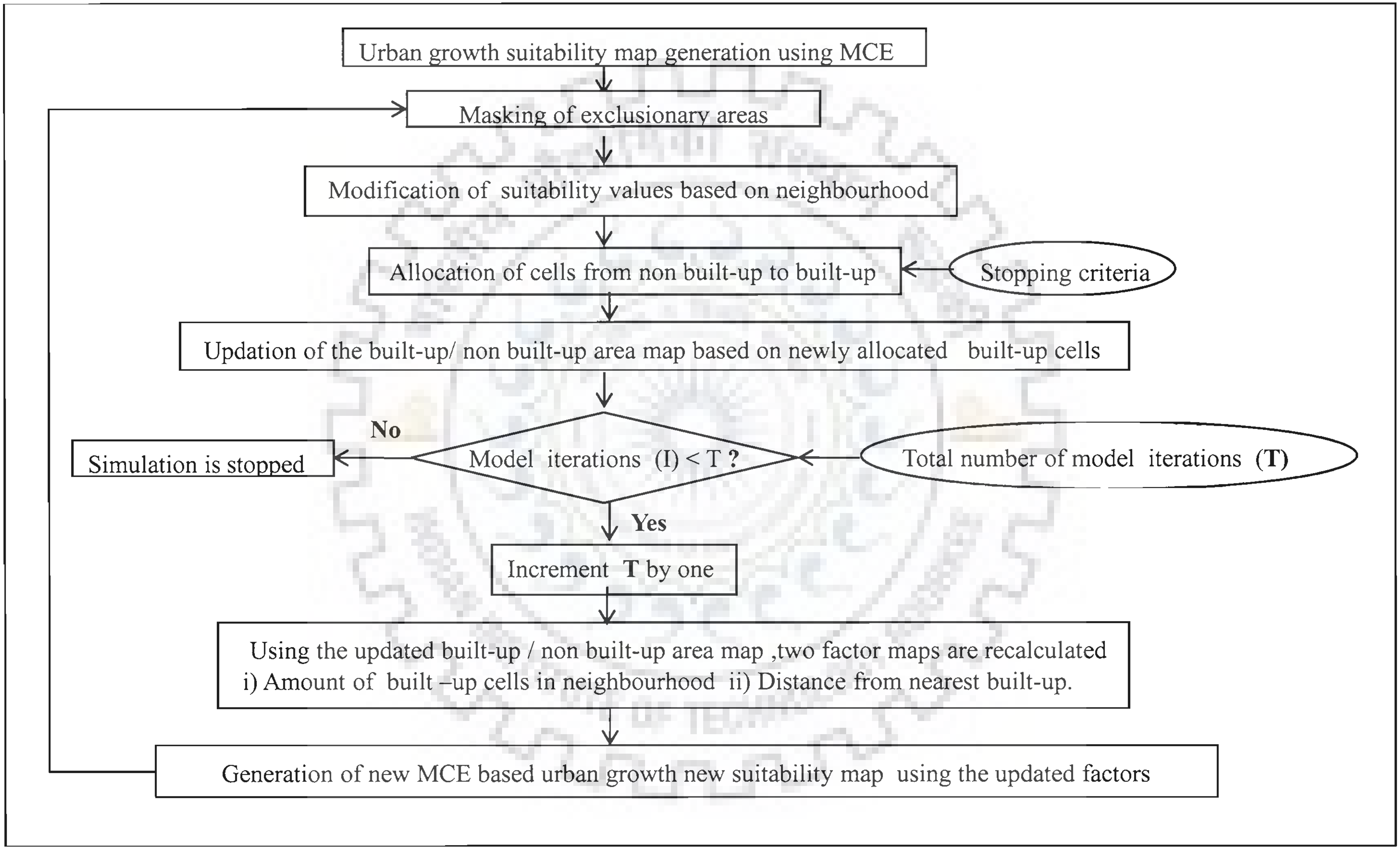

Figure 4.4: Flowchart of MCE based CA model

Following steps are followed in the running of MCE-CA model:

i) Generation of maps corresponding to factors driving urban growth in study area

ii) Generation of MCE based urban growth suitability map using maps generated in step i)

iii) Stopping criteria for the model

iv) Masking of exclusionary areas

v) Modification of suitability map based on amount of built-up cells in neighbourhood

vi) Allocation of cells from non built-up to built-up

vii) Updation of built-up/ non built-up map and factor maps

viii) Generation of urban growth suitability map based on updated factor maps

ix) The process from step iv) to step viii) is repeated, till the stopping criteria is fulfilled. The final updated built-up/non built-up map is stored as simulated urban growth map of study area.

The proposed model is implemented for study areas I and II. In order to simulate the growth of cities, it is necessary to fix the values of model parameters that are able to generate realistic patterns of urban growth. This process is called as model calibration. The proposed ANN-CA model has been calibrated for both the study areas. For study area I, the model is calibrated for period 1997-2001 whereas for study area II for the period 1993-2001. The detailed description of the calibration steps is as follows,

4.3.1 Generation of maps corresponding to factors affecting urban growth in study area

As discussed earlier, urban growth is expressed as a function of three factors, and corresponding to these three factors, four maps are created in GIS.

i) Euclidian distance of each cell from the nearest road (f1)

ii) Euclidean distance of a cell from the nearest built-up (f2)

iii) Euclidian distance of each cell from the city core (f3)

iv) Amount of built-up in neighbourhood (f4)

For generating the f4 map (i.e., amount of built-up in neighbourhood), Von Neumann and Moore neighbourhoods with cell sizes varying from 3x3 cells to 39x39 cells have been used.

4.3.2 Generation of urban growth suitability map

A suitability map created using the MCE technique (refer section 4.2) has been taken as a input.

4.3.3 Stopping criteria for the model

The stopping criterion defines the condition at which the model stops allocating non built-up cells to built-up during each iteration. For defining stopping criteria in this model, it is assumed that equal number of cells transit to built-up during each iteration. Thus, if a total of N cells transit to built-up during the entire simulation period and the number of model iterations is T, then $\frac{N}{T}$ number of cells are allocated to built-up during each iteration and is denoted by C. The process stops when C numbers of cells are allocated from non built-up to built-up.

CA models are recursive in nature (i.e., they involve a repeated procedure for a finite number of iterations, such that the model output at iteration 't' becomes the input for 't+1' iteration). It is this recursive nature that makes the CA models dynamic in nature. The proposed MCE-CA model is run for a user defined number of iterations. During each iteration, cells transit from non built-up to built-up area based on their suitability values.

For study area I, the model is calibrated for the period 1997 to 2001. Using the built-up/non built-up maps of year 1997 and 2001 (discussed in chapter 3), the total number of cells that transit from non built-up to built-up during this period are found, this defines the stopping criteria for the model. Thus, this ensures that the same number of cells transit from non built-up to built-up during the simulation, as that have actually transit from non built-up to built-up during 1997-2001. Similarly, for study area II, the model is calibrated for the period 1993 to 2001. The built-up/non built-up maps of year 1993 and 2001 (discussed in chapter 3) have been used to determine the actual number of cell that transit from non built-up to built-up, which define the stopping criteria .

Using different combinations of the neighborhood and number of iterations, the MCE-CA model has been executed several times for each of the study areas so as to determine the optimum values of the parameters.

4.3.4 Masking of exclusionary areas

The restricted areas, reserved forests, water bodies, public grounds and gardens have been treated as exclusionary zones and the model makes no prediction in these areas. A mask corresponding to these areas has been generated based on Survey of India topographical map, guide map and master plan of the study areas. Since the model only simulates transition from non built-up to built-up with no reverse process taking place, so the built-up cells are also masked out. At the end of each model iteration when cells are allocated from non built-up to built-up, the built-up mask is also updated.

4.3.5 Modification of suitability value based on neighbourhood

The concept of neighbourhood is central to CA (i.e., a non built-up cell having a larger proportion of built-up cells in its neighbourhood has a higher potential for transiting to built-up as compared to non built-up cell, which has a lower proportion of built-up cells in its neighbourhood). Thus, the urban growth suitability map generated using MCE, has been modified by multiplying the suitability value at each cell with the amount of built-up cells in its neighbourhood (Equation 4.4). Thus, for a cell to be a likely choice for transition to built-up, it should be both inherently suitable and near to built-up areas. Thus, the modified suitability value is given as,

$$S_c = S_{mce} \times \Omega \qquad \ldots 4.4$$

where, S_c is the modified suitability value, S_{mce} is the MCE derived suitability value and Ω is the amount of built-up cells in the neighbourhood. The amounts of built-up cells in neighbourhood are updated after each model iteration as explained in later steps.

4.3.6 Allocation of cells from non built-up to built-up

On the basis of their MCE and neighbourhood information derived urban growth suitability value, the cells in study area are ranked in a descending order. The first *C* ranked cells are only allocated to built-up (refer section 4.3.3), while the rest of the cells remain as non built-up.

4.3.7 Updation of built-up/non built-up map and factor maps

On the basis of the cells that have transit from non built-up to built- up, the built-up/ non built-up area map is updated for study area I and II. Other factor maps such as, distance to nearest built-up and amount of built-up in neighbourhood are then recalculated on the basis of this updated map.

4.3.8 Generation of urban growth suitability map based on updated factor maps

The urban growth suitability map is generated again using MCE technique and the updated factor maps. During suitability map generation, the same factor weights are used as computed initially using Satty's method.

4.3.9 Model iterations

The process from step 4.3.4 to step 4.3.8 is repeated, until the total number of iteration as decided in step 4.3.3 are executed. The updated built-up/ non built-up map in the last iteration is the final simulated urban growth map of the study area.

4.4 Evaluation of simulated growth patterns

The MCE-CA model has been executed several times for each of the study areas, using different model parameters. The simulated urban growth patterns have been evaluated on the basis of cell by cell matching of simulated growth with actual growth using Percent correct match (PCM). However, the PCM is based on independent comparison between pair of cells. Thus, small displacements between the actual and simulated urban growth maps are considered as errors and the same error is reported even if the displacement is of '*n*' cells or one cell (Barredo *et al*., 2003). The PCM, therefore, is unable to take into account the patterns or distribution of urban growth. Therefore, the model results have also been evaluated on the basis of the similarity between the actual and simulated growth patterns using Moran's Index.

a) Percent Correct Match (PCM)

The raster maps depicting simulated and actual urban growth have been overlaid and the corresponding cells, which have changed from non built-up to built-up, in both the maps are counted. PCM is defined as the ratio between correctly simulated cells and the actual total number of cells that have transited from non built-up to built-up during the simulation period (Equation 4.5).

$$PCM = \frac{N_1}{N_2} * 100 \qquad ...4.5$$

N_1= Cells correctly simulated to change to built-up by the model

N_2 = Cells actually transiting to built-up during the simulation period

A higher value of PCM implies that the model is able to accurately simulate the growth cells.

b) Moran Index

In order to evaluate growth pattern spatially, Moran Index has been used. A Moran Index is a spatial statistical indicator that reveals the pattern of clustering of the same type of class at adjacent cells (Shortridge, 2007, Wu, 2002, Li and Yeh, 2004a). The indicator reflects the extent to which built-up and non built-up cells are intermixed with each other. A value of Moran Index close to +1 indicates a compact growth pattern with less intermixing of built-up and non built-up cells. A value close to -1 indicates a dispersed pattern with more intermixing of built-up and non built-up cells. If the values of the Moran index for the simulated and the actual growth are close to each other, it implies that the model is able to simulate the urban growth pattern accurately. The other advantage of Moran Index is that it is simple and easy to compute as compared to other spatial metrics (e.g., mean patch area, total edge, shape index) and fractal dimension, which are complex in nature.

4.5 Results and Discussion

As discussed in section 4.5, in order to optimize the model parameters, the MCE-CA model has been calibrated by varying the sizes of two neighborhoods as well as the model iterations for subsequent urban growth simulation. PCM and Moran index have been used to compare the model derived simulated urban growth with actual urban growth for the two study areas and has been discussed in the following.

4.5.1 Study area I

i) Analysis based on PCM value

The PCM value has been plotted as a function of neighbourhood size for both the neighbourhoods as well as the number of iterations (Figures 4.5 and 4.6). On executing the model using Von Neumann neighbourhood, the maximum value of PCM has been obtained as 35%, for 5x5 cell size and 16 iterations. Increase in the sizes of the neighbourhood decreases the PCM. The lowest PCM of 29.5% is recorded when the model is executed using neighbourhood of 39x 39 cell size and 16 iterations. Increasing the number of iterations has also led to a further decrease in value of PCM.

Exactly similar trend has been observed in executing the model using Moore neighbourhood. Thus, for a study area, which has got dispersed urban growth pattern, neighbourhoods of small size (e.g., 5x5 cells) but large number of iterations produces realistic growth trends. The type of neighbourhood has been found to be immaterial.

ii) Analysis based on Moran Index value

The Moran index value has been plotted as a function of size in neighbourhood for both the neighbourhoods as well as the number of iterations (Figures 4.7 and 4.8). On executing the model using Von Neumann neighbourhood, a Moran index value of 0.29 has been obtained at 5x5 cell size and 1iteration. This value exactly matches with the Moran Index for actual urban growth in study area.

On increasing the neighbourhood size, the simulated growth patterns become increasingly compact. For example, the Moran index increases significantly when neighbourhood size increases from 3x3 cells to 15x15 cells. After this, the increase in Moran index is gradual. Similar trend can be seen in case of Moore neighbourhood (Figure 4.10).

Thus, increase in the neighbourhood size as well as increase in the number of iterations tend to increase the compactness of the urban growth pattern. However, since the urban growth trend in this study area is of dispersed nature, a neighbourhood of small size with less number of iterations has produced growth patterns which are close to the actual growth patterns spatially.

Hence, for study area I, which has a dispersed growth pattern, neighbourhoods of small size (i.e., 5x5 cells) produced accurate growth patterns, as cab be seen from the analysis of PCM and Moran Index values. However, while large number of model iterations resulted in higher values of PCM, but on the other hand they also generated increasingly compact patterns, as compared to the actual growth taking place in the study area.

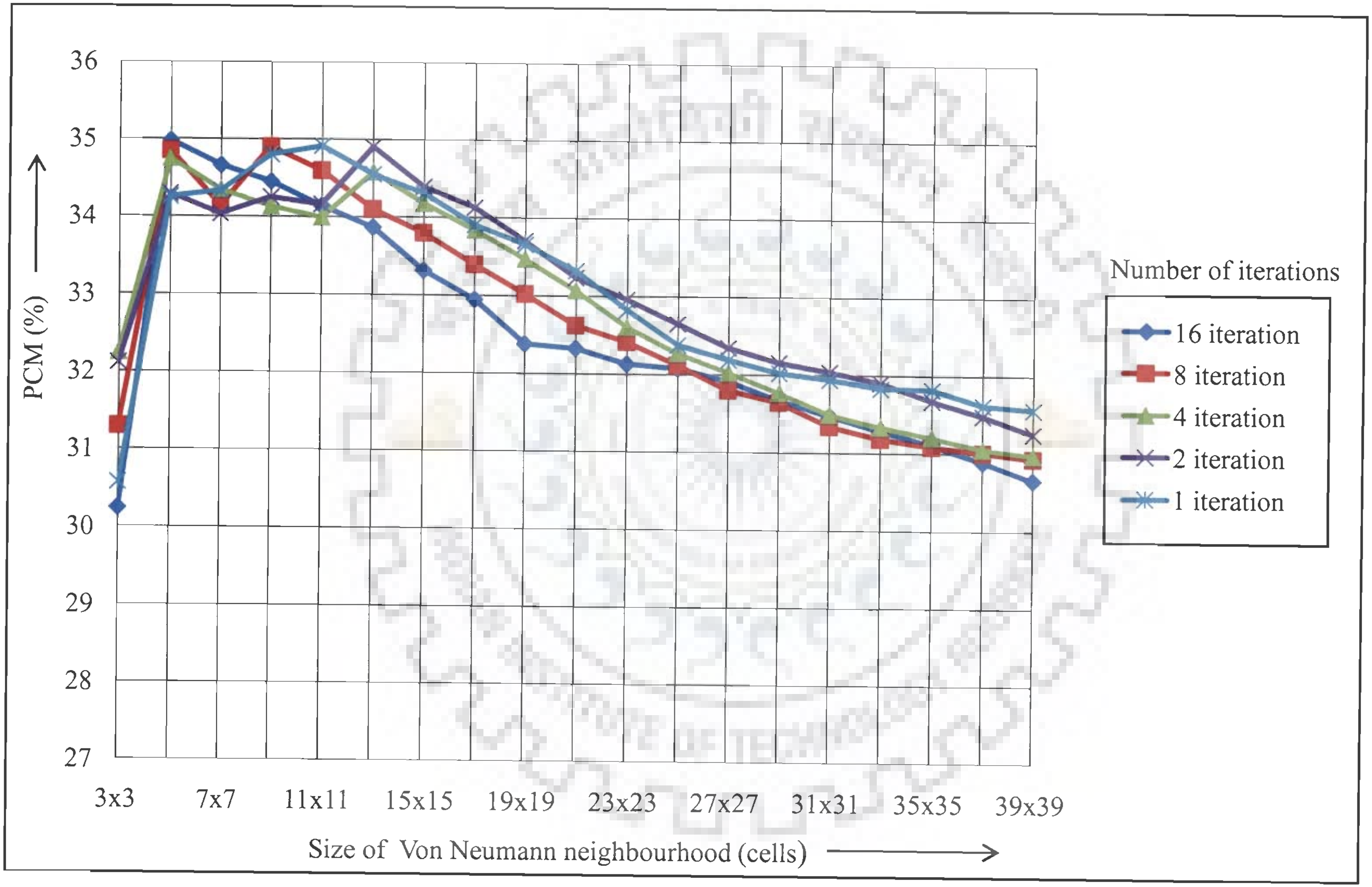

Figure 4.5 : PCM as a function of different Von Neumann neighbourhood sizes (Study area I)

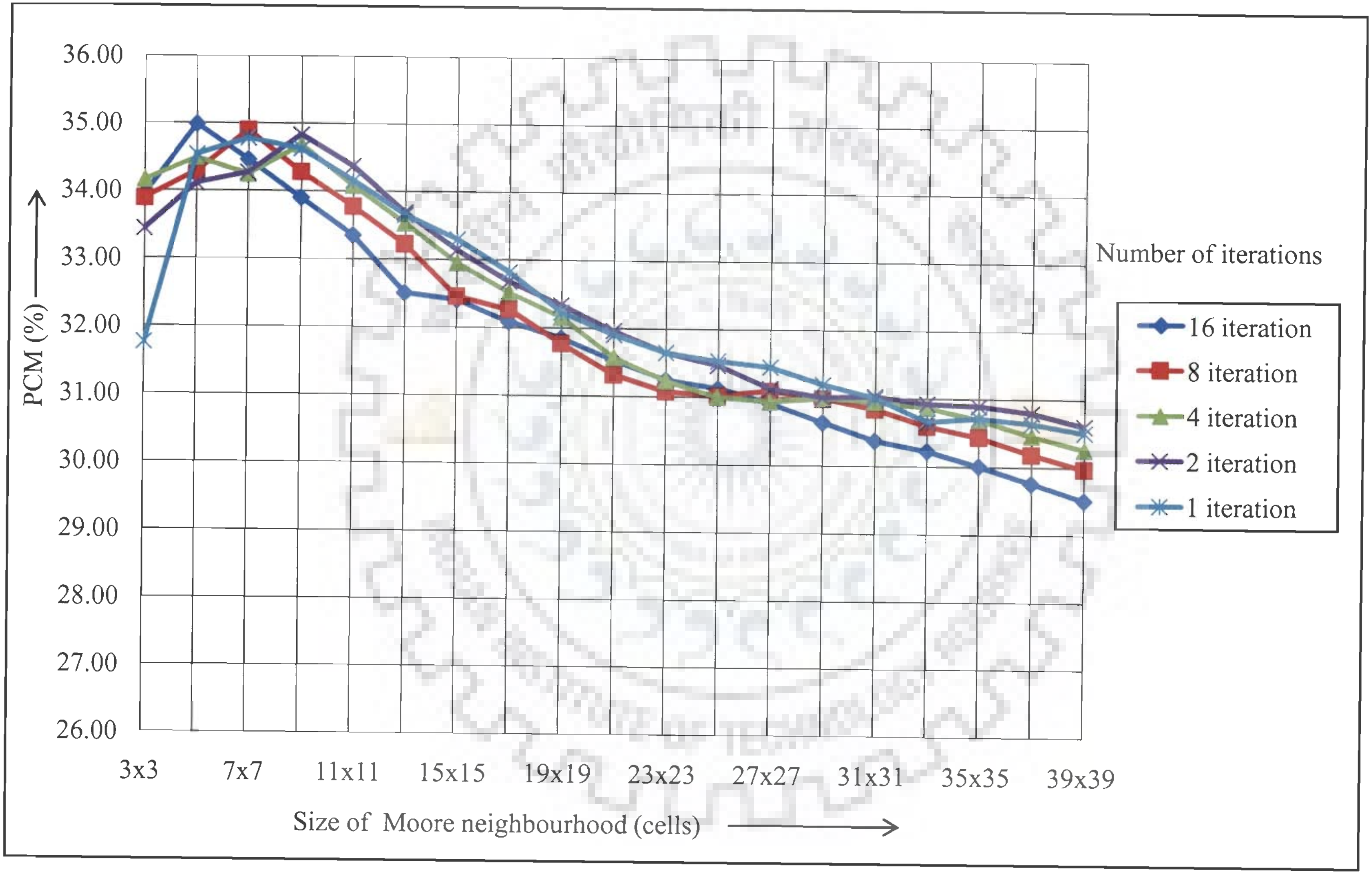

Figure 4.6: PCM as a function of different Moore neighbourhood sizes (Study area I)

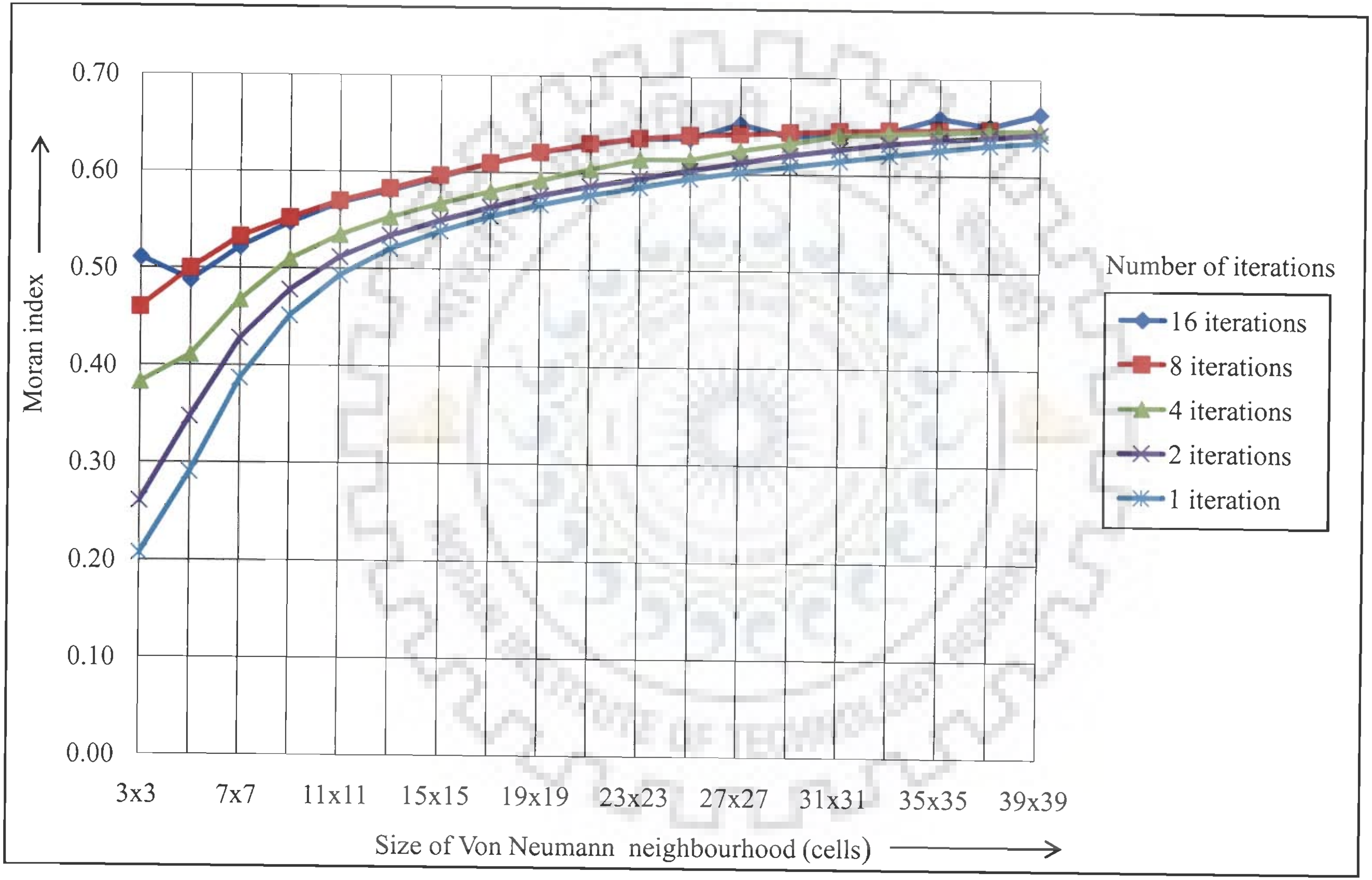

Figure 4.7: Moran Index as a function of different Von Neumann neighbourhood sizes (Study area I)

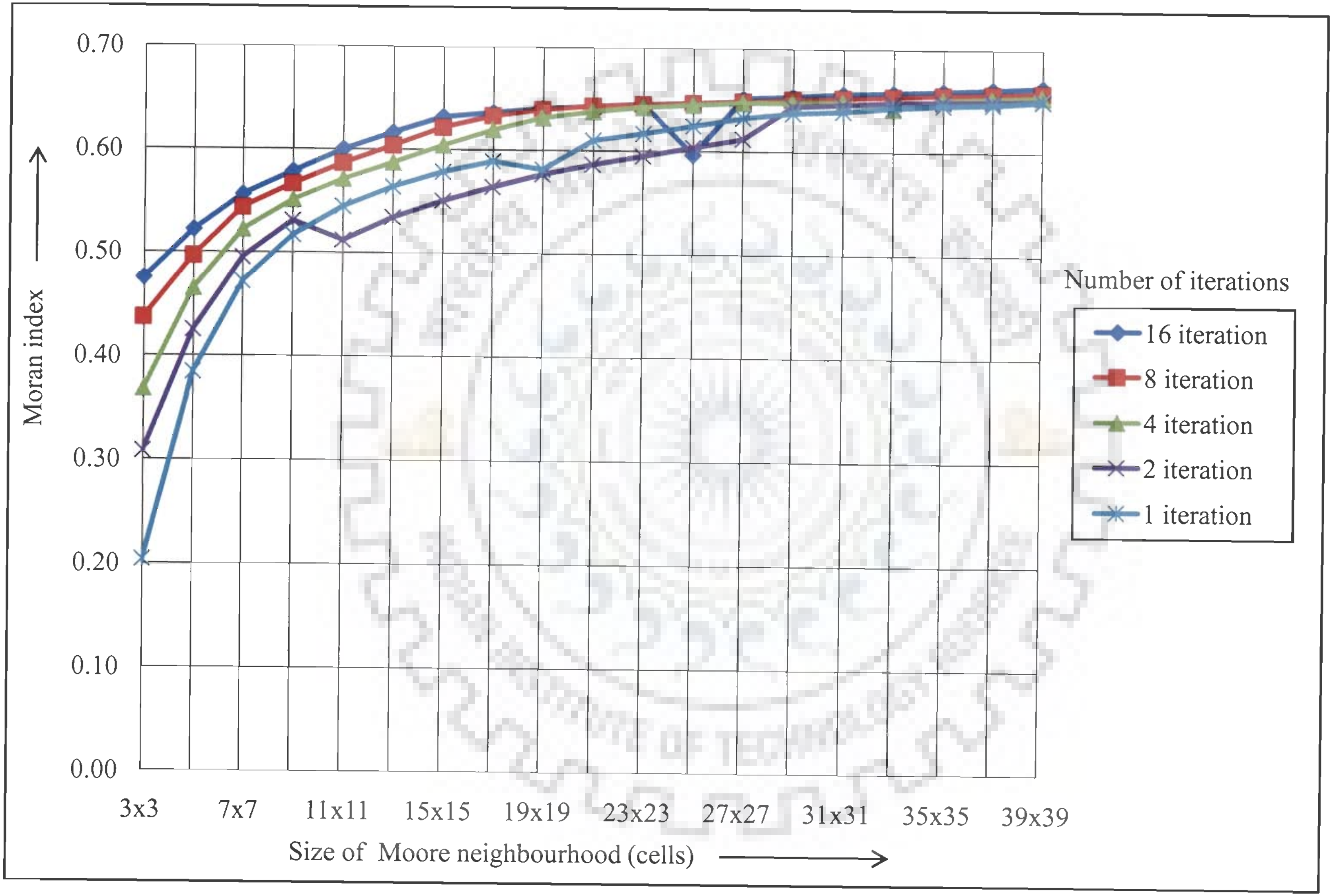

Figure 4.8 : Moran Index as a function of different Moore neighbourhood sizes (Study area I)

4.5.2 Study area II

i) Analysis based on PCM value

Looking at the plots of PCM as a function of neighbourhood sizes for different model iterations (Figures 4.9 and 4.10), it can be noticed that the maximum PCM value of 58.1% has been obtained at neighbourhood size of 39x39 cells and 1 iteration for Moore neghbourhood. Corresponding value of PCM for Von Neumann neighbourhood is 57.9% at 39x39 cell size and 2 model iterations. Thus, for study area II, which has a compact urban growth pattern, the use of larger neighourhoods but small number of model iterations has produced realistic growth patterns.

ii) Analysis based on Moran Index value

Looking at the plots of Moran index as a function of neighbourhood sizes for different model iterations (Figures 4.11 and 4.12), it can be noticed that a Moran index value of 0.75 has been obtained at neighbourhood size of 13x13 cells and 4 iterations for Moore neghbourhood. This value exactly matches with the Moran Index for actual urban growth in study area.

On increasing the neighbourhood size, the simulated growth patterns become increasingly compact. However, unlike the findings in the previous study area, the increase in value of Moran Index is gradual as the neighbourhood size increases from 3x3 cells to 39x39 cells. This can be expected also since the urban growth in this study area is largely compact in nature. Similar trend can be seen in case of Moore neighbourhood (Figure 4.12).

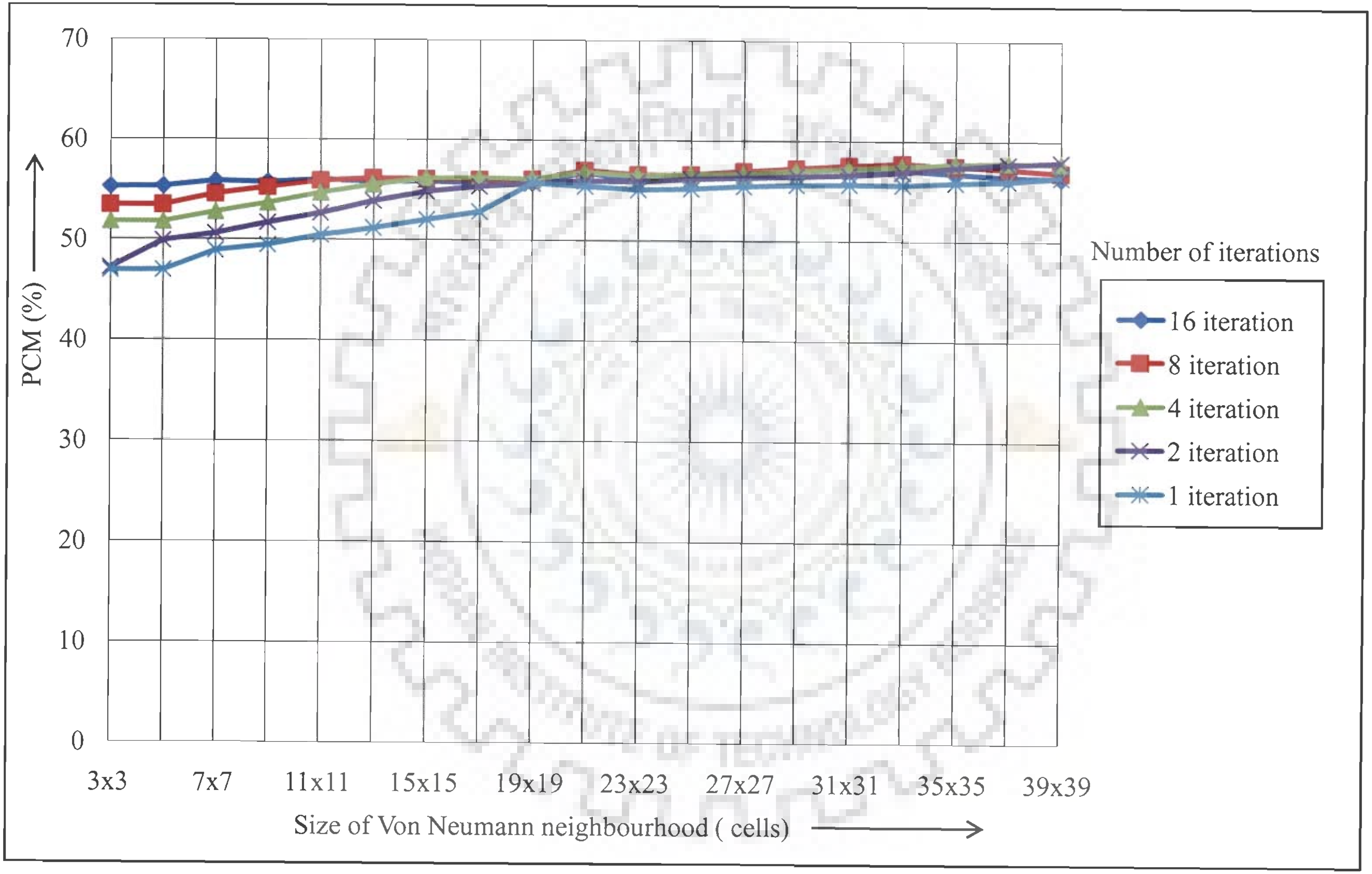

Figure 4.9: PCM as a function of different Von Neumann neighbourhood sizes (Study area II)

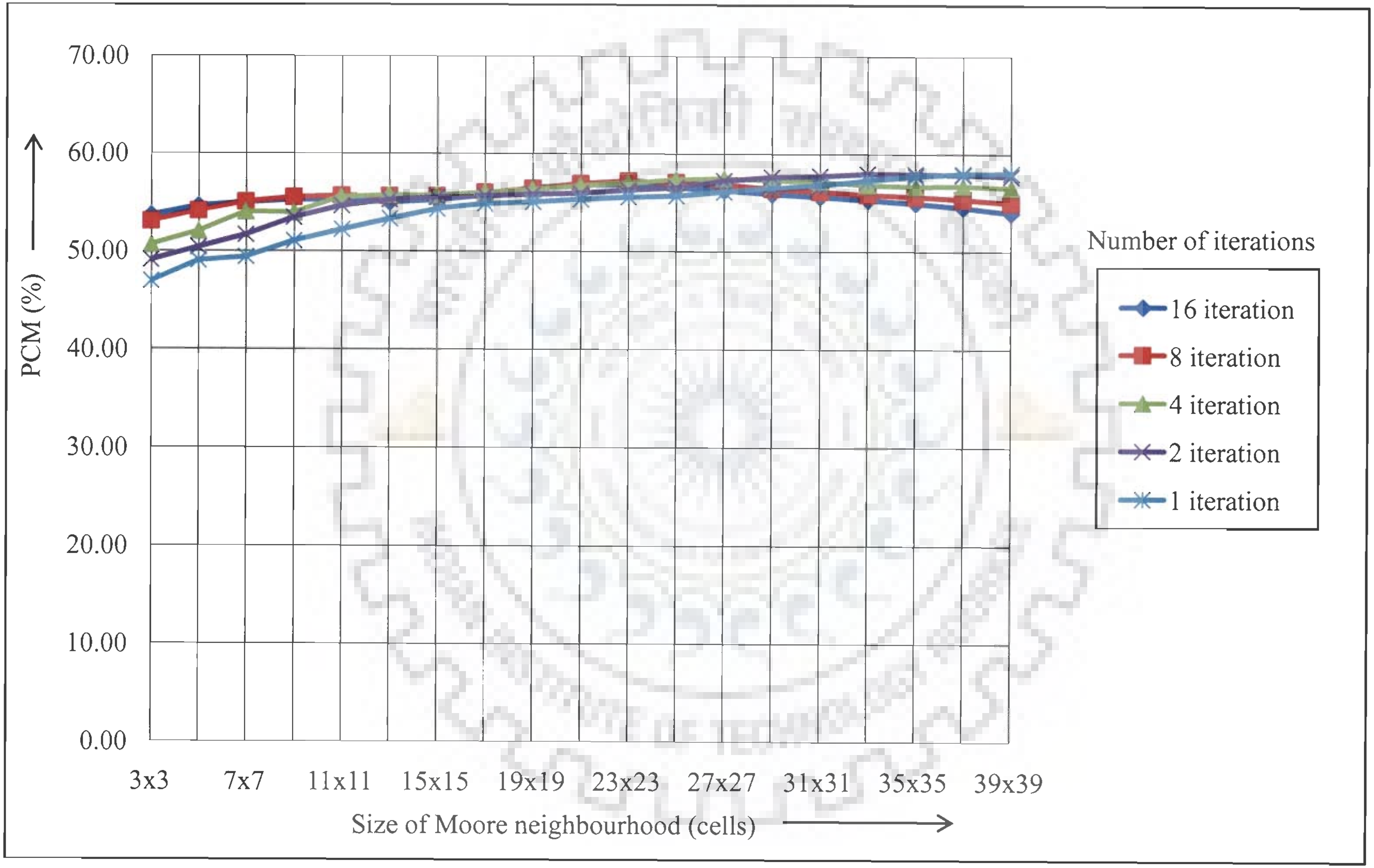

Figure 4. 10: PCM as a function of different Moore neighbourhood sizes (Study area II)

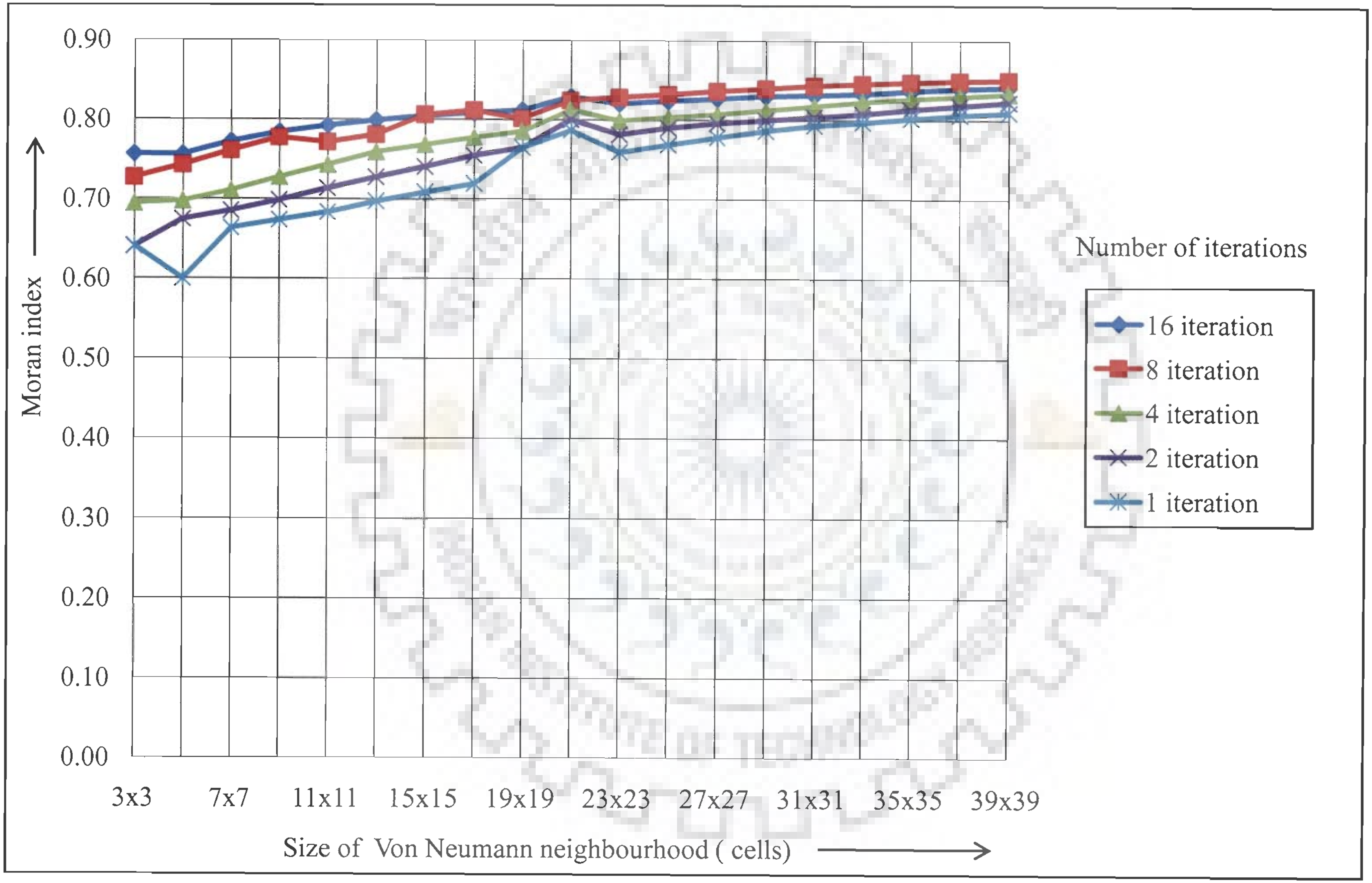

Figure 4.11: Moran Index as a function of different Von Neumann neighbourhood sizes (Study area II)

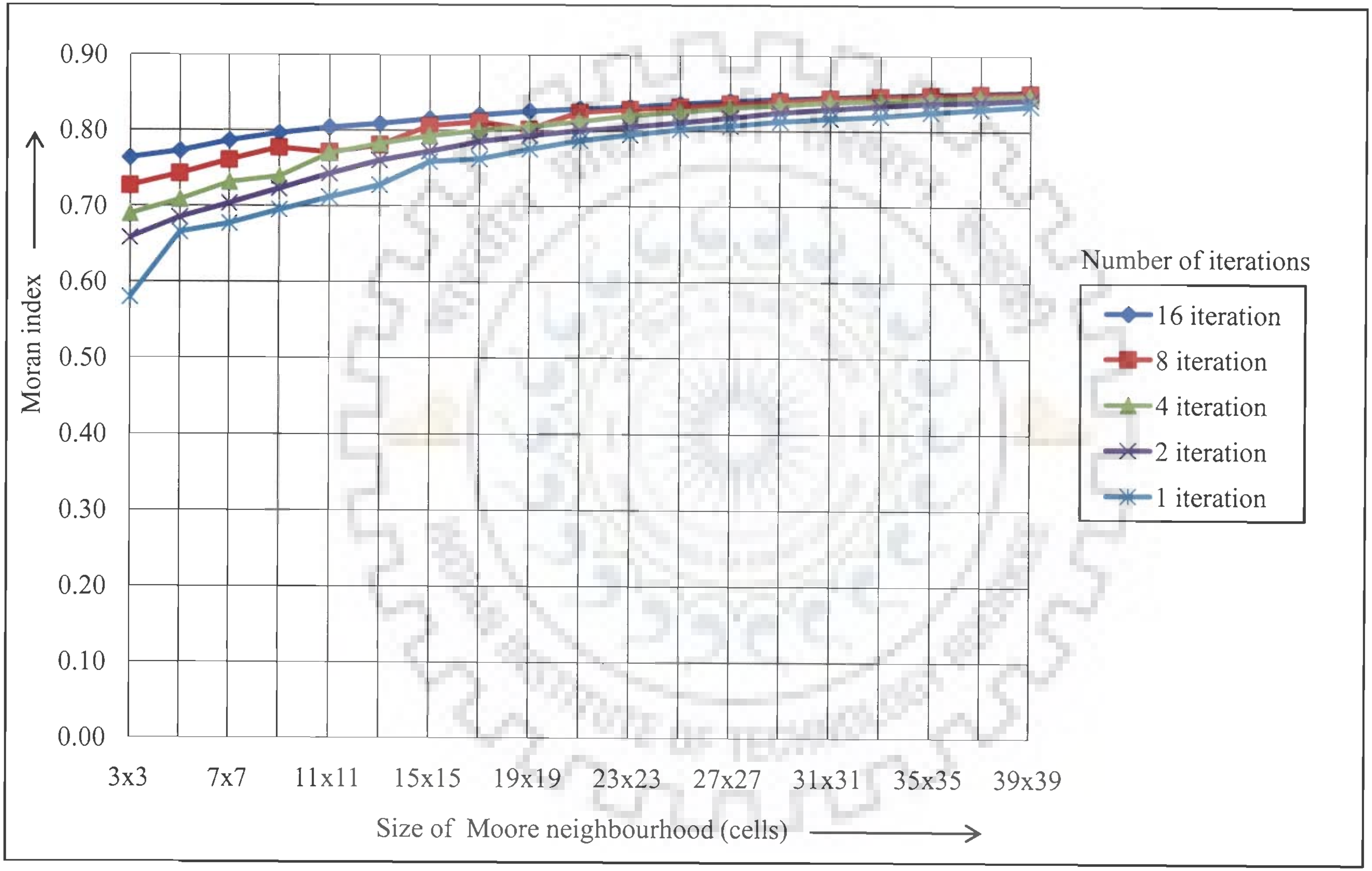

Figure 4.12: Moran Index as a function of different Moore neighbourhood sizes (Study area II)

Thus, a neighbourhood of large size with less number of iterations may produce growth patterns which are close to the actual growth patterns spatially.

Therefore, for study area II, which has a compact growth pattern, large neighbourhoods (i.e., 39x39 cells and 13x13 cells) produced the growth pattern as can be seen from the values of PCM and Moran Index. The model also required less number of iterations.

Thus, for areas having compact growth pattern, large neighbourhoods produced the best simulation results, while for areas having a dispersed growth pattern, small neighbourhoods produced the best results. Large number of iterations failed to increase the accuracy of the models. The increase in number of iterations resulted in a more compact growth pattern as compared to the actual growth pattern.

4.6 Future urban growth simulation

4.6.1 Study area I

Having defined the calibration parameters of the model, future urban growth trends have been found by execution of calibrated MCE-CA model for next 4 years and 10 years. The findings from model calibrations for the period 1997-2001 clearly indicate that 5x5 cells von–Neumann neighbourhood and 16 iterations produced the highest PCM. Further, comparison of simulated growth with actual one on spatial basis using Moran index shows that the calibration of model with 5x5 cells Von Neumann neighbourhood and 1 model iteration has resulted in exact matching of simulated growth with that of actual growth.

However, since urban growth is a stochastic process, the emphasis is usually placed on predicting the patterns of the urban growth rather than the urban growth on a particular location or point. Therefore, the model parameters which have produced realistic urban growth spatially, as identified on the basis of Moran index, have been used for simulation of urban growth in future. For this, two time windows *viz*, 2001-2005 years and 2001-2011 years, have been selected. Figure 4.13a shows the urban growth simulated by the model for the period 1997-2001. A comparison of the simulated and actual growth (Figure 4.13b) shows that the model is able to simulate the growth pattern occurring in the main city (around the city core), where the growth has taken place in a contiguous and dense manner. However, in the city fringe areas where the growth has taken place in a dispersed and isolated manner with development extending far from the core without notable concentrations or nuclei, especially in the west and south east directions of study area, the model has not been able to simulate the urban growth accuracy

Fortunately, the actual urban growth during 2001-2005 is also known. Therefore, the predictions for this period, as derived from the model, can also be validated. Thus, the calibrated model is executed for the two time windows using 5x5 cells Von Neumann neighbourhood and 1iteration for urban growth simulations.

The PCM for the simulated growth for the period 2001-2005 has been obtained as 42% which is higher than that obtained for the period 1997-2001. Similarly, the Moran index for the simulated growth for 2001-2005 has been obtained as 0.30, which matches with the Moran Index of 0.33 for the actual growth during this period. This shows that the calibrated model has been able to predict the urban growth accurately for the 4 years period of 2001-2005. The future urban growth predicted for this period is shown in Figure 4.14a. On comparing the simulated urban growth with actual growth (Figure 4.14b) for 2001-2005, it can be observed that the model is able to simulate the growth pattern in the main city where growth has occurred in the form of densification of existing built-up areas. The model is also able to simulate, to some extent, the pattern of urban growth taking place in the fringe areas mainly in the north, south east and west directions of the study area.

These figures also corroborate the findings that the model can successfully predict urban growth in future. Hence, the calibrated model is executed again for the period 2001-2011 to predict urban growth in next 10 years. The predicted urban growth from the model is shown in Figure 4.15. From this figure, it can be deduced that in the future the city will grow mainly in the south and south east directions. In addition, the densification of existing built-up areas may also. However, most of the area in the north direction is occupied by reserved forest, which is further compounded by hilly topography, whereas in the west direction, a large area is occupied by defence establishments and the tea gardens. Therefore, these two directions do not have much potential to attract future urban growth. While the land between the south and south east direction is mainly under agriculture and has a dense road network. The national highways connecting the city to other parts of the state are also located in the south and south east directions. Therefore, due to their good connectivity and availability of land for future urban growth, this area has a high potential to attract future urban growth. As observed from the field conditions in the current year (i.e., 2008), the area between the south and south east direction is experiencing a rapid growth, with a number of housing complexes and other infrastructure facilities coming up in these areas, thus validating the predictions made by the model. In the existing built-up areas, growth is taking place in the form of filling up of vacant pieces of land and by subdivision of large tracts of land holdings, resulting in densification of existing built-up areas, as predicted by the model.

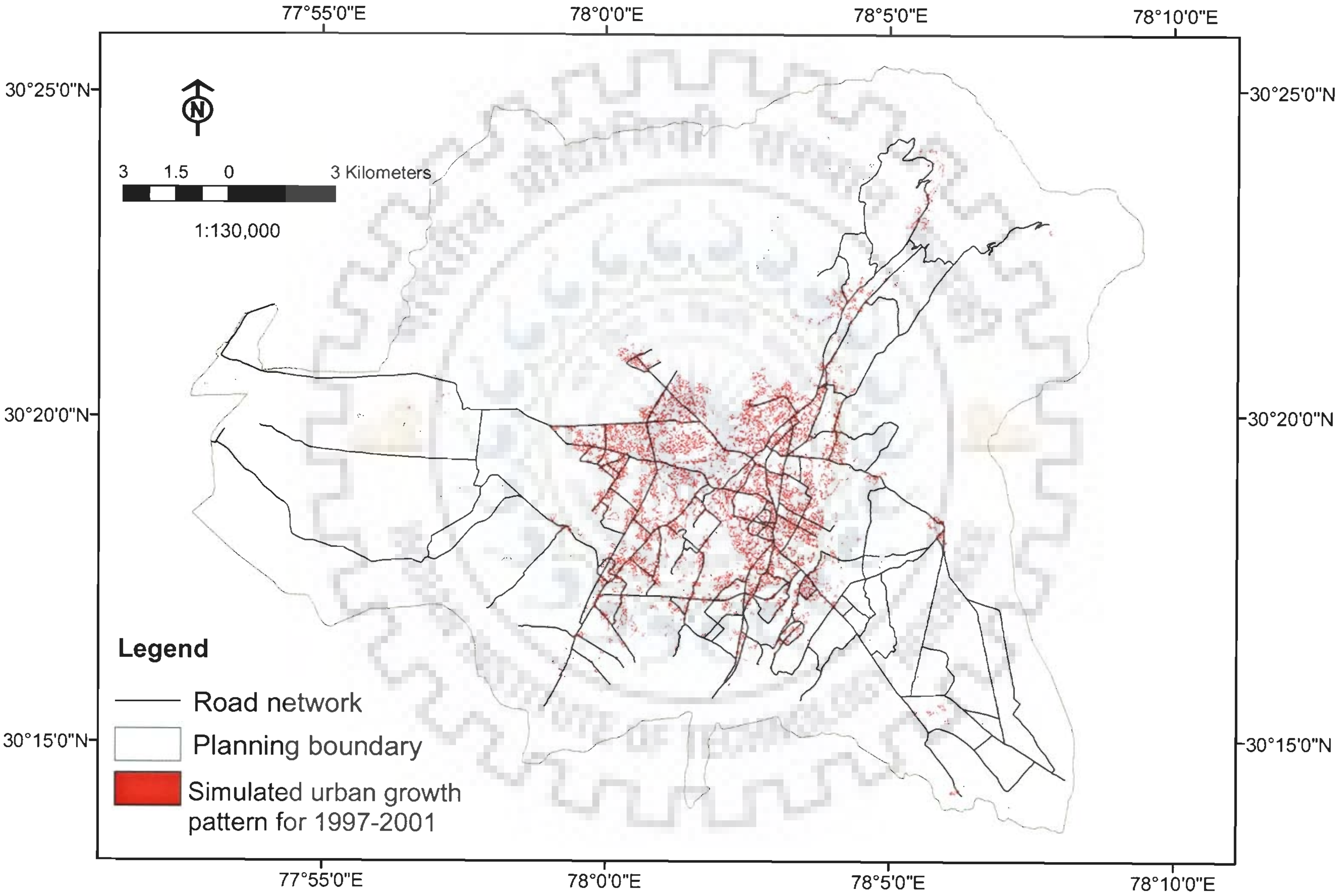

Figure 4.13a: Simulated urban growth pattern for 1997-2001 (study area I)

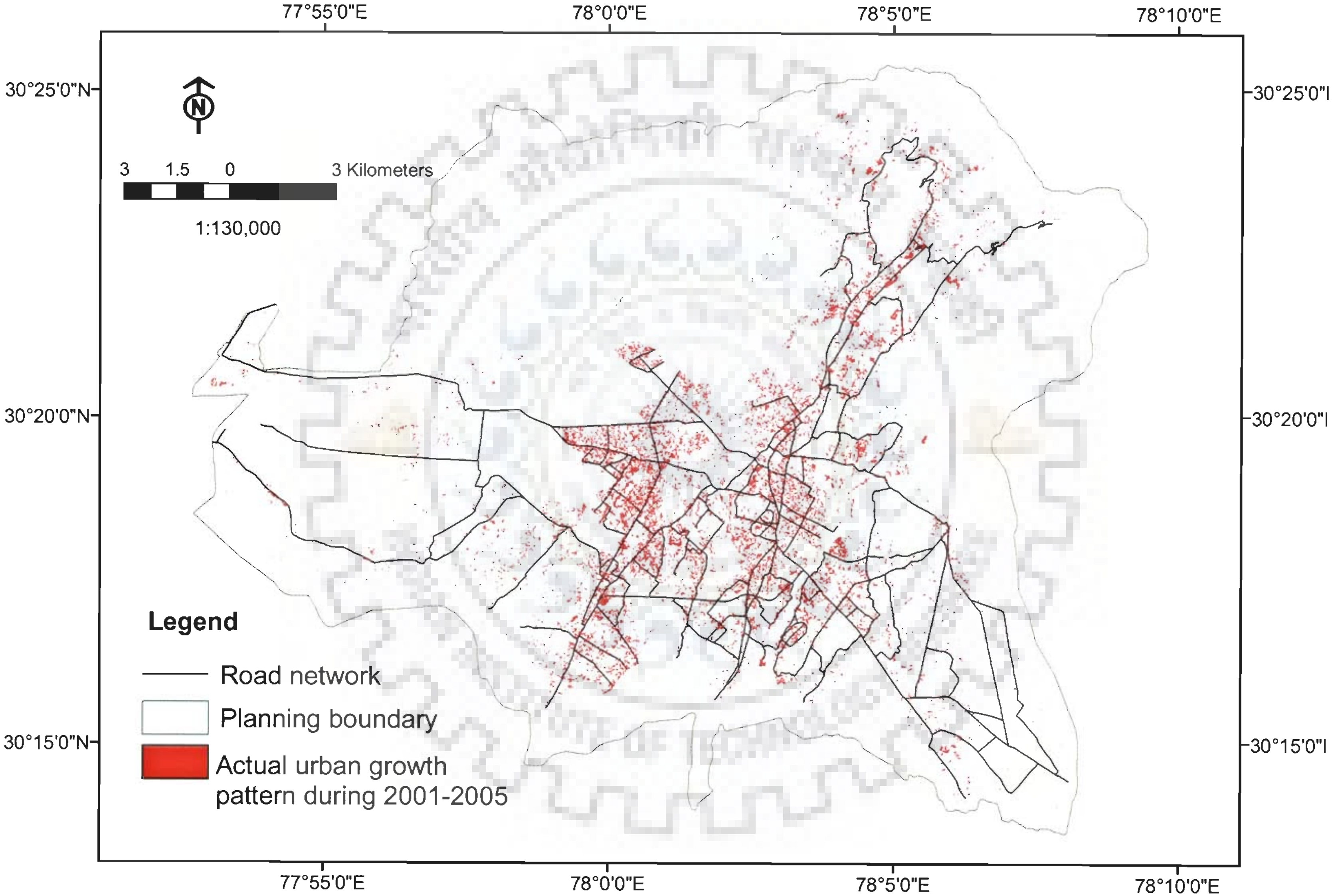

Figure 4.13b: Actual urban growth pattern during 1997-2001 (study area I)

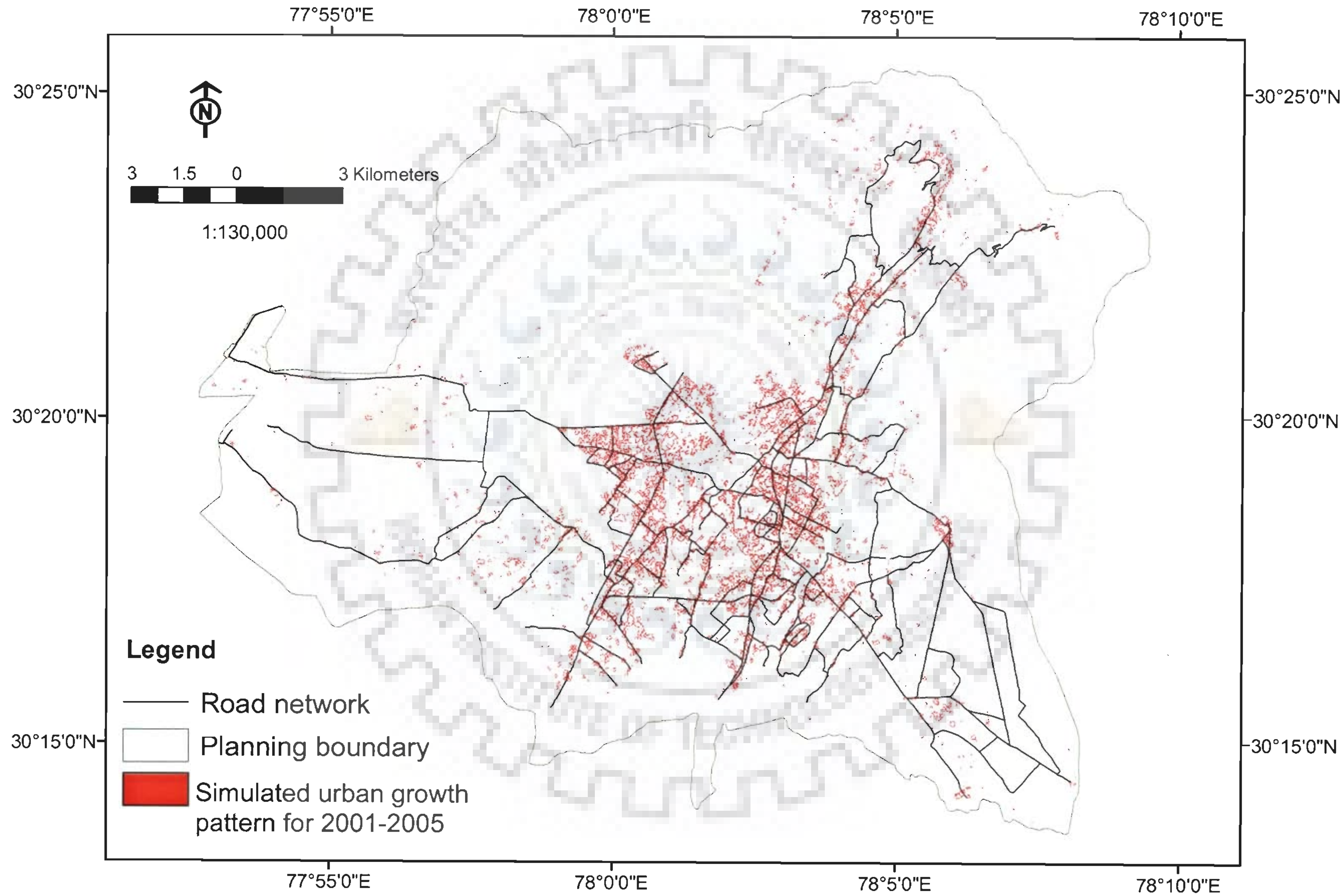

Figure 4.14a: Simulated urban growth pattern for 2001-2005 (study area I)

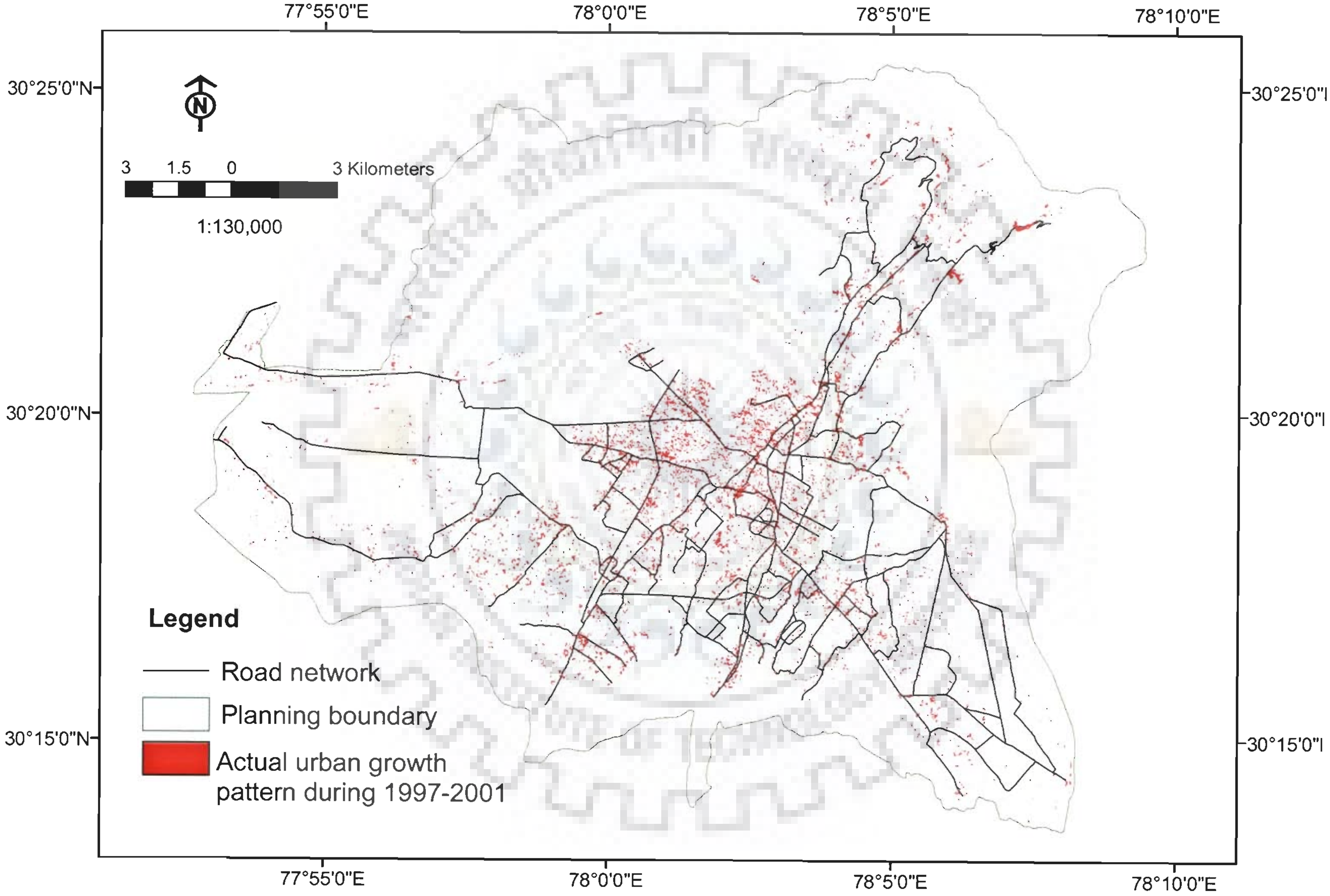

Figure 4.14b: Actual urban growth pattern during 2001-2005 (study area I)

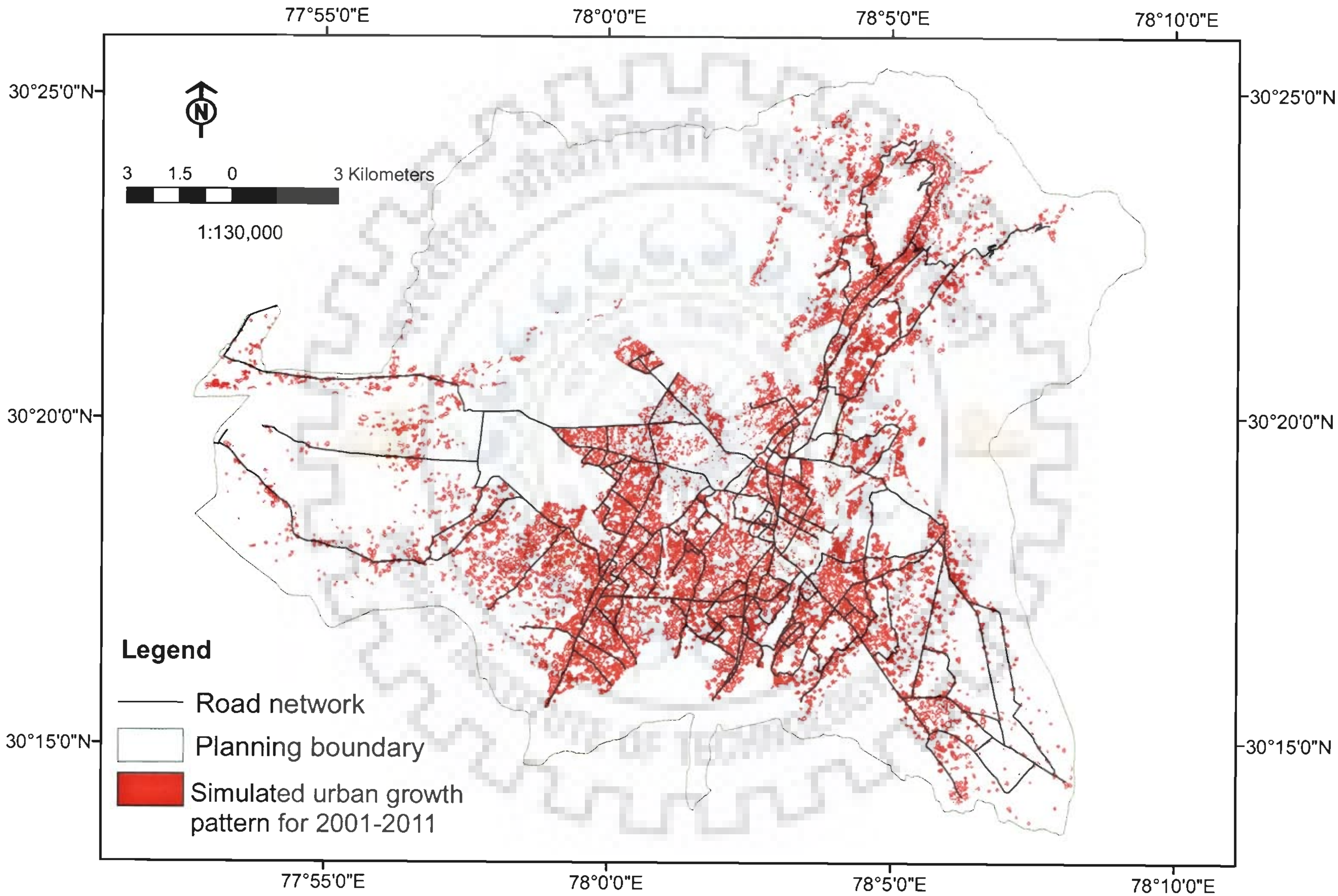

Figure 4.15: Simulated urban growth pattern for 2001-2011 (study area I)

4.6.2 Study area II

The calibrated MCE-CA model for the period 1993-2001 is executed to predict the future growth trends for next 10 years. The calibration results for the period 1993-2001 indicate that 39x39 cells Moore neighbourhood and 1 model iteration produced the maximum PCM on cell by cell basis. Further, when the simulated urban growth is compared with the actual growth on spatial basis using Moran Index, the calibration of the model with 13x13 cells Von Neumann neighbourhood and 4 model iterations produced exact matching of simulated growth with the actual growth.

Thus, Moore neighbourhood produced a higher accuracy in terms of cell by cell comparison as indicated by higher value of PCM. In terms of comparison on a spatial basis, Von Neumann neighbourhood was able to predict the spatial pattern more accurately as the Moran Index match with that of actual growth. The utility of a model is in its ability to predict the future urban growth pattern, if not the exact location of urban growth, since it is a stochastic process. Therefore, the model parameters 13x13 cells Von Neumann neighbourhood and 4 iterations have been selected for future simulation of urban growth in the study area.

The urban growth simulated for the period 1993-2001 using the calibrated parameters is shown in Figure 4.16a. A comparison of the simulated urban growth with the actual growth (Figure 4.16b) that occurred during that periods reveals, that the model is able to simulate the actual urban growth pattern which has taken place in a contiguous and concentric manner around the existing built-up area. However, some growth has taken place in an isolated and patchy form in the city fringe areas, mainly in the south and north east directions. The model is not able to predict these types of growth quite accurately. Thus, similar to study area I, the model is able to simulate the growth pattern in areas having a compact, dense and contiguous growth (city core) more accurately as compared to the areas which have a dispersed and isolated growth pattern (city fringe areas).

The calibrated model is implemented to predict the urban growth for next 10 years during the period 2001-2011 (Figure 4.17). It can be concluded from this figure, that the future urban growth may take place in a compact form and contiguous to the existing built-up areas. The area in the east direction is mainly occupied by defense establishments therefore, not much of future growth is expected in this direction. The areas in the north, north west, south and south east may experience more growth, as these areas are well served by the road network and most of the roads connecting the city to other parts of the state are located also in these areas. Growth is also expected to occur around patches of built-up areas located in vicinity of the main city. According to the model, these areas may grow in future and finally merge with the city. As observed from the existing growth trends in the current year (i.e., 2008), the city is growing mainly in the north and south directions with a number of residential areas and other facilities coming up in these areas. Besides growth is also taking place around the areas which have developed in a leap frog manner around the city. These field observations also validate the predictions made by the model for 2011.

The subjectivity in the MCE-CA model especially during, suitability map creation can be reduced by using techniques like ANN. The next chapter discusses an ANN based CA model for the same study areas, and compares the results obtained with the present ones to demonstrate the usefulness of objective techniques such as ANN in CA modelling.

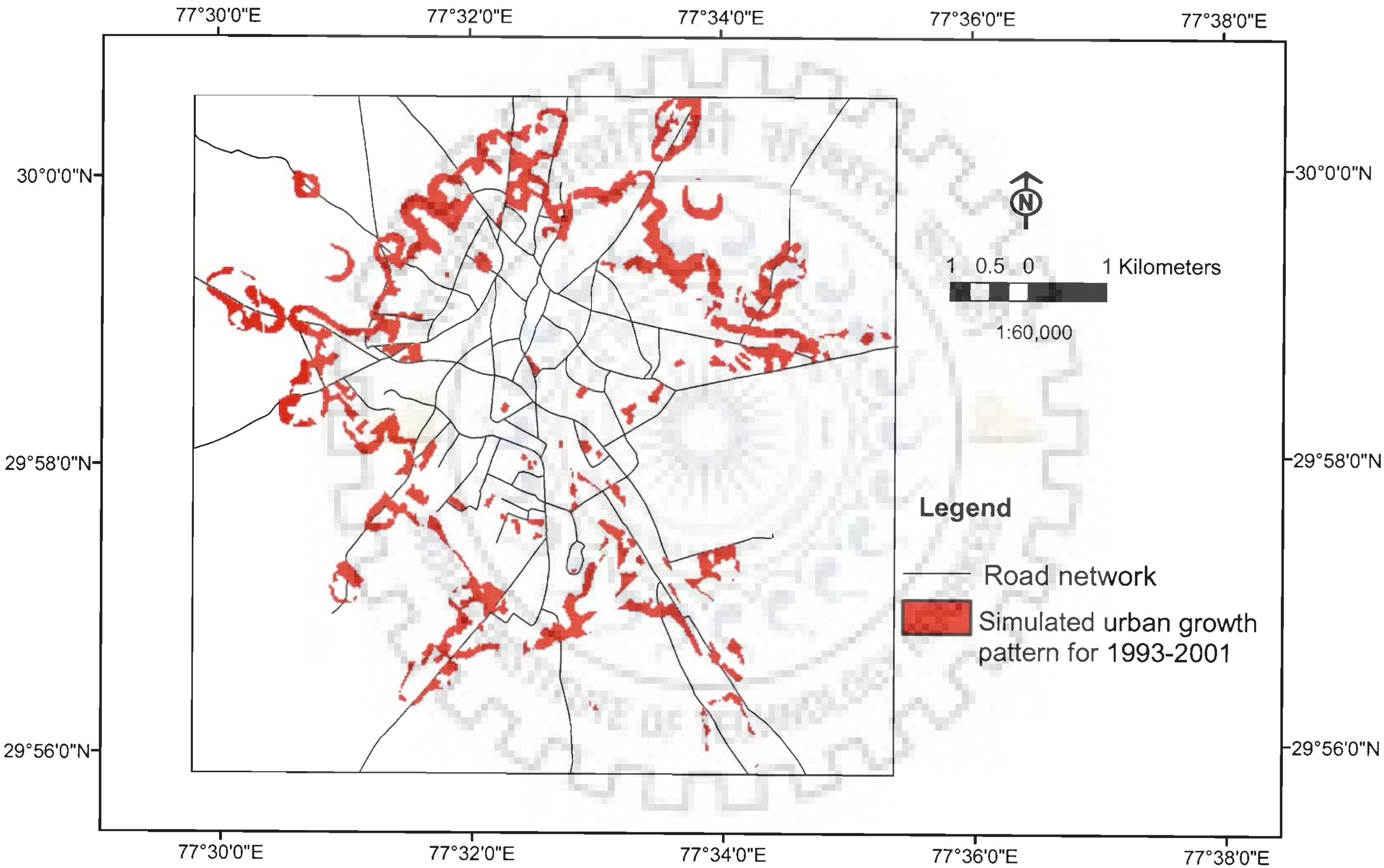

Figure 4.16a: Simulated urban growth pattern for 1993-2001 (study area II)

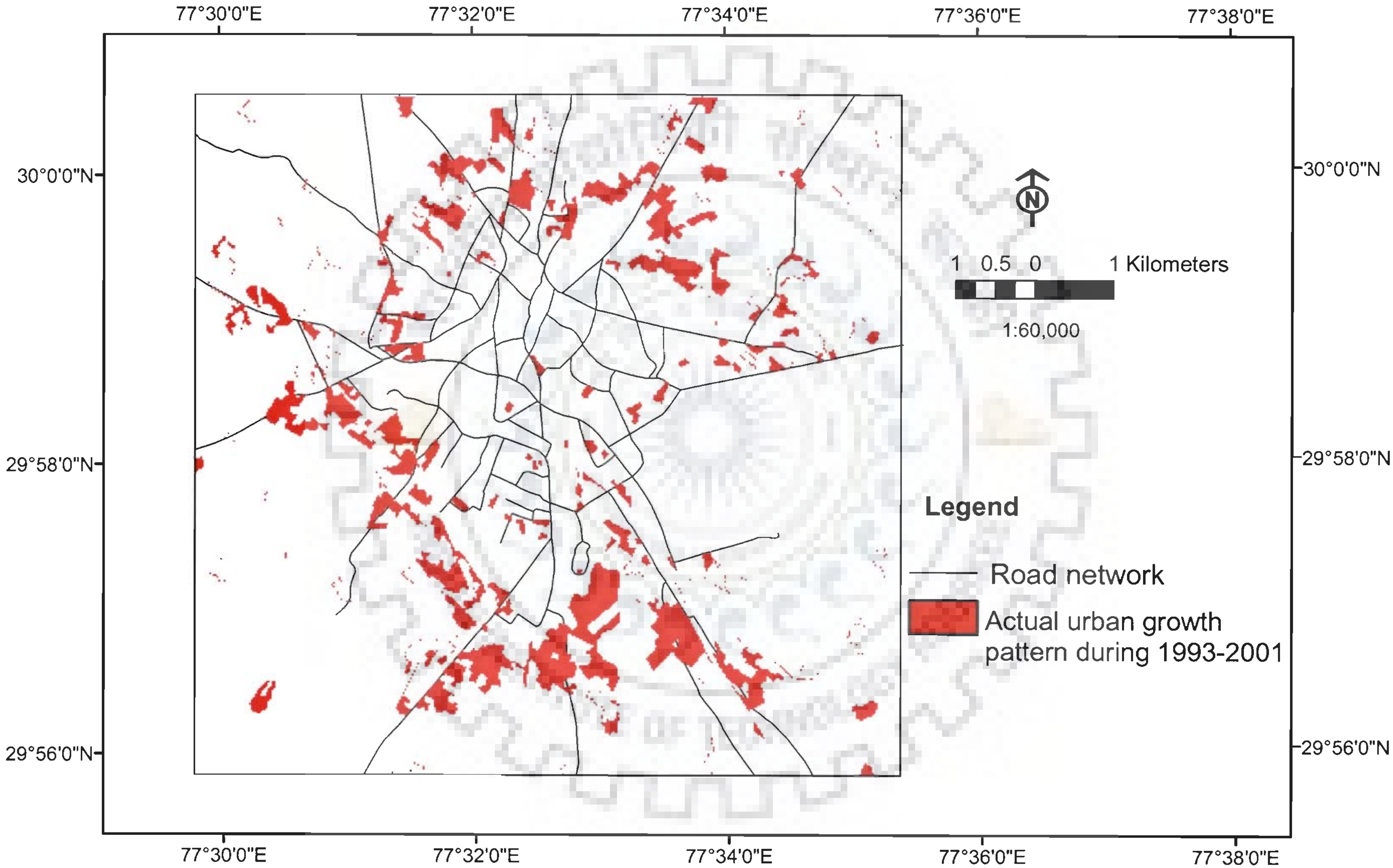

Figure 4.16b: Actual urban growth pattern during 1993-2001 (study area II)

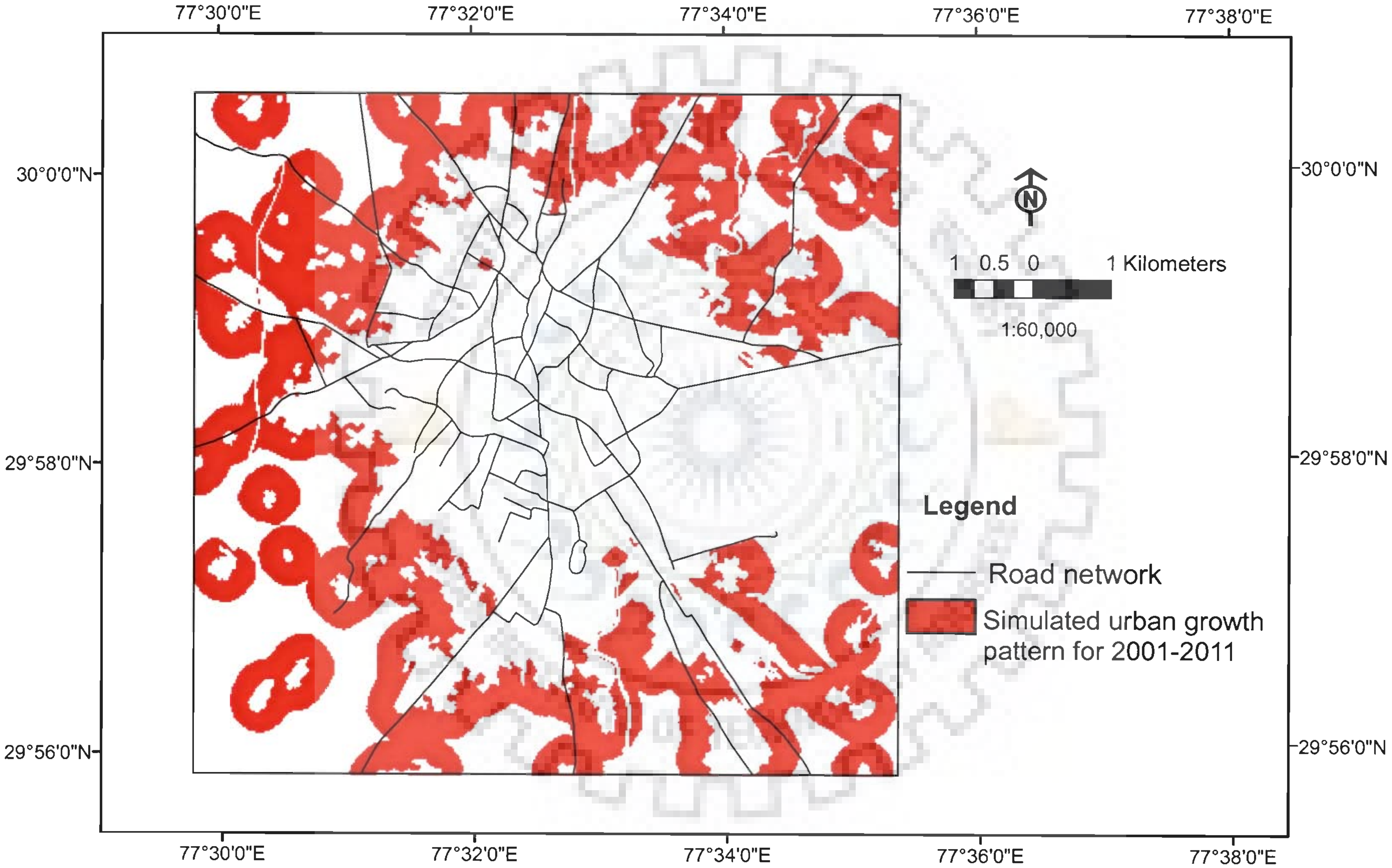

Figure 4.17: Simulated urban growth pattern for 2001-2011 (study area II)

1996, 1997), hazard zonation (Arora *et al.*, 2004; Kanungo *et al.*, 2006), land use modelling (Pijanowski *et al.*, 2002a, 2002b, 2005). Unlike the commonly used analytical methods, ANN has following advantages (Openshaw *et al.*, 1997, 2000; Haykin, 1999),

i) It makes no assumptions regarding the distributional properties of the data

ii) Mixtures of data types can be used.

iii) There are no restrictions on using non numeric data.

iv) It can solve highly non linear problems.

v) It can use many variables some of which may be redundant.

These features make ANN a promising technique for modelling nonlinear complex phenomena like urban growth assessment and prediction (Li and Yeh, 2001, 2002; Yeh and Li, 2002, 2003)

5.2.1 ANN architecture

In ANN, the basic processing elements are the neurons that work in parallel to transform input data into output entities. In order to increase the computing capabilities of ANN, the neurons are arranged in different layers. The neurons in each layer are connected to the neurons in the next successive layer and each connection carries a weight (Atkinson and Tatnall, 1997). This arrangement of neurons in layers and the pattern of connection within and in between these layers is called as ANN architecture. In the present study, the multilayer perceptron (MLP) feedforward ANN architecture has been used. The MLP consists of input, hidden and output layers consisting of neurons which are interconnected to each other layer wise. There are no interconnections between neurons within the same layer. Since the ANN is feedforward, a link is allowed from a neuron in layer i only to neurons in layer i+1 (Kavzoglu and Mather, 2003). The architecture of a three-layer MLP feedforward ANN is shown in

Figure 5.1. The black circles represent the neurons, in the input, hidden and output layers, while the lines represent the weighed connection between neurons in different layers. The ANN is described by a sequence of numbers indicating the number of neurons in each layer. For example, the ANN shown in Figure 5.1 is a **4-5-1** architecture ANN, i.e., it contains four neurons in the input layer, five neurons in the hidden layer and one neuron in the output layer.

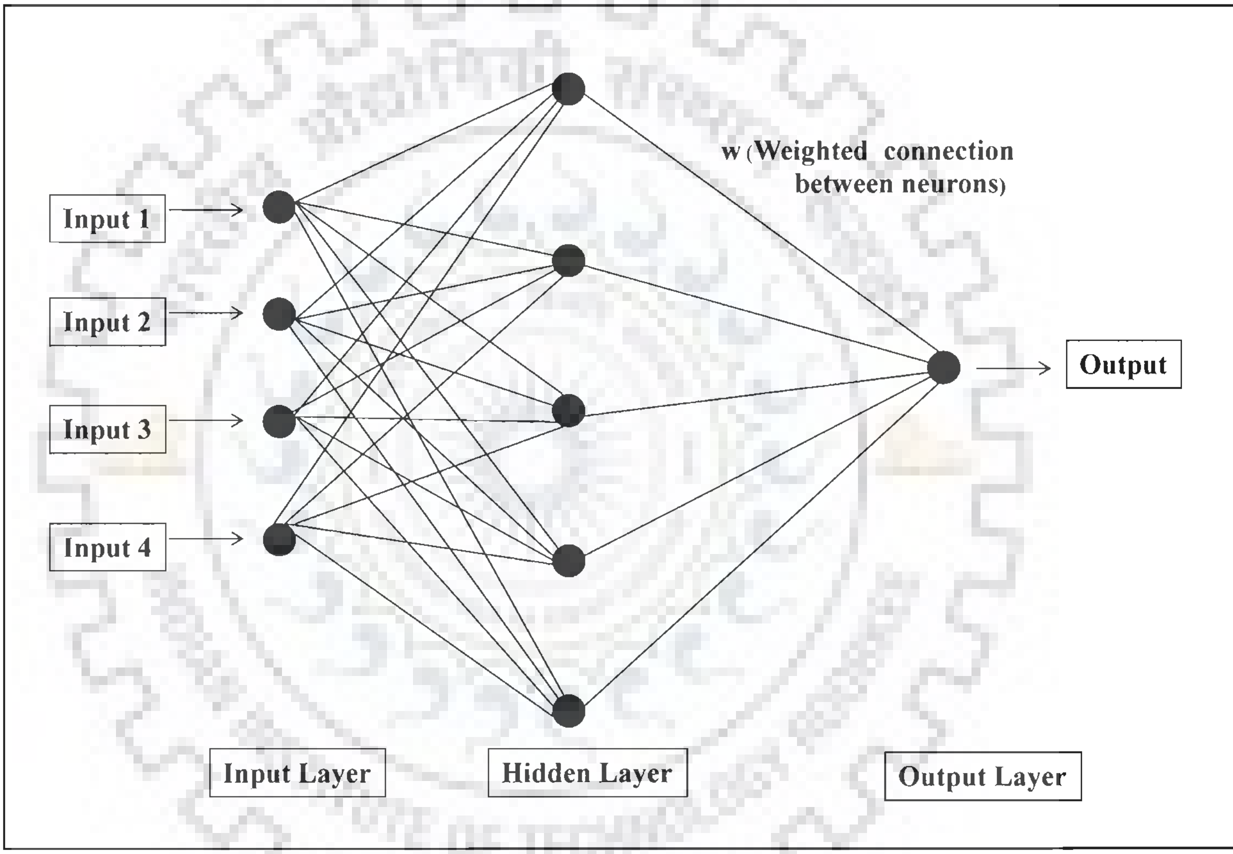

Figure 5.1: A MLP feedforward ANN architecture

The number of neurons in the input layer depends on the number of input data sources. The number of hidden layers and their neurons are often determined by trial and error or literature driven thumb rules. The number of neurons in the output layer depends on the number of class being mapped (Arora *et al.*, 1998, 2004; Kavzoglu and Mather, 2003; Kanungo *et al.*, 2006). For example, in the present case, classes will be built-up/ non built-up areas.

The neurons in the input layer only transmit data to the next layer, while the hidden and output layer neurons actively process the data. Each neuron in hidden and output layers, responds to the weighted inputs it receives from the connected neurons in the preceding input layer. If i is the sender neuron in the input layer and j is a receiver neuron in the next layer, then the weighted input (net_j) that neuron j receives is calculated as,

$$\text{net}_j = \sum_{i=0}^{n} I_i W_{ij} \qquad \text{....5.1}$$

where,

I_i = input signal from neuron i

W_{ij} = weight associated with connection between neurons i and j

net_j = weighted input at neuron j

The receiver neuron j generates an activation signal, in response to the net_j. The activation signal at each neuron becomes the input for next layer. Thus, all the hidden and output neurons collect the activation signals of the neurons in the previous layer and generate an activation signal as the input for the successive neuron. The activation signal is generated via a transfer function. Any differentiable non linear function can be used as a transfer function, but a sigmoid function is generally used (Equation 5.2) (Hayken, 1999), since the sigmoid function has useful properties like monotonicity and continuity which help in increasing the learning capacity of the ANN (Kumar, 2004; Sivanandam *et al.* 2006). The sigmoid function constraints the outputs of the ANN between 0 and 1.

$$O_j = f(net_j) = \frac{1}{1+e^{-net_j}} \quad \text{....5.2}$$

Where,

O_j = activitation signal

net_j = weighted sum of neuron inputs

5.2.2 Training of ANN

During training, the ANN is taught the salient characteristics of the dataset. Once the ANN learns the characteristics of the dataset, it can be then be used for generating outputs at unseen data. During ANN training, the network weights are continuously updated till the weights are optimized. Using these optimum network weights, the outputs for unseen data are generated (Haykin, 1999; Kumar, 2004).

In the proposed ANN-CA model, during network training, once the ANN learns the state of a cell at time t+1 as a function of various driving factors existing at t, the ANN will be able to predict the state of the cell for time t+2.

Typically, the backpropagation (BP) learning algorithm proposed by Rumelhart et al. (1986) is used for training the ANN and has been used here also. In this algorithm, the ANN weights are randomly initialized and the training data is fed to the input neurons of the network. The hidden neurons collect the activation signals of the neurons in the previous layer and generate an activation signal as the input to the next layer. The outputs generated at the output neurons, are compared with the target outputs (i.e., known output as obtained from reference data). The error (difference) between the ANN outputs and the target outputs is back propagated through the ANN and is minimized by updating the interconnection weights between the layers. This process of backpropogating the errors is repeated iteratively with weights being recomputed in each iteration, till the error is minimized and the adjusted weights are stored. The general steps in the BP algorithm can be summarized as,

i) Select a pattern X_i from the training datasets and present it to the ANN.

ii) Compute activation and output signals of input, hidden and output neurons respectively.

iii) Compute error (e) by comparing the ANN generated outputs with the target outputs.

iv) Compute the change in the connection weights based on the errors, as given in Equation 5.3 and 5.4. The ANN weights are updated iteratively until the error falls below a predefined threshold value

$$w_{ih}^{k+1} = w_{ih}^{k} + \Delta w_{ih}^{k} \quad \ldots 5.3$$

$$= w_{ih}^{k} + \eta \left(\partial e / \partial w_{ih}^{k}\right) \quad \ldots 5.4$$

where,

w_{ih}^{k+1} = weight at iteration k+1 between neuron i and h

w_{ih}^{k} = weight at iteration k between neuron i and h

Δw_{ih}^{k} = Change in weight in iteration k

η = learning rate

e = error term

η is called as *learning rate* and is a positive constant, which controls the speed of the learning process. The learning rate determines the change in weight (Δw_{ih}^{k}) at iteration k, in search for the global minimum of the error function in the training process. If the learning rate is set too high, then Δw_{ih}^{k} will be large and the ANN will become unstable and fail to converge. If the learning rate is set too low, then Δw_{ih}^{k} will be small, this will result in longer training times and there is a likelihood of the ANN, getting trapped in a local minimum (Kavzoglu and Mather, 2003).

Therefore, in order to increase the rate of learning while maintaining the ANN stability a momentum term (α) is introduced into weight update process. The momentum term uses the previous weight configuration (Δw_{ih}^{k-1}) to determine the direction of search for the global minimum of the error, as given in Equation 5.5 (Kumar, 2004). A careful selection of these two parameters is necessary during the ANN training.

$$w_{ih}^{k+1} = w_{ih}^{k} + \eta \, (\partial e / \partial w_{ih}^{k}) + \alpha \, \Delta w_{ih}^{k-1} \qquad \ldots 5.5$$

where,

w_{ih}^{k+1} = weight at iteration k+1 between neuron i and h

w_{ih}^{k} = weight at iteration k between neuron i and h

Δw_{ih}^{k-1} = Change in weight in iteration k-1

α = momentum term

η = learning rate

e = error term

Once the network is trained, an independent database known as testing data is fed to ANN to generate network output, which is then compared with target outputs to determine the accuracy of network. By varying the number of hidden layers and their neurons, the ANN is run several times to determine the most appropriate ANN architecture, based on training and testing dataset accuracy (Kanungo *et al.*, 2006)

Chapter 5

ANN based CA model

5.1 Introduction

In the MCE-CA model (chapter 4), the urban growth suitability map is produced on the basis of numerical scores assigned to the factors driving urban growth. These numerical scores were assigned depending on the ability of the factor to influence the urban growth process. However, this decision is subjective in nature and depends on the individual's knowledge and experience, which leads to subjectivity in MCE-CA model.

In order to reduce this subjectivity, an ANN based CA (ANN-CA) model has been developed. The objective is to demonstrate the advantage of using ANN in urban growth modelling. As, it allows to reverse the modelling approach, by learning the urban growth suitability values directly from the database instead of the user defining them subjectively (Diappi *et al.*, 2002; Fischer *et al.*, 2000), this makes the model simpler and objective as compared to the MCE- CA model.

5.2 Concept of ANN

ANN is a useful technique for regression and classification problems and has been successfully applied in a number of fields, such as, image classification (Arora *et al.*, 1998, 2000; Arora and Mathur 2001; Foody, 1995, 1996a, 1996b, 2001, 2004; Foody and Arora,

5.2.3 Stopping criteria for ANN training

Theoretically, the ANN is assumed to be trained, when all the patterns produce correct outputs. However, this requires a number of ANN iterations and time. Besides, the ANN may also get over-trained when the number of iterations increases. The over-trained ANN gives high accuracy on the training data, but low accuracies on other unseen data. In order to avoid these problems, other stopping criteria have also been defined for the ANN. The three stopping criteria used in the present study are listed below. The training ANN stops when any of these three criteria is met,

i) When the error falls below a threshold value.

ii) A specified number of ANN iterations have been performed.

iii) When the ANN starts over-training.

During the training of ANN, a validation dataset is used to prevent over-training. Initially, when the training of ANN is being performed, the error over training and the validation data decreases up to a point. After which the error on the training dataset keeps on decreasing, whereas the error on the validation dataset starts increasing as shown in Figure 5.3. This indicates that the ANN has become over-trained, and is not able to generalize. Therefore, the ANN training is stopped at the point when the error on the validation dataset begins to increase as shown in Figure 5.2.

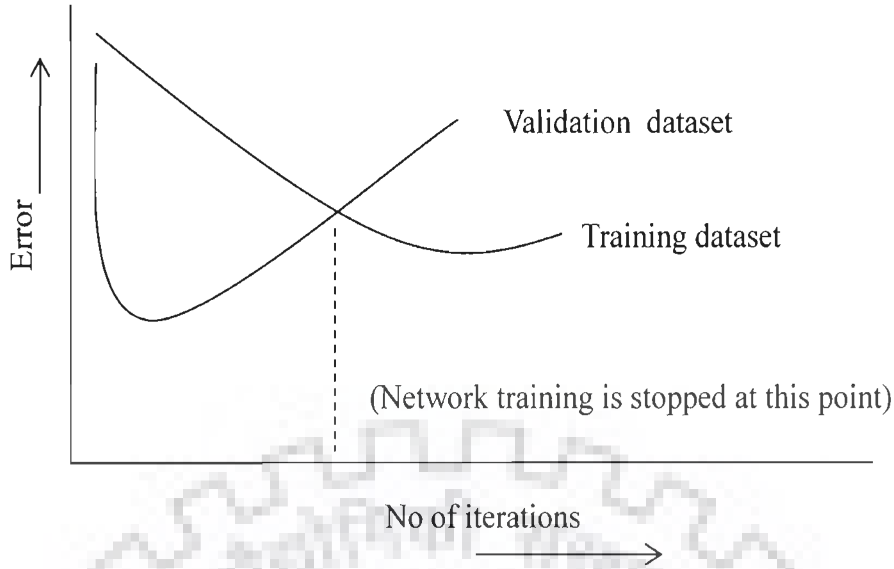

Figure 5.2: Stopping criteria to prevent the over-training of ANN

5.3 ANN-CA model

In CA models, the transition rules are defined subjectively depending on the knowledge and experience of the user. Secondly, it is extremely time consuming to find proper values of the parameters for the CA models during calibration. To get over these limitations, an ANN-CA model has been proposed. The model does not require generation of detailed and explicit transition rules and the calibration time is also reduced.

Similar to the MCE-CA model, the proposed ANN-CA model is based on the dichotomy of built-up and non built-up areas, and simulates transition from non built-up to built-up areas with no reverse process. So, the existing built–up areas and areas that do not have any development potential e.g., restricted areas, reserved forests, water bodies, existing built-up areas, public grounds (discussed in chapter 2) are treated as exclusionary areas, and the model makes no prediction of urban growth in these areas.

The user has to provide training data pertaining to built-up and non built-up area so that the ANN can learn the growth trend from these dataset. The trained ANN is then used for finding the development potential of each cell in the study area. Since CA are recursive in nature and involve number of iterations, so cells that have development potential above a certain threshold only transit to built-up in each iteration. Based on these cells, the built-up /non built-up map and other factor maps are updated. The ANN determines the development potential of cells based on the updated site attributes iteratively till the model's boundary conditions are fulfilled.

The neural network processing has been implemented using Neural Network Tool Box of MATLAB software. A schematic diagram of implementation of ANN-CA model is shown in Figure 5.3. Following steps are followed in implementing the ANN-CA model,

i) Generation of maps corresponding to factors driving urban growth in study area
ii) Generation of maps depicting actual urban growth in study area
iii) Generation of training and testing dataset from the data created in step i) and ii)
iv) Design of ANNs with different network architectures
v) Training and evaluation of ANNs
vi) Selection of optimal ANN architecture
vii) Stopping criteria for the model
viii) Estimation of the growth potential using optimal ANN
ix) Masking of exclusionary areas
x) Allocation of cells from non built-up to built-up
xi) Updation of built-up/non built-up area and other factor maps
xii) Model iterations.

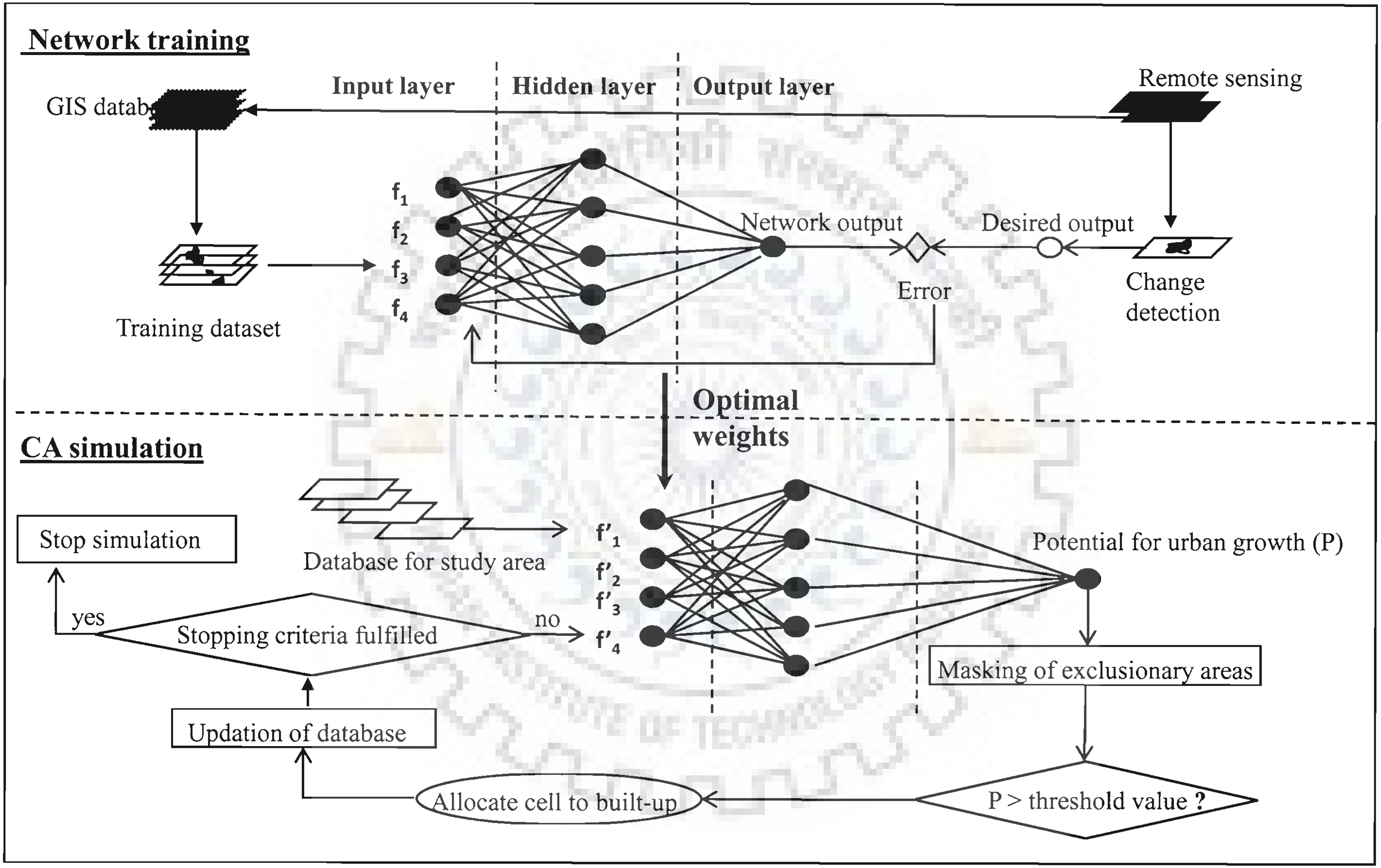

Figure 5.3 : A schematic diagram of the ANN-CA model

The proposed ANN-CA model is implemented for study areas I and II. For study area I the model is calibrated for period 1997-2001 and for study area II, it is calibrated for the period 1993-2001. The detailed description of the model steps is as follows,

5.3.1 Generation of maps corresponding to factors driving urban growth in study area

As discussed in chapter 4, urban growth in both the study areas is expressed as a function of following four raster maps created in GIS,

i) Euclidian distance of each cell from the nearest road (f1)

ii) Euclidean distance of a cell from the nearest built-up (f2)

iii) Euclidian distance of each cell from the city core (f3)

iv) Amount of built-up in neighbourhood (f4)

For generating the f4 map (i.e, amount of built-up in neighbourhood), the neighbourhood size which produced the most accurate urban growth simulation for study areas I and II in MCE-CA model have been used. Thus, 5x5 cells Moore and Von Neumann neighbourhoods, for study area I and 13x13 cells Moore and Von Neumann neighbourhods for study area II have been selected (refer chapter 4). Thus, two datasets based on both the selected neighbourhoods have been created for study areas I and II. Table 5.1 provides a description of these datasets.

Table 5.1: Datasets created using Von Neumann and Moore neighbouhood (study areas I and II)

Study area I	
Dataset I	i)Amount of built up in neighbourhod **(Calculated using 5x5 Moore neighbourhood)** ii) Distance to nearest built-up iii) Distance to city core iv) Distance to nearest road
Dataset 1I	i)Amount of built up in neighbourhod **(Calculated using 5x5 Von Neumann neighbourhood)** ii) Distance to nearest built-up iii) Distance to city core iv) Distance to nearest road
Study area II	
Dataset I	i)Amountof built up in neighbourhod **(Calculated using 13x13 Moore neighbourhood)** ii) Distance to nearest built-up iii) Distance to city core iv) Distance to nearest road
Dataset II	i)Amount of built up in neighbourhod **(Calculated using13x13 Von Neumann neighbourhood)** ii) Distance to nearest built-up iii) Distance to city core iv) Distance to nearest road

All the data pertaining to all the layers have been normalized from 0 to 1, before these are input to neural networks (Kumar, 2004). Scaling the variables also makes them compatible with the sigmoid activation function, which produces a value between 0 and 1. In the present study for normalization, each cell value in a map has been divided by the maximum cell value in the map.

5.3.2 Generation of maps depicting actual urban growth in study area

For study area I, a map depicting cells that transit from non built-up to built-up area during 1997-2001 is generated using remote sensing data and GIS tools as discussed in chapter 3. Similarly, for study area II, a similar map has been prepared for period 1993-2001

5.3.3 Generation of training and testing dataset

i) Training data

The ANN learns the growth patterns of the study area I and II, from the training dataset directly without any statistical parameters such as, mean, standard deviation, variance, co-variance derived from them. Hence, the size and characteristics of the training data has a significant impact on the performance of ANN. In the present study, the training data has been generated based on reference data, as discussed in section 5.3.2. The training data consists of two types of cells,

a) Non built-up cells that transit to built-up

b) Non built-up cells which did not transit to built-up.

A cell is assigned a target value of 1 if it transits from non built-up to built-up, and 0 if it remains non built-up during the calibration period.

Table 5.2 shows an example of the training dataset. For samples 1 to 5, the values under f1,f2,f3 and f4 columns show the attributes value at a cell corresponding to the four factors, while the target value indicates whether the cell transits to built-up or not (1 or 0).

A total of 2400 training samples have been selected based on equal stratified random sampling. Out of these 2400 samples, 1200 samples belong to cells which were non built-up and transit to built-up, while 1200 belong to cells that remained non built-up. Thus, for study area I, two training datasets are generated corresponding to Moore and Von Neumann neighbourhoods. Similarly, two training datasets have been prepared for study area II.

Table 5.2: Example of training dataset consisting of cell attributes and the target value

	f1	f2	f3	f4	Target output
Sample 1	0.132	0.407	0.010	0.345	0
Sample 2	0.015	0.343	0.010	0.181	0
Sample 3	0.015	0.390	0.007	0.089	1
Sample 4	0.009	0.409	0.007	0.236	1
Sample 5	0.009	0.402	0.007	0.222	1

ii) Testing dataset

In order to determine the accuracy of ANN and hence to test its generalization, capabilities, a testing dataset of 1200 cells has been created in the same manner as the training data set. However the training and testing datasets are mutually exclusive, i.e., they do not have common samples (Foody and Arora, 1997). Thus, two testing datasets; one each for Von Neumann and Moore neighbourhood have been generated for both the study areas.

5.3.4 Design of ANNs having different network architecture

Different MLP feed forward ANN architectures have been designed, the basis of variations in network architecture is discussed in the following:

Input layer: The number of neurons in the input layer has been kept equal to the number of factors used in the creation of model. Hence, four neurons are kept in the input layer corresponding to the four maps representing data pertaining to four factors.

Hidden layer: The number of hidden layers and the number of neurons in each layer has been determined heuristically. A number of thumb rules exist but none is universally accepted, as each real life problem may be unique. ANN having small number of hidden neurons can not identify the internal structure of the data (a state known as under-fitting) and therefore produce lower accuracies. While ANN having large number of hidden neurons become overspecific to the training data (over-fitting or over-training the data). These over-trained ANN may give high accuracy on the training data, but perform badly in processing of unknown dataset.

In the present study, maximum two hidden layers have been used, as these are sufficient for most of the classification like problems (Kanellopoulos and Wilkinson, 1997; Arora *et.al.*, 2004). Different ANN architectures having single and double hidden layers have been generated, some of these networks are shown in Table 5.3. Out of the different ANN architectures, 3 ANNs having a single hidden layer with 4-3-1, 4-9-1 and 4-12-1 architectures are based on heuristics given by Kanellopoulos and Wilkinson (1997), Hush (1989), Hecht-Nielsen (1987), Wang (1994), Ripley (1993) and Paola (1994). Table 5.4 illustrates these thumb rules and the corresponding ANN architectures.

Output layer: There is one neuron in the output layer. Its value ranges from 0-1. A value of 1 indicates maximum potential for transiting from non built-up to built-up and 0 denotes the minimum potential. The intermediate values between 0 and 1, indicate different potential for transiting from non built-up to built-up area.

Table 5.3: ANN architectures based on trial and error

4-6-1	4-3-3-1	4-6-3-1	4-9-3-1	4-12-3-1	4-15-3-1	4-18-3-1	4-21-3-1
4-15--1	4-3-6-1	4-6-6-1	4-9-6-1	4-12-6-1	4-15-6-1	4-18-6-1	4-21-6-1
4-18-1	4-3-9-1	4-6-9-1	4-9-9-1	4-12-9-1	4-15-9-1	4-18-9-1	4-21-9-1
4-21-1	4-3-12-1	4-6-12-1	4-9-12-1	4-12-12-1	4-15-12-1	4-18-12-1	4-21-12-1
	4-3-15-1	4-6-15-1	4-9-15-1	4-12-15-1	4-15-15-1	4-18-15-1	4-21-15-1
	4-3-18-1	4-6-18-1	4-9-18-1	4-12-18-1	4-15-18-1	4-18-18-1	4-21-18-1
	4-3-21-1	4-6-21-1	4-9-21-1	4-12-21-1	4-15-21-1	4-18-21-1	4-21-21-1

Table 5.4: ANN architectures based on literature driven thumb rules

Thumb rule	Number of hidden neurons	ANN architecture
Hecht-Nielsen (1987)	$2N_i + 1$	4-9-1
Hush (1989)	$3N_i$	4-12-1
Ripley (1993)	$(Ni + N_o) / 2$	4-3-1
Wang (1994)	$2N_i /3$	4-3-1
Paola (1994)	$\dfrac{2 + N_o. N_i + \frac{1}{2} N_o (N_i^2 + N_i) - 3}{N_i + N_o}$	4-3-1
Kanellopoulos and Wilkinson (1997)	$3N_i$	4-12-1

* Number of input = N_i, Number of output = N_o (Note: Here N_i= 1 and N_o=4)

5.3.5 Training and evaluation of ANNs

The different ANN architectures have been trained using the training datasets, as discussed earlier. The backpropagation (BP) training algorithm given by Rumelhart et al. (1986) has been used to train these ANNs. The training process is initiated by assigning arbitrary connection weights, which are constantly updated until acceptable training data accuracy is achieved. Table 5.5 shows the network parameters and stopping criteria used during network training. These network parameters are based on the recommendation given Kavzoglu and Mather (2003), after rigorous experiments on different datasets. The adjusted weights are subsequently used to process the testing dataset, in order to find the generalization capability of the trained ANN. The performance of the networks is evaluated by determining the training and testing data accuracies in terms of percent correct or overall classification accuracy (Congalton, 1991).

Table 5.5: Network parameters and stopping criteria used during ANN training

1. Training parameter	**Value used**
1.1 Learning rate	0.10
1.2 Momentum factor	0.50
2. Stopping Criteria	
2.1 Acceptable error	0.01
2.2 Maximum number of iterations	10,000
2.3 Validation dataset	1200 samples

5.3.6 Selection of optimal ANN architecture

The acceptable ANN is the one for which the difference between the training and testing accuracy is minimum, as it reflects the ANN is able to train accurately as well as generalize. For study area I, the 4-9-1 and 4-6-1 ANN architectures based on literature driven thumb rules and the 4-20-1 ANN architecture based on trial and error produced the most accurate outputs. Table 5.5 shows the training and testing accuracies for these ANNs and the nature of dataset used.

For study area II, the 4-9-1 and 4-3-1 architecture based on literature driven thumb rules and the 4-12-21-1, architecture based on trial and error, produces the most accurate outputs. Table 5.5 shows the training and testing accuracies for these ANN and the dataset used.

The weights of these optimal networks for study area I and II are saved for future subsequent use.

Table 5.6: Acceptable ANN architectures (study area I)

Network architecture	Training data accuracy	Testing data accuracy	Dataset from which training data is created
4-9-1	78%	74%	Dataset II
4-6-1	79%	73%	Dataset II
4-20-1	71.2%	67.7%	Dataset I

Table 5.7: Acceptable ANN architectures (study area II)

Network architecture	Training data accuracy	Testing data accuracy	Dataset from which training data is created
4-12-21-1	76.8%	74.3%	Dataset II
4-9-1	73.2%	70.7%	Dataset II
4-3-1	70.4%	69.1%	Dataset I
4-12-21-1	75.2%	73.2%	Dataset I

5.3.7 Stopping criteria for the model

For study area I, the model has been, implemented for the period 1997 to 2001. The total number of cells that transit from non built-up to built-up areas during the period is found. These cells define the stopping criteria for the model. The model is stopped stops, when the total number of cells that transit from non built-up to built-up area in all model iterations equals the number of cells that have actually transited to built-up area in 1997-2001. This ensures the number of cells which transit from non built-up to built-up area during processing are same as the actual cells transiting from non built-up to built-up during the period selected.

Similarly for study area II, the model has been calibrated for the period 1993 to 2001. The built-up/non built-up maps of year 1993 and 2001 have been used to find the actual number of cell that transit from non built-up to built-up area, which are subsequently used for defining the stopping criteria .

5.3.8 Estimation of growth potential using optimal network

For study area I, the dataset created using 5x5 cells Von Neumann neighbourhood is passed through the 4-9-1 and 4-6-1 ANN architectures, while the 5x5 cells Moore neighbourhood dataset is passed through the 4-20-1 ANN architecture. For study area II, the dataset created using 13x13 cells Von Neumann neighbourhood is passed through the 4-9-1 and 4-12-21-1 ANN architectures, while and the 13x13 cells Moore neighbourhood dataset is passed through the 4-3-1 and 4-12-21-1 ANN architectures.

5.3.9 Masking of exclusionary areas

The restricted areas, water bodies, public grounds and gardens have been treated as exclusionary zones and the model makes no prediction in these areas. A mask corresponding to these areas has been generated based on Survey of India topographical map, guide map and master plan of the study areas. Since the model only simulates transition from non built-up to built-up with no reverse process taking place, so the built-up cells are also masked out. At the end of each model iteration when cells are allocated from non built-up to built-up, the built-up mask is also updated.

5.3.10 Allocation of cells from non built-up to built-up

The outputs obtained from the different ANN for study area I and II, show the development potential of each cell. However, all the non built-up cells are not transitioned to built-up cells simultaneously. Only cells that have a development potential above a certain threshold value transit to built-up. This is necessary since CA models are recursive in nature and involve many iterations with the output of iteration t being the input for iteration t+1.

The model is executed with different values of threshold, i.e., 0.8, 0.85, 0.9 and 0.95. These values are decided based on experiments and literature survey. In the proposed ANN-

CA model when the threshold value is kept low (i.e., 0.8) a large number of cells qualify for transiting to built-up in each model iteration. Thus, less number of model iterations are required for the stopping criteria to be fulfilled. In contrast when the threshold value is kept high (i.e., 0.95) a small number of cells qualify for transiting to built-up in each iteration. Hence, it requires a large number of model iterations for the stopping criteria to be fulfilled.

Thus, for study area I, the ANN-CA model is executed using 4-9-1, 4-6-1 and 4-20-1 ANN architectures. Using each of these ANN architecture, the ANN-CA model is executed 4 times using the threshold values 0.8, 0.85, 0.9 and 0.95.

For study area II, the ANN-CA model is executed using 4-9-1, 4-3-1 and 4-12-21-1 ANN architecture. Using each of these ANN architectures, the ANN-CA model is executed 4 times using the threshold values 0.8, 0.85, 0.9 and 0.95.

5.3.11 Updation of built-up/non built-up and other factor maps

The built-up/non built-up area map is updated for study area I and II, based on the cells that have transit from non built-up to built-up. Other factors maps such as, distance to nearest built-up and amount of built-up in neighbourhood are then recalculated on the basis of this updated map.

5.3.12 Model iterations

Using the updated factor maps, the process from section 5.3.8 to section 5.3.11 is repeated, until the stopping criteria is fulfilled. The updated built-up/non built-up map in the last iteration is the final simulated urban growth map of the study area.

5.4 Results and Discussion

5.4.1 Study area I

Similar to the MCE-CA model, the ANN-CA model for 1997-2001 has been evaluated on a cell by cell basis and spatially using PCM and Moran Index respectively. For study area I, the 4-9-1 ANN architecture produced the highest accuracy of 33.4% using the 5x5 cells Von Neumann neighbourhood as can be seen from Table 5.8. The Moran Index for the simulated growth using 4-9-1 architecture is 0.29, which is equal to the Moran Index of 0.29, calculated for actual growth in the study area during 1997-2001.

The values of Moran Index for other two ANN architecture are 0.48 and 0.47 which are significantly higher than 0.29. Thus, the 4-9-1 ANN architecture based on literature driven thumb rules produced comparable and even higher accuracy than that obtained from the acceptable network 4-20-1 as identified from processing of several ANN architectures.

Figure 5.8: Performance of ANN-CA model for urban growth (study area I)

ANN architecture	Neighbourhood used	Threshold value	PCM	Moran Index
4-9-1	Von-Neumann	0.8	33.4%	0.29
4-6-1	Von-Neumann	0.9	22.6%	0.48
4-20-1	Moore	0.85	28.4%	0.47

A comparison of the simulated urban growth map generated using 4-9-1 ANN architecture (Figure 5.4a) and actual growth map (Figure 5.4b), shows that the model is able to successfully, simulate the urban growth pattern taking place in the main city (i.e., around the city core) where there is contiguous urban growth. However, in the fringe areas where growth has taken place in a dispersed and patchy form, the model has not been able to simulate growth pattern. These results are similar to the ones obtained for the simulated urban growth using MCE-CA model.

For study area I, the 4-9-1 ANN produced the maximum accuracy, at a low threshold value i.e., 0.8 (refer Table 5.8). The low value of threshold results in less number of iterations as large number of cells are able to transit to built-up in each iteration. Similarly, in the MCE-CA model for study area I (chapter 4), the best simulation results are obtained when the number of iterations are less. Thus, both the ANN-CA and MCE-CA model have been able to provide acceptable results at less number of iterations.

On implementing the model for the period 1997-2001, the simulated results obtained using the MCE-CA model for study area I (chapter 4), also produced a Moran Index of 0.29 and PCM value of 34.3% when it was calibrated for 1997-2001. This shows that the ANN–CA model has produced accuracy comparable to the MCE-CA model. Thus, ANNs are able to learn the urban growth process objectively without much human intervention.

Since, actual urban growth for 2001-2005 is known, the urban growth has been simulated for the period 2001-2005 to validate the model. The 4-9-1 ANN and 5x5 cells Von Neumann neighbourhood data has been used. After implementing the model, the simulated growth has a PCM of 44.3%. Similarly, the Moran Index for the simulated growth for the period 2001-2005 is 0.34, which matches the Moran Index of 0.33 for actual growth. Correspondingly, the accuracy of simulation results from MCE-CA model are; PCM of 42%, Moran Index: 0.3, which are similar to ANN-CA model. This further demonstrates the usefulness of ANN-CA model in urban growth simulation.

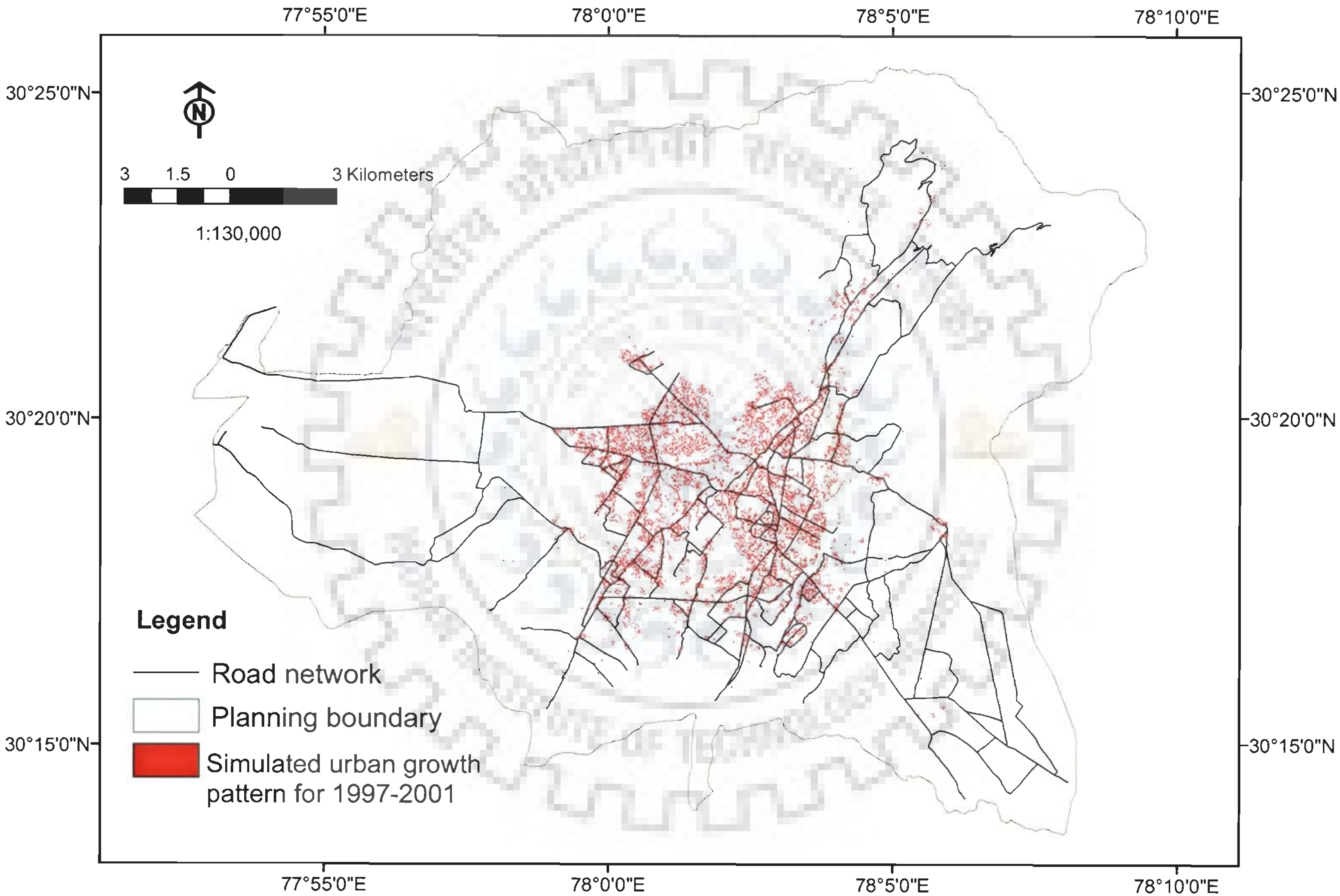

Figure 5.4 a: Simulated urban growth pattern for 1997-2001 using ANN-CA model (study area I)

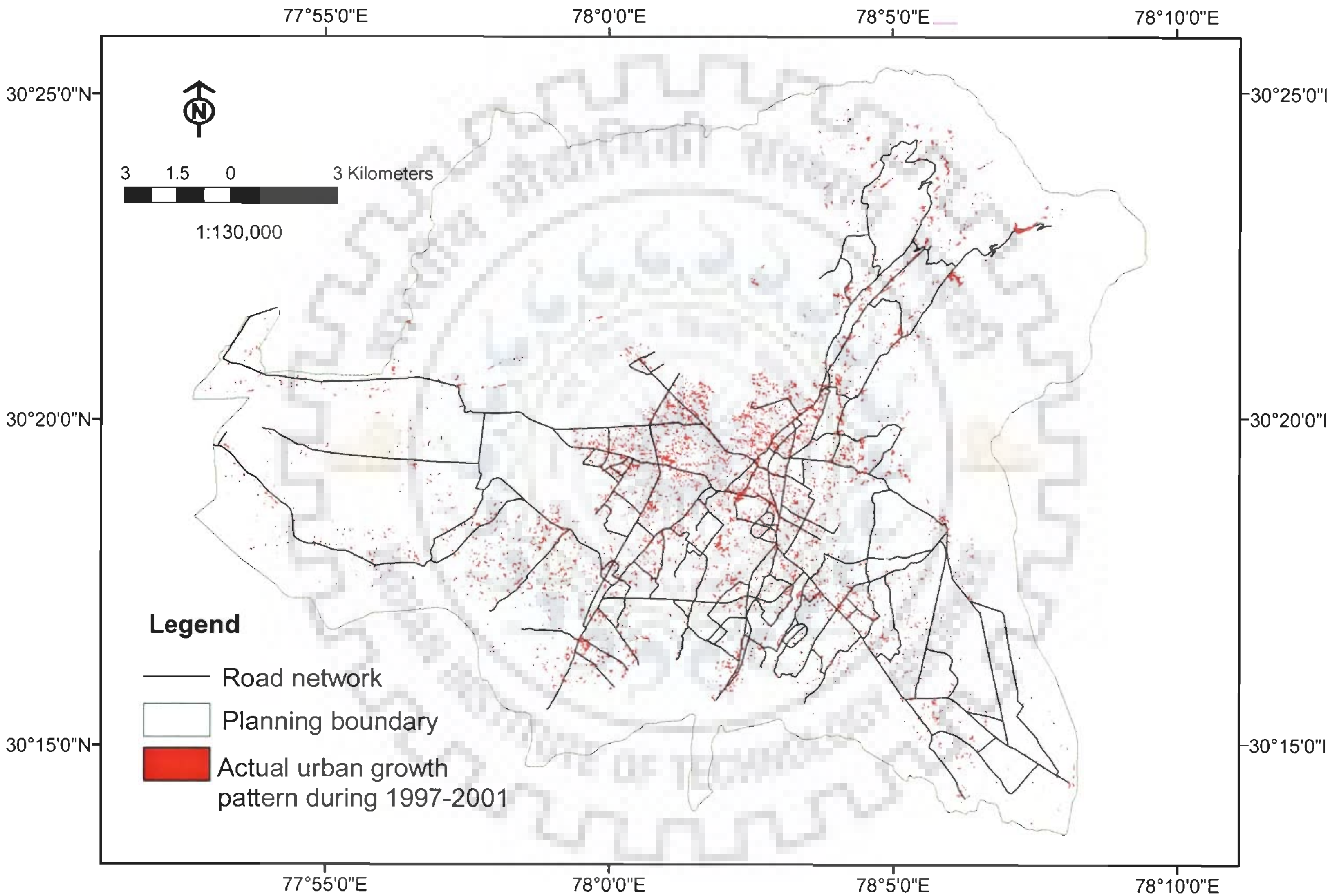

Figure 5.4b: Actual urban growth pattern during 1997-2001 (study area I)

On comparing the simulated growth with the actual growth (Figures 5.5a and 5.5b), it is observed that the model is able to simulate the contiguous growth pattern that has occurred in the main city and its surrounding areas. The model, to some extent, is also able to simulate the urban growth pattern that has occurred in the fringe area in the north, south east and south west directions.

5.4.2 Study area II

For study area II, the 4-12-21-1 ANN architecture using 13x13 cells Moore neighbourhood based dataset produced the maximum accuracy of 56% whereas the three other ANNs produced a PCM of 54% (refer Table 5.9). The Moran Index of the simulated growth using 4-12-21-1 ANN is 0.77, the other three ANNs produced a Moran Index of 0.76 and 0.74, which is comparable with the value of 0.75 obtained for actual growth during the 1993-2001 period.

Further, the 4-9-1 and 4-3-1 ANN architecture based on literature driven thumb rules produced comparable accuracy with that obtained from the acceptable network 4-12-21-1 as identified from trial and error.

Figure 5.9: Performance of ANN-CA model for urban growth (study area II)

ANN architecture	Neighbourhood used	Threshold value	PCM	Moran Index
4-9-1	Von-Neumann	0.8	54.72%	0.76
4-12-21-1	Von-Neumann	0.8	54.93%	0.74
4-3-1	Moore	0.8	54.78%	0.76
4-12-21-1	Moore	0.8	56.08%	0.77

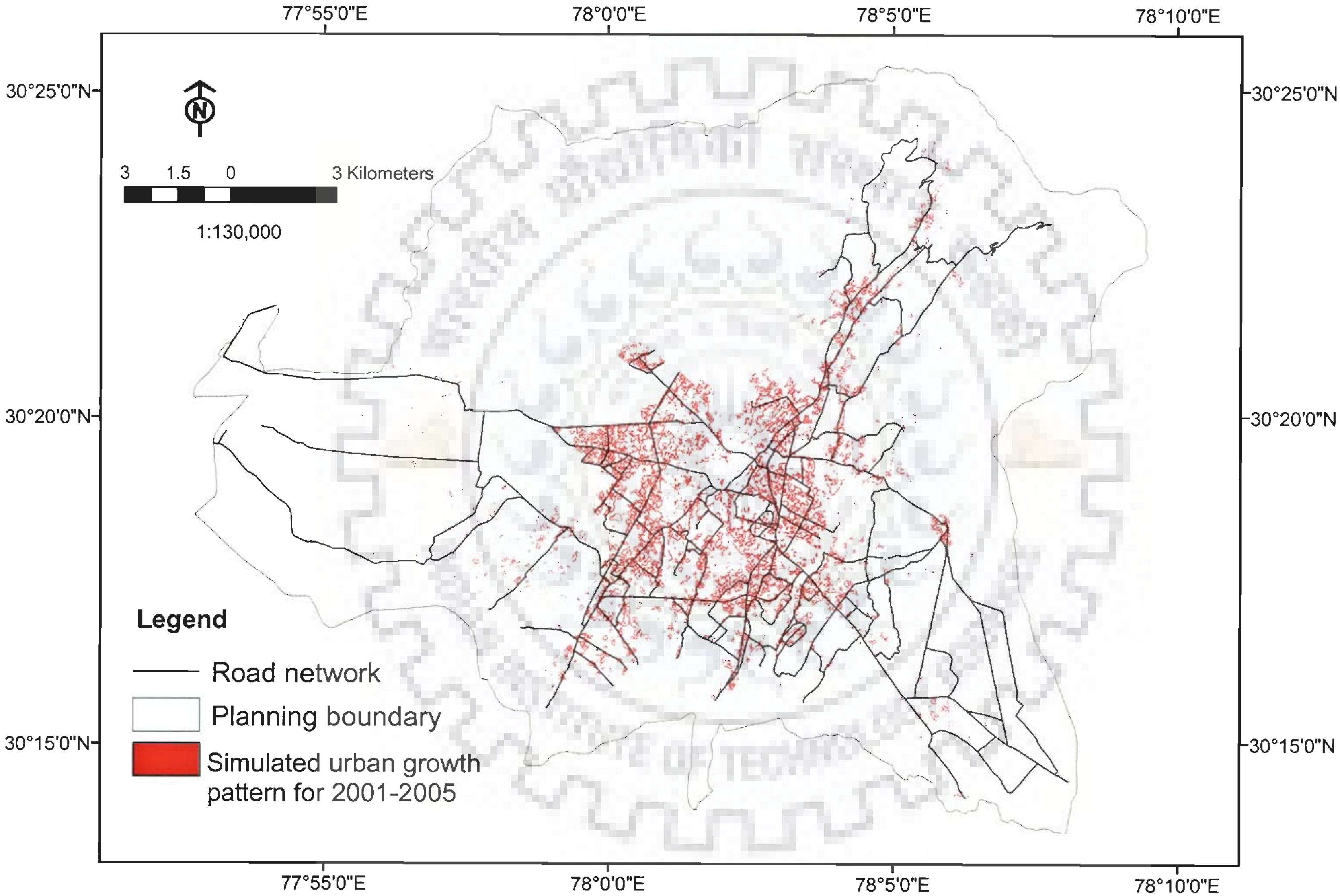

Figure 5.5 a: Simulated urban growth pattern for 2001-2005 using ANN-CA model (study area I)

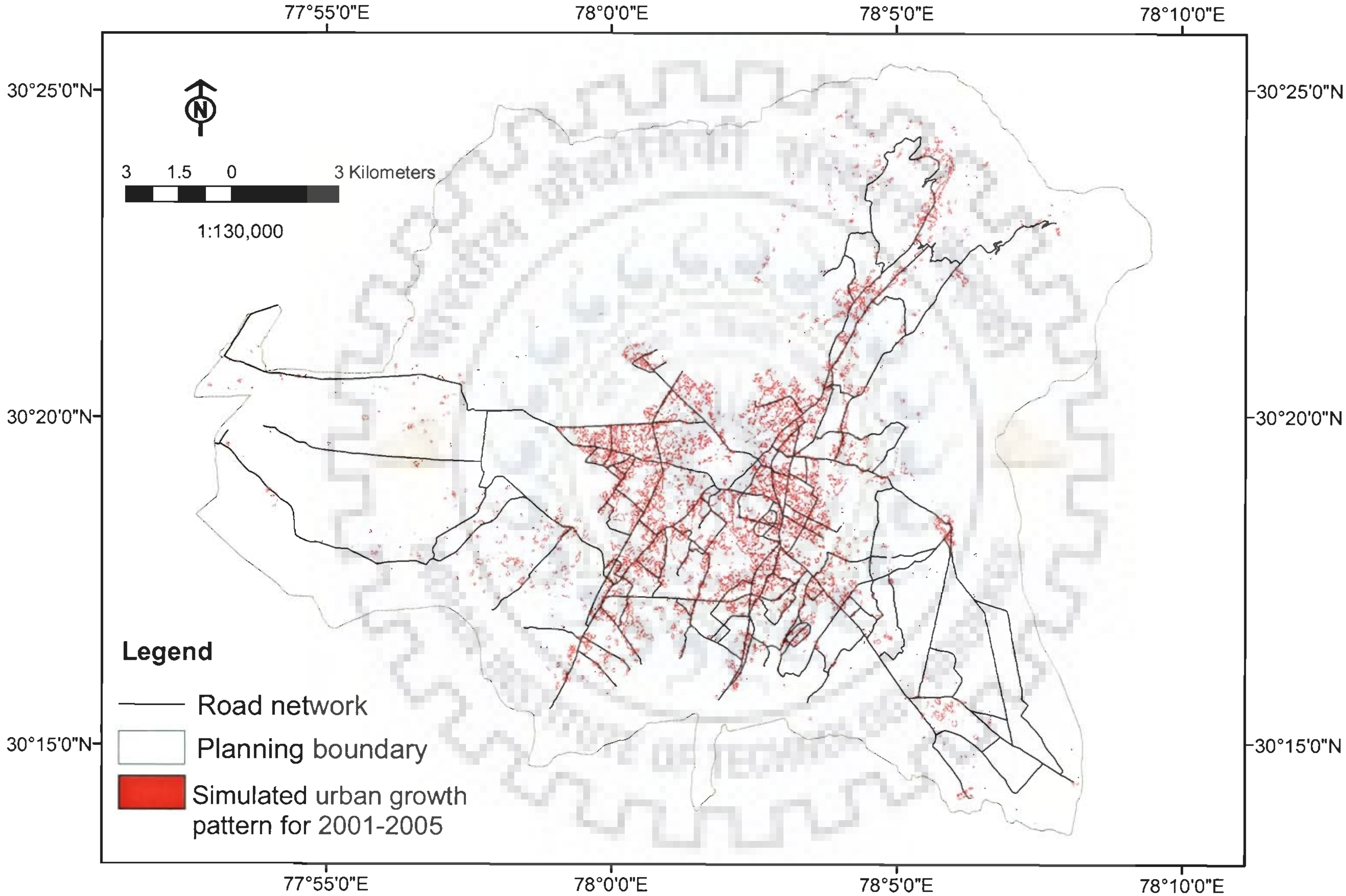

Figure 5.5b: Actual urban growth pattern for 2001-2005 (study area I)

For study area II, the 4-12-21-1 ANN produced the maximum accuracy, at low threshold value (i.e., 0.8). The low threshold value results in less number of model iteration. Similarly, in case of the MCE-CA model for study area II, the best simulation results were obtained for less number of iterations (Moran Index: 0.76 and PCM of 55.6%). Thus, the ANN-CA model in study area II has been able to simulate the urban growth process thereby increasing the objectivity in the simulation process.

A comparison of the simulated growth for year 1993-2001 (Figure 5.6a) using the 4-12-21-1 architecture with the actual growth during this period (Figure 5.6b), shows that the model has been able to simulate urban growth pattern that has taken place around the existing built-up areas. However, it is not able to accurately simulate the isolated patches of growth that has taken place in the study area. These results are also similar to those obtained for simulated growth during the same period using the MCE-CA model.

5.5 Comparative analysis of CA based models for both cities

The Moran Index and PCM values for MCE-CA and ANN-CA model for study areas I and II are given in Table 5.10. It can be inferred from this table that for both the study areas the ANN-CA model in which the network architecture was decided based on thumb rules gave comparable and even better results than that obtained from the network architecture which was decided by trial and error.

Table 5.10: Comparative Analysis of models results for both study area

Model	Study area I		Study area II	
	Moran Index	PCM	Moran Index	PCM
ANN-CA (trial and error)	0.47	28.41%	0.74	54.93%
ANN-CA (thumb rule)	0.29	33.44%	0.76	54.78%
MCE-CA	0.29	34.26%	0.76	55.57%

Nevertheless, for both the study areas I and II the ANN-CA model produced accuracy comparable to the MCE-CA model results, demonstrating that the ANN are able to learn the urban growth process objectively without any human intervention. The next chapter discusses how the ANN output can be used for defining the urban growth zonation maps which are a important input in many planning applications

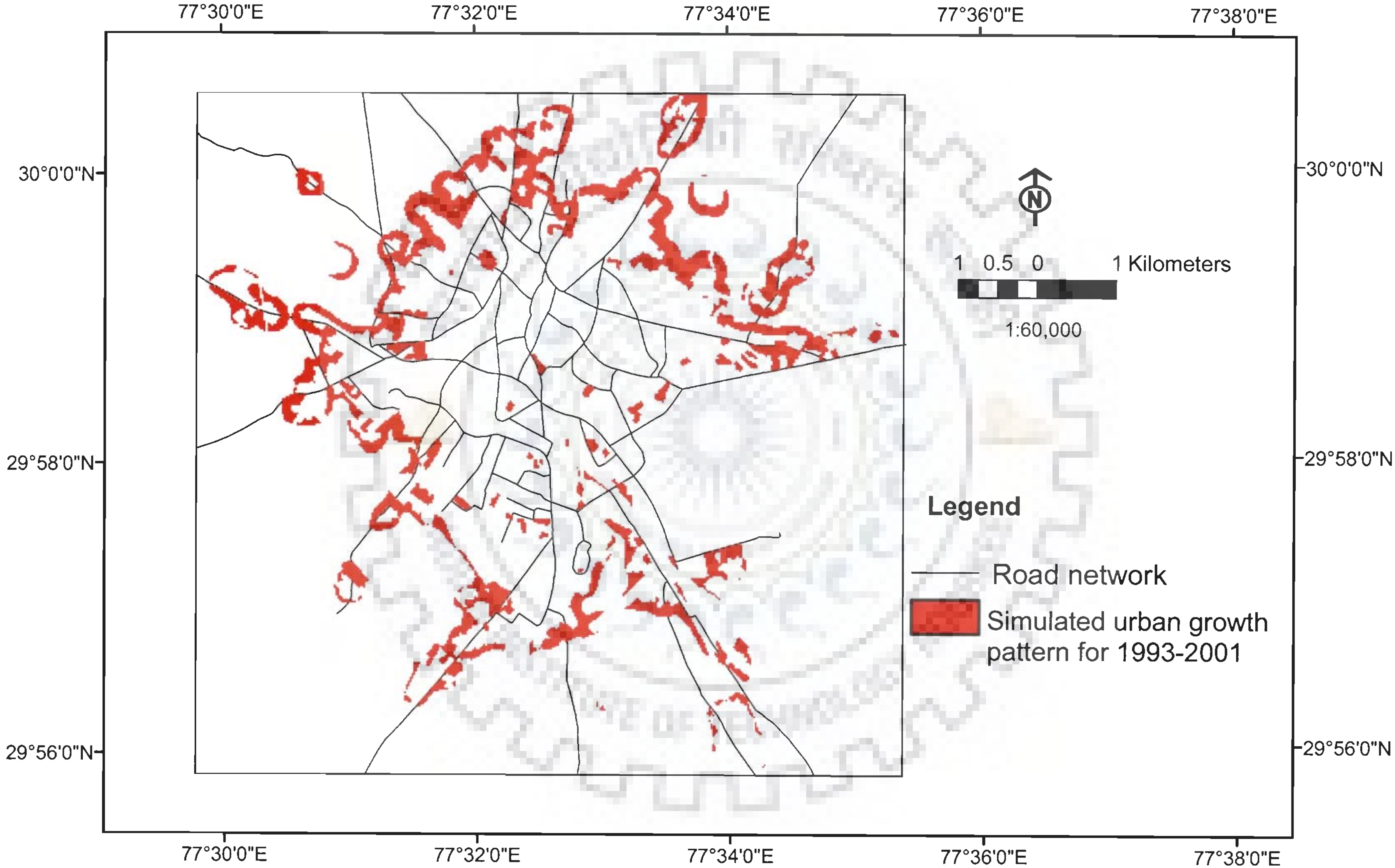

Figure 5.6a: Simulated urban growth pattern for 1993-2001 using ANN-CA model (study area II)

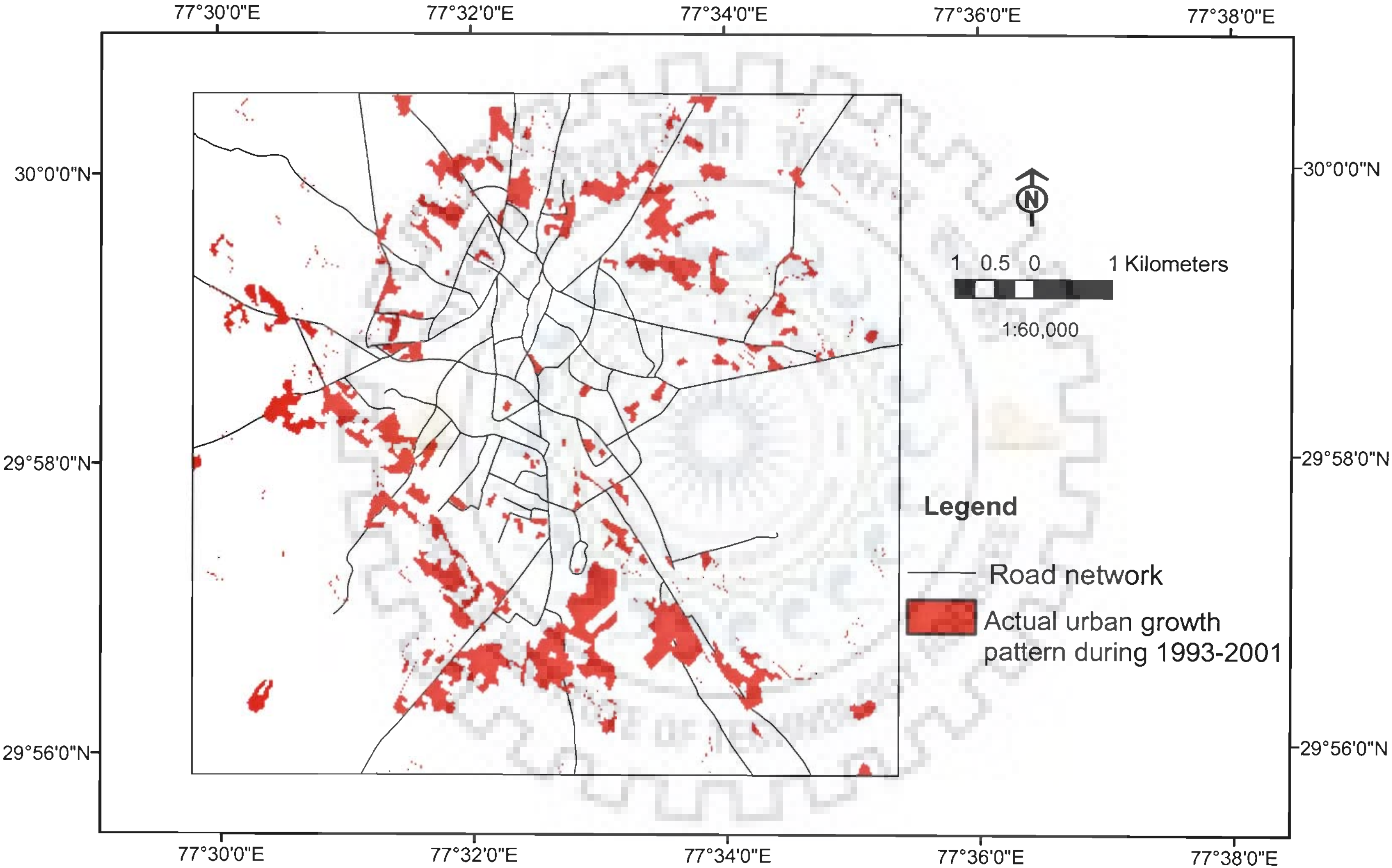

Figure 5.6b: Actual urban growth pattern during 1993-2001 (study area II)

Chapter 6

ANN based approach for Urban Growth Zonation

6.1 Introduction

Most of the Indian cities are undergoing a rapid growth. This growth if left unregulated will not only create environmental problems such as, depletion of natural resources, increased pollution levels, loss of green cover etc., but will also lead to lack of infrastructural facilities such as water supply, sewerage etc., in the cities.

In order to regulate the future growth of cities, the urban planning authorities draft a master plan, which provides a framework for future growth of the city and aims at controlling the growth along preconceived and predetermined paths. In the master plan, the planning authorities delineate future urbanizable zones and propose different land uses, such as, high, medium and low density residential areas, commercial, recreation etc., for these zones depending on their growth potential. Therefore, there is an urgent need to generate urban growth zonation maps depicting zones with varying urban growth potential (i.e. high, medium and low). These zonation maps can serve as an important input to the master plan preparation, as they provide a rational scientific ground on which the planning authorities can base their decisions regarding the future growth of the city. Besides, the urban growth zonation maps can also be used as inputs for disaster relief plans and environmental related studies.

Although in other fields, such as, landslide hazard zonation (LHZ) a number of techniques like ANN (Arora *et al.*, 2004), Fuzzy, combined neural and fuzzy (Kanungo *et al.*, 2006) and the conventional weighting assignment procedure (Saha *et al.*, 2002) have been used for generating zones having different landslide susceptibility. However, in the field of urban planning, only the conventional weighting assignment procedure has been implemented (Pathan *et al.*, 2004) for generating urban growth potential zones. In the conventional weight assignment procedure, the factor weights are assigned based on experience and previous knowledge. This makes the generation of zonation maps subjective in nature and might therefore contain some implicit biases towards the assumptions made.

This chapter intends to make the process of urban growth zonation more objective, by utilizing ANN to generate urban growth zonation maps. After having predicted urban growth at a cell location using ANN-CA model, the present study has been further extended to define zones having different urban growth potential using ANN.

6.2 ANN based urban growth zonation

The inputs to urban growth zonation are the same as were used for simulating urban growth based on CA models and are listed again,

i) Distance to road network
ii) Accessibility to infrastructural facilities
iii) Distance to city core

Thus, corresponding to above three factors, the following four raster maps have been used as an input to the ANN,

i) Euclidian distance of each cell from the nearest road (f1)
ii) Euclidean distance of a cell from the nearest built-up (f2)

iii) Euclidian distance of each cell from the city core (f3)

iv) Amount of built-up in neighbourhood (f4)

Since the datasets used here are the same as before, the network that produced the highest training and testing accuracy in the ANN-CA model have been used here also. Thus, for study area I, the 4-9-1 ANN architecture using Von Neumann neighbourhood has been selected, while for study area II, the 4-12-21-1 architecture using Moore neighbourhood has been selected (refer Tables 5.6 and 5.7). The trained networks are run on the whole dataset to produce the output at each cell.

The ANN outputs show the development potential of each cell on a 0 to 1 scale. The cell with value of 1 being the most potential cell for future development while the cell with value 0 being the least potential.

The ANN output values ranging between 0 and 1, have been categorized into three classes which show the urban growth potential on an ordinal scale and are listed as,

i) Low potential zone

ii) Medium potential zone

iii) High potential zone

The categorization can be done in a number of ways. A judicious way for such categorization is to search for abrupt change in the values (Davis, 1986) or to divide the data into classes representing near equal distribution (van Westen, 1997). Saha (2004) also attempted to categorize the data using a probabilistic approach called as 'success rate curve'. However, in the present study, the class boundaries have been determined statistically, in order to avoid the subjectivity in fixing the class boundaries. Assuming that data are normally distributed, the boundaries for categorization have been defined as,

i) Low potential zone < (μ-σ)

ii) (μ-σ) < Medium potential zone < (u+ σ)

iii) (u+ σ) < High potential zone

where, μ is mean and σ is the standard deviation of the ANN output over all cells

A histogram plot of the ANN outputs for the study areas I and II (Figure 6.1a), show that the ANN outputs do not follow a normal distribution. Therefore in order to make these outputs normally distributed, a number of mathematical transformations can be applied to these ANN outputs. The logit transformation (Petruccelli et.al., 1999), as given in Equation 6.1 has been selected,

$$O_j' = \ln\left(\frac{O_j}{1-O_j}\right) \qquad \ldots 6.1$$

where,

O_j = ANN output

O_j' = Transformed ANN output

The histogram of the logit transformed ANN output is given in Figure 6.1b, which clearly shows the data are now normally distributed. These transformed ANN outputs are then categorized into the 3 urban growth potential zones using the class definitions as discussed above.

Figure 6.2 shows a schematic diagram of the ANN based urban growth zonation process. For study area I, Figure 6.3 shows the zonation map generated for year 2001 taking 1997 as base year. For study area II, Figure 6.4 shows the zonation map generated for year 2001 taking 1993 as the base year.

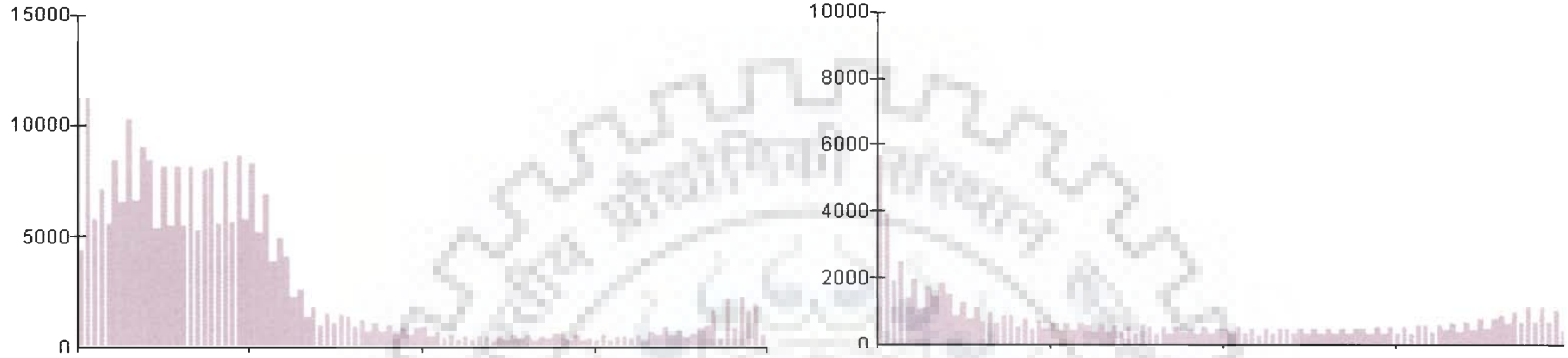

Study area I

Study area II

Figure 6.1 a: Histograms of ANN outputs for study area I and II

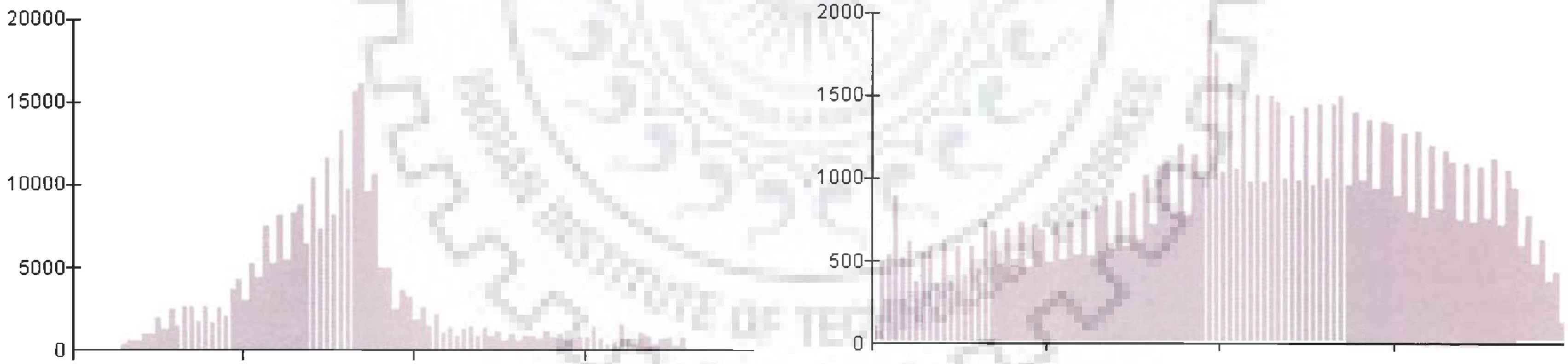

Study area I

Study area II

Figure 6.1 b: Histograms of the logit transformed ANN outputs for study area I and II

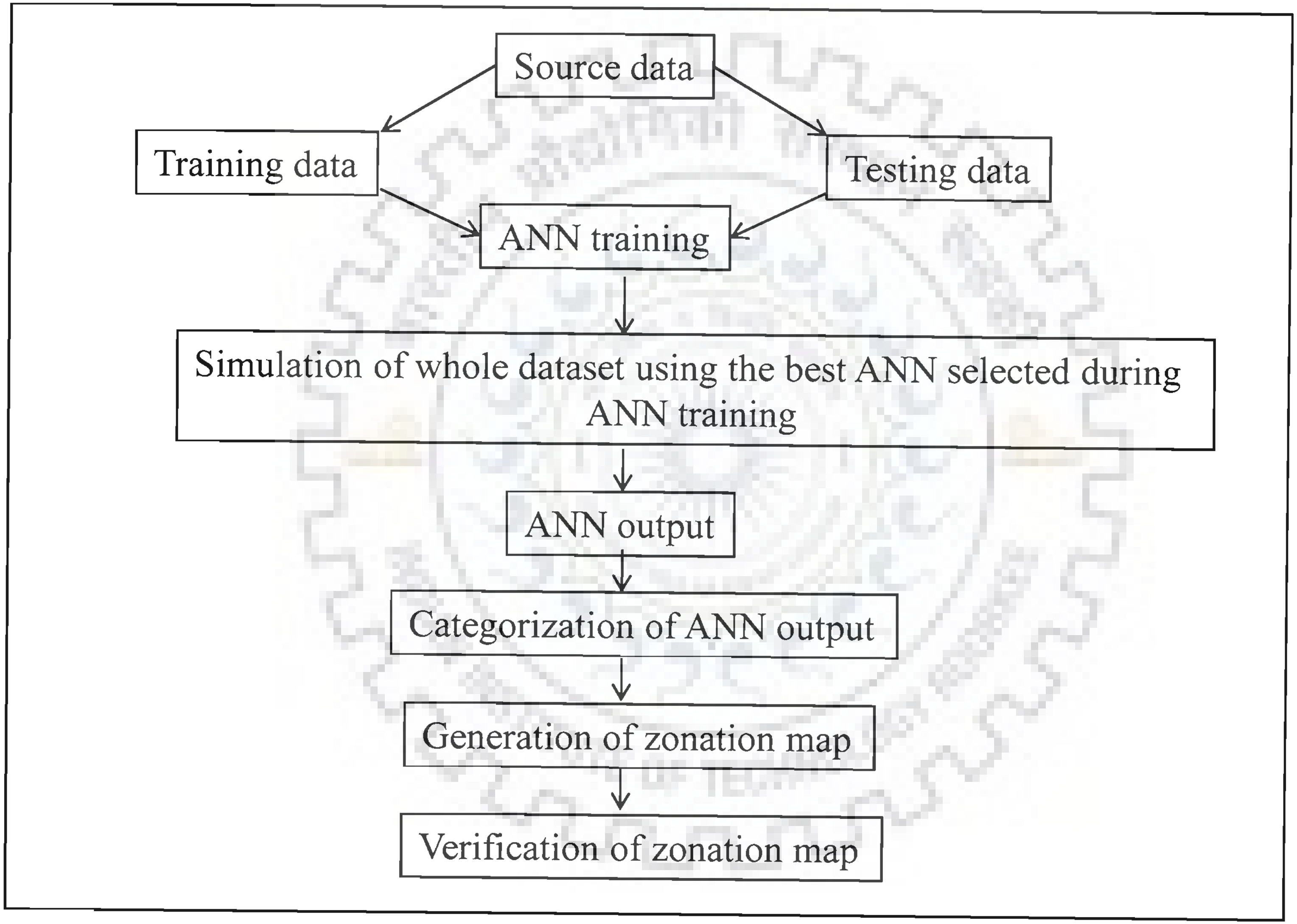

Figure 6.2: Schematic diagram of urban growth zonation process from ANN

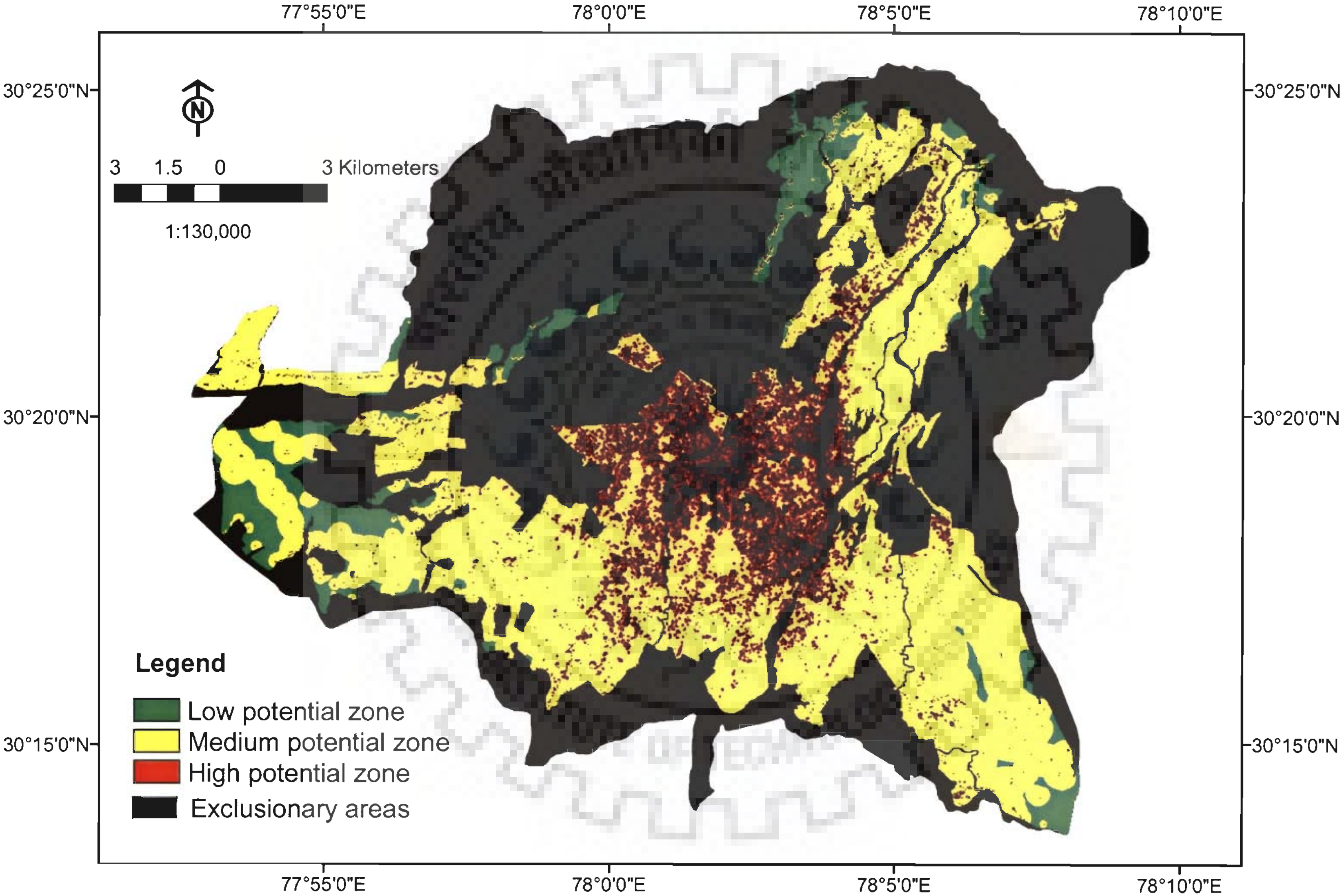

Figure 6.3: Urban growth zonation map for 2001 (study area I)

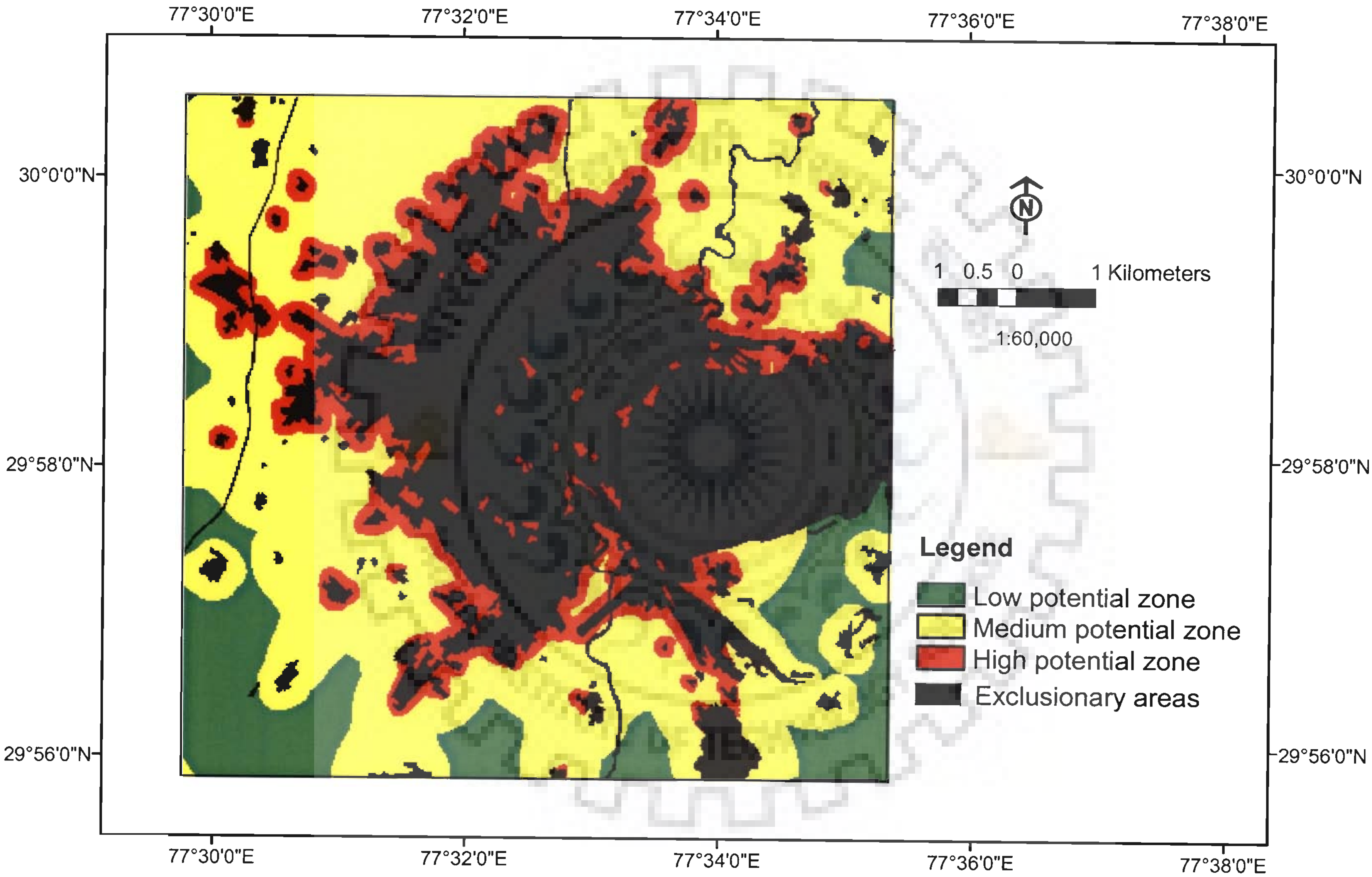

Figure 6.4 : Urban growth zonation map for 2001 (study area II)

6.3 Evaluation of the zonation maps

The distribution of the actual urban growth in study area I and II, has been used to evaluate the validitiy of the urban growth zonation map.

6.3.1 Study area I

In the urban growth zonation map generated for 2001 taking 1997 as base year (refer Figure 6.3), the high potential zone occupies 11.85% of the total study area, the medium and low potential zones occupy 76.43% and 11.72% of the study area respectively. The high potential zones are contiguous to the existing built up area, the medium potential zones occupy most of the agricultural areas surrounding the city, while the low potential zones are situated in patches at the periphery of the study area mainly in the North, west and South-east direction

In order to evaluate the validity of the urban growth zonation map generated, the map of actual urban growth that occurred during 1997-2001 is overlayed with the zonation map created to find the number of growth cells lying in each zone. It has been found that 50% of the growth cells (cells that changed from non built-up to built-up) are located in high potential zone, 48% of the growth cells in medium potential zone and 2% growth cells in low potential zone. Relative frequency of urban growth occurring in different buffer zones has been found out by dividing the percentage of growth cell lying in a zone with the percentage of study area occupied by the particular zone (Table 6.1).

Table 6.1: Areas and relative frequencies of urban growth with respect to different zones for 1997-2001 (study area I)

	Low potential zone	Medium potential zone	High potential zone
Percentage of growth cells lying in the zone (**A**)	2.00	48.00	50.00
Percentage of study area occupied by the zone (**B**)	11.72	76.43	11.85
Relative frequency (**A/B**)	0.17	0.63	4.22

Ideally, the relative frequency value should increase from low potential zone to high potential zone, since the high potential zones will have more urban growth compared to other zones (Arora *et al.,* 2004). Figure 6.5 shows the plot of the relative frequency values. It can be observed that there is a increase in the relative frequency values from low potential to high potential zone. The high value of relative frequency for high potential zone compared to other zones is due to the fact that a lot of urban growth (50%) has taken place in the high potential zone which only constitutes 11.85% of the study area. Thus, ANN has been able to zone the areas effectively.

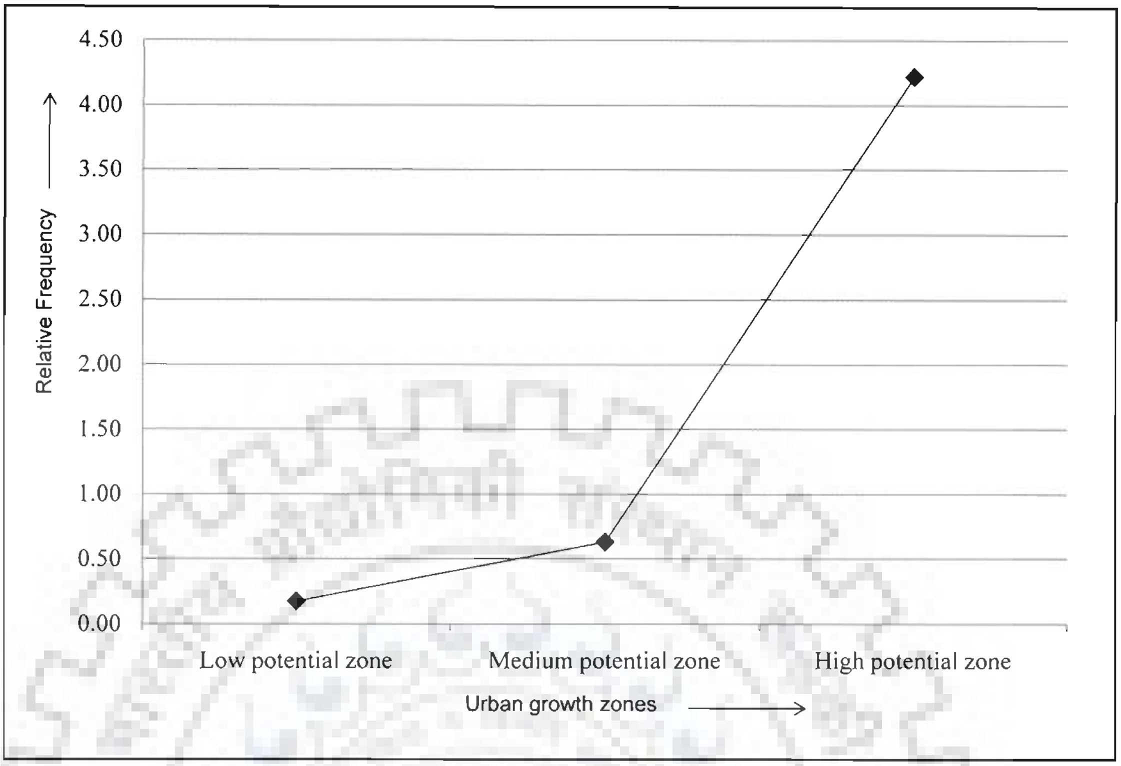

Figure 6.5: Plot of relative frequency versus urban growth zones for the period 1997-2001 (study area I)

Since actual growth for 2001-2005 is also known, so an urban growth zonation map has also been generated, taking 2001 as the base year and is shown in Figure 6.6. In the zonation map, the high potential zone occupies 12.71% of the total study area, the medium and low potential zones occupy 76.82% and 10.47% of the study area respectively.

In order to evaluate the validity of the urban growth zonation map generated, the map depicting actual urban growth during 2001-2005 is overlayed with the zonation map created to find the number of growth cells lying in each zone. It is found that 57% of the growth cells are located in high potential zone, 42% in medium potential zone and 1% in low potential zone. A relative frequency table has been generated (Table 6.2). The relative frequencies have been plotted as shown in Figure 6.7.

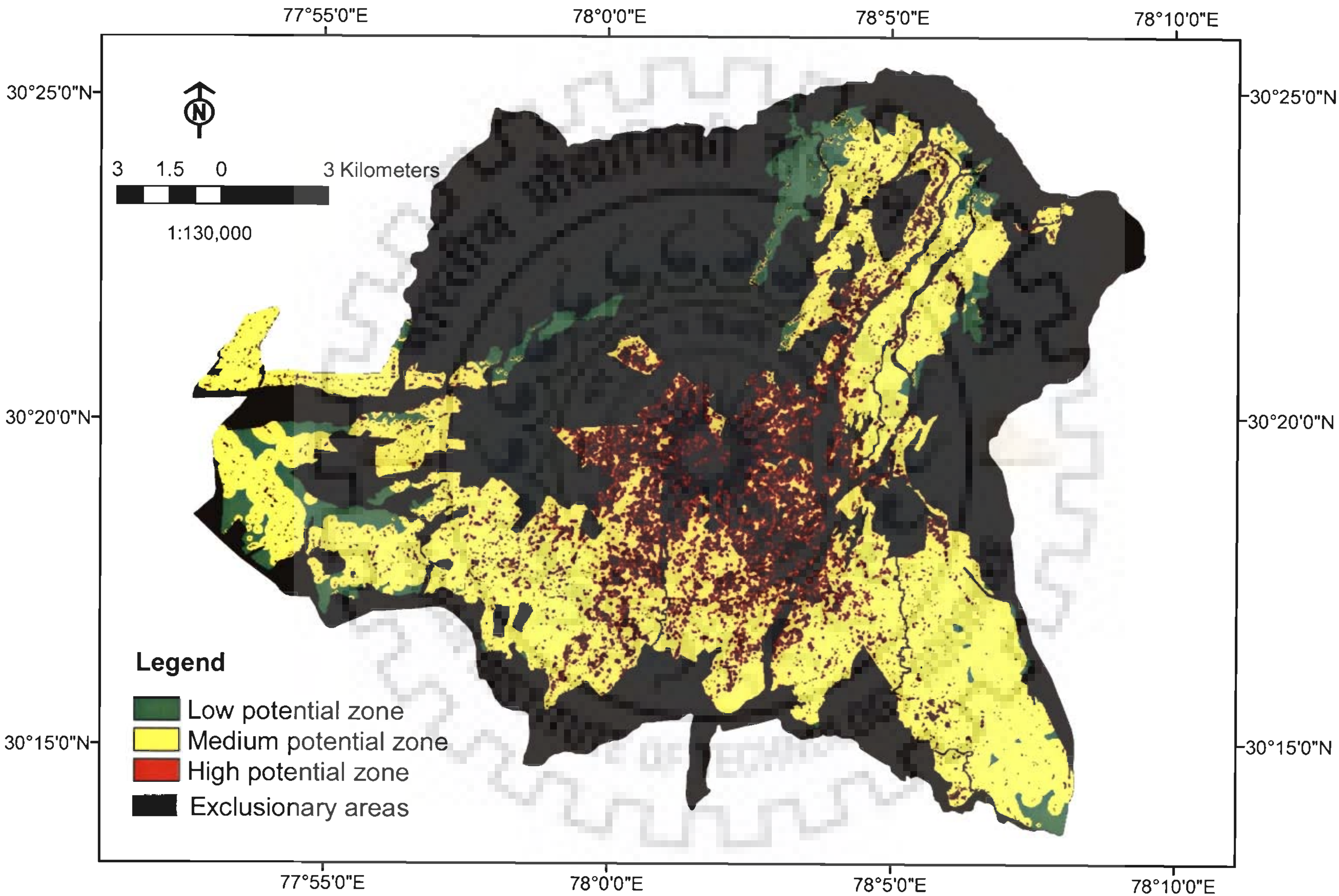

Figure 6.6: Urban growth zonation map for 2005 (study area I)

It can be seen that there is an increase in the frequency from low potential to high potential zone. This further corroborates the applicability of ANN for zonation.

Table 6.2: Areas and relative frequencies of urban growth with respect to different zones for 2001-2005 (study area I)

	Low potential zone	Medium potential zone	High potential zone
Percentage of growth cells lying in the zone **(A)**	1.00	42.00	57.00
Percentage of study area occupied by the zone **(B)**	10.47	76.82	12.71
Relative frequency **(A/B)**	0.10	0.55	4.48

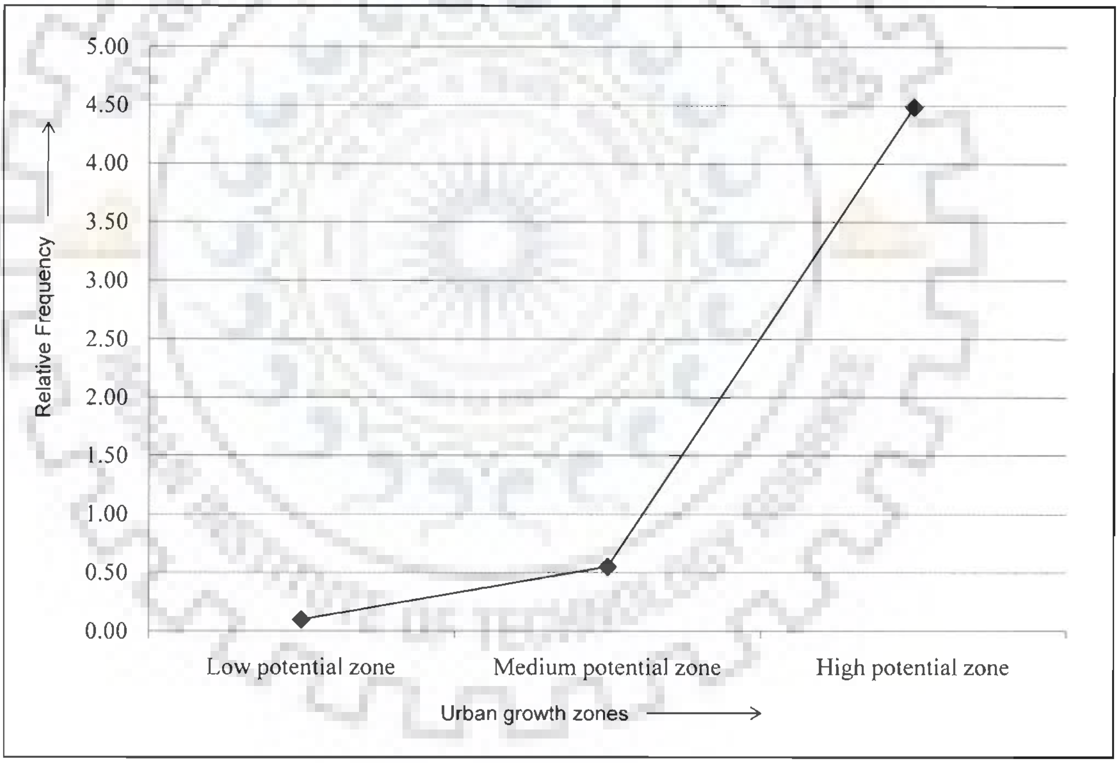

Figure 6.7: Plot of relative frequency versus urban growth zones for the period 2001-2005 (study area I)

An overlay of this zonation map with the 2001 zonation maps reveals that 27.6% of low potential zone in 2001 has changed to medium potential zone, while 4.4% of medium potential zone in 2001 has changed to high potential zone. From Tables 6.2 and 6.3 it can also be observed that in the two zonation maps created, the area occupied by low, medium and high potential is nearly same, but the percentage of urban growth taking place in high potential zone has increased from 50% during 1997-2001 to 57%, during 2001-2005. While the urban growth in medium potential zone has decreased from 48% in 1997-2001 to 42% in 2001-2005. This shows that densification of built-up area has taking place, with most of the new growth occurring in contiguity of already built-up areas in the high potential zone. This can also be observed from the fact that the value of relative frequency increased from 4.42 in 1997-2001 to 4.48 in 2001-2005.

6.3.2 Study area II

In the urban growth zonation map generated for 2001 taking 1993 as base year (refer Figure 6.4), the high potential zone occupies 18.69% of the total study area, the medium and low potential zones occupy 62.68% and 18.63% of the total study area respectively. The high potential zones are mainly contiguous to the existing built up area, the medium potential zones are adjacent to the high potential zones, and cover most of the agricultural areas around the city. The low potential zones are situated mainly in the south of the city and consists of areas which are situated at a distance from the road network or are adjacent to the restricted areas.

The map showing actual urban growth that occurred during 1993-2001 is overlayed with the zonation map to find the number of growth cells lying in each zone. It has been found that 68% of the growth cells are located in high potential zone, 31% in medium potential zone and 2% in low potential zone. A relative frequency table has been generated (Table 6.3) and the frequencies have been plotted and are shown in Figure 6.8. It can be seen that there is a increase in the relative frequency from low potential to high potential zone.

Table 6.3: Areas and relative frequencies of urban growth with respect to different zones for 1993-2001 (study area II)

	Low potential zone	Medium potential zone	High potential zone
Percentage of growth cells lying in the zone **(A)**	2.00	31.00	68.00
Percentage of study area occupied by the zone **(B)**	18.63	62.68	18.69
Relative frequency **(A/B)**	0.11	0.49	3.64

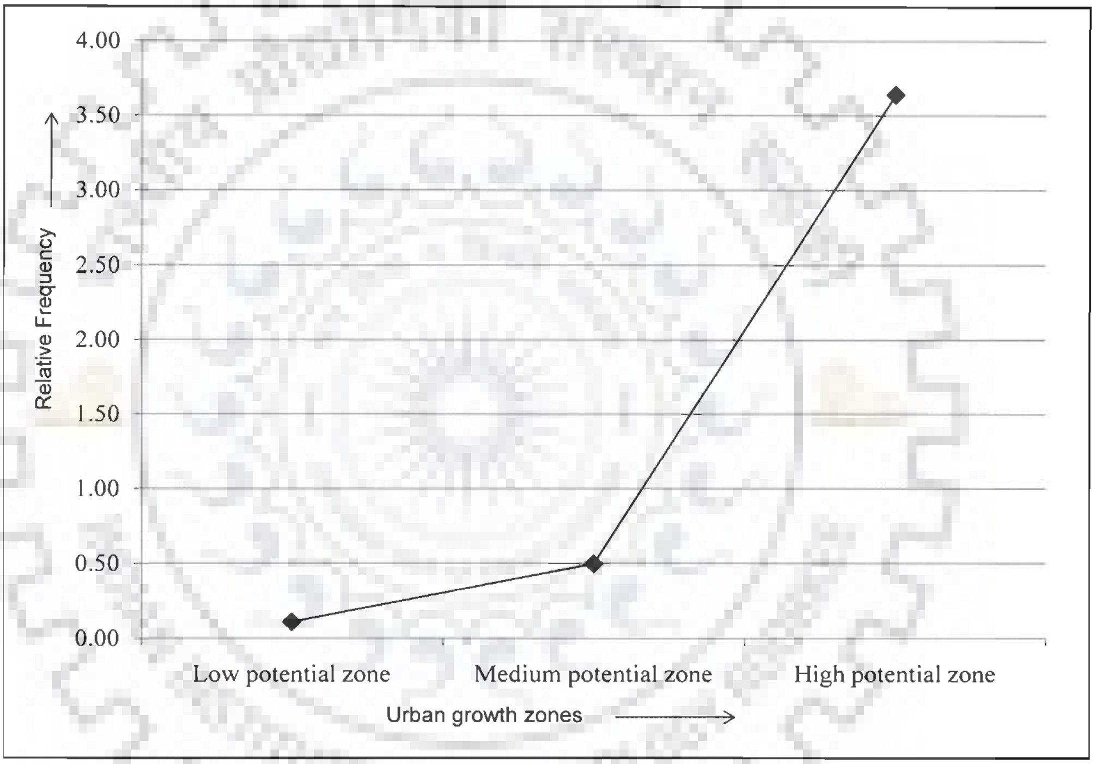

Figure 6.8: Plot of relative frequency versus urban growth zones for the period 1993-2001 (study area II)

Thus for both study areas, the relative frequency follows the ideal trend, thereby validating the urban growth potential zones generated using ANN. In the zonation maps generated for both the study areas, the medium potential zones occupy the maximum study area, while the high potential zones occupy relatively less areas but in comparison have a high intensity of urban growth. The low potential zones are located in the fringes of the study areas in proximity of reserved forests, restricted areas and other areas which have no development potential. It can be inferred that the ANN based methodology for integration of various factors seems to be quite applicable for urban growth zonation. The next chapters discusses the evaluation of simulation results using entropy method

Chapter 7

Evaluation of Urban Growth using Entropy

7.1 Introduction

In chapters 4 and 5, the MCE-CA and ANN-CA models for urban growth were discussed and evaluated using PCM and Moran Index respectively. The PCM compares the simulated and actual urban growth maps on cell by cell basis only. Moran Index is a spatial statistical indicator that measures the clustering of the growth cells (cells which transit from non built-up to built-up during the simulation period) and is used to assess the closeness of simulated growth pattern to the actual one.

However, both PCM and Moran index evaluate the urban growth at the finest possible scale (i.e., at the cell level), and thus have limitations in explaining the growth pattern at macroscopic level (i.e., whether the urban growth is compact or distributed, with respect to an individual factor such as road network , city core etc).

In the proposed models, since urban growth has been expressed as a function of factors, such as distance to road network and city core, there is a need to identify indices which can evaluate the simulated growth patterns, in terms of their distribution and orientation with respect to these factors.

According to Li and Yeh (2004), the Shannon entropy is an effective indicator to evaluate whether patterns of urban growth are dispersed or compact with regard to a factor. Therefore, in this study, the Shannon entropy has been used for evaluating the simulated urban growth patterns with respect to road network and city core.

7.2 Shannon entropy

SE measures the degree of spatial concentration or dispersion of phenomenon (e.g., urban growth) in *n* different zones. It is calculated as (Lata *et. al.*, 2001; Yeh and Li, 2001a; Li and Yeh, 2004b),

$$SE = \sum_{i=1}^{n} p_i * \log \frac{1}{p_i} \qquad \ldots 7.1$$

p_i, is the proportion of the phenomenon occurring in the i^{th} zone and is defined as,

$$p_i = \frac{x_i}{\sum_{i=1}^{n} x_i} \qquad \ldots 7.2$$

x_i is the observed value of the phenomenon in the i^{th} zone, and n is the total number of zones.

The value of SE ranges from a minimum of 0 to a maximum of log (n). Relative entropy (RE) may be used to scale the SE value in range from 0 to 1 and is defined as,

$$RE = \frac{SE}{\log(n)} \qquad \ldots 7.3$$

If the phenomenon is maximally concentrated in one zone, the value of relative entropy will be 0. Conversely, if the phenomenon is evenly dispersed across all the zones, the value of relative entropy will be 1 (Sudhira *et. al.*, 2003; Yeh and Li, 2001a).

7.3 Relative entropy (RE) of simulated and actual urban growth

For both the study areas, the simulated urban growth, as obtained from MCE-CA model has been evaluated with respect to actual urban growth using relative entropy (RE).

Since urban growth is expressed as a function of distance from road network and city core, the simulation results and the actual growth have been evaluated using RE calculated with respect to these factors. The buffer function in GIS has been used to create buffer zones along the roads and around the city core. These buffer zones are based on distances, as given in Tables 3.6 and 3.7 (refer chapter 3) decided on the basis of opinions of the experts from the local planning authorities.

The buffer zones along the roads and around the city core for study area I are shown in Figures 7.1 and 7.2 respectively. The buffer zones along roads and city core for study area II are shown in Figures 7.3 and 7.4 respectively.

7.3.1 Study area I

The two time periods for which the RE has been calculated are 1997-2001 and 2001-2005. The RE is calculated for both simulated and actual urban growths.

<u>RE for the period 1997-2001</u>

The map showing simulated urban growth for the period 1997-2001 has been overlaid on the buffer zones created along the road network (Figure 7.1) and around the city core (Figure 7.2). The spatial distribution of the simulated urban growth in these buffer zones is shown in Figures 7.5 and 7.6 respectively. The stepwise computation of RE, with respect to road network and city core, is shown in Tables 7.1 and 7.2.

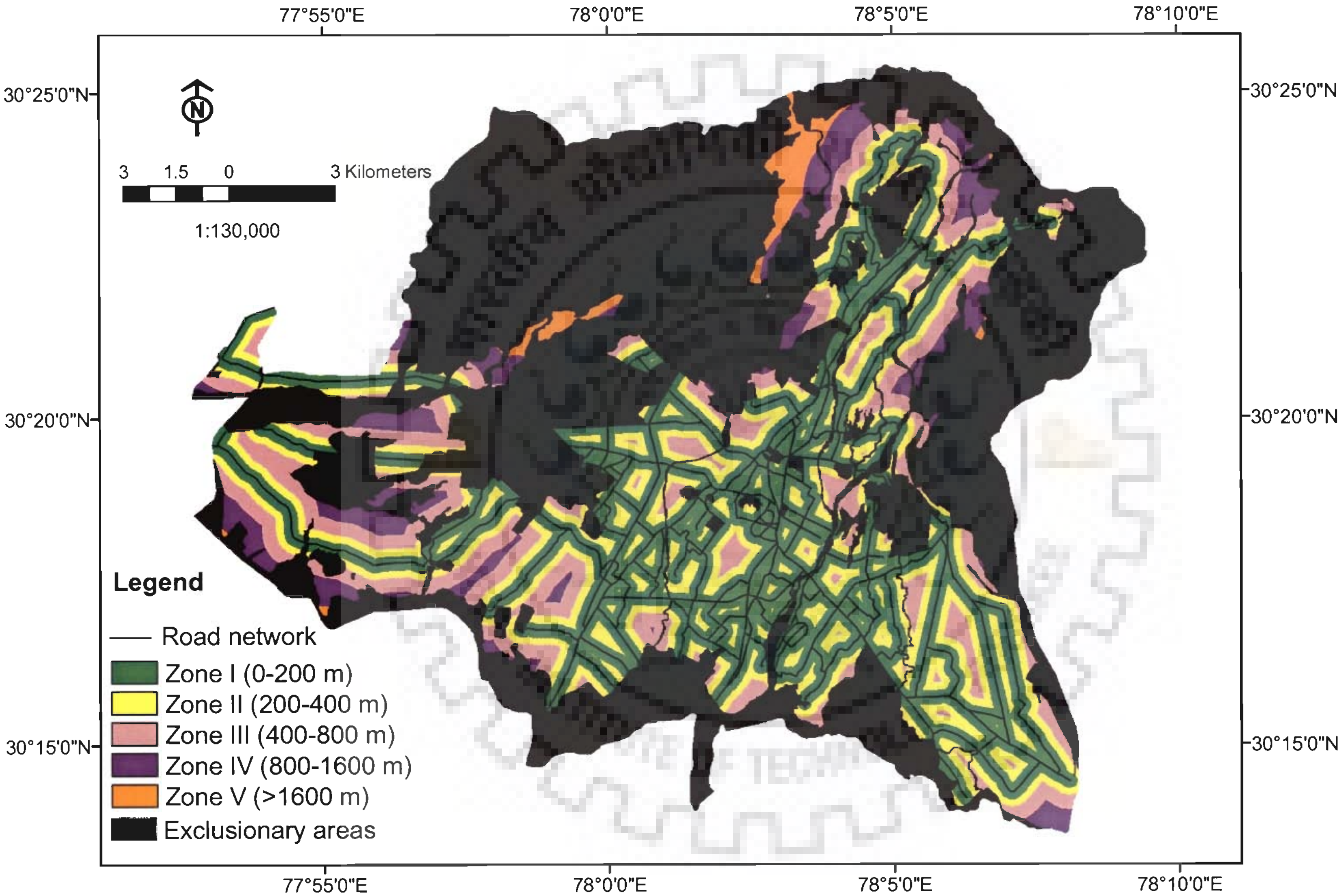

Figure 7.1 : Buffer zones along road network (study area I)

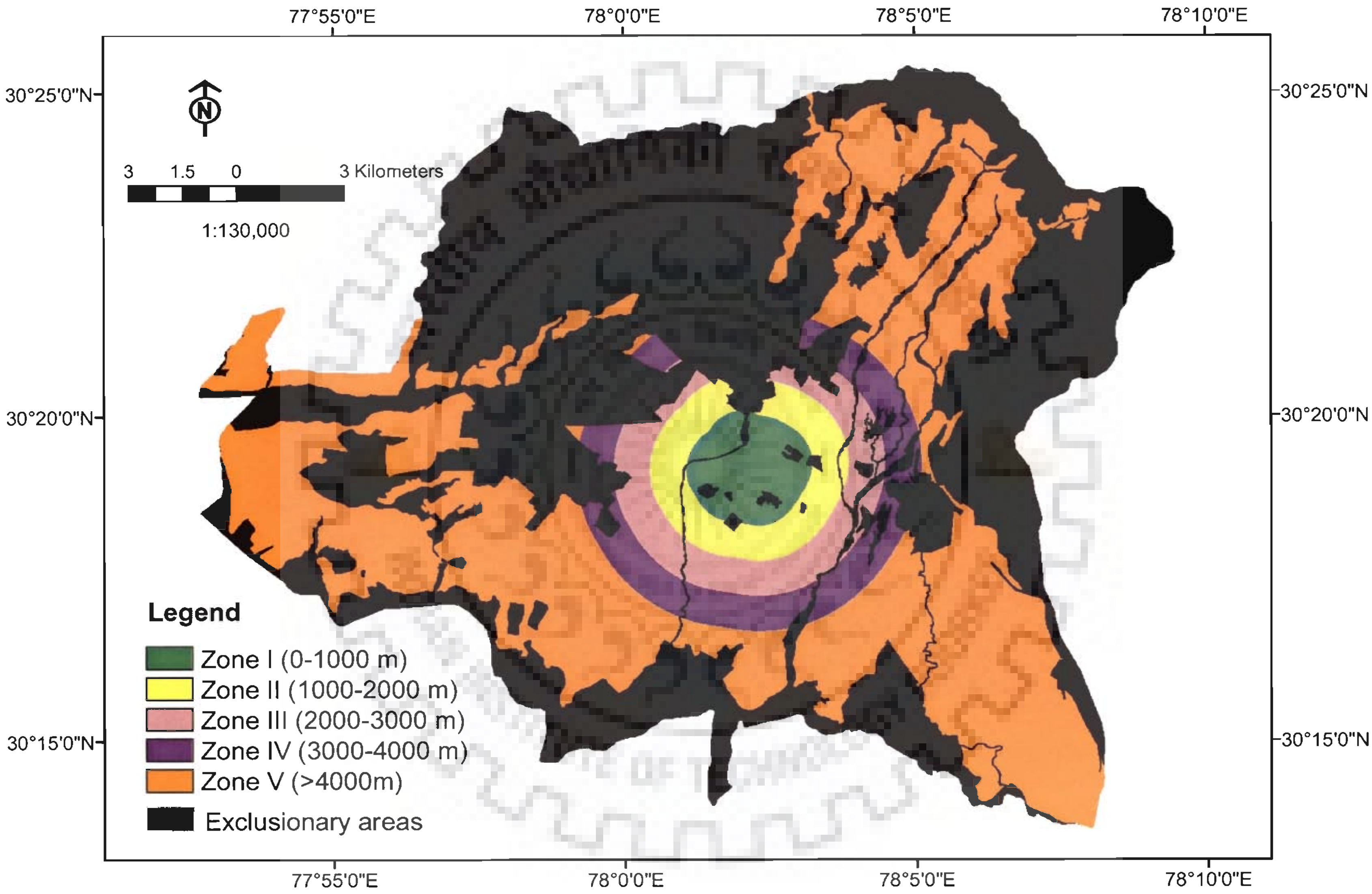

Figure 7.2 : Buffer zones around city core (study area I)

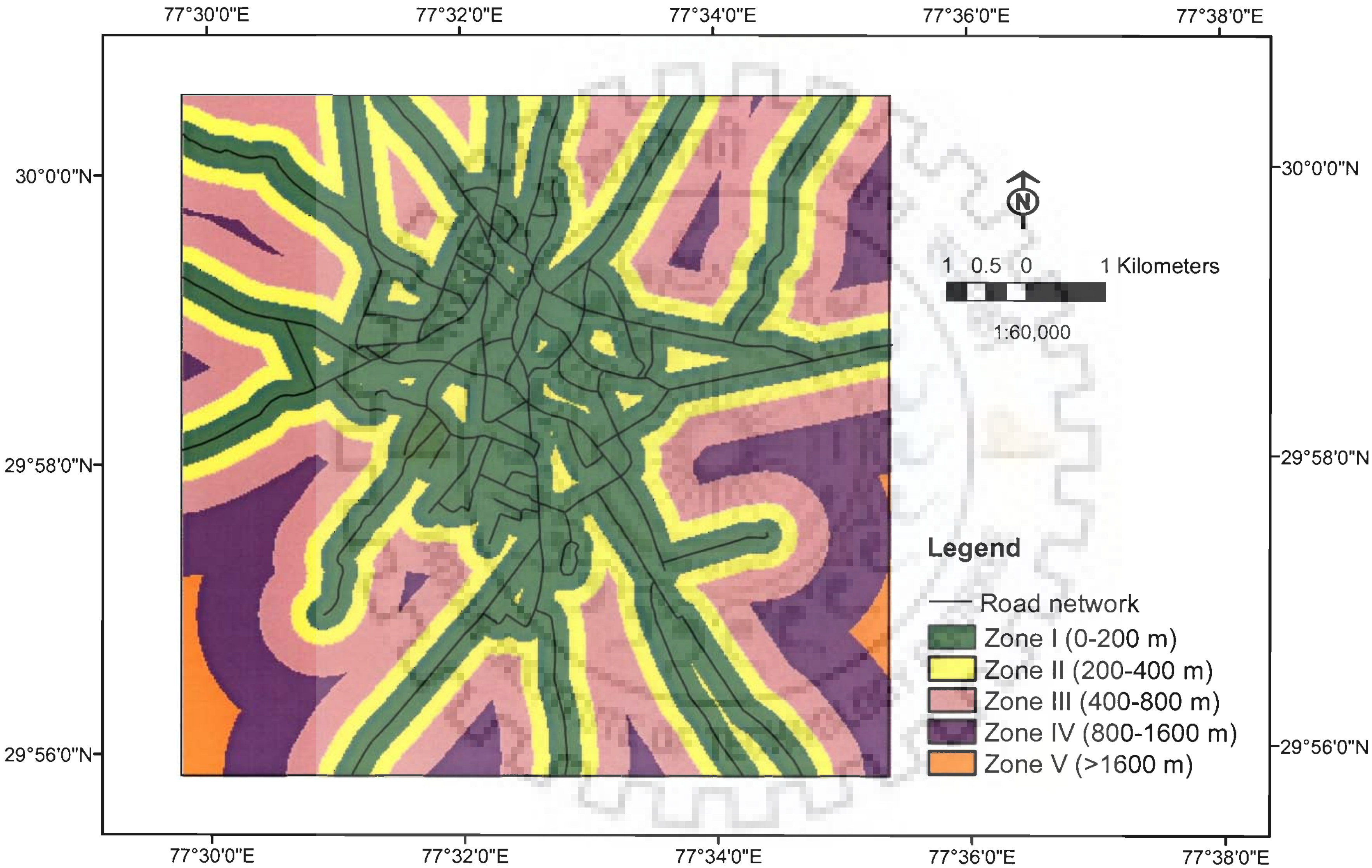

Figure 7.3 : Buffer zones along road network (study area II)

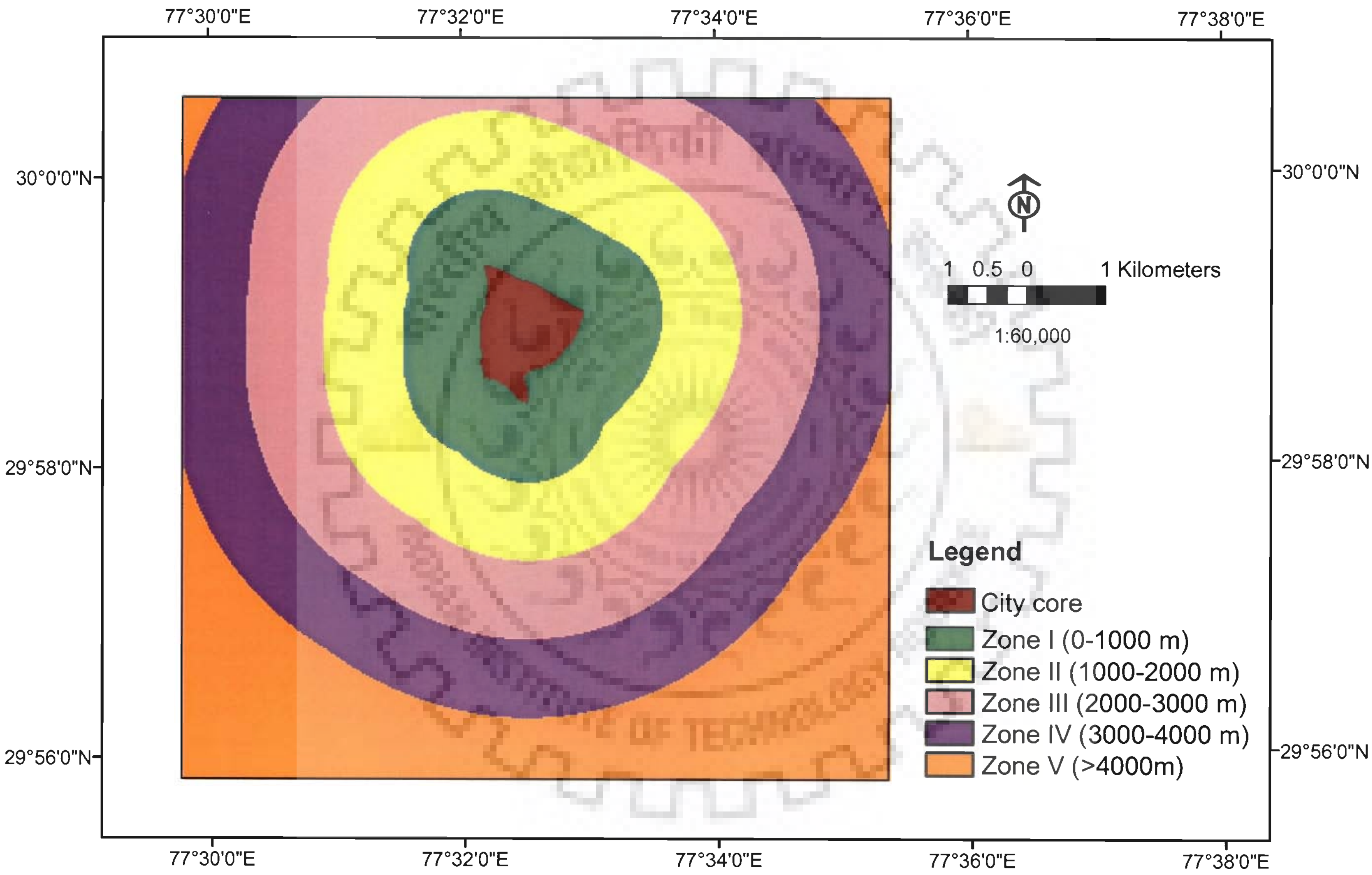

Figure 7.4 : Buffer zones around city core (study area II)

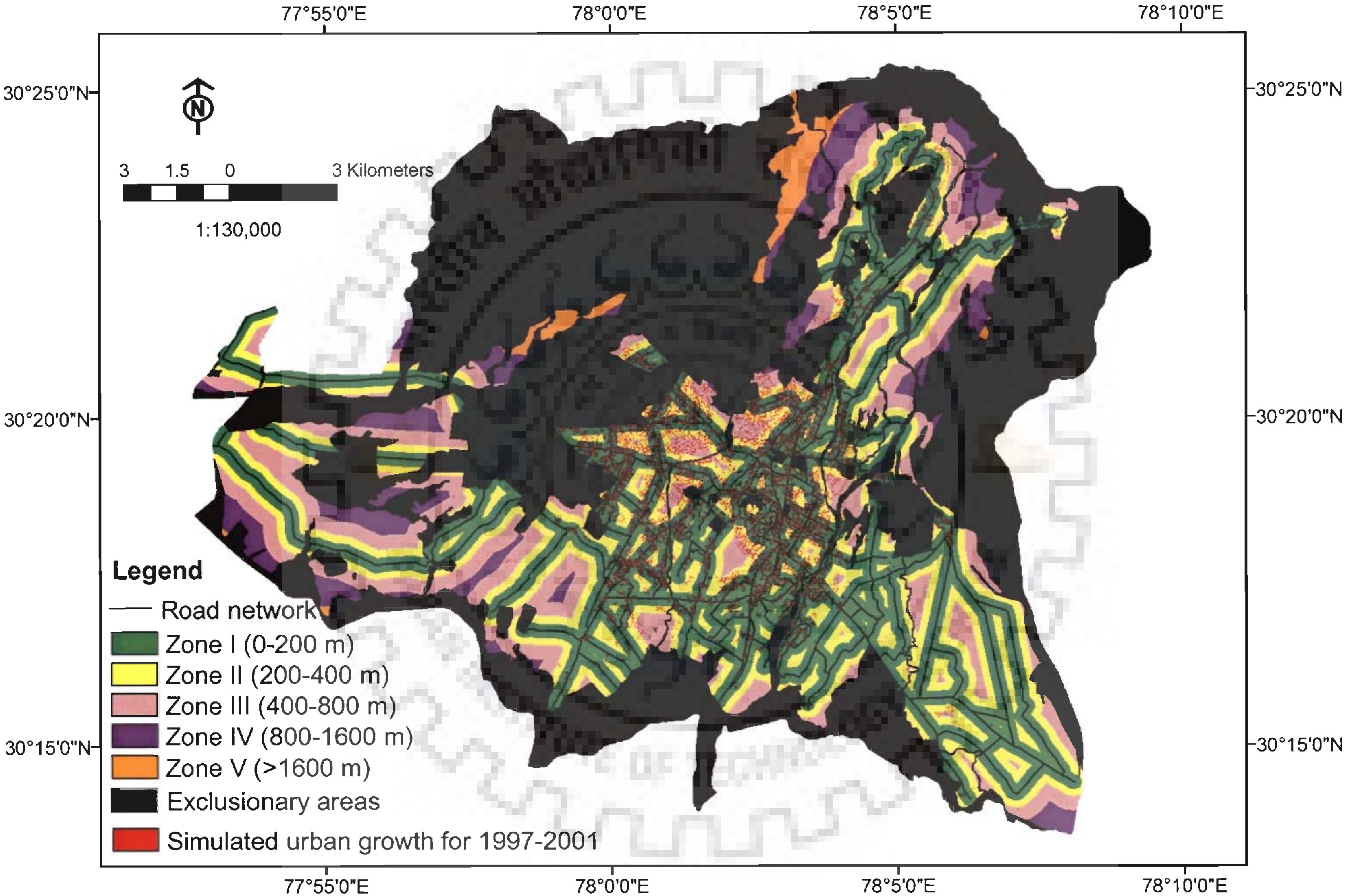

Figure 7.5 : Spatial distribution of simulated urban growth for 1997-2001 in different buffer zones along road network (study area I)

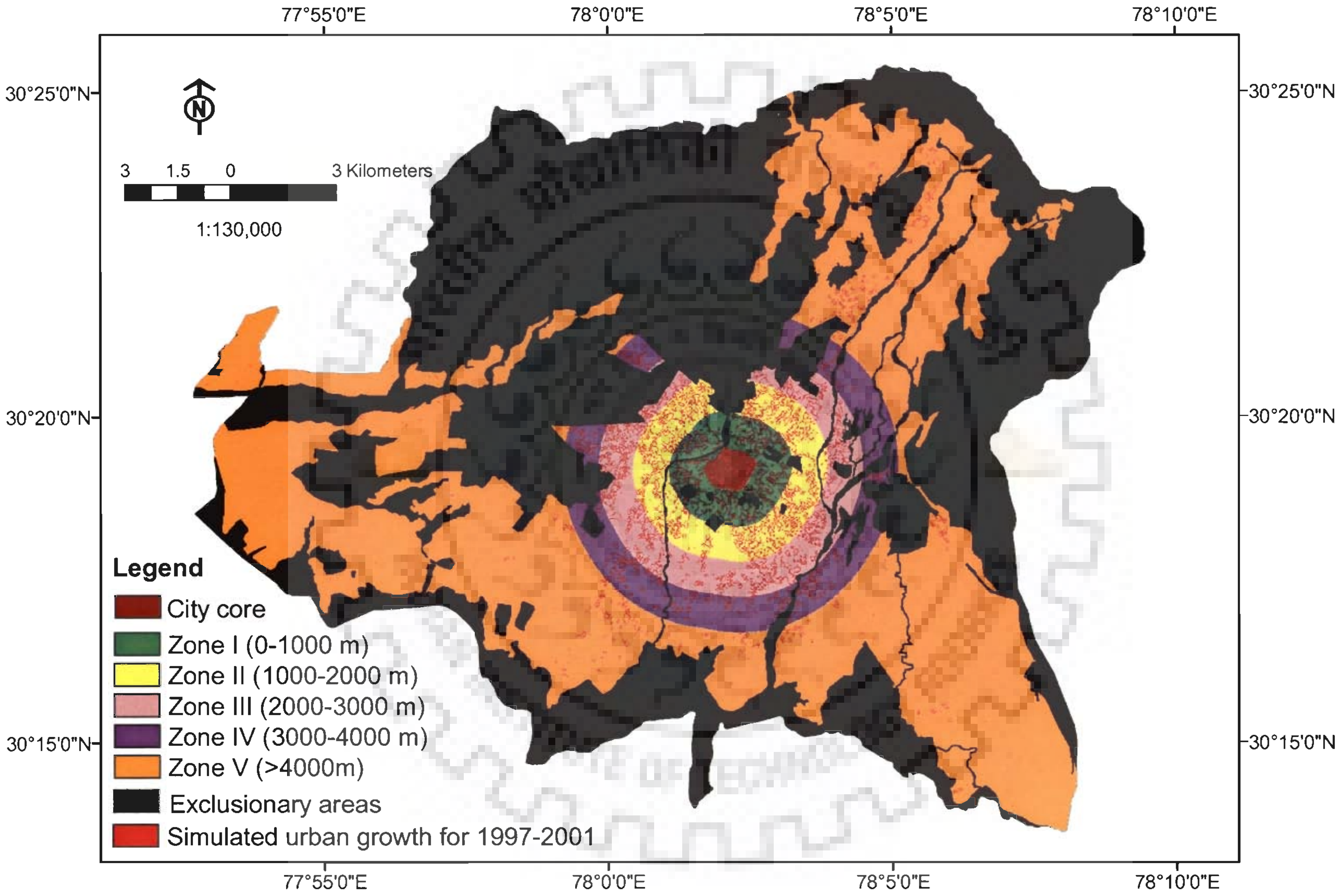

Figure 7.6 : Spatial distribution of simulated urban growth for 1997-2001 in different buffer zones around city core (study area I)

Table 7.1: Calculation of RE with respect to road network for simulated urban growth (1997-2001)

		Step 1	Step 2	Step 3
Buffer zones	Number of growth cells	p	log 1/p	p*log 1/p
Zone I	10733	0.743	0.129	0.096
Zone II	2641	0.183	0.738	0.135
Zone III	977	0.068	1.170	0.079
Zone IV	66	0.005	2.340	0.011
Zone V	25	0.002	2.762	0.005

Step 4: $SE = \sum_{i=1}^{5} p_i * \log \frac{1}{p_i} = (0.096 + 0.135 + 0.079 + 0.011 + 0.005) = 0.325$

Step 5: $RE = SE/\log 5 = 0.325/\log 5 = 0.46$

Table 7.2: Calculation of RE with respect to city core for simulated urban growth (1997-2001)

		Step 1	Step 2	Step 3
Buffer zones	Number of growth cells	p	log 1/p	p*log 1/p
Zone I	2640	0.183	0.738	0.135
Zone II	4081	0.283	0.549	0.155
Zone III	3896	0.270	0.569	0.154
Zone IV	2075	0.144	0.843	0.121
Zone V	1750	0.121	0.917	0.111

Step 4: $SE = \sum_{i=1}^{5} p_i * \log \frac{1}{p_i} = (0.135 + 0.155 + 0.154 + 0.121 + 0.111) = 0.676$

Step 5: $RE = SE/\log 5 = 0.676/\log 5 = 0.96$

Similarly, in order to calculate the RE for actual urban growth, the map showing urban growth is overlaid on the buffer zones created with respect to road network and city core (refer Figures 7.1 and 7.2). The spatial distribution of these actual growth cells in these buffer zones is shown in Figures 7.7 and 7.8 respectively. The stepwise computation of RE with respect to road network and city core for actual urban growth is shown in Tables 7.3 and 7.4 respectively.

Table 7.3: Calculation of RE with respect to road network for actual urban growth (1997-2001)

		Step 1	Step 2	Step 3
Buffer zones	Number of growth cells	p	log 1/p	p*log 1/p
Zone I	9005	0.624	0.205	0.128
Zone II	3043	0.211	0.676	0.143
Zone III	1873	0.130	0.887	0.115
Zone IV	458	0.032	1.498	0.048
Zone V	61	0.004	2.374	0.010

Step 4: SE = $\sum_{i=1}^{5} p_i * \log \frac{1}{p_i}$ = (0.128 + 0.143 + 0.115+ 0.048+0.01) = 0.443

Step 5: RE = SE/log 5= 0.443/log 5 = 0.63

Table 7.4: Calculation of RE with respect to city core for actual urban growth (1997-2001)

		Step 1	Step 2	Step 3
Buffer zones	Number of growth cells	p	log 1/p	p*log 1/p
Zone I	1938	0.134	0.872	0.117
Zone II	2395	0.166	0.780	0.129
Zone III	2339	0.162	0.791	0.128
Zone IV	1398	0.097	1.014	0.098
Zone V	6372	0.441	0.355	0.157

Step 4: SE = $\sum_{i=1}^{5} p_i * \log \frac{1}{p_i}$ = (0.117 + 0.129 + 0.128+ 0.098+ 0.157) = 0.629

Step 5: RE = SE/log 5= 0.629/log 5 = 0.90

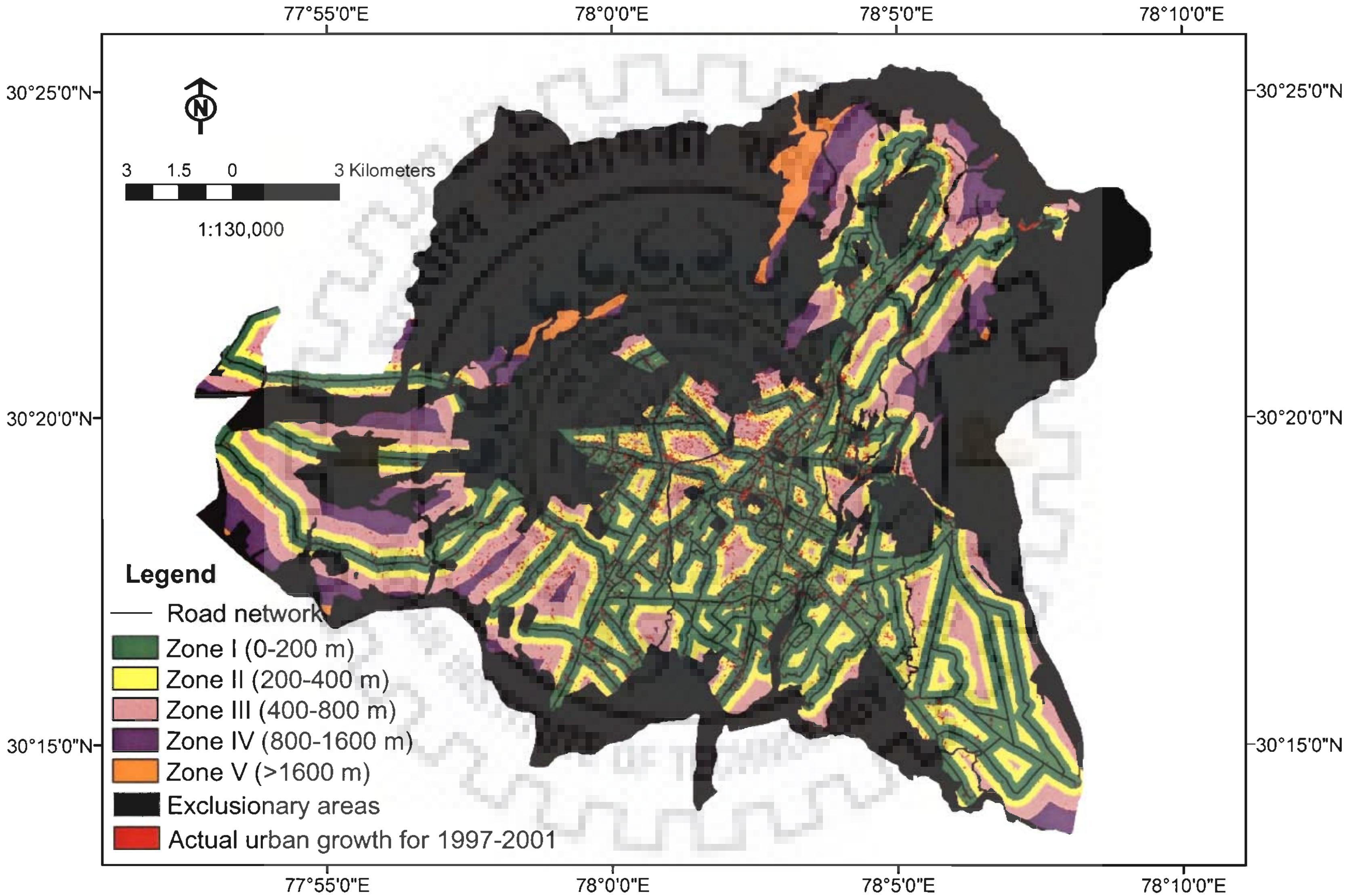

Figure 7.7: Spatial distribution of actual urban growth during 1997-2001 in different buffer zones along road network (study area I)

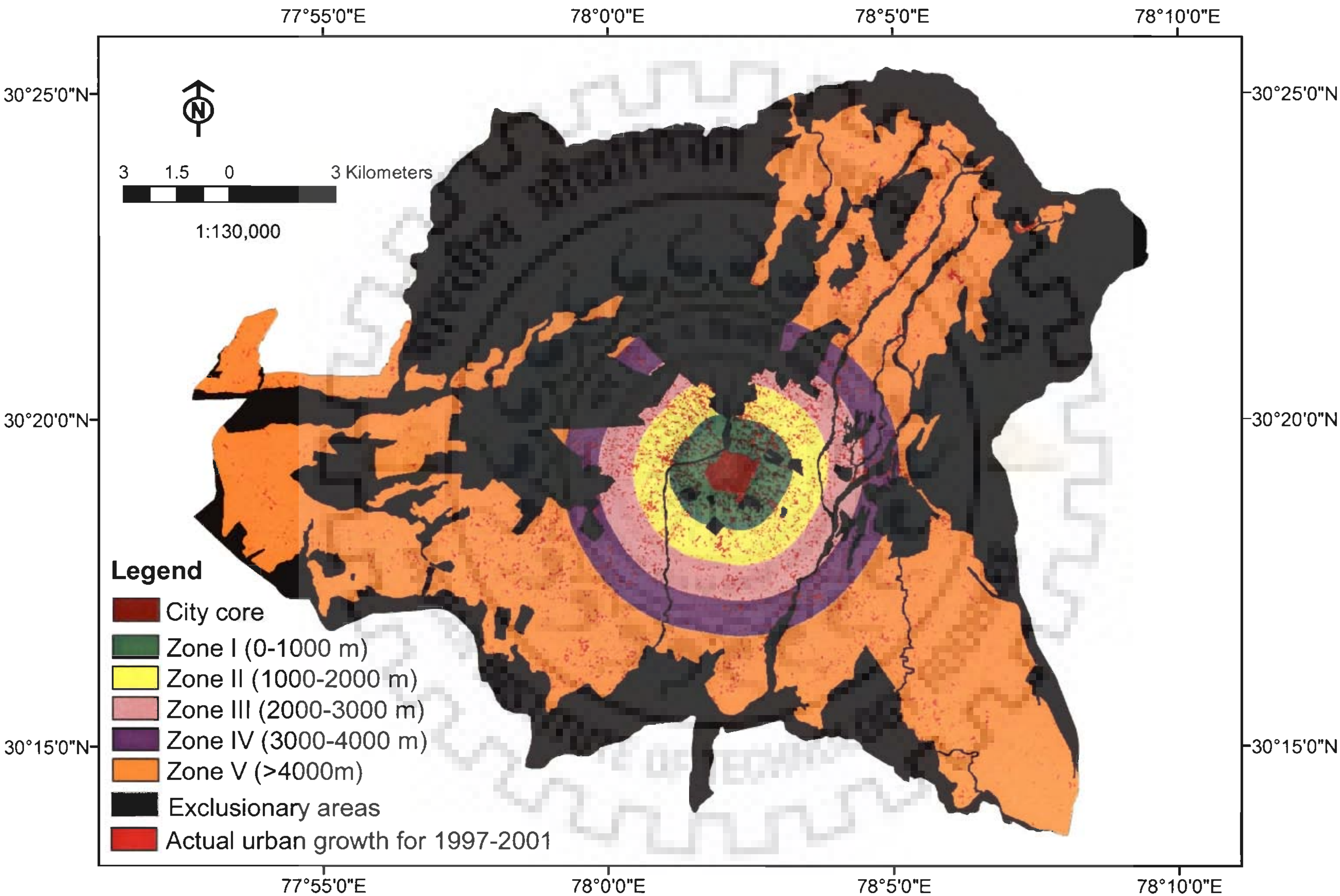

Figure 7.8 : Spatial distribution of actual urban growth during 1997-2001 in different buffer zones around city core (study area I)

RE for the period 2001-2005

Similar to 1997-2001, the map showing simulated and actual urban growth for period 2001-2005 are overlaid on the buffer zones created with respect to road network and city core (Figure 7.1 and 7.2). Figures 7.9 and 7.10 show the spatial distribution of the simulated growth for 2001-2005 in the buffer zones. Figures 7.11 and 7.12 show the spatial distribution of the actual urban growth during 2001-2005 in the buffer zones.

The stepwise computation of RE with respect to road network and city core for simulated urban growth is given in Tables 7.5 and 7.6. Similarly, Tables 7.7 and 7.8 show the stepwise computation of RE with respect to road network and city core for actual urban growth.

Table 7.5: Calculation of RE with respect to road network for simulated urban growth (2001-2005)

		Step 1	Step 2	Step 3
Buffer zones	Number of growth cells	p	log 1/p	p*log 1/p
Zone I	14436	0.719	0.143	0.103
Zone II	3531	0.176	0.755	0.133
Zone III	1674	0.083	1.079	0.090
Zone IV	319	0.016	1.799	0.029
Zone V	113	0.006	2.250	0.013

Step 4: $SE = \sum_{i=1}^{5} p_i * \log \frac{1}{p_i}$ = (0.103 + 0.133 + 0.09+ 0.029+ 0.013) = 0.367

Step 5: RE = SE/log 5= 0.367/log 5 = 0.52

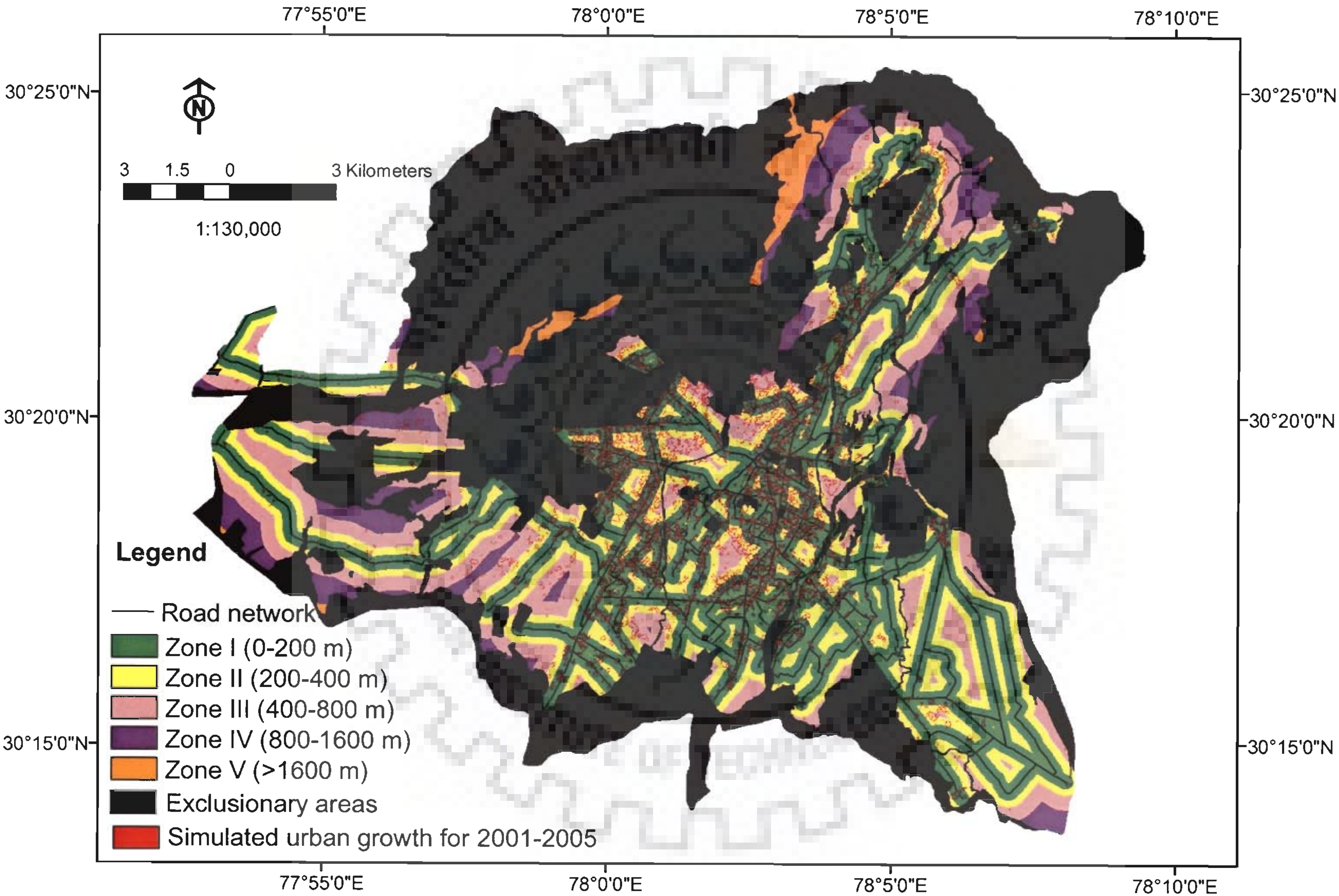

Figure 7.9: Spatial distribution of simulated urban growth for 2001-2005 in different buffer zones along road network (study area I)

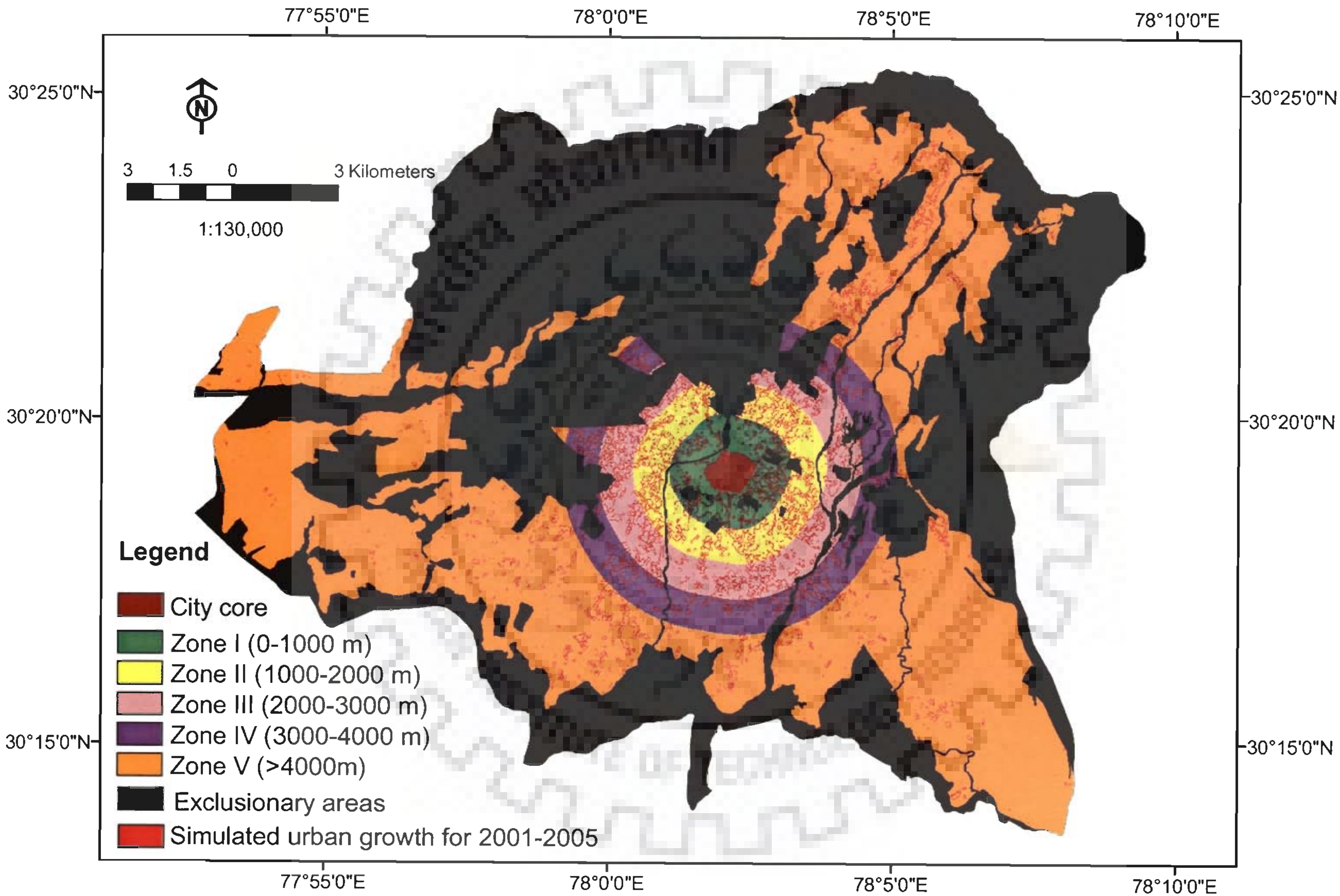

Figure 7.10: Spatial distribution of simulated urban growth for 2001-2005 in different buffer zones around city core (study area I)

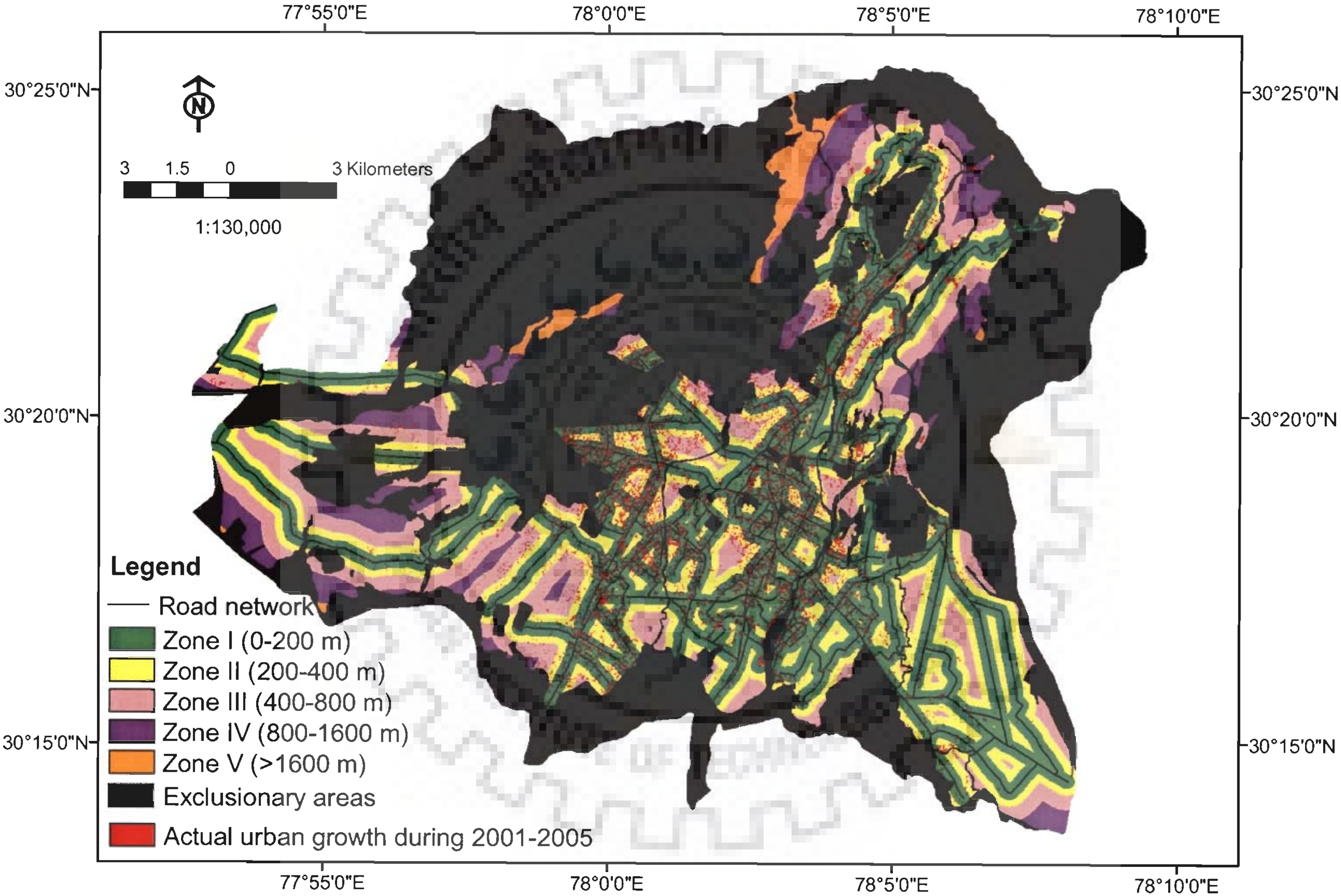

Figure 7.11: Spatial distribution of actual urban growth during 2001-2005 in different buffer zones along road network (study area I)

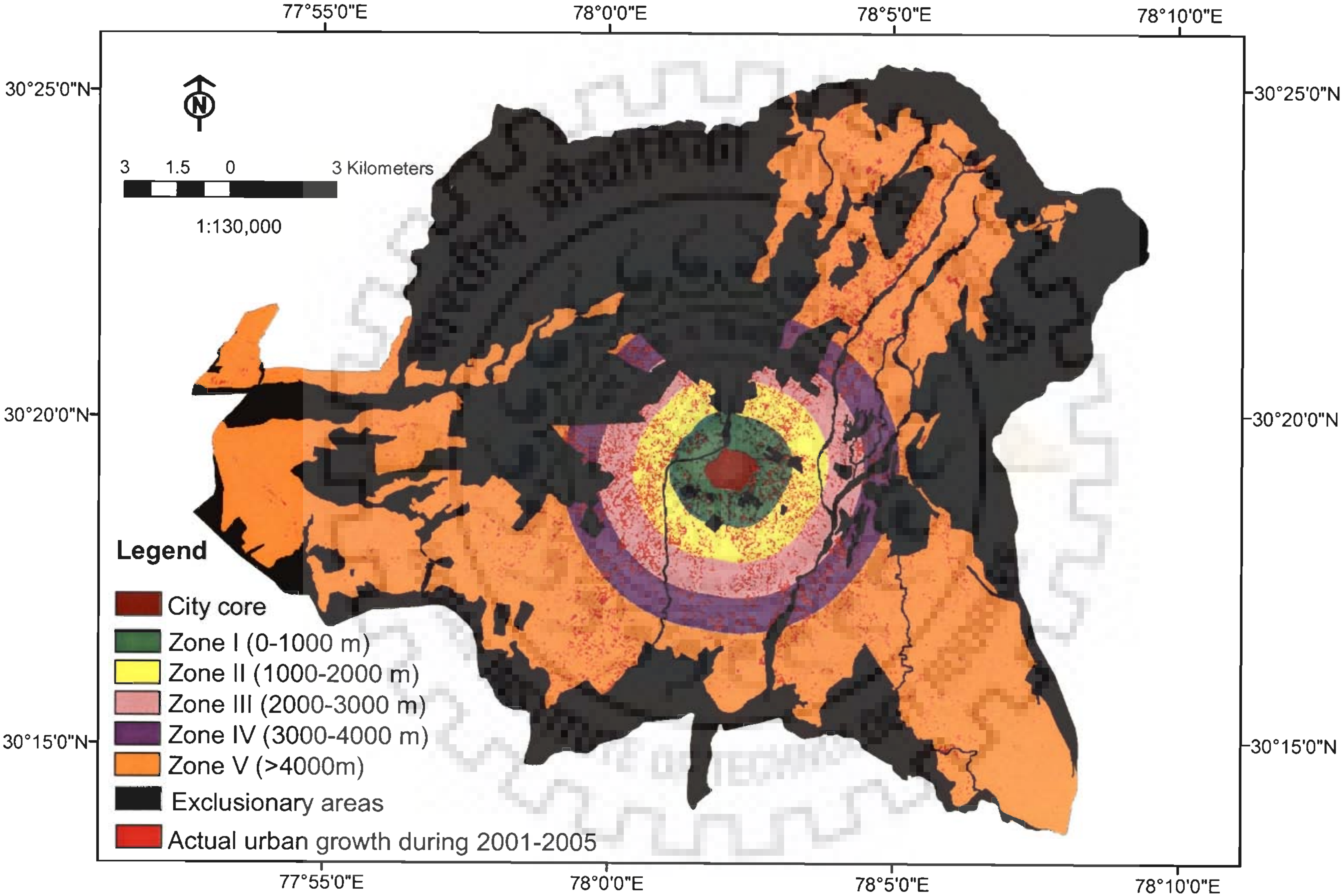

Figure 7.12: Spatial distribution of actual urban growth during 2001-2005 in different buffer zones around city core (study area I)

Table 7.6: Calculation of RE with respect to city core for simulated urban growth (2001-2005)

		Step 1	Step 2	Step 3
Buffer zones	Number of growth cells	p	log 1/p	p*log 1/p
Zone I	2241	0.112	0.952	0.106
Zone II	4294	0.214	0.670	0.143
Zone III	4461	0.222	0.653	0.145
Zone IV	2870	0.143	0.845	0.121
Zone V	6207	0.309	0.510	0.158

Step 4: $SE = \sum_{i=1}^{5} p_i * \log \frac{1}{p_i}$ = (0.106 + 0.143 + 0.145+ 0.121+ 0.158) = 0.673

Step 5: RE = SE/log 5= 0.673/log 5 = 0.96

Table 7.7: Calculation of RE with respect to road network for actual urban growth (2001-2005)

		Step 1	Step 2	Step 3
Buffer zones	Number of growth cells	p	log 1/p	p*log 1/p
Zone I	13753	0.685	0.164	0.113
Zone II	4116	0.205	0.688	0.141
Zone III	1723	0.086	1.066	0.092
Zone IV	396	0.020	1.705	0.034
Zone V	85	0.004	2.373	0.010

Step 4: $SE = \sum_{i=1}^{5} p_i * \log \frac{1}{p_i}$ = (0.113 + 0.141 + 0.092+ 0.034+ 0.01) = 0.389

Step 5: RE = SE/log 5= 0.389 /log 5 = 0.55

Table 7.8: Calculation of RE with respect to city core for actual urban growth (2001-2005)

		Step 1	Step 2	Step 3
Buffer zones	Number of growth cells	p	log 1/p	p*log 1/p
Zone I	1613	0.080	1.095	0.088
Zone II	3621	0.180	0.744	0.134
Zone III	3953	0.197	0.706	0.139
Zone IV	3255	0.162	0.790	0.128
Zone V	7631	0.380	0.420	0.160

Step 4: $SE = \sum_{i=1}^{5} p_i * \log \frac{1}{p_i} = (0.088 + 0.134 + 0.139 + 0.128 + 0.16) = 0.649$

Step 5: RE = SE/log 5= 0.649/log 5 = 0.92

7.3.2 Study area II

RE for 1993-2001 period

The map showing urban growth simulated for 1993-2001 is overlaid on the buffer zones created along the road network and around the city core (refer Figures 7.3 ad 7.4). The spatial distribution of the simulated growth in these buffer zones is shown in Figures 7.13 and 7.14. Tables 7.9 and 7.10 show the stepwise computation of RE with respect to road network and city core for simulated growth,

Similarly, the map showing actual urban growth that occurred during 1993-2001 is overlaid on the buffer zones created with respect to road network and city core (refer Figures 7.3 and 7.4) . The spatial distribution of the actual growth in these buffer zones is shown in Figures

7.15 and 7.16 respectively. The stepwise calculation of RE with respect to road network and city core for actual growth is shown in Tables 7.11 and 7.12.

Table 7.9: Calculation of RE with respect to road network for simulated urban growth (1993-2001)

		Step 1	Step 2	Step 3
Buffer zones	Number of growth cells	p	log 1/p	p*log 1/p
Zone I	7106	0.622	0.206	0.128
Zone II	3042	0.266	0.575	0.153
Zone III	1242	0.109	0.963	0.105
Zone IV	32	0.003	2.553	0.007
Zone V	0	0.000	0.000	0.000

Step 4: SE = $\sum_{i=1}^{5} p_i * \log \frac{1}{p_i}$ = (0.128 + 0.153 + 0.105+ 0.007+ 0) = 0.393

Step 5: RE = SE/log 5= 0.393/log 5 = 0.56

Table 7.10: Calculation of RE with respect to city core for simulated urban growth (1993-2001)

		Step 1	Step 2	Step 3
Buffer zones	Number of growth cells	p	log (1/p)	p*log 1/p
Zone I	1072	0.094	1.027	0.096
Zone II	3431	0.300	0.522	0.157
Zone III	3523	0.308	0.511	0.158
Zone IV	2306	0.202	0.695	0.140
Zone V	1090	0.096	1.020	0.097

Step 4: SE = $\sum_{i=1}^{5} p_i * \log \frac{1}{p_i}$ = (0.096 + 0.157 + 0.158+ 0.14+ 0.097) = 0.649

Step 5: RE = SE/log 5= 0.649/log 5 = 0.92

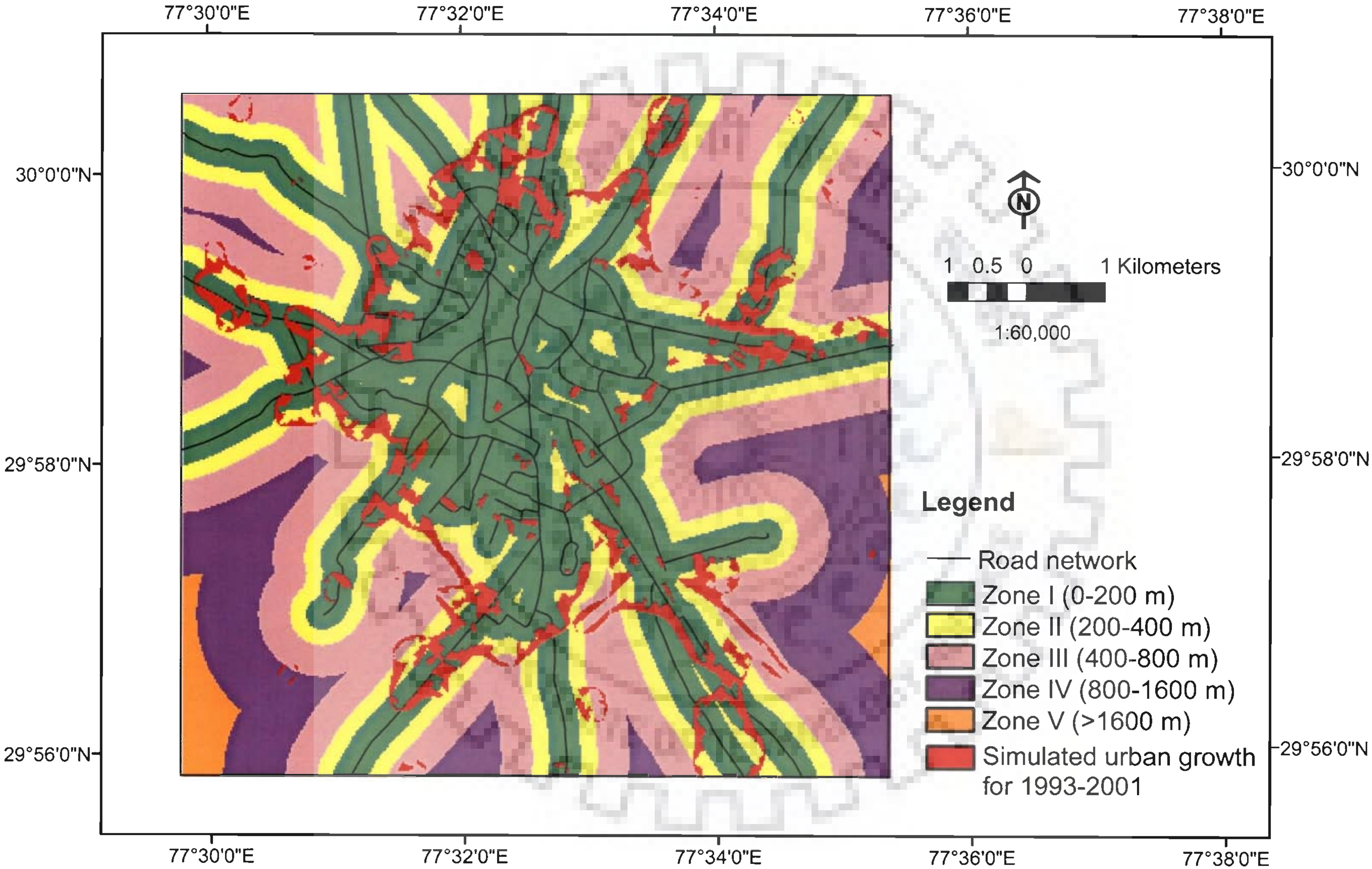

Figure 7.13: Spatial distribution of simulated urban growth for 1993-2001 in different buffer zones along road network (study area II)

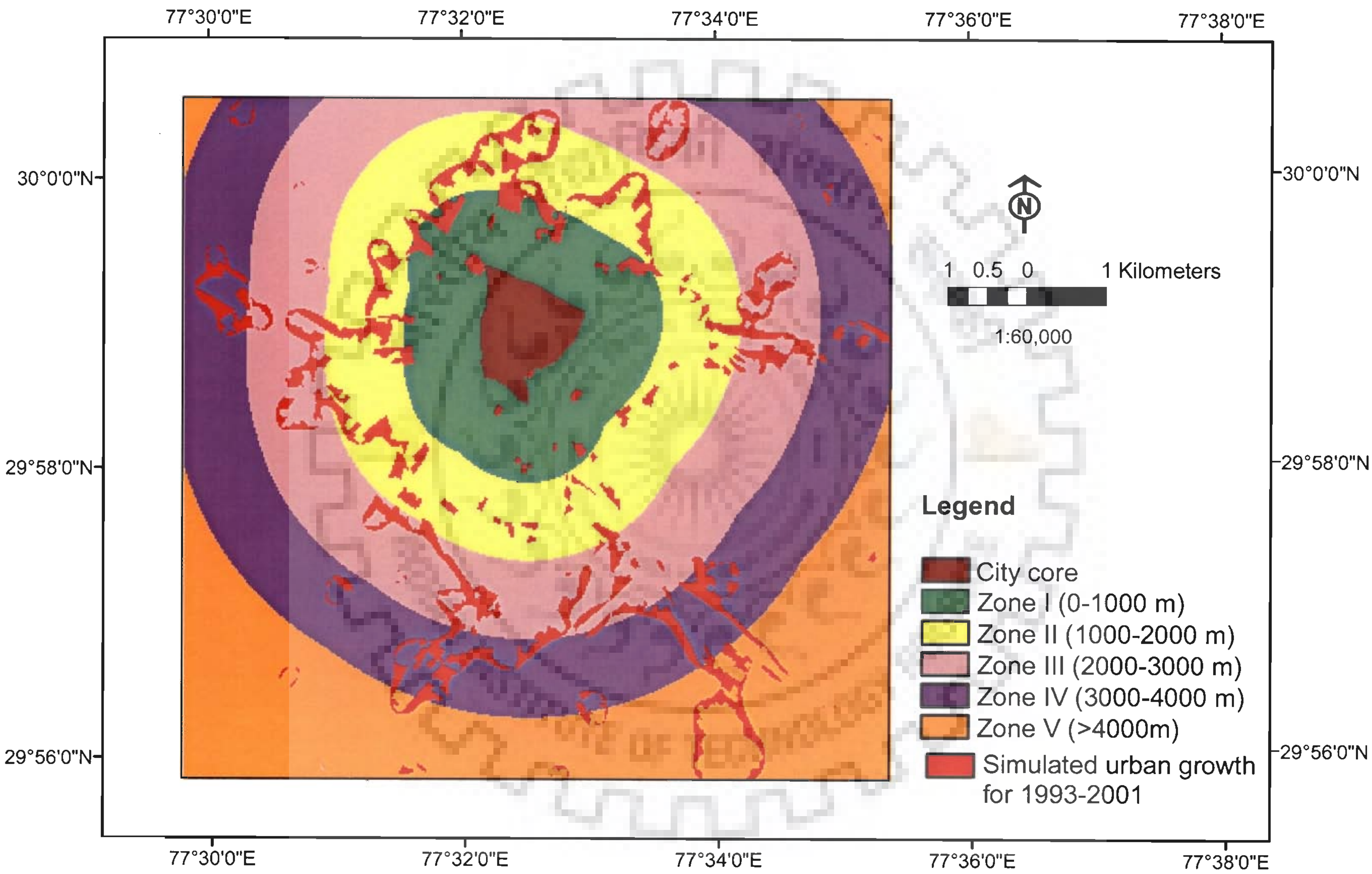

Figure 7.14: Spatial distribution of simulated urban growth for 1993-2001in different buffer zones around city core (study area II)

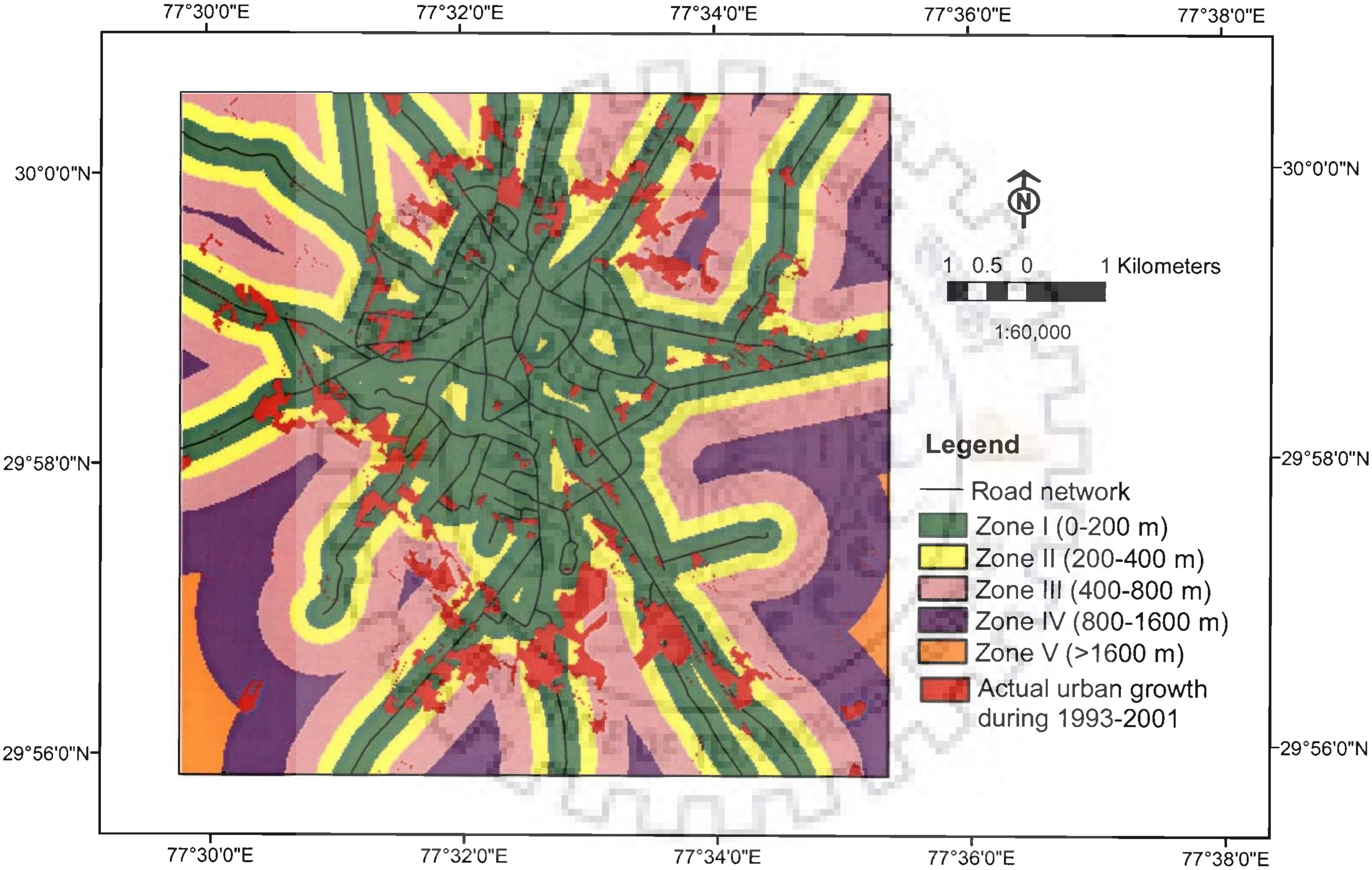

Figure 7.15: Spatial distribution of actual urban growth during 1993-2001 in different buffer zones along road network (study area II)

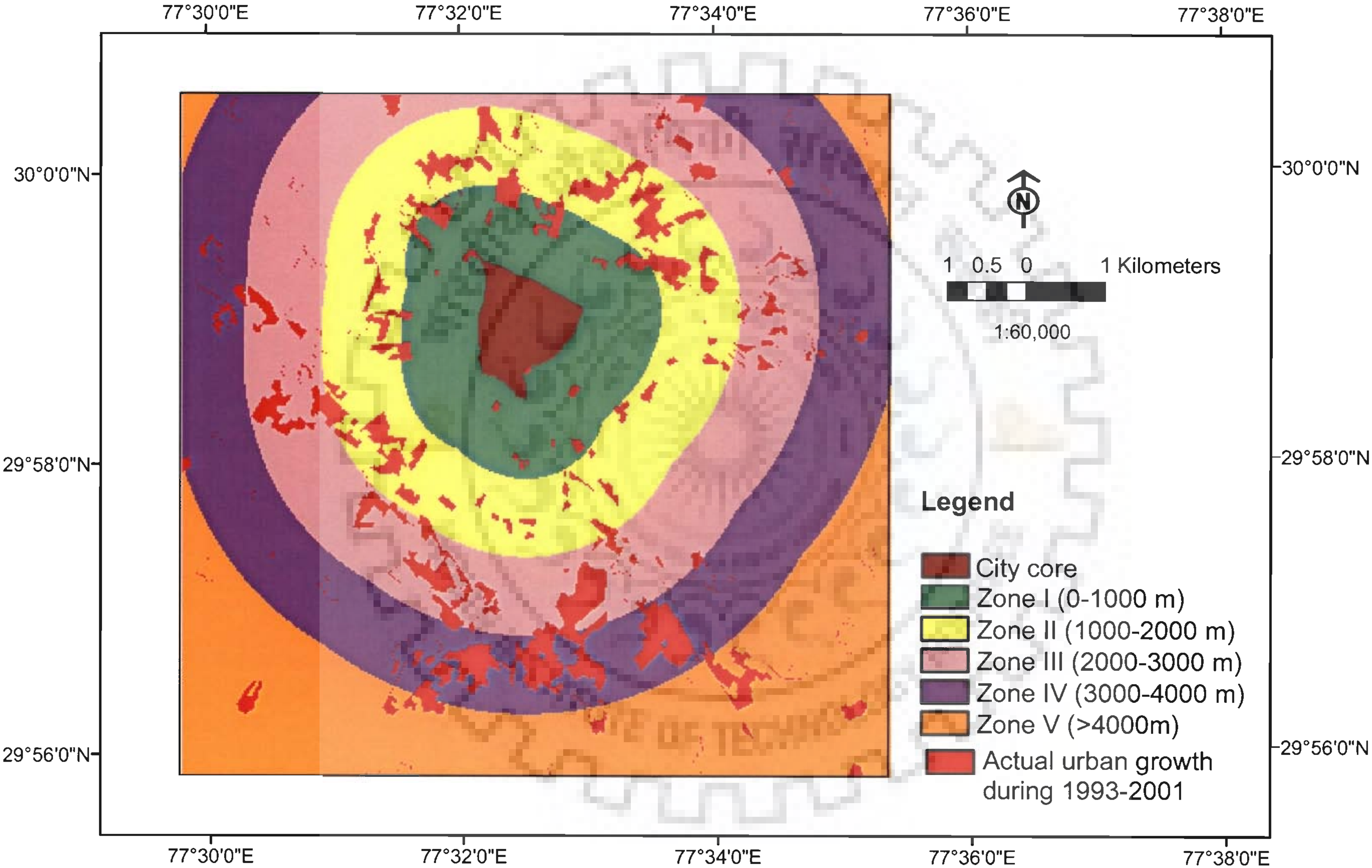

Figure 7.16: Spatial distribution of actual urban growth during 1993-2001 in different buffer zones around city core (study area II)

Table 7.11: Calculation of RE with respect to road network for actual urban growth (1993-2001)

Buffer zones	Number of growth cells	Step 1 p	Step 2 log (1/p)	Step 3 p*log 1/p
Zone I	5893	0.516	0.287	0.148
Zone II	3079	0.270	0.569	0.153
Zone III	2094	0.183	0.737	0.135
Zone IV	356	0.031	1.509	0.047
Zone V	0	0.000	3.757	0.001

Step 4: $SE = \sum_{i=1}^{5} p_i * \log \frac{1}{p_i}$ = (0.148 + 0.153 + 0.135+ 0.0475+ 0.001) = 0.484

Step 5: RE = SE/log 5= 0.484/log 5 = 0.69

Table 7.12: Calculation of RE with respect to city core for actual urban growth (1993-2001)

Buffer zones	Number of growth cells	Step 1 p	Step 2 log 1/p	Step 3 p*log 1/p
Zone I	909	0.080	1.099	0.087
Zone II	3532	0.309	0.510	0.158
Zone III	3201	0.280	0.552	0.155
Zone IV	2762	0.242	0.617	0.149
Zone V	1018	0.089	1.050	0.094

Step 4: $SE = \sum_{i=1}^{5} p_i * \log \frac{1}{p_i}$ = (0.09 + 0.16 + 0.15+ 0.15+ 0.09) = 0.643

Step 5: RE = SE/log 5= 0.643/log 5 = 0.91

7.4 Assessment of urban growth using Relative Entropy

7.4.1 Study area I

In this section, in the first part, RE with respect to road network, for 1993-2001 and 2001-2005 periods has been analyzed. While in the second part, the RE with respect to city core for the same two time periods has been analyzed.

7.4.1.1 RE with respect to road network

<u>1997-2001 period</u>

The RE values for simulated and actual urban growth with respect to road network have been obtained as 0.46 and 0.64 respectively (refer Tables 7.1 and 7.3). The value of RE for simulated urban growth is smaller than that obtained for actual urban growth. This indicates that the simulated urban growth cells are concentrated in a few zones whereas the actual urban growth cells are dispersed with respect to road network. This can further be substantiated from Figure 7.17 that shows the percentage of growth cells lying in different buffer zones along the roads in the road network layer. It can be observed from the figure that in zone I, the percentage of simulated growth cells (i.e., 72.3%) is significantly higher than that of actual growth cells (i.e., 62.3%). For other zones, the reverse trend can be seen. However, for zones other than zone I, the difference between percentages of growth cells for the two growth patterns is insignificant. Due to this higher concentration of simulated urban growth in zone I, a lower value of RE has been obtained for the simulated growth than for the actual urban growth.

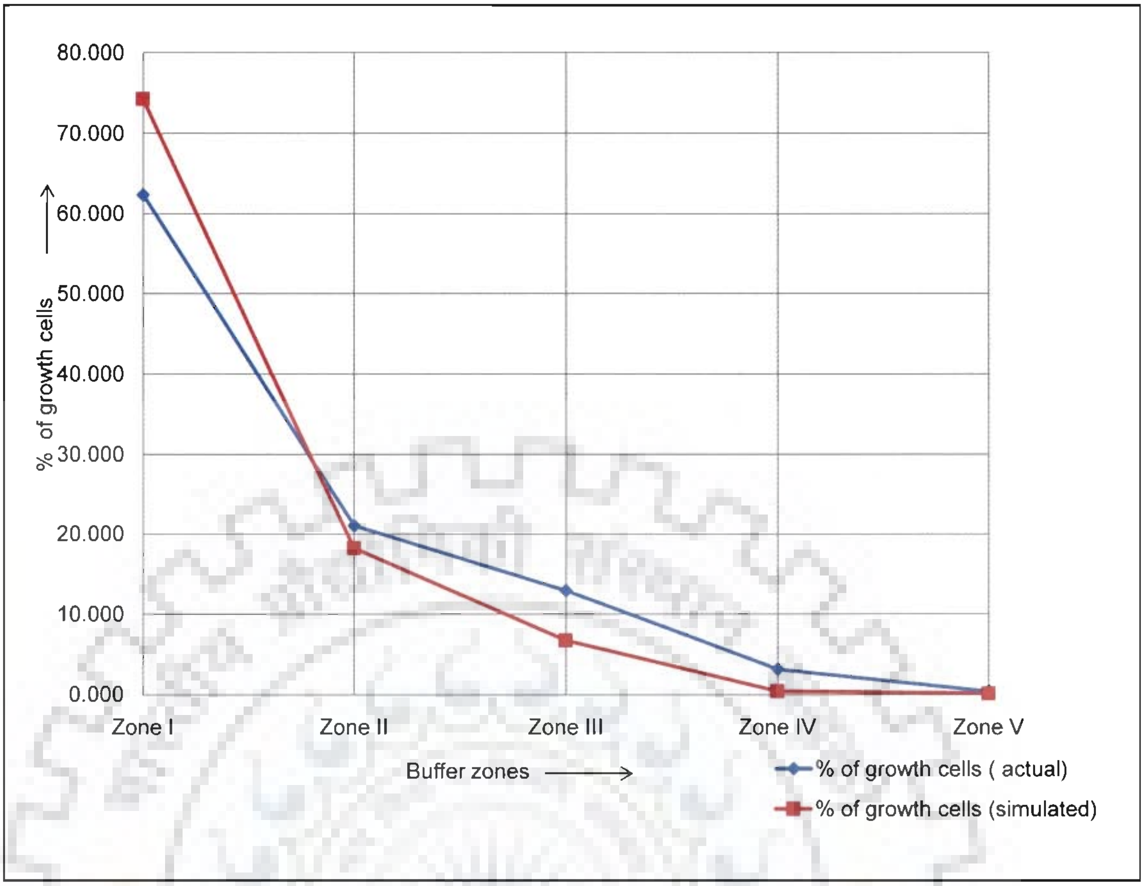

Figure 7.17: Percentage of actual and simulated growth cells lying in different zones along the road network for 1997-2001 (Study area I)

<u>2001-2005 period</u>

The RE for simulated and actual urban growth, with respect to road network have been obtained as 0.52 and 0.54 respectively (refer Tables 7.5 and 7.7). The value of RE for simulated growth is nearly equal to that obtained for actual growth. This indicates that the simulated and actual urban growth cells are distributed in a same manner in the buffer zones along the roads.

This can be explained from Figure 7.18, which shows the percentage of the growth cells lying in different buffer zones along the roads. It can be observed from the figure, that the distribution patterns of simulated and actual growth cells in different zones are identical.

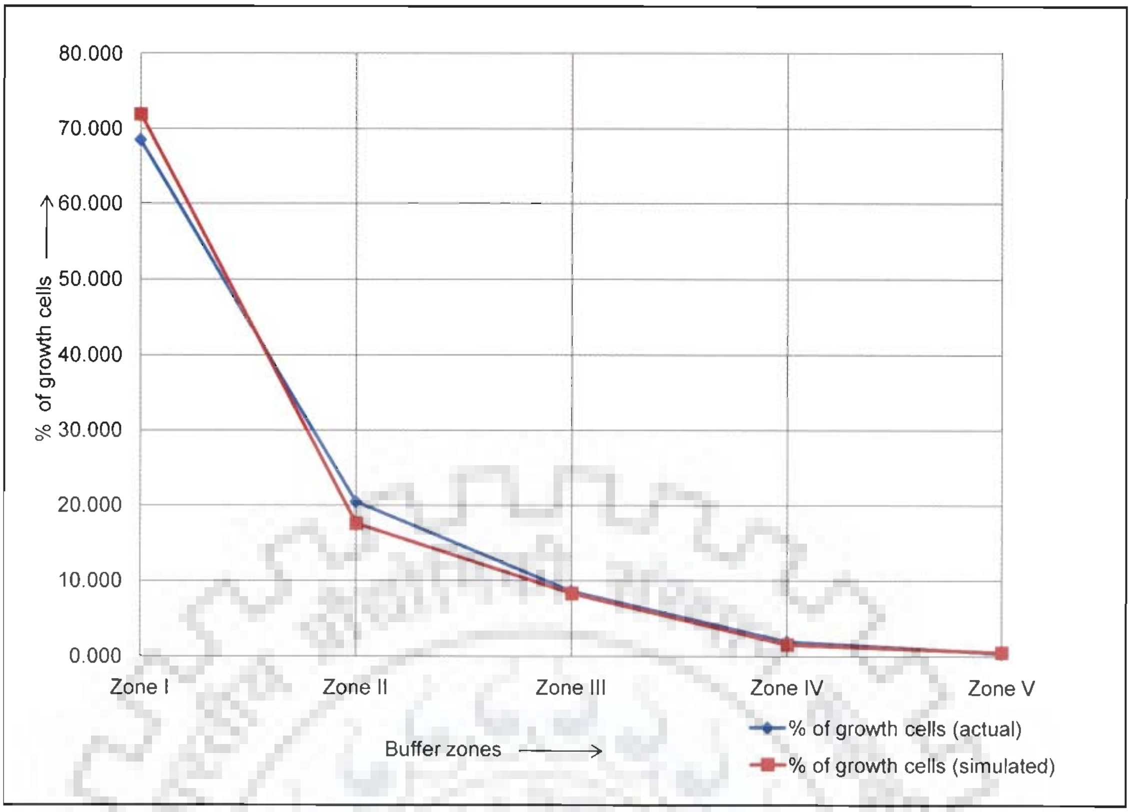

Figure 7.18: Percentage of actual and simulated growth cells lying in different zones along the road network for 2001-2005 (Study area I)

The RE with respect to road network for the actual and simulated growth for 1997-2001 and 2001-2005 period have been summarized in Table 7.13

Table7.13: RE with respect to road network for actual and simulated growth

	RE for simulated growth	RE for actual growth
1997-2001 period	0.46	0.64
2001-2005 period	0.52	0.54

On comparing the values of RE for actual growth during 1997-2001 and 2001-2005 periods (refer Table 7.13), it has been found that the value of RE for actual growth during 1997-2001 is greater than that for 2001-2005 period. This indicates that the actual growth cells during 1997-2001 are more dispersed with respect to the road network as compared to 2001-2005. The growth during 2001-2005 has taken place mainly in the form of densification of existing built-up areas that are in close vicinity of the road. Therefore, the growth in 2001-2005 is more compact compared to 1997-2001.

From Table 7.13, it can be inferred that for period 1997-2001, the model simulated a more compact growth compared to actual growth, with respect to roads. However, for 2001-2005 period the model has been able to simulate the growth with respect to roads accurately, as it matches with the actual growth pattern.

7.4.1.2 RE with respect to city core

1997-2001 period

The RE for simulated and actual urban growth, with respect to city core have been obtained as 0.96 and 0.90 respectively (refer Table 7.2 and 7.4). Since the two RE values are nearly equal, it indicates that the simulated and actual urban growth cells are distributed in a similar manner in different zones around the city core. As can be substantiated from Figure 7.19, the distribution pattern of actual and simulated growth cells in different zones is generally same, except in zone V. It can be observed that in zone V, 44.1% of actual growth cells are located compared to 12.1% of simulated growth cells. While for rest of the zones, the reverse trend is observed. It is due to this heavy concentration of cells in zone V, that the RE with respect to city core, for actual growth is 0.90 as compared to 0.96 for simulated growth.

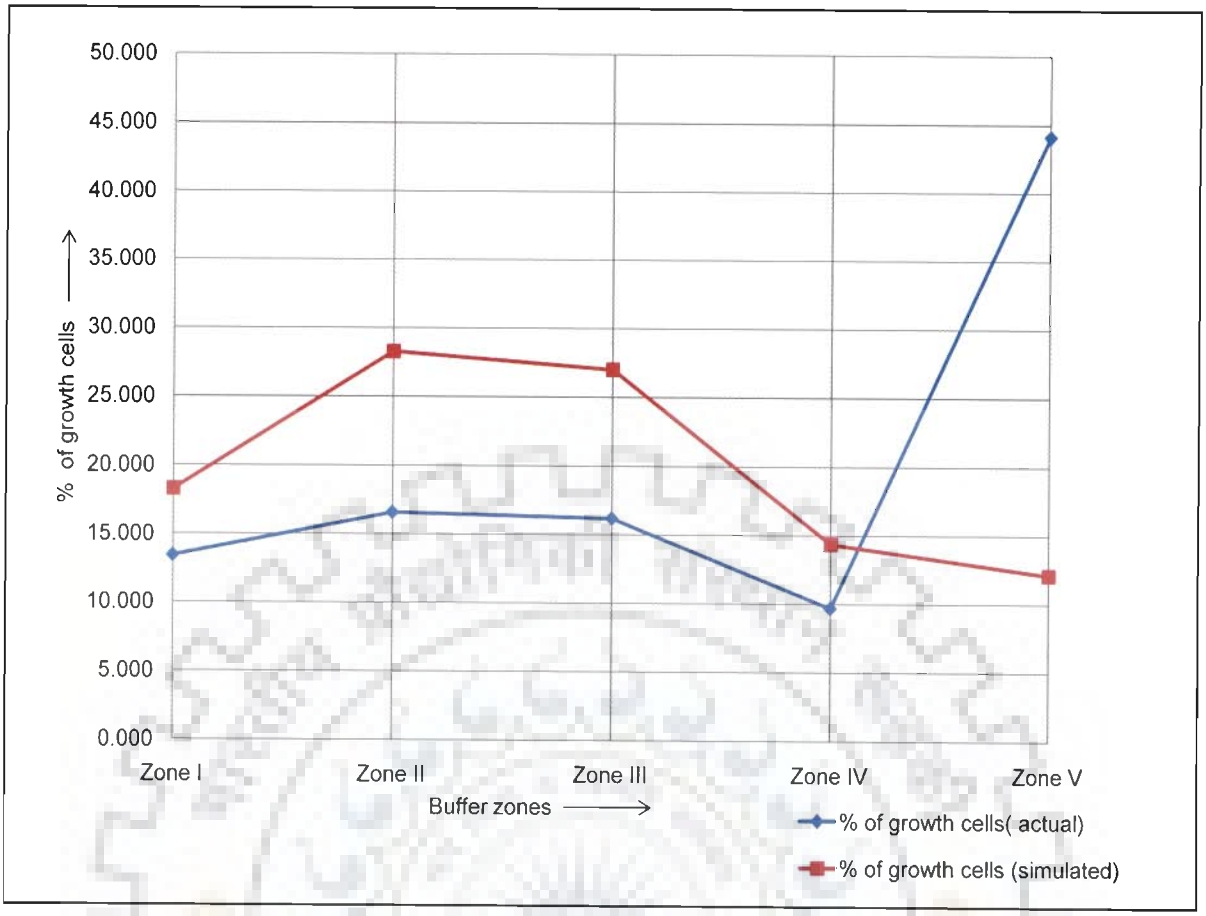

Figure 7.19: Percentage of actual and simulated growth cells lying in different zones around the city core for 1997-2001 (Study area I)

<u>2001-2005 period</u>

The RE for simulated and actual urban growth, with respect to city core have been obtained as 0.96 and 0.92 respectively (refer Tables 7.6 and 7.8). The two equal values of RE, indicate that the simulated urban growth cells are distributed in a similar manner as the actual growth cells with respect to the city core. As can be seen from Figure 7.20 also, the distribution patterns of simulated and tual growth cells in different zones are identical.

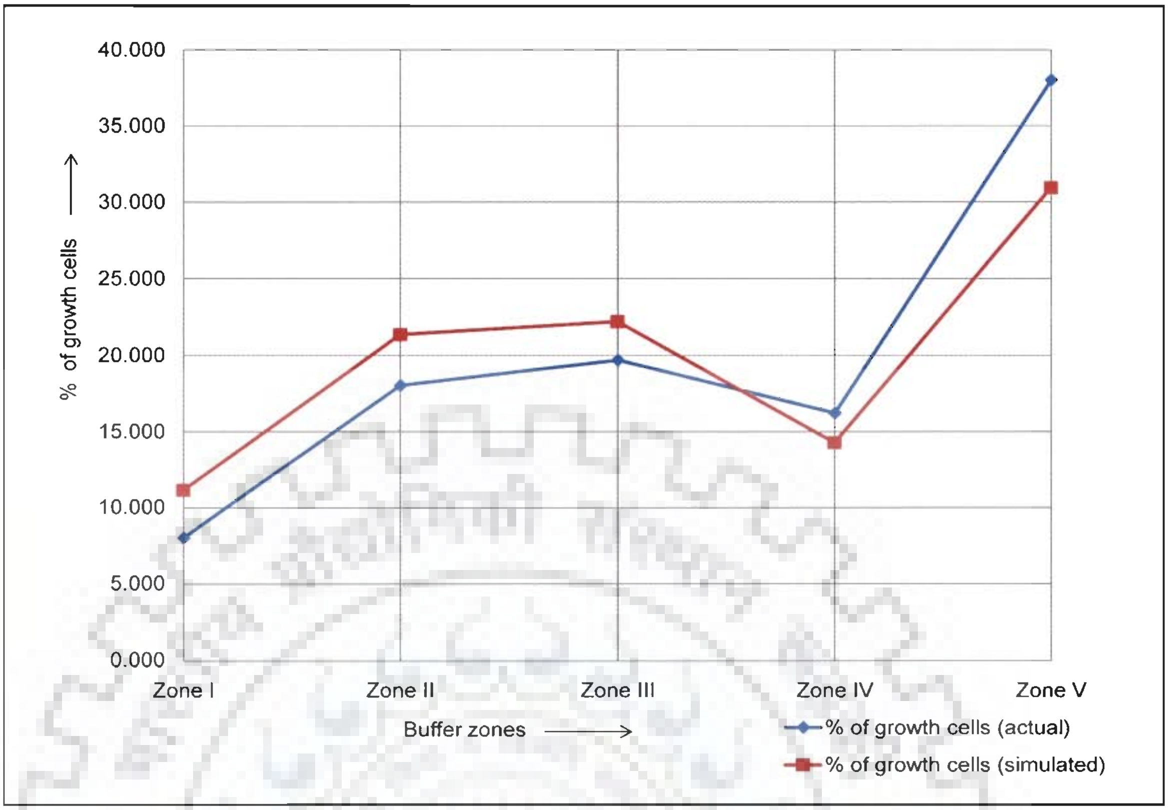

Figure 7.20: Percentage of actual and simulated growth cells lying in different zones around the city core for 2001-2005 (Study area I)

The RE with respect to city core, for the actual and simulated growth for 1997-2001 and 2001-2005 periods have been summarized in Table 7.14

Table 7.14: RE with respect to city core for actual and simulated growth

	Simulated growth	Actual growth
1993-2001 period	0.96	0.90
2001-2005 period	0.96	0.92

On comparing the RE with respect to city core, for actual growth during periods 1997-2001 and 2001-2005 (refer Table 7.14), it can be observed that the growth pattern with respect to city core has been identical. Thus, the model has been able to simulate the growth pattern with respect to roads quite accurately.

From the above analysis, it can be inferred that the model has been able to simulate the growth with respect to roads and city core accurately, except for urban growth with respect to roads for 1997-2001 period. This may be due to dispersed urban growth, which might have taken place along the roads during this period.

7.4.2 Study area II

Similar to study area I, the RE with respect to roads for 1993-2001 period is analyzed, in the first part of this section, whereas the RE with respect to city core for 1993-2001 is analyzed in second part.

7.4.2.1 RE with respect to road network

1993-2001 period

The RE values for simulated and actual urban growth with respect to road network have been obtained as 0.56 and 0.69 respectively (refer Tables 7.9 and 7.11). Thus, the value of RE for simulated growth is less than that obtained for actual growth. This shows that the actual urban cells are dispersed with respect to the road network while the simulated growth cells are concentrated in a few zones. This can be explained from Figure 7.21, which shows the percentage of growth cells lying in different buffer zones along the roads. It can be observed from the figure that in zone I, the percentage of simulated growth cells (i.e., 62.2%) is higher than the actual growth cells (i.e., 51.6%). In zone II, a reversal takes place wherein the percentage of simulated growth cells (i.e., 10.8%) is lower than that of actual growth cells (i.e., 18.3%). This trend continues in other zones also, although the difference between percentages of growth cells in simulated and actual growth patterns is insignificant. Thus, due to higher concentration of growth cells in zone I, a lower value of RE has been obtained for the simulated growth than for the actual urban growth.

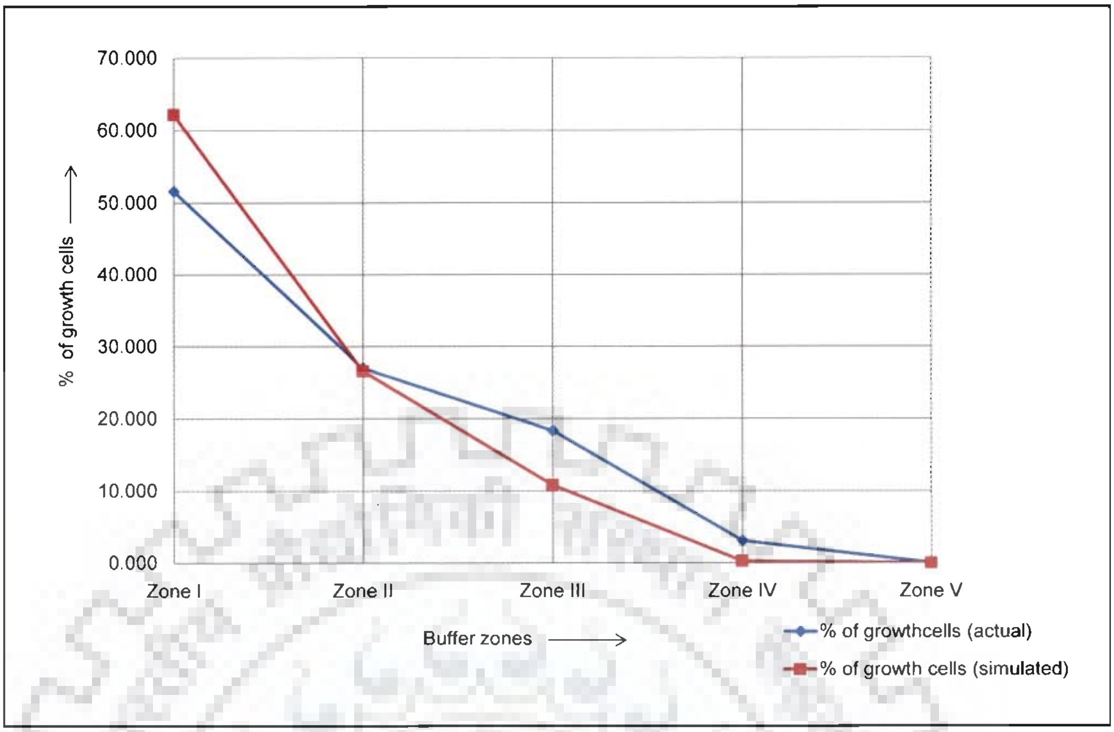

Figure 7.21: Percentage of actual and simulated growth cells lying in different zones along the road network for 1993-2001 (Study area II)

7.4.2.2 RE with respect to city core

<u>1993-2001 period</u>

The RE values for simulated and actual urban growth with respect to city core have been obtained as 0.93 and 0.92 respectively (refer Tables 7.9 and 7.11). Thus, the RE values for simulated and actual growth are nearly equal. This indicates that the simulated and actual growth cells are distributed in a similar manner in the buffer zones created around the city core. This can be explained with the help of Figure 7.22, which shows the percentage of simulated and actual growth cells lying in different buffer zones around the city core. It can be seen from the figure that the distribution pattern for simulated and actual growth cells in different zones are identical.

From the assessment of RE with respect to road network and city core in section 7.4.2.1 and 7.4.2.2 respectively, it can be inferred that the model has simulated a more compact growth

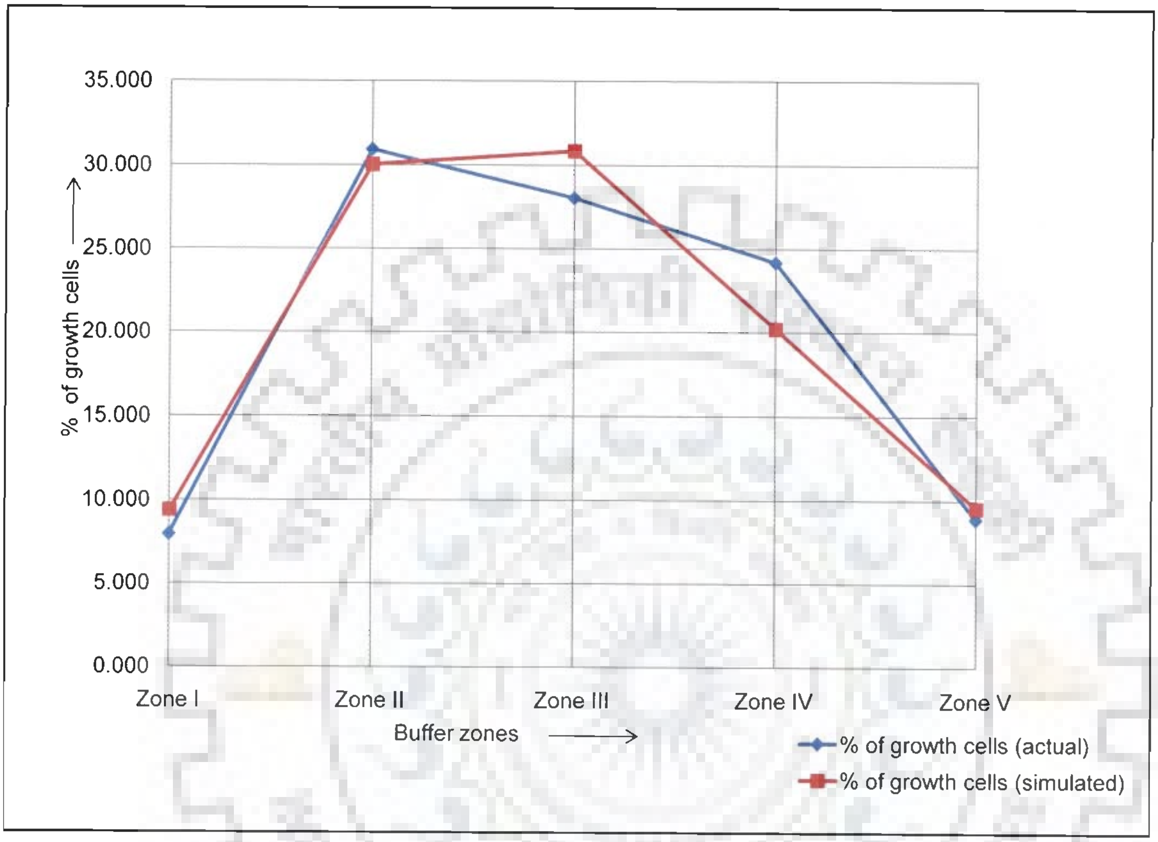

Figure 7.22: Percentage of actual and simulated growth cells lying in different zones around the city core (Study area II)

along the roads as compared to the actual growth. While with respect to the city core, the model has been able to simulate quite accurately the distribution of urban growth.

The results presented in this chapter clearly reflect that RE can serve as a potential index for evaluation of simulated and actual growth with respect to a given factor affecting the urban growth.

Chapter 8

Conclusions and Further Research

8.1 Introduction

India is experiencing a rapid pace of urbanization. As the limited land resources in the city diminish, the pressure mounts, which result in an increasing demand for land. This leads to an outward growth from the city. The outward growth often outpaces the planning efforts of the government. Thus, an urgent need was felt to develop models that could predict future urban growth in accurate manner as this may help the authorities to take proper policy and planning measures.

The failure of a number of traditional models to deal with the spatial and temporal aspects of urban growth has led to the development of Cellular Automata (CA) based urban growth models. The main aim of this thesis was to investigate the efficiency of CA based models for assessment of urban growth in a GIS environment.

8.2 Overview of methodology

In the present thesis, urban growth was defined in terms of increase in built-up area, which could be interpreted with ease from the remote sensing data. The proposed CA model was based on the dichotomy of built-up and non built-up areas and simulated urban growth as a function of three factors,

i) Distance to road network

ii) Accessibility to infrastructural facilities

iii) Distance to city core

Spatial data layers corresponding to the three factors were generated using remote sensing and GIS tools. For Dehradun city study area, the data acquired by IRS 1D satellite LISS-III and PAN sensor at a spatial resolution of 23.5 and 5.8 m respectively was used for generation of spatial data layers. For Saharanpur city study area, aerial photographs at 1:10,000 scale and remote sensing images from PAN sensor were used for data layer preparation.

These data layers formed the input for urban growth simulation using the MCE based CA model (MCE-CA) and an ANN based CA model (ANN-CA). In the MCE-CA model, weights were assigned to the factors based on their relative importance in the urban growth process using the Analytical Hierarchy Process (AHP). These factors were then combined by weighted linear combination to create an urban suitability map. The cell values in the suitability map were modified based on the amount of built-up area in the neighbourhood. Different sizes of Von Neumann and Moore neighbourhoods were used to estimate the amount of built-up area in neighbourhood. Thus, for a cell to be a likely candidate for transition from non built-up to built-up area, it must be both inherently suitable and near to built-up area. The number of cells to transit to built-up were determined exogenously and divided into equal parts depending on the number of model iterations. The data pertaining to factors were dynamically updated after each iteration. The simulated results were then evaluated using two indices:

i) Percentage correct match

ii) Moran Index.

Further, in order to reduce the subjectivity in CA modelling, an ANN based CA (ANN-CA) was also implemented to simulate the urban growth. The ANN was used to derive the suitability from the data itself rather than assigning the user defined subjective weights. Several ANNs were formulated and trained using backpropogation algorithm. The ANN which produced the highest accuracy was used for urban growth simulation. The result of the ANN-CA based model were compared with those obtained from the MCE-CA model.

The ANN outputs were also used directly for the creation of zones showing the urban growth potential on an ordinal scale (i.e. high, medium and low). Since the ANN outputs were not normally distributed, a logit transformation was applied to bring the data normally distributed. The transformed data was divided into three classes as,

i) Low potential zone < (μ-σ)

ii) (μ-σ) < Medium potential zone < (u+ σ)

iii) (u+ σ) < High potential zone

where, μ is mean and σ is the standard deviation of the transformed data.

The simulated growth patterns for both the study areas were also evaluated using Shannon's Entropy. It is a structural measurement index that assesses the goodness of fit according to the spatial domain of interest, which in this case was the distribution of urban growth with respect to the distance from roads and distance from city core. The spatial relationships between urban growth and the two distance variable were established using a two–dimension entropy space.

8.3 Conclusions

From the analysis of the results obtained after implementation of the proposed models for assessing urban growth in the two example study areas, following general conclusions have been drawn,

1. Dehradun city has experienced a dispersed growth. Therefore, small neighbourhood of 5x5 cells produced the highest accuracy in predicting the pattern and location of growth. In Saharanpur city, the urban growth has taken place in a compact and concentric form. Therefore, large neighbourhoods produced the most accurate simulation results.

2. Von Neumann neighbourhood of small size was found appropriate for city having dispersed growth, whereas for city having a compact development, both Von Neumann and Moore neighbourhoods were found appropriate.

3. Large number of model iterations failed to increase the accuracy of the models. The increase in number of iterations resulted in a more compact growth pattern as compared to the actual growth pattern. This may be due to unplanned and stochastic behavior of urban growth process in Indian cities, which the CA models have are not been able to simulate completely.

4. Percent correct match and Moran Index were found to be useful and simple indicators, for matching the simulated growth pattern with the actual growth. The former was able to match the two on a pixel by pixel basis. Whereas the later was found effective in matching pattern of growth in the region.

5. The accuracy of ANN-CA model was comparable with that of MCE-CA model for the data set considered. The, neural networks were, however, able to define the transition rules for CA from the data itself, without any human intervention, in an objective manner. This proves the usefulness ANN-CA based modelling for urban growth simulation.

6. The design of ANN architecture, which can be defined in many different ways, is a key issue in this study. The ANN architecture designed on the basis of literature driven thumb rules produced comparable and even better accuracy with that obtained from the optimal network as identified from processing of several ANN architectures.

7. The urban growth potential zonation maps derived from neural network outputs conveyed the actual growth pattern in the respective areas. Thus, preparing such zonation maps may be a valuable input for planning exercises like master and zonal plan preparation.

8. Shannon's Entropy is a useful indicator for assessing the urban growth in terms of spatial distribution of urban growth with respect to road network and city core. Since urban growth is a function of these elements, so Shannon's Entropy is a useful index that can evaluate the growth pattern and simulated results with respect to these elements.

8.4 Major Contributions

The research work reported in this thesis has resulted into following major contributions,

1. The applicability of Cellular Automata (CA) techniques for modeling growth of two Indian cities having varied growth patterns has been investigated fruitfully.

2. The application of ANN in cellular automata modelling helps in deriving the transition rules in an objective manner thereby reducing the human intervention.

3. The optimum sizes and types of neighbourhood to be used in CA modelling have been recommended for two Indian cities, one having dispersed growth pattern and another having compact growth pattern.

4. A methodology for generating zoning maps depicting areas with different urban growth potential based on ANN has been proposed. The zonation maps will be very useful for urban planners.

8.5 Further Research

The work presented in this thesis may be envisaged as a contribution to the development of CA based modelling for urban growth simulation, with special reference to Indian cities. Since, the work on CA based modelling for urban growth prediction in India has just started, some research directions are now put forth,

1. In this research, the urban growth is modelled as a function of physical factors only, therefore other socio-economic factors may also be incorporated in the proposed models.
2. The limitation of the proposed model is that it is based on the dichotomy of built-up and non built-up areas. Therefore, detailed urban land use information can be incorporated as now a day's high spatial resolution satellite data is also available.
3. The proposed CA based models can be applied to other cities with different characteristics such as coastal and hill towns. This would establish the general capabilities of the proposed models.

References

Alberti, M., 1999, Modelling the urban ecosystem: a conceptual framework. E*nvironmental and planning B*, **26(4)**, pp. 605-630.

Almeida, C. M., Batty, M., Monteiro, A. M. V., Camara, G., Soares-Filho, B. S., Cerqueira, G. C., and Pennachin,C. L., 2003, Stochastic cellular automata modeling of urban land use dynamics: empirical development and estimation. *Computer Environment and Urban Systems*, **27**, pp. 481-509

Anderson, J. R., Hardy, E. E., Roach, J. T., and Witmer, R. E., 1976, A land use and land cover classification system for use with remote sensor data. *USGS Professional Paper* **964**, USA.

Arora, M. K., Narsimham, G., and Mohanty, B., 1998, Neural network approach for the classification of remotely sensed data*, Asian Pacific Remote Sensing and GIS Journal,* **10(2)**, pp.11–18.

Arora, M. K., Tiwari, K.C., and Mohanty, B., 2000, Effect of neural network variables on image classification. *Asian Pacific Remote Sensing and GIS Journal*, **13**, pp. 1-11.

Arora, M. K., and Mathur, S., 2001, Multi-source image classification using neural network in a rugged terrain, *Geo Carto International*, **16(3)**, pp. 37 – 44.

Arora, M. K., 2002, Land cover classification from remote sensing data.G*IS@ development*, **6(3)**, pp. 24-25, 30-31.

Arora, M. K., and Agarwal, K., 2002, A program for sampling design for image classification accuracy assessment, *Photogrammetry Journal Finland*, **18(1)**, pp. 33-43.

Arora, M. K., Das Gupta, A.S., and Gupta, R.P., 2004, An artificial neural netwok approach for landslide hazard zonation in the Bhagirathi (Ganga) valley, Himalayas. *International Journal of Remote Sensing,* **25**, pp. 559-572.

Atkinson, P. M. and Tatnall, A. R. L., 1997, Neural networks in remote sensing. *International Journal of Remote Sensing,* **18(4)**, pp. 699-709.

Barredo, J. I., Kasanko, M., McCormick, N., and Lavalle, C., 2003, Modelling dynamic spatial process: simulation of urban future scenarios through cellular automata. *Landscape and Urban Planning*, **64**, pp. 145-160.

Barredo, J. I., Demicheli, L., Lavalle, C., Kasanko, M., and McCormick, N., 2004, Modelling future urban scenarios in developing countries: an application case study in Lagos,Nigeria. *Environment and Planning B: Planning and Design*, **32**, pp. 65-84.

Batty, M., and Longley, A., 1986, The fractal simulation of urban structure, *Environment and Planning A*, **18**, pp. 1143-1179.

Batty, M., 1994, A chronicle of scientific planning: the Anglo-American modeling experience. *Journal of the American Planning Association,* **60**, pp. 7-16.

Batty, M., and Longley, P., 1994, *Fractal Cities: A Geometry of Form and Function* (London: Academic Press).

Batty, M., and Xie, Y., 1994a, Modelling inside GIS. Part 1: Model structures, exploratory spatial data analysis and aggregation. *International Journal of Geographical Information Systems*, **8(3)**, pp. 291-307.

Batty, M., and Xie, Y., 1994b, Modelling inside GIS. Part 2: Selecting and calibrating urban models using ARC/INFO. *International Journal of Geographical Information Systems*, **8(1)**, pp. 451-470.

Batty, M., and Xie, Y., 1994c, From cells to cities. *Environment and Planning B*, **21**, pp. 31-48.

Batty, M., 1996, Urban change, *Environment and Planning B*, **23**, pp. 513-514.

Batty, M., and Xie, Y., 1997, Possible urban automata. *Environment and Planning B*, **24**, pp. 175-192.

Batty, M., 1998, Urban evolution on the desktop: simulation with the use of extended cellular automata. *Environment and Planning A*, **30**, pp. 1943-1967.

Batty, M., Xie, Y., and Zhanli, S., 1999, Modeling urban dynamics through GIS-based cellular automata. *Computers, Environment and Urban Systems*, **23**, pp. 205-233.

Batty, M., 2000, Geocomputation using cellular automata. In *Geo Computation,* Openshaw S. and Abrahart, R.J.(Eds), pp. 95-126 (London: Taylor & Francis, 2000).

Batty, M., 2001, Models in planning: technological imperatives and changing roles. *International Journal of Applied Earth Observation and Geoinformation,* **3(3),** pp. 252-266.

Batty, M. and Torrens, P.M., 2001, Modelling complexity: the limits to prediction, *CASA working paper series, paper* **36**, available online at: www.casa.ucl.uk (accessed 1 August 2005).

Benati, S., 1997, A cellular automaton for the simulation of competitive location. *Environment and Planning B*, **24**, pp. 205-218.

Benenson, I. and Torrens, P.M., 2004, *Geosimulation-Automata based modelling of urban phenomena* (New York : John Willey & Sons).

Bivand, R., and Lucas, A., 2000, Integrating models and Geographical Information Systems. In *Geocomputation*, Openshaw, S. and R. J. Abrahart, R.J. (Eds), pp.331-364 (London: Taylor & Francis, 2000).

Burrough, P. A., and McDonnell, R. A., 1998, *Principles of Geographical Information Systems* (New York: Oxford University Press).

Cabral, P., and Zamyatin, A., 2006, Three land change models for urban dynamics analysis in the Sintra-Cascais area. In *1st workshop of the EARSeL Special Interest Group Urban Remote Sensing*, 2-3 March, Berlin, Germany.

Cecchini, A., 1996, Urban modelling by means of cellular automata: generalised urban automata with help on-line (AUGH) model. *Environment and Planning B*, **23**, pp. 721-732.

Census of India, 2001, (New Delhi: Government of India).

Clarke, K. C., Gaydos, L., and Hoppen, S., 1997, A self-modifying cellular automaton model of historical urbanization in the San Francisco Bay area. *Environment and Planning B*, **24**, pp. 247–261

Clarke, K. C., and Gaydos, L., 1998, Loose-coupling a CA model and GIS: long-term urban growth prediction for San Franciso and Washington/Baltimore. *International Journal of Geographical Information Science*, **12(7)**, pp. 699-714.

Congalton, R. G., 1991, A review of assessing the accuracy of classifications of remotely sensed data. Remote Sensing of Environment, **37**, pp. 35-46.

Congalton, R. G., and Green, K., 1999, Assessing the Accuracy of Remotely Sensed Data: Principles and Practices (Florida: CRC Press, Inc.).

Couclelis, H., 1985, Cellular worlds: a framework for modeling micro-macro dynamics. *Environment and Planning A*, **17**, pp. 585-596.

Couclelis, H., 1989, Macrostructure and microbehaviour in metropolitan area. *Environment and Planning A*, **16**, pp. 141-154.

Couclelis, H., 1997, From cellular automata to urban models: new principles for model development and implementation. *Environment and Planning B*, **24**, pp. 165-174.

Couclelis, H., 2002, Modeling Frameworks, paradigms and approaches. In *Geographic Information Systems and Environmental Modeling*, Clarke, K.C., Parks, B.O., and Crane, M.P (Eds), pp. 36-50 (Upper Saddle River: Prentice Hall).

Davis, J. C., 1986, Statistics and data analysis in Geology (New York: John Wiley and Sons.).

Diappi, L., Bolchi, P., Franzini, L., Buscema, M., and Intraligi, M., 2002, The urban sprawl dynamics: does a neural network understand the spatial logic better than a cellular automata. In *42nd Congress of the European Regional Science Association, 27-31* August 2002, Dortmund.

Fazal, S., 2000, Urban expansion and loss of agricultural land – a GIS based study of Saharanpur city, India. *Environment & Urbanization*, **12(2)**, pp. 133-149.

Fischer, M. M., and Abrahart, R. J., 2000, Neurocomputing- tools for geographers. In *GeoComputation,* Openshaw S. and Abrahart, R.J.(Eds), pp. 187-218 (London: Taylor & Francis, 2000).

Foody, G. M., 1995, Land cover classification by an artificial neural network with ancillary information. *International Journal of Remote Sensing*, **16**, pp. 527-542.

Foody, G. M., 1996a, Approaches for the production and evaluation of fuzzy land cover classifications from remotely sensed data. *International Journal of Remote Sensing.* **17**, pp. 1317-1340.

Foody, G. M., 1996b, Relating the land-cover composition of mixed pixels to artificial neural network classification output. *Photogrammetric Engineering and Remote Sensing*, **62**, pp. 491-499.

Foody, G. M., and Arora, M. K., 1996, Incorporating mixed pixels in the training allocating and testing stages of supervised classifications. Pattern Recognition letters, **17,** pp. 1389-1398.

Foody, G. M., and Arora, M. K., 1997, An evaluation of some factors affecting the accuracy of classification by an artificial network. *International Journal of Remote Sensing,* **18(4)**, pp. 799-810.

Foody, G. M., 2001, Thematic mapping from remotely sensed data with neural networks: MLP, RBF and PNN based approaches. *Computers and Geosciences,* **26**, pp. 469-478.

Foody, G. M., 2004, Supervised image classification by MLP and RBF neural networks with and without an exhaustively defined set of classes. *International Journal of Remote Sensing*, **25**, pp. 3091-3104.

Forrester, J. W., 1969, *Urban Dynamics* (Cambridge, MA: MIT Press).

Gautam, N. C., 1976, Aerial photo-interpretation techniques for classifying urban land use. *Photogrammetric Engineering and Remote Sensing*, **42(6)**, pp.815-822.

GGIM, Good governance India magazine, available online at: www.infochangeindia.org (accessed on 4 April 2005).

Gowda, K., 1998, Forces of urban form, In *International Symposium on Changing Environmental Scenario in South Asia During The Past Five Decades*. 20-22 December 1998, Calcutta.

Gowda, K. and Sridhara, M. V., 2000, Sustainable city: experiences and perspectives. In *International Conference on urbanisation and housing*, 2000, Bangalore.

Gupta, J. K. and Bawa, P., 2004, Selecting sites for urban development projects. *Spatio-Economic Development Record,* **11(3),** pp. 29-33.

Hägerstrand, T., 1968, A monte carlo approach to diffusion. *In Spatial Analysis: A reader in Statistical Geography*, Berry, J.L. and Marble, D.F. (Eds), pp.368-384 (Englewood Cliffs, NJ: Prentice-Hall).

Haykin, S., 1999, *Neural Networks: A Comprehensive Foundation* (New Jersey: Prentice Hall).

Hecht-Nielsen, R., 1987, Kolmogorov's mapping neural network existence theorem. In *Proceedings of the first IEEE International conference on neural networks*. 21-24 June 1987, San Diego, CA

Hush, D., R., 1989, Classification with neural networks: a performance analysis. In *Proceedings of the IEEE International conference on systems engineering*. Daon, Ohio, USA, pp. 277-280.

Itami, R. M., 1994, Simulating spatial dynamics: cellular automata theory. *Landscape and Urban Planning*, **30**, pp. 27-47.

Jacob, N., Krishnan, R., Harmsen, K., and Murali Krishna, I.V., 2006, Spatial dynamic modeling through cellular automata for simulating land use change dynamics. *International Journal of Geoinformatics*, **2(2)**, pp. 31-38.

Jain, R. K., 2002, Massive urbanisation and urban governance: Some issues. *Spatio-Economic Development Record*, **9(2)**, pp. 25-27.

Jain, Sadhana and Jain, R. K., 2003, An integrated information system for urban and regional planning: Some suggestions. *Spatio-Economic Development Record*, **10(2)**, pp. 16-21.

Jensen, J. R., 1986, *Introductory Digital Image Processing: A Remote Sensing Perspective* (USA: Prentice Hall PTR).

Kanellopoulos, I., and Wilkinson, G. G, 1997, Strategies and best practice for neural network image classification. *International Journal of Remote Sensing*, **18(4)**, pp. 711-725.

Kanungo, D. P., Arora, M. K., Sarkar, S., and Gupta, R. P., 2006, A comparative study of conventional ANN black box, fuzzy and combined neural and fuzzy weighting procedures for landslide susceptibility zonation in Darjeeling Himalayas. *Engineering Geology*, **85**, pp. 347-366.

Kasetkasem, T., Arora, M. K., and Varshney, P. K, 2005, Super resolution land cover mapping using a Markov Random field based approach. *Remote Sensing Environment,* **96,** pp.302-314.

Kavzoglu, T., and Mather, P.M., 2003, The use of back propagation artificial neural networks in land cover classification. *International Journal of Remote Sensing*, **24**, pp. 4097-4938.

Knowles, R., and Wareing, J., 1976, *Economic and social geography* (Delhi: Rupa and Co.).

Kulshrestha, S. K., 2004. Some Suggestions on the Mixed Land Use Approach for Madhya Pradesh. In *53rd National Town & Country Planners Congress*, 27-29 December 2004, Indore, pp. 177-181.

Kulshrestha, S. K., 2007a. Emerging challenges in spatial development and need for reforms in urban and regional planning legislations. In *55th National Town & Country Planners Congress*, 9-11 January 2007, Kerala, pp. 5-11.

Kulshrestha, S. K., 2007b. Peri-Urban areas: The concept, concerns, and planning and development policies. In *56th National Town & Country Planners Congress*, 20-22 December 2007, Kolkatta, pp. 31-37.

Kumar, J. A. V., Pathan, S. K., and Bhanderi, R. J., 2007, Spatio-temporal analysis for monitoring urban growth- a case study from Indore city. *Journal of Indian Society of Remote Sensing,* **35(1)**, pp. 11-20.

Kumar, S., 2004, *Neural Networks: A Classroom Approach* (New Delhi: Tata McGraw Hall).

Lata, K., M., Rao, C., H., S., Prasad, V., K., Badrinath, K., V., S., and Raghavaswamy, 2001, Measuring urban sprawl of Hyderabad. *GIS @ development*, **5(12)**, pp. 26-29.

Laurini, R. and Thompson, D., 1996, *Fundamentals of spatial information systems* (London: Academic Press).

Leao, S. Z., 2002, Spatial-temporal model for demand and allocation of landfills in growing urban regions. Ph.D. thesis, Melbourne: University of Melbourne, Melbourne.

Lee, C., 1973, *Models in Urban Planning* (New York: Pergamon Press).

Li, X., and Yeh, A.G.O., 2001, Calibration of cellular automata by using neural networks for the simulation of complex urban systems. *Environment and Planning A: Planning and Design*, **33**, pp. 1445-1462.

Li, X., and Yeh, A. G. O., 2002, Neural-network-based cellular automata for simulating multiple land use changes using GIS. *International Journal of Geographical Information Science*, **16(4)**, pp. 323-343.

Li, X., and Yeh, A. G. O., 2004a, An extended cellular automaton using case-based reasoning for simulating urban development in a large complex region. *International Journal of Geographical Information Science,* **20(10)**, pp. 1109-1136.

Li, X., and Yeh, A. G. O., 2004b, Analyzing spatial restructuring of land use patterns in a fast growing region using remote sensing and GIS. *Landscape and urban planning,* **69**, pp. 335-354.

Lillesand, T. M., and Kiefer, R. W., 2000, *Remote sensing and image interpretation* (John Wiley & Sons, New York).

Longley, P., and Batty, M., 1996, Spatial analysis: modelling in a GIS environment. (New York: John Wiley and Sons).

Mahavir and Galema, M., 1991, Monitoring urban growth using Spot images and aerial photographs. *ITC Journal*, 2, pp.63-69.

Malczewski, J., 1999, *GIS and multicriteria decision analysis* (New York: John Wiley & Sons).

Malczewski, J., 2006, GIS-based multicriteria decision analysis: a survey of the literature. *International Journal of Geographical Information Science*, **20(7)**, pp.703-726.

Mather, P. M., 1999, *Computer processing of remotely sensed images: an introduction* (Chichester: John Wiley & Sons).

Meaille, R., and Wald, L., 1990, Using Geographical Information Systems and satellite imagery within a numerical simulation of regional growth. *International Journal of Geographical Information Systems*, **4(4)**, pp. 445-456.

Mundia, C. N. and Aniya, M., 2005, Analysis of land use/cover changes and urban expansion of Nairobi city using remote sensing and GIS. *International Journal of Remote Sensing,* **13(10)**, pp. 2831-2849.

Openshaw, S., and Abrahart, R.J., 2000, *GeoComputation* (London: Taylor and Francis).

Openshaw,O., and Openshaw,C.,1997, *Artificial intelligence in Geography* (New York: John Wiley & Sons).

Paola, J. D., 1994, Neural network classification of multispectral imagery. MSc thesis, The University of Arizona, Tucson, USA.

Pathan S. K., Jothimani, P., Choudhary G. K., Pendharkar, S. P., and Sampat Kumar, D., 1989, Urban landuse mapping and zoning of Bombay metropolitian region using remote sensing data. *Journal of Indian Society of Remote Sensing*, **17(3)**, pp. 11-22.

Pathan, S. K., Shukla, V. K., Patel, R. G., and Mehta, K. S., 1991, Urban land use mapping-A case study of Ahmedabad city and its environs. *Journal of Indian Society of Remote Sensing*, **19(2)**, pp. 95-112.

Pathan, S. K., Sastry, S. V. C., Dhinwa, P. S., Rao, M., Majumdar ,K. L., Kumar, D. S., Patkar, V. N., and Phatak, V. N., 1993, Urban growth trend analysis using GIS techniques-A case study of the Bombay Metropolitan Region. *International Journal of Remote Sensing*, **14(17)**, pp. 3169-3179.

Pathan, S.K., 2004, Urban Planning with specific reference to Indore Master. In international conference on "Spatial Data Infrastructure for Sustainable Development. 20-22 December,Ahmedabad.

Pathan, S.K., 2005, Space Science and Technology for Geographical Research and Applications (Ahmedabad: BS Publications).

Pathan, S.K., 2006, Geoinformatics techniques for urban and regional planning", (New Delhi: IGU Publication).

Paul, R. and Bharat, A., 1997, Solutions for metropolitan development. In *International Conference on Planning for 21st century (concepts & systems)* , 2-4 October 1997, Roorkee.(Department of Architecture and Planning, Univ. of Roorkee), pp. 257-265.

Petruccelli, Nandram, and Chen, 1999, *Applied Statistics for Engineers and Scientists* (New Jersey: Prentice-Hall Inc.).

Phipps, M., and Langlois, A., 1997, Spatial dynamics, cellular automata, and parallel processing computers, *Environment and Planning B*, 24, pp. 193-204.

Pijanowski, B. C., Brown, D. G., Shellito, B.A., and Manik, G. A., 2002a, Using neural networks and GIS to forecast land use changes: A Land Transformation Model. *Computers, Environment and Urban Systems*, **26**, pp. 553-575.

Pijanowski, B. C., Shellito, B. A., Pithadia, S., and Alexandridis, K., 2002b, *Forecasting and assessing the impact of urban sprawl in coastal watersheds along eastern lake Michigan. Lakes & Reservoirs: Research and Management*, **7**, pp. 189-199.

Pijanowski, B. C., Pithadia, S., Shellito, B. A , and Alexandridis, K., 2005, Calibrating a neural network-based urban change model for two metropolitan areas of the Upper Midwest of the United States. *International Journal of Geographical Information Science,* **19(2)**, pp.197-215.

Portugali, J., Benenson, I., and Omer, I., 1994, Sociospatial residential dynamics: stability and instability within a self-organising city, *Geographical Analysis*, **25**, pp. 321-340.

Portugali, J., 2000, *Self-organisation and the city (* Berlin: Springer-Verlag).

Ramachandran, R., 1991, *Urbanization and Urban Systems in India* (Delhi: Oxford University Press).

Rashid, S. M., 1993, Identification of suitable sites for construction and conservation : a case study of Delhi metropolitan area. In *Remote Sensing in Geography*, Rashid, S.M., (Eds) (New Delhi: Manak Publications).

Rashid, S. M., 1999a, Remote sensing of urban environment. In *Remote Sensing of Urban Environment,* Sokhi, B.S. and Rashid, S.M. (Eds), pp.1-41 (New Delhi: Manak Publications).

Rashid, S. M., 1999b, Suitability analysis of vacant lands for urban development: a case study of Guirim and Porvorim Towns . In *Remote Sensing of Urban Environment,* Sokhi, B.S. and Rashid, S.M. (Eds), pp. 285-301 (New Delhi: Manak Publications).

Reif, B., 1973, Models in urban and regional planning (New York: Prentice-Hall Inc.).

Ripley, B. D., 1993, Statistical aspects of neural networks. In *Networks and Chaos – Statistical and Probabilistic Aspects*, Barndorff-Nielsen, O., E., Jensen, J., L., and Kendall, W., S (Eds), pp. 40–123 (London: Chapman & Hall).

Routray, J. K., 1990, Data Base: An aid to GIS application for decentralized micro-level planning in developing countries - Indian experience. *HSD Working Paper No.* **34**, *Asian Institute of Technology Bangkok.*

Routray, J.K., 1993, Urban and regional planning in practice in India. *Habitat International*, **17(3)**, pp. 55-74.

Routray, J.K., Rath, K.C. and Sahoo, N.N., 2000, Urban land development and informal settlement planning:A study on Bhubaneswar city in eastern India. HSD Research Monograph **40**, *School of Environment, Resources and Development, Asian Institute of Technology, Bangkok.*

Rumelhart, D. E., Hinton, G. E., and Williams, 1986, Learning representatons by Back-propogating errors. *Nature*, **23**, pp. 533-536.

Saha, A. K., Gupta, R. P., and Arora, M. K., 2002, GIS-based landslide hazard zonation in the Bhagirathi (Ganga) valley, Himalayas. *International Journal of Remote Sensing,* **23(2)**, pp. 357--369.

Saha, A. K., 2004, GIS based study for route planning in landslide susceptible terrain, PhD thesis, IIT Roorkee, Roorkee, India.

Sembolini, F., 1997, An urban and regional model based on cellular automata. *Environment and Planning B*, **24(4)**, pp. 589-612.

Shortridge, A., 2007, Practical limits of moran's autocorrelation index for raster class maps. *Computers, Environment and Urban Systems*, **31**, pp. 362-367.

Silva, E. A., and Clarke, K. C., 2002, Calibration of the SLEUTH urban growth model for Lisbon and Porto, Portugal. *Computers, Environment and Urban Systems,* **26**, pp. *525-552.*

Singh, A., K., 2003, Modelling land use land over changes using Cellular Automata in a geo spatial environment. MSc thesis, International Institute for Geo-information Science and Earth Observation, The Netherlands.

Sipper, M., 1997, *Evolution of Parallel Cellular Machines: The Cellular Programming Approach* (Heidelberg: Springer-Verlag).

Sivanandam, S.N., Sumathi, S., Deepa, S.N., 2006, Introduction to neural networks using Matlab 6.0 (New Delhi: Tata Mcgraw-Hill).

Subudhi, A.P., 1998, Monitoring and mapping:Urban growth and changing land use pattern in and around Saharanpur city. Ph.D thesis, Ch. Charan Singh University, Meerut, India.

Sudhira, H., S., Ramachandra, T., V., and Jagadish, K., S., 2003, Urban sprawl pattern analysis using GIS. (CES Technical report no.99, Indian Institute of Science, Bangalore).

Sudhira, H., S., 2004, Integration of agent based and Cellular Automata models for simulating urban sprawl. MSc thesis, International Institute for Geo-information Science and Earth observation, The Netherlands.

Sui, D. Z., and Zeng, H., 2001, Modeling the dynamics of landscape structure in Asia's emerging Desakota regions: a case study in Shenzhen. *Landscape and Urban Planning*, **53(1-4)**, pp. 372.

Sullivan, D. O., and Torrens, P. M., 2000a, Cellular models of urban systems, *CASA working paper series, paper* **22**, available online at :www.casa.ucl.uk (accessed 01 August 2005).

Sullivan, D. O., and Torrens, P. M., 2000b, Cellular models of urban systems. In *Theoretical issues on cellular automata*, Bandini, S. and Worsch, T. (Eds), pp. 108-117 (London: Springer-Verlag).

Tayal, T. and Bharat, A., 1997, Managing urban environment: a case of Bhopal. In *International Conference on Planning for 21st century (concepts & systems)*, 2-4 October 1997, Roorkee.(Department of Architecture and Planning, Univ. of Roorkee), pp. 77-86.

Tobler, W. R., 1970, A computer movie simulating urban growth in the Detroit Region. *Economic Geography*, **46**, pp. 234-240.

Tobler, W. R., 1979. Cellular geography. In *Philosophy in Geography*, Gales, S. and Olson, G. (Eds), pp. 339-346 (Dortrecht: D Reidel).

Toffoli, T., and Margolus, N., 1987, Cellular Automata Machines: A New Environment for Modelling (Cambridge: MIT Press).

Torrens, P.M., 2000, How cellular models of urban systems work. *CASA working paper series, paper* **28,** available online at: www.casa.ucl.uk (accessed 26 June 2005).

Torrens, P. M., 2001, Can geocomputation save urban simulation? Throw some agents into the mixture, simmer and wait…, *CASA working paper series, paper* **32**, available online at www.casa.ucl.uk (accessed 1 August 2005).

Torrens, P. M., and Sullivan, D.O., 2001, Cellular Automata and urban simulation: where do we go from here. *Environment and Planning B: Planning and Design*, **28**,pp. 163-168.

Town and Country Planning Department, 2001, *Master plan of Saharanpur for 2021*, Govt. of Uttar Pradesh, Uttar Pradesh, India.

Town and Country Planning Department, 2005, *Draft Master plan of Dehradun for 2005 - 2025*, Govt. of Uttranchal, Uttranchal,India.

Van Westen, C., J., 1997, Statistical landslide hazard analysis. Application guide, In: ILWIS 2.1 for Windows, ITC, The Netherlands, pp. 73-84.

Varanka, D., 2001, Modeling Urban Expansion in the Philadelphia Metropolitan Area, available online at: http://mcmcweb.er.usgs.gov/phil/modeling.html (accessed on March 26 March 2002).

Waddell, P., 2002, UrbanSim: Modeling urban development for land use transportation and environmental planning. *Journal of the American Planning Association*, **68(3)**, pp. 297-314.

Wagner, D. F., 1997, Cellular automata and geographic information systems, *Environment and Planning B*, **24**, pp. 219-234.

Wang, F., 1994, The use of artificial neural networks in geographical information system for agricultural land-suitability assessment. *Environment and Planning A*, **26**, pp.265–284.

Ward, D. P., Murray, A.T., and Phinn, S.R., 2000, A stochastically constrained cellular model of urban growth. *Computers, Environment and Urban Studies*, **24**, pp. 539-558.

Waters, N., 2002, Modelling the environment with GIS: A historical perspective from Geography. Clarke, K.C., Parks, B.O., and Crane, M.P (Eds), pp. 1-35 (Upper Saddle River: Prentice Hall).

Wegener, M., 2000, Spatial Models and GIS. In *Spatial models and GIS. New Potential and New Models*, Forthringham, A.S. and Wegener, M., pp. 3-20 (London: Taylor and Francis).

White, R., and Engelen, G., 1993, Cellular automata and fractal urban form: a cellular modeling approach to the evolution of urban land use patterns. *Environment and Planning A*, **25**, pp. 1175-1199.

White, R., and Engelen, G., 1994. Cellular dynamics and GIS: modelling spatial complexity. *Geographical Systems*, **1**, pp. 237-253.

White, R., and Engelen, G., 1997, Cellular automata as the basis of integrated dynamic regional modelling. *Environment and Planning B*, **24**, pp. 235-246.

White, R., Engelen, G., and Uljee, I., 1997, The use of constrained cellular automata for high-resolution modelling of urban land-use dynamics. *Environment and Planning B: Planning and Design*, **24**, pp. 323-343.

White, R., 1998, Cities and cellular automata. *Discrete Dynamics in Nature and Society*,**2**, pp. 111-125.

Wolff, S. B., and Wu, J., 2004, Modeling urban landscape dynamics: A review. E*cological Research*, **19**, pp. 119-129.

Wolfram, S.,1984, Cellular automata as models of complexity. *Nature*, **311**, pp. 419-424.

Wolfram, S., 1986, *Theory and Applications of Cellular Automata* (Singapore: World Scientific.

Wu, F., 1998a, An empirical model of intrametropolitan land use changes in a Chinese city, *Environment and Planning B*, **25**, pp. 245-263.

Wu, F., 1998b, Simland: A prototype to simulate land conversion through the integrated GIS and CA with AHP-derived transition rules. I*nternational Journal of Geographical Information Science*, **12**, 63–82.

Wu, F., and Webster, C., 1998, Simulation of land development through the integration of cellular automata and multicriteria evaluation. *Environment and Planning B*, **25**, pp.103-126.

Wu, F., 1999, GIS-based simulation as an exploratory analysis for space-time processes.*The Journal of Geographical Systems*, **1(3)**, pp. 199-218.

Wu, F., and Webster, C. J., 2000, Simulation artificial cities in a GIS environment: urban growth under alternative regulation regime. *International Journal of Geographical Information Science*. **14(7)**, pp. 625-648.

Wu, F., 2002, Calibration of stochastic cellular automata: the application to rural-urban land conversions. *International Journal of Geographical Information Science*, **16(8)**, pp.795-818.

Yates, P. M., and Bishop, I. D., 1998, The integration of existing GIS and modeling systems: with urban applications. *Computers Environment and Urban Systems*, **22(1)**, pp. 71-80.

Yeh, A. G. O., and Li, X., 2001a, Measurement and monitoring of urban sprawl in a rapidly growing region using entropy. *Photogrammetric Engineering & Remote Sensing*, **67(1)**, pp.83-90

Yeh, A. G. O., and Li, X., 2001b, A constrained CA model for simulation and planning of sustainable urban forms by using GIS. *Environment and Planning B*, **28**, pp. 733-753.

Yeh, A. G. O., and Li, X., 2002, Urban simulation using neural networks and cellular automata for land use planning. In symposium on Geospatial theory, Processing and Applications, 2002 Ottawa.

Yeh, A. G. O., and Li, X., 2003, Simulation of development alternatives using neural networks, cellular automata, and GIS for urban planning. *Photogrammetric Engineering & Remote Sensing*, **69(9)**, pp. 1043-1052.